Geometric Spanners for Topology Control in Wireless Networks

Dissertationsschrift

von

Klaus Volbert

Schriftliche Arbeit zur Erlangung des Grades
eines Doktors der Naturwissenschaften

Fakultät für Elektrotechnik, Informatik und Mathematik
Institut für Informatik und Heinz Nixdorf Institut
Universität Paderborn

Paderborn, im Februar 2005

Acknowledgements

First of all, I would like to thank my advisors, Prof. Dr. Friedhelm Meyer auf der Heide and Dr. Christian Schindelhauer, for their great support. We had a pretty good time and a very nice atmosphere in the research group of Prof. Dr. Friedhelm Meyer auf der Heide. I always had the freedom to choose the content and direction of my research. Furthermore, I would like to thank all (former) members of the research group "Algorithms and Complexity", especially the persons with whom I had close collaborations in research, teaching, or just in daily conversations. Namely, in alphabetic order, these are: Olaf Bonorden, Matthias Fischer, Jan Klein, Dr. Tamás Lukovszki, Peter Mahlmann, Jana Neuhaus, Stefan Rührup, Dr. Rolf Wanka, and Dr. Martin Ziegler. In addition, I am very grateful to Matthias Grünewald and, a second time, Stefan Rührup (also for reading and commenting on parts of this work) and Dr. Christian Schindelhauer for our joint research in the subproject C6 of the DFG-Sonderforschungsbereich 376 where I was heavily involved.

Last but not least, besides my colleagues, I would like to thank my wife Birgit and my parents Marianne and Karl-Heinz for their continuous support in all other circumstances.

Thanks to all for the great time and for supporting me in finishing this thesis.

Paderborn, February 2005 *Klaus Volbert*

This thesis was supported by

- DFG-Sonderforschungsbereich 376 "Massive Parallelität: Algorithmen, Entwurfsmethoden, Anwendungen" (Subproject C6 "Mobile Ad-hoc-Netzwerke"),
- EU Project "Algorithms and Complexity - Future Technologies (ALCOM-FT)", and by
- EU Project "Dynamically Evolving, Large Scale Information Systems (DELIS)"

Abstract

In this thesis titled “Geometric Spanners for Topology Control in Wireless Networks” we develop and analyze algorithms for communication in wireless networks. Especially, we consider ad hoc networks which are known as spontaneous wireless networks without a fixed infrastructure and without centralized administration. We distinguish between static, dynamic, and mobile ad hoc networks. In a static ad hoc network, we do not allow the participants any dynamics and movements and all hosts are stationary. In a dynamic ad hoc network, we allow the hosts to enter and/or leave the network. Finally, in a mobile ad hoc network (MANET), every host can move around without any restriction.

A special feature of this work is that we consider *power-variable* ad hoc networks, i.e. networks in which every participant is allowed to adjust the transmission range(s) of its sender(s). In addition, we distinguish between omnidirectional (radio) and directional (beam radio, infrared) communication.

The goal of this work is the development and the analysis of resource-efficient wireless communication structures (topologies). We focus on the resources routing time and energy consumption. For this purpose we introduce models, develop algorithms, and identify suitable measures. We use mathematical analyses to develop topologies with provably good graph and communication properties. Furthermore, we demonstrate experimentally that the results of our work are also suitable for real-world applications. Therefore we have developed and implemented different testbeds and present the outcome of our extensive experimental evaluations. We show that it is possible to build up and maintain wireless topologies using distributed, local algorithms without the need for any geographical positioning system.

In this work we model wireless networks using geometric graphs and use and extend methods in computational geometry.

Most of the results presented in this work have already been published in preliminary form in various international conference proceedings and journals. The results of Chapter 3 extend the results in [SVZ04]. Chapter 4 is based on [MSVG02, GLSV02, MSVG04] and contains technical motivation and background discussed in [GRSV03]. The results of Chapter 5 partially extend [SLRV03]. Finally, Chapter 6 summarizes and partially extends [Vol02, RSVG03, Vol04a].

Contents

Chapter 1

Introduction

The idea of long-distance wireless communication is not new. It already existed 100 years ago when morse codes were transmitted from ships to shore via wireless telegraphs. Since then there has been a long history of different radio and cellular systems. Nevertheless, wireless networks are very popular and widely used today. Nearly everyone has a mobile phone or other wireless device and wants to have wireless connections, e.g., to the Internet. For example, people access voice and data services via mobile phones, bluetooth technology replaces awkward cables with wireless links and wireless networking is possible via IEEE 802.11 compatible network equipment. These wireless networks can be divided into two categories: wireless networks with infrastructure (see Figure 1.1(a)) and wireless networks without infrastructure (see Figure 1.1(b)). Usually, in a wireless network with infrastructure, devices exchange their data packets with fixed base-stations (access points) that connect them with a wired backbone. However, in applications such as search and rescue missions, spontaneous get-together via laptops, space exploration, or environmental monitoring, no explicit communications infrastructure is available. In addition, the wireless devices usually have a very limited power supply and their communication range is limited, so that target devices are not always (directly) reachable. In these cases the data has to be routed via intermediate devices (multi-hop communication). For this purpose, each device has to have router capabilities. Such spontaneous multi-hop networks without fixed infrastructure and without centralized administration are called *ad hoc networks*.

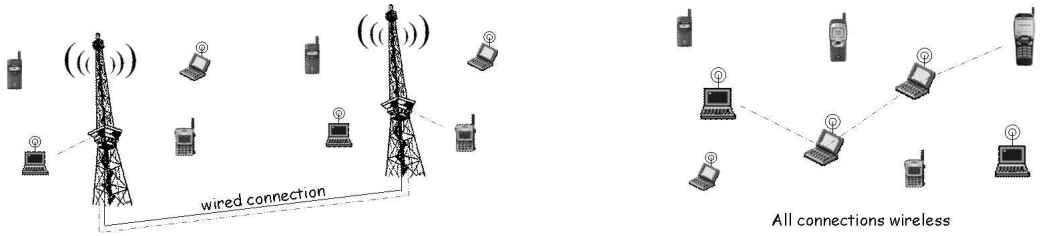

(a) With fi xed infrastructure (b) Without fi xed infrastructure

Figure 1.1: Wireless networks: fixed versus ad hoc

An ad hoc network is a collection of (mobile) hosts connected by wireless links (dynamically)

forming a temporary network without the aid of any established infrastructure or centralized administration [JM96, Per01]. In this thesis we concentrate on three special types of wireless networks without a fixed infrastructure: *static* ad hoc networks, *dynamic* ad hoc networks and *mobile* ad hoc networks. In a static ad hoc network, we do not allow the participants any dynamics and movements and all hosts are stationary. In a dynamic ad hoc network, we allow the hosts to enter and/or leave the network. Finally, in a mobile ad hoc network (MANET), every host can move around without any restriction.

Since ad hoc networks change their topology frequently and often without any regular pattern, topology maintenance and enabling fast and reliable communication is a challenging task in such spontaneous networks. The network's wireless topology may dynamically change in an unpredictable manner. One of the most important challenges in designing MANETs is how to provide high throughput and low-energy wireless access to mobile nodes. Energy efficiency is of paramount importance for MANETs design, since the mobile nodes in such networks are typically battery powered, which are often not rechargeable. The main goal of this thesis is to design and analyze topologies as basic network structures for ad hoc networks of the different types which allow us efficient point-to-point communication with regard to routing time and energy consumption. By point-to-point communication we mean the process of moving information across a network from a source to a destination. For this purpose we develop models, algorithms, and measures and present topologies for wireless networks which provably optimize routing time and/or energy consumption. Furthermore, we point out technical limitations, e.g., we show that, in general, it is not possible to optimize routing time and energy consumption in a wireless network at the same time.

A special feature of this thesis is that we consider so-called *power-variable* ad hoc networks, i.e. networks in which every participant is allowed to adjust its transmission range(s). We will show that we can achieve improvements in energy consumption and routing time. Furthermore, we distinguish between omnidirectional (radio) and directional (beam radio, infrared) communication. Both communication models allow us different possibilities to form networks. To give an example, the question "what is the minimum transmission range for every node of a set of wireless devices each equipped with an omnidirectional antenna that guarantees connectivity?" is very hard to solve. Its decision problem is known to be NP-hard [KKKP00, CPS04]. We show that this problem is easy to solve using the directional communication model. Here, we present localized algorithms that do not need any geographical positioning system to build up power-efficient and routing time-efficient topologies. We model our networks using geometric graphs, use and prove geometric properties, investigate communication features and test our algorithms experimentally using realistic settings. For the mobility of the hosts in a MANET, we introduce a worst case model and show how to maintain a network with arbitrary movements.

1.1 Outline

Most of the chapters focus on point-to-point communication problems. We start with a theoretical study on spanners which builds the fundament for the results on topology control in wireless networks. We first present analyses on static ad hoc networks, then we extend our model and

allow station dynamics, where radio stations can enter and/or leave the network, and finally, we investigate networks using worst case movements of its participants. In the last chapter, we present our results concerning realistic mobile ad hoc networks based on extensive simulations. In the following, we give a detailed overview of the chapters of this thesis.

Chapter 2 - Preliminaries. In Chapter 2 we give a short summary of the basic terminology for topology control in wireless networks using geometric graphs. We introduce the omnidirectional (radio) and the directional (beam radio, infrared) communication model and review physical aspects of wireless transmissions. In the most common attenuation model the received signal power at distance d from a sender falls proportionally to $1/d^\delta$ for any δ between 2 and 4 or even 8. Since we assume in this thesis that there is only one given transmission frequency, we discuss the problem of interference. Furthermore, we introduce basic definitions, e.g., the δ-cost of a path in a geometric graph, and present the challenges of topology control. A good topology has low stretch, low degree, low energy consumption, and is locally constructable. We use spanners, weak spanners, and power spanners to build up topologies that provably fulfill these requirements and review the theoretical background. Finally we discuss (multi-hop) point-to-point communication and mention traditional routing protocols for MANETs such as AODV, DSDV, and DSR.

Chapter 3 - Spanners, Weak Spanners, and Power Spanners. In Chapter 3 we investigate the relations between spanners, weak spanners, and power spanners in $\mathbb{R}^\mathcal{D}$ for any constant $\mathcal{D}$. For $c \in \mathbb{R}$, a *c-spanner* is a subgraph of the complete Euclidean graph satisfying the condition that between any two vertices there exists a path of length at most c-times their Euclidean distance. Based on this ability to approximate the complete Euclidean graph, sparse spanners have found many applications, e.g., in FPTAS, geometric searching, and radio networks. In a *weak* c-spanner, this path may be arbitrarily long, but must remain within a disk or sphere of radius c-times the Euclidean distance between the vertices. Finally in a *c-power* spanner, the total energy consumed on such a path, where the energy is given by the sum of the squares of the edge lengths on this path, must be at most c-times the square of the Euclidean distance of the direct edge or communication link.

While it is known that any c-spanner is also both a weak C_1-spanner and a C_2-power spanner for appropriate C_1, C_2 depending only on c but not on the graph under consideration, we show that the converse is not true: there exists a family of c_1-power spanners that are not weak C-spanners and also a family of weak c_2-spanners that are not C-spanners for any fixed C. However a main result of this thesis reveals that any weak c-spanner is also a C-power spanner for an appropriate constant C.

We further generalize the latter notion by considering (c, δ)-power spanners where the sum of the δ-th powers of the lengths has to be bounded; so $(c, 2)$-power spanners coincide with the usual power spanners and $(c, 1)$-power spanners are classical spanners. Interestingly, these (c, δ)-power spanners form a strict hierarchy where the above results still hold for any $\delta \geq \mathcal{D}$; some even hold for $\delta > 1$ while counter-examples exist for $\delta < \mathcal{D}$. We show that every self-similar curve of fractal dimension $\mathcal{D}_f > \delta$ is not a (C, δ)-power spanner for any fixed C, in general.

Chapter 4 - Static and Dynamic Ad Hoc Networks. In Chapter 4 we investigate static and dynamic ad hoc networks and present solutions concerning the problem of point-to-point communication for a set of n radio stations. We concentrate on single frequency ad hoc networks in which every station is allowed to adjust its transmission range to decrease energy consumption and to avoid interference. Such networks are also called *power-variable* ad hoc networks. Furthermore, we distinguish between omnidirectional (radio) and directional (beam radio or infrared) communication. In both communication models we first investigate static vertex sets, before we extend our considerations to dynamic vertex sets.

For static point-to-point communication we define measures for congestion, dilation, and energy consumption that take interference among communication links into account. Furthermore, we introduce the (bidirectional) interference number and show that energy-optimal path selection for radio networks can be computed in polynomial time. Then we introduce the diversity $g(V)$ of a set $V \subseteq \mathbb{R}^{\mathcal{D}}$ for any constant $\mathcal{D}$. It can be used to upper bound the number of interfering edges. For real-world applications it can be regarded as $\Theta(\log n)$.

A main result is that every weak c-spanner allows us to approximate an energy-optimal path system with a constant factor and a congestion-optimal path system with a factor of $\mathcal{O}(g(V))$. We introduce the Hierarchical Layer Graph (HL-graph) and show that this graph is a c-spanner for a constant c. Since the (bidirectional) interference number in the HL-graph can be upper bounded by $\mathcal{O}(g(V)$, the HL-graph allows us an $\mathcal{O}((\log n)^2)$ approximation of a congestion optimal path system in real-world applications. Furthermore, we investigate trade-offs and show that it is not possible to optimize more than one measure at the same time, in general. The relation between congestion and energy is even worse.

Then we show that we can construct better topologies using the directional communication model than using the omnidirectional one. We introduce the unidirectional interference number and present a sectorized, theoretically interference-free topology, the so-called sparsified Yao-graph (SparsY-graph), which allows us to approximate an energy-optimal path system with a constant factor and a congestion-optimal path system with a factor of $\mathcal{O}(g(V))$, i.e. with $\mathcal{O}(\log n)$ in realistic settings. A main result is that we prove that the SparsY-graph is a weak c-spanner for a constant c. Hence, we can apply our results of Chapter 3 to show that the SparsY-graph is a C-power spanner for some constant C depending only on c. We compare the SparsY-graph with other sectorized topologies, known as the Yao-graph and the SymmY-graph and investigate degree and spanner properties as well as communication features with regard to interference. In general, we show that the SymmY-graph is neither a weak spanner nor a power spanner, but nevertheless it is connected. Note that some of these results require an appropriate number of sectors/senders per node. But most of our results hold already if this number is greater than 6.

Finally, we discuss the handling of interference and compare the abilities of these topologies to handle dynamic changes of the network when radio stations enter or leave the network and present other geometric structures that can be used as basic network topologies in wireless networks.

Chapter 5 - Mobile Ad Hoc Networks In Chapter 5 we investigate distributed algorithms for moving radio hosts with adjustable transmission power in a worst case scenario. We consider

two models to find a reasonable restriction on the worst case mobility. In the pedestrian model we assume a maximum speed $v_{\max}$ of the radio hosts, while in the vehicular model we assume a maximum acceleration $a_{\max}$ of the participants.

Our goal is to maintain persistent routes with good communication network properties like small diameter, low energy-consumption, low congestion, and low interference. A route is persistent, if we can guarantee that all edges of this route can be upheld for a given time span Δ, which is a parameter denoting the minimum time the mobile network needs to adopt changes, i.e. update routing tables, change directory entries, etc. This Δ can be used as the length of an update interval for a proactive routing scheme.

We extend some known notions such as transmission range, interference, spanner, weak spanner, power spanner, and congestion to both mobility models and introduce a new parameter called crowdedness that states a lower bound on the amount of radio interference. Then we prove that a mobile weak spanner hosts a path system that polylogarithmically approximates the optimal path system for congestion.

We present distributed algorithms based on a grid clustering technique and a high-dimensional representation of the dynamic start situation which construct mobile (weak) spanners with low congestion, low interference, low energy-consumption, and low degree. We measure the optimality of the output of our algorithm by comparing it with the optimal choice of persistent routes under the same circumstances with respect to pedestrian or vehicular worst case movements. Finally, we present solutions for dynamic position information management under both mobility models.

Chapter 6 - Experimental Analyses and Results In Chapter 6 we present the results of our extensive experimental evaluations. We have developed two different testbeds to perform a number of significant simulations that demonstrate the properties of our algorithms and/or analyses using realistic settings.

We describe our simulation environment for mobile ad hoc networks, SAHNE, developed for analyzing (directional) communication in MANETs. SAHNE allows us both, simulating omnidirectional as well as directional wireless transmissions. We use it to close the gap between theoretical investigations of communication protocols in wireless networks and real-world applications. For this purpose we have implemented realistic models for radio and infrared transmissions. For point-to-point communication we examine experimentally the Yao-graph, the SparsY-graph, the SymmY-graph, and the HL-graph. First, we present communication strategies using idealized assumptions. Then we consider topology control using realistic propagation models. Our distributed algorithms build up the sectorized graphs in time $\mathcal{O}(\log n)$ per node without the use of any geographical positioning system. They are based only on local knowledge and local decisions and make use of power control to establish communication links with low energy-cost. We compare these algorithms with respect to congestion, dilation, and energy. For congestion we introduce different measures that allow us to investigate the difference between real-world wireless networks and models for wireless communication at a high level of abstraction. Our experimental results show that these topologies and algorithms work well in a distributed environment.

Furthermore, we present our interactive tool for checking graph properties, ITGraP. Here,

our aim was not to go into technical detail, but more to present a theoretical study of important graph properties on normal vertex sets where the nodes are placed uniformly at random. We have implemented the Yao-graph and its variants as well as the Hierarchical Layer Graph to perform simulations and to find out about the performance of our topologies. In general, it is assumed that the sectors of the nodes underlie a fixed orientation or that they are oriented as a result of the movement of nodes. We extend this model and allow each node to adjust the orientation of its senders independently of any other conditions. We introduce new optimization tasks and present algorithms which improve the stretch factors of known sectorized topologies only by adjusting the orientation of some sectors of the nodes. Our aim is to improve the quality, especially the stretch factors, of the sectorized topologies. We show improvements experimentally and present algorithms to compute exactly the stretch factors of a given graph $G = (V, E)$ in time $\mathcal{O}(|V|^2 \log |V| + |V||E|)$. Hence, we can determine these factors for sparse graphs in time $\mathcal{O}(|V|^2 \log |V|)$. We use the algorithms to compute a lower bound for an optimal orientation of all senders, e.g., with regard to energy consumption, in polynomial time. We use this bound to analyze the simulation results.

Our extensive experimental evaluation of the sectorized topologies on random vertex sets using different sector alignments shows that we can improve the known stretch factors and that the considered topologies perform well on "normal" vertex sets where the nodes are placed uniformly at random.

1.2 Bibliographic Notes

Most of the results presented in this thesis have already been published in preliminary form in various international conference proceedings and journals. In the following I give a list of my own contributions with regard to topology control in wireless networks.

- K. Volbert. *A Simulation Environment for Ad Hoc Networks Using Sector Subdivision*, 2002 [Vol02].
- F. Meyer auf der Heide, C. Schindelhauer, K. Volbert, and M. Grünewald. *Energy, Congestion and Dilation in Radio Networks*, 2002 [MSVG02].
- M. Grünewald, T. Lukovszki, C. Schindelhauer, and K. Volbert. *Distributed Maintenance of Resource Efficient Wireless Network Topologies*, **distinguished paper**, 2002 [GLSV02].
- S. Rührup, C. Schindelhauer, K. Volbert, and M. Grünewald. *Performance of Distributed Algorithms for Topology Control in Wireless Networks*, 2003 [RSVG03].
- M. Grünewald, U. Rückert, C. Schindelhauer, and K. Volbert. *Directed power-variable infrared communications for the mini robot Khepera*, 2003 [GRSV03].
- C. Schindelhauer, T. Lukovszki, S. Rührup, and K. Volbert. *Worst Case Mobility in Ad Hoc Networks*, 2003 [SLRV03].

- F. Meyer auf der Heide, C. Schindelhauer, K. Volbert, M. Grünewald. *Congestion, Dilation, and Energy in Radio Networks*, 2004 [MSVG04].
- K. Volbert. *Experimental Analysis of Adjustable Sectorized Topologies for Static Ad Hoc Networks*, 2004 [Vol04a].
- C. Schindelhauer, K. Volbert, and M. Ziegler. *Spanners, Weak Spanners, and Power Spanners for Wireless Networks*, 2004 [SVZ04].

The results of Chapter 3 extend the results in [SVZ04]. Chapter 4 is based on [MSVG02, GLSV02, MSVG04] and contains technical motivation and background discussed in [GRSV03]. The results of Chapter 5 partially extend [SLRV03]. Finally, Chapter 6 summarizes and partially extends [Vol02, RSVG03, Vol04a].

Chapter 2

Preliminaries

In this thesis we try to contribute to solutions to the problem of topology control in ad hoc networks using geometric structures. We use this chapter to present basic definitions and foundations concerning wireless transmissions, geometric structures, topology control, and routing. We model wireless networks using geometric graphs and suggest a graph-theoretical point of view for topology control. Based on our topologies, other tasks like forwarding packets and selecting routing paths can take place. Our focus lies on the problem of point-to-point communication.

2.1 Wireless Transmission

In an ad hoc network, each node is equipped with a wireless transmitter and a receiver with appropriate antenna, which may be omnidirectional, highly directional, possibly steerable, or some combination thereof [AZ03]. In this work we distinguish between two types of wireless networks. In the first one, the omnidirectional communication network, every node is equipped with an omnidirectional antenna whereas in the second one, the directional communication network, every node has k sending and receiving devices (e.g., directional antennae, adaptive antennae, beam-forming antennae, infrared diodes) which are located such that a node can communicate in parallel within each of its k (non-overlapping) sectors with angle $\theta = 2\pi/k$ (see Figure 2.1).

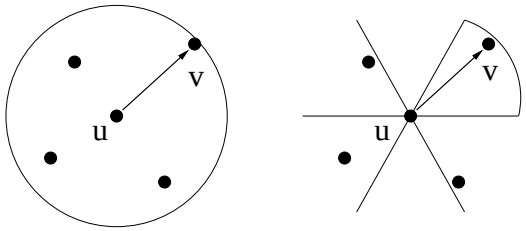

Figure 2.1: Omnidirectional versus directional transmission

In our analyses, e.g., in Chapter 4, we assume that these sectors are non-overlapping and have fixed borders. In reality, sectors overlap, borders are not fixed, and physical effects like areas with no reception occur. One aim of our experiments, presented in Chapter 6, was to

evaluate our theoretical results using realistic settings. For this purpose we simulate realistic signal propagation and deal with overlapping sectors in simulations.

It is very important to understand distinguishing features of radio transmissions when designing and analyzing topologies for wireless networks. When electrons move, they create electromagnetic waves that can propagate through space (even in a vacuum). The number of oscillations per second of a wave is called its frequency f and is measured in *Hz* (Hertz). The distance between two consecutive maxima (or minima) is called the wavelength, which is usually designated by λ. When an antenna of the appropriate size is attached to an electrical circuit, the electromagnetic waves can be broadcast efficiently and received by a receiver some distance away. All wireless communication is based on this principle [Tan96]. In vacuum, all electromagnetic waves travel at the speed of light c (approximately $3 \cdot 10^8$ m/sec), no matter what their frequency is. The fundamental relation between f, λ and c in vacuum is

$$\lambda \cdot f = c \, .$$

Waves of different frequencies are assigned to frequency bands. An overview of the electromagnetic spectrum and its uses for communication is given in Figure 2.2.

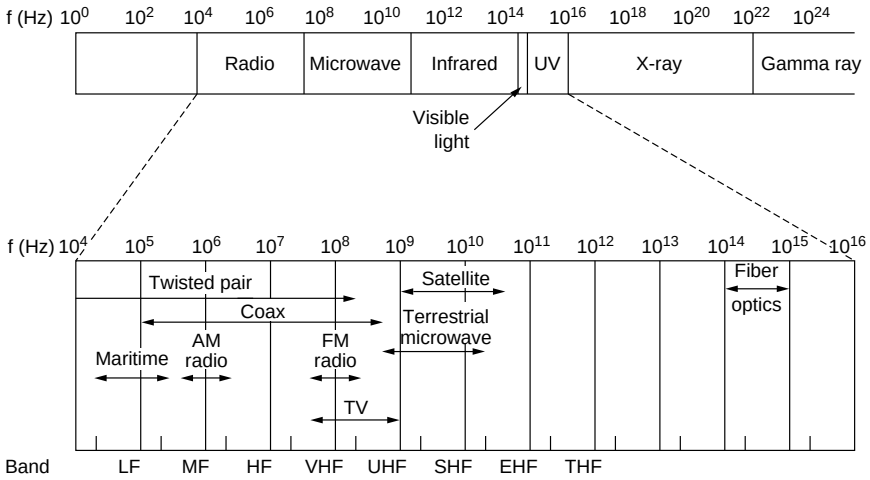

Figure 2.2: Frequencies and frequency bands [Tan96]

The radio, microwave, infrared, and visible light portions of the spectrum can all be used for transmitting information by modulating the amplitude, frequency, or phase of the waves. Ultraviolet light, X-rays, and gamma rays would be even better, due to their higher frequencies, but they are hard to produce and modulate, do not propagate well through buildings, and are dangerous to living things. In this thesis we assume that only one frequency for transmission is given, e.g., radio or infrared. These waves follow the ground or they are refracted/reflected by the ionosphere and sent back to the earth. One advantage of radio waves is that they pass through obstacles, infrared waves do not. In the rest of this thesis we assume propagation in free space and without any obstacles. We neglect effects like reflection, diffraction, and scattering [AZ03]. Free space is an ideal propagation medium. The received signal power at distance d from a sender

falls proportionally to $1/d^\delta$ where δ, the propagation exponent, is a constant between 2 and 6 or even 8 depending on side-effects like absorption, multi-path propagation or fading [Rap96]. For example, for the ideal free space propagation model we have $\delta = 2$, for the so-called two ray model, which also considers multipath fading, we have $\delta = 4$.

Energy conservation is one of the most important issues in wireless networks for node and network lifetime, as the nodes, in general, have only limited power supply.

Since we allow the hosts only one transmission frequency, signals can interfere and this effect may result in data loss. A common measure for interference is the signal-to-interference-ratio (SIR) or signal-to-interference-plus-noise-ratio (SINR). We will discuss and use this in Chapter 6. In our analyses we use a model that is easier to handle. We assume that if there is a node receiving more than one signal at the same time, e.g., two or more nodes are sending at the same time with the necessary transmission range, then this node can not receive anything. In Chapter 4 we introduce interference models for the omnidirectional model as well as for the directional model. There, we also review some special interference problems known as the hidden terminal problem (HTP) and the exposed terminal problem (ETP). Since we consider single frequency power-variable ad hoc networks, i.e. each host is allowed to adjust its transmission power to decrease energy consumption and to avoid interference, a third interference problem can occur. We will introduce this as the asymmetric interference problem.

2.2 Geometric Graphs

We model wireless networks using geometric graphs. A geometric graph $G = (V, E)$ consists of a set of vertices (or nodes) $V \subset \mathbb{R}^{\mathcal{D}}$ for $\mathcal{D} \in \mathbb{N}$ and a set of edges (or links) E. We define the size of G as the number of nodes contained in G denoted by $|V|$. For all $u, v \in V$, let (u, v) denote a directed edge from u to v, and $\{u, v\}$ denote an undirected edge connecting u and v. We call G undirected if $E \subseteq \{\{u, v\} \mid u, v \in V\}$, and directed if $E \subseteq \{(u, v) \mid u, v \in V\}$. For all $u, v \in V$ let $|u - v|$ be defined as the Euclidean distance between u and v, this is, for completeness, $\sqrt{\sum_{i=1}^{\mathcal{D}}(u_i - v_i)^2}$. A finite sequence $P = (u = u_1, u_2, \ldots, u_\ell = v)$ of nodes $u_i \in V$ such that $(u_{i-1}, u_i) \in E$ for all $i \in \{2, \ldots, \ell\}$ is called a path from u to v in G. Occasionally, we also encounter the more general situation of a path from u to v that is not necessarily in G. This means that $u_i \in V$ still holds, but the requirement $(u_{i-1}, u_i) \in E$ is dropped. The radius of P is the real number $\max_{i=1,\ldots,\ell} |u - u_i|$. The (Euclidean) length of P is given by $\sum_{i=2}^{\ell} |u_i - u_{i-1}|$. Then the hop length is $\ell - 1$ and for $\delta \geq 0$ we define the δ-cost of a path P by

$$||P||^\delta := \sum_{i=2}^{\ell} |u_i - u_{i-1}|^\delta \, .$$

The length is just the 1-cost whereas the hop length coincides with the 0-cost. The δ-cost for $\delta \geq 2$ reflects the transmission properties of radio networks. In this case δ is also called the propagation exponent. The graph G is called connected if for every pair of nodes $u, v \in V$, there is a path in G from u to v. If $\{u, v\} \in E$ then u is called a neighbor of v. The number of neighbors of v gives the degree of v denoted by $\deg(v)$. The degree of G is defined as $\deg(G) :=$

$\max_{v \in V} \deg(v)$. For directed graphs, we define the number of edges ending at a node v the in-degree of v, and the number of edges leaving v the out-degree of v.

In Chapter 3 we concentrate on families of graphs. A family of graphs

$$\mathcal{G} = \{G_n \mid G_n \text{ is a geometric graph for } n \in \mathbb{N}\}$$

fulfills a given property if and only if G_n fulfills this property for all $n \in \mathbb{N}$. Later on, if it is clear to which family a graph belongs, we say that this graph fulfills a property if and only if its family fulfills the same property.

2.3 Topology Control in Wireless Networks

The simplest topology for a wireless network is given by the complete geometric graph denoted by K_n for n nodes. But, typically, the transmission range of a node in such a network is limited. For a wireless network consisting of a set V of wireless nodes where the maximum transmission range is given by a constant and is equal on all nodes, the most commonly used topology is the *unit disk graph* $\texttt{UDG}(V)$. Using proper scaling, we assume that all nodes have a maximum transmission range equal to one unit. Then for $u, v \in V$ the edge $\{u, v\}$ is contained in $\texttt{UDG}(V)$ if and only if $|u - v| \leq 1$.

Both topologies, the complete geometric graph and the unit disk graph, have the major drawback that the number of edges in these graphs can be as large as the square of the number of nodes in the network. Maintaining such a number of links is not practicable and would tend to a network with high interference which results in high congestion. Hence, a subgraph of the complete geometric graph or of the unit disk graph has to be constructed which has to contain some important properties. First of all, the number of edges should be linear in the number of nodes. A graph satisfying this requirement is called *sparse* graph. Furthermore, the degree of each node should be upper bounded by a constant and the complete structure should be buildable locally in an efficient way; all this under the side condition that the subgraph, the topology, is still relatively good regarding the quality of the routes between nodes compared to the complete graph or the unit disk graph (low stretch). We will use geometric spanners to build up wireless topologies that provably fulfill these requirements. It is known that low degree and/or sparseness alone does not imply low interference, see Figure 4.5 in Section 4.1 or [BvRWZ04].

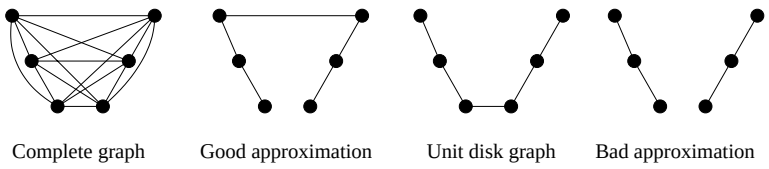

Figure 2.3: A good approximation of the complete graph can result in a bad approximation of the corresponding unit disk graph

Note that in general a good approximation of the complete graph will not always result in a good approximation of the unit disk graph (see Figure 2.3). We present topologies that give good approximations of the complete graph as well as of the unit disk graph.

The field of topology control for wireless networks is relatively new. Recently, lots of papers have been published concerning topology control and routing. Excellent surveys are presented by X.-Y. Li [Li03b, Li03a, Li03c] and R. Rajaraman [Raj02]. In the following chapters we will mention some related works in more detail. To the best of our knowledge, we are one of the first to combine theoretical algorithmic research and prototypical realization of the directional communication model. On the one hand, we present mathematical analyses and prove interesting properties. On the other hand, we have implemented our algorithms in testbeds as well as in prototypical environments in cooperation with electrical engineers and show that they perform well in realistic scenarios.

2.4 Geometric Spanners

First of all, we give the definition of a spanner, a weak spanner, and a power spanner. Let $G = (V, E)$ be a directed geometric graph with finite $V \subseteq \mathbb{R}^2$ and $c > 0$. G is a *c-spanner*, if for all $u, v \in V$ there is a path P from u to v in G of length $\|P\|^1$ at most $c \cdot |u - v|$. G is a *weak c-spanner*, if for all $u, v \in V$ there is a path P from u to v in G of radius at most $c \cdot |u - v|$, i.e. the path P lies completely in a bounded disk of radius at most $c \cdot |u - v|$. For $\delta \geq 0$, G is a *(c, δ)-power spanner* if for all $u, v \in V$ there is a path P from u to v in G of δ-cost $\|P\|^\delta$ at most $c \cdot |u - v|^\delta$. G is a *c-power spanner*, if G is a $(c, 2)$-power spanner. We call factor c the *length stretch factor*, *weak stretch factor* or *power stretch factor*, respectively. Roughly speaking, spanners approximate the complete Euclidean graph on a set of geometric vertices. Mostly, another goal is to have only linearly many edges.

Finally, when power consumption is of minor interest and the focus lies on the routing time, which is dominated by the number of individual steps, sparse graphs are desired which guarantee that any two vertices are connected by a path containing at most c additional vertices. These are the so-called *c-hop* spanners [ALW+03]. In Chapter 5 we extend these notions and introduce *mobile* spanners to investigate worst case mobility in MANETs.

Geometric spanners were first introduced to computational geometry by Chew [Che86]. Peleg and Schaffer introduced them in the context of distributed computing [PS89]. They have applications in motion planning [Cla87], they were used for approximating the minimum spanning tree [Yao82], and for a fully polynomial time approximation scheme for the traveling salesman and related problems [AGK+98, RS98]. A good survey of spanning trees and spanners is given by Eppstein in [Epp00].

Weak spanners were introduced for special range searching problems in walkthrough systems [FLZ98, FMS97]. We use them in Chapter 4 for optimizing routing time in wireless networks, i.e. for approximating congestion-optimal path systems.

Recently, (power) spanners have been used for routing and topology control in ad hoc networks to build up power efficient wireless network topologies [ALW+03, Raj02, JRS03, GLSV02, MSVG04, Li03b, Li03a, Li03c].

In Chapter 3 we investigate the relations between these various types of spanners. The question on the relation between spanners and weak spanners is whether any weak c-spanner is a C-spanner for some value C depending only on c. Based on a construction from [Epp96], we

answer this negatively. For some weak c-spanners it is proven that they are also C-power spanners for some value C [GLSV02, JRS03] using elaborated constructions. One major contribution of Chapter 3 generalizes and simplifies such results by showing that in $\mathbb{R}^{\mathcal{D}}$ in fact any weak c-spanner is a C-power spanner with $C = \mathcal{O}(c^{2\mathcal{D}})$. Moreover, we introduce and investigate the notion of a (c, δ)-power spanner which

- for $\delta = 0$ coincides with c-hop spanners, i.e. graphs with diameter c
- for $\delta = 1$ coincides with c-spanners
- for $\delta = 2$ coincides with (usual) c-power spanners
- for $\delta > 2$ reflects transmission properties of radio networks (e.g., for $\delta \leq 8$) .

We show that these form a strict hierarchy: for $\Delta > \delta > 0$, any (c, δ)-power spanner is also a (C, Δ)-power spanner with C depending only on c and Δ/δ; whereas we give examples of (C, Δ)-power spanners that are not (c, δ)-power spanners for any fixed c. Our main contribution is that any weak c-spanner is also a (C, δ)-power spanner for arbitrary $\delta \geq \mathcal{D}$ with C depending on c and δ only. Finally, we show that this claim is best possible by presenting weak c-spanners which are not (C, δ)-power spanners for arbitrary $\delta < \mathcal{D}$ and any fixed C.

Sometimes we shorten the notion of a spanner, a weak spanner and a power spanner and omit constant parameters. So, if we say that a family of graphs is a (good) *spanner*, then there exists a constant c such that all its members are c-spanners. If it is clear to which family a graph belongs, we say that this graph is a spanner, a weak spanner or a power spanner, if and only if its family is a spanner, a weak spanner or a power spanner.

2.5 Point-to-Point Communication (Multi-hop)

Suppose that we are given an ad hoc network and a set of source-destination pairs. For each of these source-destination pairs, we want to solve the resulting point-to-point communication problem (routing problem), i.e. we want to choose a selection of edges on which it is possible to transmit the data, in the form of packets, from the source to the destination. Mainly, routing is the process of moving information across a network from a source to a destination. It can be divided into two parts: the determination of routing paths (path selection) and the transport of information units (typically called packets) along the paths. Our focus is on path selection. Since the nodes in our network have limited energy supply and since the links have limited bandwidth, we have to ensure that all packets reach their destinations power-efficiently and quickly, in the sense of routing time.

In this thesis we concentrate on analyzing and constructing topologies as basic structures for routing in wireless networks. Based on these topologies the routing task takes place and the developer of a routing protocol can decide in some cases which criteria he wants to optimize. Traditional routing protocols for MANETs such as AODV, DSDV, and DSR [Per01] usually choose the path with the lowest hop count. There also exist power-aware routing protocols that use different metrics (e.g., energy consumed per packet, variance in node power level) to choose the best route in order to extend the lifetime of individual nodes or the whole network

[SR98, SW98, CT00]. The congestion of a route is usually not regarded directly, but some routing protocols choose routes with the shortest route discovery, assuming that the route with the quickest response is less congested (e.g., SSA [DRWT97]). All these routing protocols assess the paths that have been found by route discoveries according to a cost function. Many further routing algorithms have recently been proposed for mobile ad hoc networks. In all these protocols, the routing task is performed using a proactive, a reactive scheme, or a combination of both. Examples of proactive protocols that have been suggested are OLSR, DSDV, and WRP. Examples of reactive protocols are DSR, LAR, RDMAR, AODV, and TORA. A combination of both concepts can be found in ZRP and LANMAR. Surveys can be found in [Per01, RT99].

Chapter 3

Spanners, Weak Spanners, and Power Spanners

In this chapter we investigate the relations between spanners, weak spanners, and power spanners in $\mathbb{R}^{\mathcal{D}}$ for $\mathcal{D} \in \mathbb{N}$. First, for simplicity, we formulate our results for the case $\mathcal{D} = 2$, and then we extend our results to the more general, higher-dimensional case. In Section 2.4 we already defined that for $c \in \mathbb{R}$ a *c-spanner* is a subgraph of the complete Euclidean graph satisfying the condition that between any two vertices there exists a path of length at most c-times their Euclidean distance. In a *weak* c-spanner, this path may be arbitrarily long, but must remain within a disk of radius c-times the Euclidean distance between the vertices, i.e. the path has a radius of at most c-times the Euclidean distance between the vertices. Finally in a *c-power* spanner, the total energy consumed on such a path, where the energy is given by the sum of the squares of the edge lengths on this path, must be at most c-times the squares of the Euclidean distance of the direct link.

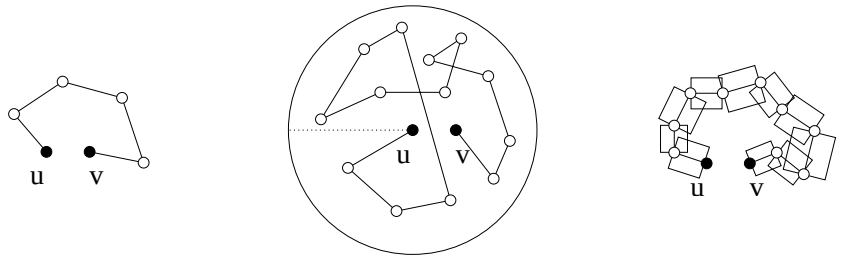

(a) Bounded length (b) Bounded radius (c) Bounded energy

Figure 3.1: Spanner, weak spanner, and power spanner

The attentive reader might have observed that our definition of a power spanner does not exactly match that from [GLSV02]. The latter required that the δ-cost of some path P from u to v in G is bounded by c-times the δ-cost of any path Q (not necessarily in G) from u to v, i.e. there exists a path P in G with $||P||^{\delta} \leq \min_{Q=(u_1,\ldots,u_\ell),\ell\in\mathbb{N}} \sum_{i=1}^{\ell-1} |u_i - u_{i+1}|^{\delta}$. However, both approaches are in fact equivalent: let $G = (V, E)$ be a (c, δ)-power spanner, $u, v \in V$, and let Q denote some path $Q = (u = u_1, \ldots, u_\ell = v)$ (not necessarily in G) from u to v of minimum

δ-cost. For each $i = 2, \ldots, \ell$ there exists by presumption a path P_i in G from u_{i-1} to u_i of δ-cost at most $c \cdot |u_i - u_{i-1}|^\delta$. The concatenation of all these paths yields a path P from u to v in G with δ-cost $\|P\|^\delta$ at most $c \cdot \|Q\|^\delta$.

Observe that any strongly connected finite geometric graph is a C-spanner for some value C. For this, e.g., consider for any pair u, v of vertices some path from u to v and the ratio of its length to the distance between u and v. Then taking for C the maximum over the (finitely many) pairs u, v will give the value C. Therefore the question on the relation between spanners and weak spanners rather asks whether any weak c-spanner is a C-spanner for some value C depending only on c. While it is known that any c-spanner is also both, a weak C_1-spanner and a C_2-power spanner for appropriate C_1, C_2 depending only on c, but not on the graph under consideration, we show that the converse is not true: there exists a family of c_1-power spanners that are not weak C-spanners and also a family of weak c_2-spanners that are not C-spanners for any fixed C. However the most significant result in this chapter reveals that any weak spanner is also a power spanner. We further generalize the latter notion by considering (c, δ)-power spanners where the sum of the δ-th powers of the lengths has to be bounded; so $(c, 2)$-power spanners coincide with the usual power spanners and $(c, 1)$-power spanners are classical spanners. Interestingly, these (c, δ)-power spanners form a strict hierarchy where the above results still hold for any $\delta \geq \mathcal{D}$; some even hold for $\delta > 1$ while counter-examples exist for $\delta < \mathcal{D}$. We show that every self-similar curve of fractal dimension $\mathcal{D}_f > \delta$ is not a (C, δ)-power spanner for any fixed C.

This chapter is organized as follows. In Section 3.1, we show that, while any c-spanner is also a weak c-spanner, a weak c-spanner is, in general, not a C-spanner for any C depending just on c. Section 3.2 similarly reveals the relations between spanners and power spanners. In the main Section 3.3 of this chapter, we investigate the relation between weak spanners and power spanners. Theorem 3.3 gives an example of a power spanner which is not a weak spanner. Our major contributions then prove that, surprisingly, any weak c-spanner is also a C-power spanner with C depending only on c. For different values of δ, we obtain different upper bounds to C in terms of c: for $\delta = 2$ (power spanners in the original sense), we show $C \leq \mathcal{O}(c^8)$, see Theorem 3.5; for $\delta > 2$, we have $C \leq \mathcal{O}\big(c^{2+\delta}/(1 - 2^{2-\delta})\big)$, see Theorem 3.4. However for $\delta < 2$, we present counter-examples of unbounded C, that is, in this case provably not every weak c-spanner is a (C, δ)-power spanner, see Theorem 3.6. Furthermore, we generalize our construction and analysis to self-similar fractal curves. Section 3.4 finally shows that for different δ, the respective classes of (c, δ)-power spanners form a strict hierarchy. In Section 3.5 we extend our results to higher-dimensional cases, before we summarize our results in Section 3.6.

3.1 Spanners versus Weak Spanners

Every c-spanner is also a weak c-spanner. Our first result shows that the converse is not true, in general.

Theorem 3.1 *There is a family of graphs $\mathcal{G} = (V, E)$ with $V \subseteq \mathbb{R}^2$ all of which are weak $(\sqrt{3} + 1/2)$-spanners but not C-spanners for any fixed $C \in \mathbb{R}$.*

Figure 3.2: EPPSTEIN'S construction: a fractal curve with high dilation (not a spanner but a weak spanner)

Proof: We show the claim using the fractal construction presented in [Epp96] (see Figure 3.2). We briefly review its recursive definition which is similar to that of a KOCH Curve. At the beginning, there are two vertices with distance 1. In the following steps we replace each edge by 5 new edges of equal length as follows: one horizontal, one at angle $\pi/4$, a second horizontal, another one at angle $-\pi/4$ and a third horizontal. After i steps we have a graph consisting of 5^i edges and $5^i + 1$ vertices. As shown in [Epp96] this graph has unbounded length stretch factor. We argue that there exists a constant c such that it is a weak c-spanner. It is known that the area under the constructed curve is bounded by a constant and that the path between two vertices $u, v \in V$ lies completely in a disk around the midpoint of the segment between u and v with radius at most $(2 \cdot \sqrt{3}/2) = \sqrt{3}$ (see KOCH's Snowflake, Figure 3.9). Applying Observation 3.1 proves the claim. ■

The following observation says that, except for constants, it makes no difference in the definition of a weak spanner whether the radius is bounded with respect to center u (the starting one of the two points) or with respect to center $(u + v)/2$ (the midpoint of the segment between the two points).

Observation 3.1 *Let $P = (u = u_1, \ldots, u_\ell = v)$ be a path in the geometric graph $G = (V, E)$ such that $|u - u_i| \leq c \cdot |u - v|$ for all $i = 1, \ldots, \ell$. Then $w := (u + v)/2$ satisfies by the triangle inequality*

$$|w - u_i| \quad = \quad |u - u_i + (v - u)/2| \quad \leq \quad |u - u_i| + |v - u|/2 \quad \leq \quad (c + \tfrac{1}{2}) \cdot |u - v| \ .$$

Conversely if P has $|w - u_i| \leq c \cdot |u - v|$ for all i, then

$$|u - u_i| \quad = \quad |w - u_i + (u - v)/2| \quad \leq \quad |w - u_i| + |u - v|/2 \quad \leq \quad (c + \tfrac{1}{2}) \cdot |u - v| \ .$$

3.2 Spanners versus Power Spanners

The first result of this section shows that, for $\delta > 1$, every c-spanner is also a (c^δ, δ)-power spanner.

Theorem 3.2 *For $\delta > 1$, every c-spanner is also a (c^δ, δ)-power spanner.*

Proof: Let $G = (V, E)$ be a c-spanner, $u, v \in V$, and $P_{\texttt{OPT}} = (u = u_1, u_2, \ldots, u_\ell = v)$ be an optimal path from u to v concerning the δ-cost (not necessarily in G). Since G is a c-spanner, for each edge (u_i, u_{i+1}) on the path $P_{\texttt{OPT}}$, there is a path $P_i = (u_i = w_1, w_2, \ldots, w_{\ell_i} = u_{i+1})$ in G with $||P_i|| = \sum_{j=1}^{\ell_i - 1} |w_j - w_{j+1}| \leq c \cdot |u_i - u_{i+1}|$. Now let P be the concatenation of all these paths P_i for $i = 1, \ldots, \ell - 1$, then we get a path P from u to v in G with:

$$||P||^\delta = \sum_{i=1}^{\ell-1} ||P_i||^\delta \leq \sum_{i=1}^{\ell-1} (c \cdot |u_i - u_{i+1}|)^\delta = c^\delta \cdot \sum_{i=1}^{\ell-1} (|u_i - u_{i+1}|)^\delta = c^\delta \cdot ||P_{\texttt{OPT}}||^\delta$$

■

However, conversely, for any $\delta > 1$, there are (c, δ)-power spanners which are not C-spanners for any fixed C: this follows from Theorem 3.3 presented below, in Section 3.3, as any C-spanner is a weak C-spanner as well.

3.3 Weak Spanners versus Power Spanners

Now we turn to the main contribution of this chapter and present our results concerning the relation between weak spanners and power spanners. Surprisingly, it turns out that any weak c-spanner is also a C-power spanner for some C depending only on c. But first observe that the converse is not true, in general:

Theorem 3.3 *In the plane and for any $\delta > 1$, there is a family of (c, δ)-power spanners which are not weak C-spanners for any fixed C.*

Proof: Let $V := \{u = v_1, \ldots, v_n = v\}$ be a set of n vertices placed on a circle scaled such that the Euclidean distance between u and v is 1 and $|v_i - v_{i+1}| = 1/i$ for all $i = 1, \ldots, n-1$. Now consider the graph $G = (V, E)$ with edges (v_i, v_{i+1}). First observe that G is a (c, δ)-power spanner with c independent of n. Indeed, its δ-power stretch factor is dominated by the δ-cost of the (unique) path P in G from u to v which amounts to

$$\|P\|^\delta \quad = \quad \sum_{i=1}^{n-1} (1/i)^\delta \quad \leq \quad \sum_{i=1}^{\infty} (1/i)^\delta \quad =: \quad c$$

a convergent series since $\delta > 1$. This is compared to the cost of the direct link from u to v of 1. On the other hand, the Euclidean length (the 1-cost) of the polygonal chain from u to v is given by the unbounded harmonic series $\sum_{i=1}^{n-1} (1/i) = \Theta(\log n)$. Therefore the radius of this polygonal chain also cannot be bounded by any C independent of n, either. ■

Subsequently, we show that, conversely, any weak c-spanner is a (C, δ)-power spanner for both $\delta > 2$ (Subsection 3.3.1) and $\delta = 2$ (Subsection 3.3.2) with C depending only on c and δ. A counter-example in Subsection 3.3.3 reveals that this, however, does not hold for $\delta < 2$. We extend our results in Section 3.5 to higher dimensions.

3.3.1 Weak Spanners are Power Spanners for $\delta > 2$

In this subsection, we show that any weak c-spanner is also a (C, δ)-power spanner for any $\delta > 2$ with C depending only on c and δ. By definition between vertices u, v, there exists a path P in G from u to v that remains within a disk around u of radius $c \cdot |u - v|$. However on the course of

this path, two of its vertices u' and v' might come very close so that P, considered as a subgraph of G, in general, is not a weak c-spanner. On the other hand, G being a weak c-spanner, there also exists a path P' of small radius between u' and v'. Based on such repeated applications of the weak spanner property, we first assert the existence of a path which, considered as a subgraph of G, is a weak $2c$-spanner.

Definition 3.1 *Let $G = (V, E)$ be a directed geometric graph and $e_1 := (u_1, v_1)$, $e_2 := (u_2, v_2)$ two of its edges. By their* distance *we mean the number*

$$\min\left\{|u_1 - u_2|, |v_1 - v_2|, |u_1 - v_2|, |v_1 - u_2|\right\} \ ,$$

that is, the Euclidean distance of the closest pair of their vertices (see Figure 3.3(b)).

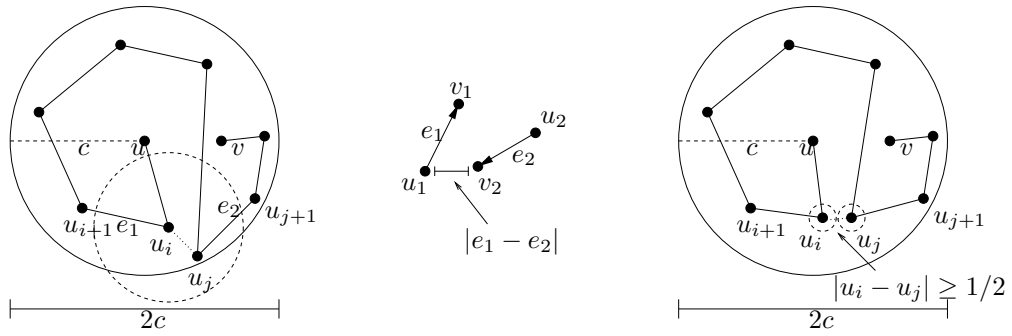

(a) Improving paths (b) Edge distance (c) Counting edges

Figure 3.3: Construction of a path with low power stretch factor in a weak spanner

Lemma 3.1 *Let $G = (V, E)$ be a weak c-spanner and $u, v \in V$. Then there is a path P from u to v in G which, as a subgraph of G, is a weak $2c$-spanner.*

Proof: We consider a path P from u to v in G that fulfills the weak spanner property and modify this path step by step until the required property is guaranteed. The idea is to locally replace each part of P connecting vertices u' and v' that violates the weak spanner property in $G(P)$ by a path from u' to v' in G. However for these iterated improvements to eventually terminate, we perform them in decreasing order of the lengths of the edges involved.

W.l.o.g. we assume $|u - v| = 1$. Since G is a weak c-spanner, there exists a path $P = (u = u_1, \ldots, u_\ell = v)$ from u to v in G that lies completely within a disk around u of radius c. In particular, any edge on this path has a length of at most $2c$, see Figure 3.3(a).

Now consider all edges on this path of length between c and $2c$. For any pair $e_1 = (u_i, u_{i+1})$ and $e_2 = (u_j, u_{j+1})$ with $j > i$ closer than $\frac{1}{2}$ (Definition 3.1), w.l.o.g. let u_i and u_j be the closest pair of their vertices, replace the path from u_i to u_j with a path according to the weak spanner property. This improvement is applied to vertices of distance at most $\frac{1}{2}$, so this sub-path remains within a disk of radius $c/2$; in particular, any edge introduced to P has length at most c and thus does not affect the edges of length between c and $2c$ currently considered. Moreover, after having

performed such improvements to all edges of length between c and $2c$, the modified path P has radius $c + c/2$, although it might now leave the disk around u of radius c.

Next, we apply the same process to edges of length between c and $c/2$ and perform improvements on those closer than $\frac{1}{4}$. The path P thus obtained remains within a disk of radius $c + c/2 + c/4$ while, for any pair of vertices u' and v' improved in the previous phase, the sub-path between them might increase in radius from $c \cdot |u' - v'|$ to at most $(c + c/2) \cdot |u' - v'|$.

As G is a finite graph, repeating this process for edges of length between $c/2$ and $c/4$ and so on, will eventually terminate and yield a path P from u to v remaining within a disk of radius $c + c/2 + c/4 + \ldots = 2c$. Moreover, for any pair of vertices u', v' in P, the sub-path between them has radius at most $(c + c/2 + c/4 + \ldots) \cdot |u' - v'|$ which proves that P is indeed a weak $2c$-spanner. ∎

Lemma 3.2 *Let $P = (u_1, \ldots, u_\ell)$ be a weak $2c$-spanner, $u_i \in \mathbb{R}^2$, $|u_1 - u_\ell| = 1$. Then P contains at most $(8c + 1)^2$ edges of length greater than c; more generally, P contains at most $(8c + 1)^2 \cdot 4^k$ edges of length greater than $c/2^k$.*

Proof: Consider two edges (u_i, u_{i+1}) and (u_j, u_{j+1}) on P both of length at least c with $j > i$. P being a weak $2c$-spanner implies that, between vertices u_i and u_j, the sub-path in P from u_i to u_j (which is unique and passes through u_{i+1}), satisfies $c \leq |u_i - u_{i+1}| \leq 2c \cdot |u_i - u_j|$; hence, $|u_i - u_j| \geq \frac{1}{2}$, see Figure 3.3(c). In particular, placing an Euclidean disk B_i of radius $\frac{1}{4}$ around each starting vertex u_i of an edge of length at least c results in these disks being mutually disjoint. If m denotes the number of edges of length at least c, these disks thus cover a total area of $m\pi(\frac{1}{4})^2$. On the other hand, as all u_i lie within a single disk around u_1 of radius $2c$, all disks B_i together cover an area of at most $\pi(2c + \frac{1}{4})^2$. Therefore,

$$m \quad \leq \quad \frac{\pi(2c + \frac{1}{4})^2}{\pi(\frac{1}{4})^2} \quad = \quad (8c + 1)^2 \, .$$

For edges (u_i, u_{i+1}) and (u_j, u_{j+1}) on P longer than $c/2^k$, one similarly obtains $|u_i - u_j| \geq 2^{-k-1}$ so that, here, Euclidean disks of radius 2^{-k-2} can be placed mutually disjoint within the total area of $\pi(2c + 2^{-k-2})^2$. ∎

Theorem 3.4 *Let $G = (V, E)$ be a weak c-spanner with $V \subseteq \mathbb{R}^2$. Then G is a (C, δ)-power spanner for $\delta > 2$ where $C := (8c + 1)^2 \cdot \dfrac{(2c)^\delta}{1 - 2^{2-\delta}}$.*

Proof: Fix $u, v \in V$, w.l.o.g. $|u - v| = 1$. In the following we analyze the δ-cost of the path P constructed in Lemma 3.1 for $\delta = 2 + \epsilon$. We consider all edges on this path and divide them into classes depending on their lengths. According to Lemma 3.2, there are at most $(8c + 1)^2$ edges of length between c and $2c$, each one inducing δ-cost at most $(2c)^\delta$. More generally, we have at most $(8c + 1)^2 \cdot 4^k$ edges of length between $c/2^k$ and $2c/2^k$ and the δ-cost of any such edge is at most $(2c/2^k)^\delta$. Summing up over all possible edges of P, thus yields a total δ-cost of P of at most

$$\|P\|^\delta \quad \leq \quad \sum_{k=0}^{\infty} (8c + 1)^2 \cdot 4^k \cdot \left(\frac{2c}{2^k}\right)^\delta \quad = \quad (8c + 1)^2 \cdot \frac{(2c)^\delta}{1 - 2^{2-\delta}}$$

∎

3.3.2 Weak Spanners are Power Spanners for $\delta = 2$

The preceding subsection showed that, for fixed $\delta > 2$, any weak c-spanner is also a (C, δ)-power spanner. The present subsection yields the same for $\delta = 2$, a case which, however, turns out to be much more involved. Moreover, our bounds on C in terms of c become slightly worse. In fact, the most significant result of this chapter is the following:

Theorem 3.5 *Let $G = (V, E)$ be a weak c-spanner with $V \subseteq \mathbb{R}^2$. Then G is a $(C, 2)$-power spanner for $C := \mathcal{O}(c^8)$.*

Proof: First recall that between vertices $u, v \in V$ there is a path P in G from u to v which remains inside a square of length $\ell := 2c \cdot |u - v|$ and center u. We denote such a square by $S_u(\ell)$. By s we denote the starting point of the path and by t the end (target) point. We denote by $V(P)$ the vertex set of a path and by $E(P)$ the edge set of a path.

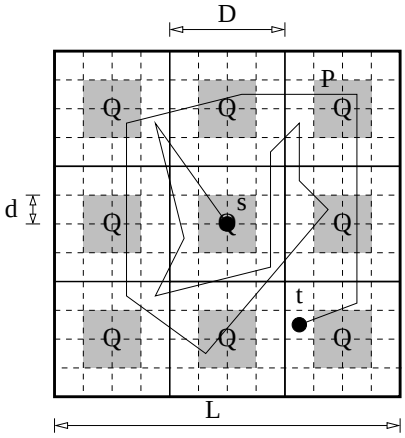

Figure 3.4: Idea and most important parameters for the proof of Theorem 3.5

We give a constructive proof of the Theorem, i.e. given a path in G obeying the weak spanner property we construct a path which obeys the $\big(\mathcal{O}(c^8), 2\big)$-power spanner property. For this we iteratively apply a procedure called **clean-up** to a path, yielding paths with smaller and smaller costs. Besides the path P in G this procedure has parameters $L, d, D \in \mathbb{R}^+$. Hereby, L denotes the edge length of a square with central point s containing the whole path. The parameters d, D are in the range $0 < 3(2c\sqrt{5}+2)d \leq D \leq L$ and can be chosen arbitrarily, yet fulfilling $D/d \in \mathbb{N}$ and $L/D \in \mathbb{N}$. These parameters define two edge-parallel grids G_d and G_D of grid size d and D such that boundaries of G_D are also edges of G_d. These grids fill out the square $S_u(L)$, while the boundary edge of $S_u(L)$ coincides with the boundary of G_d and G_D, see Figure 3.4. The outcome of the procedure **clean-up** is a path $P' = \text{clean-up}(P, L, d, D)$ which reduces the cost of the path while obeying other constraints, as we show shortly.

In Figure 3.6 we describe the procedure **clean-up** which uses the procedure **contract** described in Figure 3.5. Let $D(A)$ denote the diameter of the area A.

Lemma 3.3 *Let $P = (v_1, \ldots, v_m)$ and $P' =$ **contract**$(P, A) = (v_1, \ldots, v_{i-1}, v_i = w_1, \ldots, w_k = v_j, v_{j+1}, \ldots, v_m)$. Then the following properties are satisfied.*

Procedure contract $(P = (v_1, \ldots, v_m) : \text{path}, A : \text{area})$
begin
Let v_i be the first vertex of P in A
Let v_j be the last vertex of P in A
Let $P' = (w_1, \ldots, w_k)$ be a path between $v_i = w_1$ and $v_j = w_k$ satisfying the weak spanner property
return $(v_1, \ldots, v_{i-1}, w_1, \ldots, w_k, v_{j+1}, \ldots, v_m)$
end

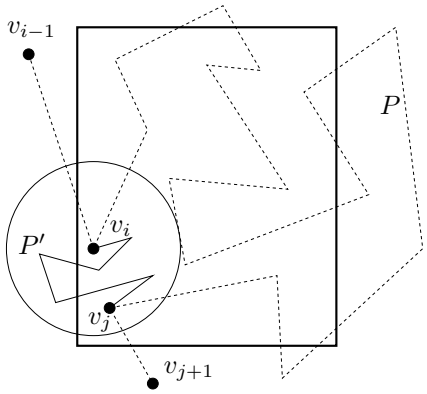

Figure 3.5: The **contract** procedure

- *Locality:* $\forall u \in \{w_1, \ldots, w_k\}$*:* $\min_{p \in A} |u - p| \leq c \cdot D(A)$ *and* $\max_{p \in A} |u - p| \leq (c+1) \cdot D(A)$.
- *Continuity of long edges:* $\forall e \in E(P') : |e| > 2c \cdot D(A) \Longrightarrow e \in E(P)$.

Proof: The maximum distance between v_i and v_j is at most $D(A)$. The replacement path $(w_1, \ldots, w_k)$ is inside a disk of radius $c \cdot D(A)$. Hence for all vertices u of this replacement path we have $|u - v_i| \leq cD(A)$ and therefore $\min_{p \in A} |u - p| \leq |u - v_i| \leq cD(A)$. From the triangle inequality it follows

$$\max_{p \in A} |u - p| \leq D(A) + \min_{p \in A} |u - p| \leq D(A) + cD(A) = (c+1)D(A) \; .$$

The second property follows from the fact that all new edges inserted in P' lie inside a disk of radius $cD(A)$. ■

Lemma 3.4 *For $D \geq 3(2c\sqrt{5}+2)d$ the procedure $P' =$***clean-up***(P, L, d, D) satisfies the four properties power efficiency, locality, empty space, and continuity of long edges.*

1. **Locality** *For all vertices $u \in V(P')$ there exists $v \in V(P)$ such that*

$$|u - v| \;\leq\; (\sqrt{2} + \sqrt{5}) \cdot c \cdot d \; .$$

2. **Continuity of long edges** *For all edges $e \in E(P')$ with $|e| > 2c\sqrt{5}d$ it holds $e \in E(P)$.*

3. **Power efficiency** *For all $k > 2c\sqrt{5}$:*

$$\sum_{e \in E(P') : 2c\sqrt{5}d < |e| \leq kd} |e|^2 \;\leq\; k^2 \, d^2 \, \#F(P, G_d) \; ,$$

where $\#F(P, G_d)$ denotes the number of grid cells of G_d where at least one vertex of P lies which is the end point of an edge of length at least $2c\sqrt{5}d$.

4. **Empty space** *For all grid cells C of G_D we have at least one G_d-sub-cell within C without a vertex of P'.*

Proof: All cells of G_d are called sub-cells in this proof for distinguishing them from the cells of G_D

Procedure clean-up (P, L, d, D)
begin
while three edges exist in P longer than $2c\sqrt{2}d$ starting or ending in the same cell of G_d
do
Let C be such a cell in G_d
$P \leftarrow$ **contract**(P, C)
od
while there exists a cell in G_D where at least one vertex of P is in each of its G_d-sub-cells
do
Let C be such a cell of G_D
Let $\text{rank}_P(u)$ be the position of a vertex u in P
Sort all cells $Z_1, \ldots, Z_{(D/d)^2}$ of G_d in C according to $\min_{u \in Z_i \cap V(P)}\{\text{rank}_P(u)\}$
Sort all cells $Z'_1, \ldots, Z'_{(D/d)^2}$ of G_d in C according to $\max_{u \in Z'_i \cap V(P)}\{\text{rank}_P(u)\}$
$i \leftarrow 1$
while cell Z_i is **neither** horizontally neighboring to one of the cells $\{Z'_1, \ldots, Z'_i\}$
nor cell Z'_i is horizontally neighboring to one of the cells $\{Z_1, \ldots, Z_i\}$
do
$i \leftarrow i + 1$
od
Let z and z' be the two neighboring cells from $\{Z_1, \ldots, Z_i\}$ and $\{Z'_1, \ldots, Z'_i\}$
$P \leftarrow$ **contract**$(P, z \cup z')$
od
return P
end

Figure 3.6: The **clean-up** procedure

Observe that the **clean-up** procedure uses only contract-operations to change the path. As parameters for this procedure we use either a grid sub-cell C of edge length d and diameter $D(C) = \sqrt{2}d$ or two horizontally neighboring grid sub-cells Z and Z' with edge lengths d with diameter $D(Z \cup Z') = \sqrt{5}d$.

Further note that in the first loop each sub-cell C of the grid G_d will be treated by the contract-procedure once. The reason is that the contract procedures produce edges with lengths of at most $2c\sqrt{2}d$, while each sub-cell will lose all but two edges of P with minimum length greater than $2c\sqrt{2}d$. This also proves that the first loop always halts.

Now consider the second while-loop and concentrate on the part inside the loop before the contract-operation takes place. Since in every sub-cell of C we have a vertex of P we can

compute the ordering Z_i and Z_i' as described by the algorithm. The main observation is that until the first two neighboring sub-cells Z and Z' from these sets are found, no two sub-cells Z and Z' from $Z \in \{Z_j\}_{j\leq i}$ and $Z' \in \{Z_j'\}_{j\leq i}$ are horizontally neighboring. Considering only points of P lying in these sub-cells implies that there is at least one empty sub-cell in C.

The situation changes slightly if we apply the contract-operation. Then an intermediate path will be added and possibly some of the empty sub-cells will start to contain vertices of the path. However, only sub-cells in a Euclidean distance of $c\sqrt{5}d$ from sub-cells Z and Z' are affected by this operation. Now consider a square Q (see Figure 3.4) of $(2c\sqrt{5}+2)d \times (2c\sqrt{5}+2)d$ sub-cells in the middle of C. Then at least two horizontally neighboring sub-cells will not be influenced by this contract-operation and thus remain empty.

One cannot completely neglect the influence of this operation to a neighboring grid cell of C. However, since $D \geq 3(2c\sqrt{5}+2)d$ the inner square Q is not affected by contract-operation in neighboring grid cells of C because of the locality of the contract-operation.

This means if a cell C was object to the second while-loop, then an empty sub-cell will be produced which remains empty for the rest of the procedure. Hence, the second loop also terminates. We now check the four required properties.

Locality. After the first loop the locality is satisfied even within a distance of $c\sqrt{2}d$. For this, observe that all treated cells contain end points of edges longer than $2c\sqrt{2}d$ which cannot be produced by contract-operations in this loop. Hence, if a cell is object to the contract-operation it was occupied by a vertex of P from the beginning. Then from Lemma 3.3 it follows that for all new vertices on the path P there exists at least one old vertex in distance $c\sqrt{2}d$ after the first loop.

For the second loop we need to distinguish two cases. First, consider a cell C where in the inner square an empty sub-cell exists. In this case this cell will never be treated by this second loop. If new vertices are added to the path within this cell, then this will be caused by a contract-operation in a neighboring cell and will be considered in the second case.

Now consider all cells with preoccupied inner squares (preoccupation refers to the outcome of the first loop). These cells can be object to contract-operations of the second loop. However, they will add only vertices to their own sub-cells or to the outer sub-cells of neighboring cells. So, new vertices are added within a distance of $c\sqrt{5}d$ of vertices in the path at the beginning of the second loop. As we have seen above every such vertex is only $c\sqrt{2}d$ away from an original vertex of a path. This gives a locality of distance $(\sqrt{2}+\sqrt{5})cd$.

Continuity of long edges. Since the parametrized areas for the contract operation have a maximum diameter of $\sqrt{5}d$ this property follows directly from Lemma 3.3.

Power efficiency. After the first loop the number of edges longer than $2c\sqrt{2}d$ is bounded by $\#F(P, G_d)$, because in every occupied sub-cell at most two edges start or end and each edge has two end points. Clearly, this number is an upper bound for edges longer than $2c\sqrt{5}d$. In the second loop no edges longer than $2c\sqrt{5}d$ will be added. This directly implies the wanted bound.

Empty space. As we have already pointed out the second loop always halts. Therefore the empty space property holds. ∎

Lemma 3.5 *Given a path P_1 with source s and target t such that $\forall u \in V(P_1) : |u-s| \leq L$, where $L = c \cdot |s-t|$. Iteratively apply $P_{i+1} =$ clean-up(P_i, L_i, d_i, D_i) for $i = 1, 2, \ldots$*

where $L_i = \sum_{j=1}^{i} D_j, D_i = L\beta^{1-i}$, $d_i = L\beta^{-i}$ *for* $\beta = 3(2c\sqrt{5}+2)$. *Then* P_m *for* $m = \max\{1, \lceil \log_{\beta^{-1}}(\min_{u,v\in V} |u-v|)/L \rceil\}$ *is a path connecting* s *to* t *obeying the* $\big(\mathcal{O}(c^8), 2\big)$*-power spanner property.*

Proof: For this proof we make use of the four properties of the clean-up procedure. First note that the square of edge length L_i containing all vertices of path P_i can increase (see Figure 3.7). However we can bound this effect by the locality property, giving $L_{i+1} \leq L_i + 2(\sqrt{2}+\sqrt{5})cd_i$, where $d_i = L \cdot \beta^{-i}$. Since, $2(\sqrt{2}+\sqrt{5})c \leq 8c \leq 6c\sqrt{5}+6 = \beta$ for $c \geq 1$, we get $L_{i+1} \leq L_i + D_i$. Hence, our choice of L_i fulfills the requirements and we get an upper bound of $L_i = L_{i-1} + D_{i-1} \leq L + \sum_{j=2}^{\infty} D_j \leq 2L$ for all $i > 1$.

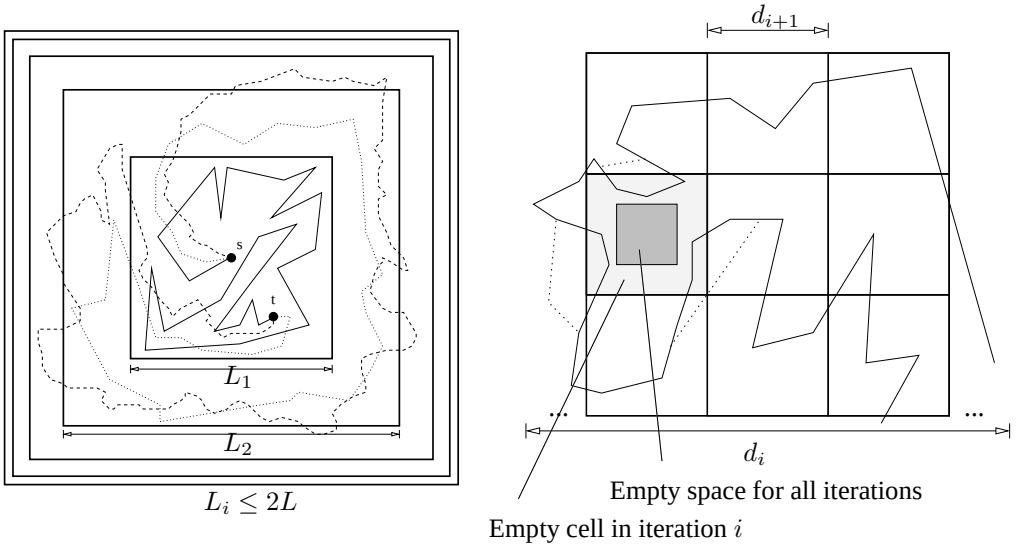

Figure 3.7: Increase in path and lower bound for empty space

Let $F_i = \#F(P_i, G_{d_i})$. Then $A_i = (d_i)^2 F_i$ denotes the area of all grid cells in G_{d_i} with a vertex of the path P_i which is the end point of an edge with length of at least $2c\sqrt{5}d_i$. In the next iteration near the middle in each of these cells an empty space will be generated with an area of $(d_{i+1})^2$ (see Figure 3.7). Because of the locality property at most the following term of the side length of this area is subtracted

$$\sum_{j=i+2}^{\infty} (\sqrt{2}+\sqrt{5})cd_j \leq \sum_{j=i+2}^{\infty} \frac{\beta(\sqrt{2}+\sqrt{5})cd_j}{\beta} < \frac{1}{3}\sum_{j=i+2}^{\infty} d_{j-1} \leq \frac{1}{3}\sum_{j=i+1}^{\infty} d_j \leq \frac{1}{3}d_{i+1}\ .$$

Hence, an empty area of at least $\frac{1}{9}(d_{i+1}^2)$ remains after applying all clean-up procedures. Let E_i be the sum of all these areas in this iteration, then $E_i \geq F_i \cdot (\frac{1}{9}) \cdot (d_{i+1})^2 = F_i \cdot (\frac{1}{9}) \cdot (d_i)^2 \cdot \frac{1}{\beta^2}$. Therefore we have $A_i \leq 9\beta^2 E_i$. Clearly, these empty areas in this iteration do not intersect with empty areas in other iterations (since they arise in areas which were not emptied before). Therefore all these spaces are inside the all-covering square of side length $2L$ yielding $\sum_{i=1}^{\infty} E_i \leq 4L^2$.

Because of the long edge continuity property, edges of minimum length $2c\sqrt{5}d_i$ do not appear in rounds later than i. Therefore, the following sum S gives an upper bound on the power of the constructed path.

$$S = \sum_{i=1}^{\infty} \sum_{\substack{e \in E(P_i): \\ 2c\sqrt{5}d_i \leq |e| < 2c\sqrt{5}\beta d_i}} |e|^2 .$$

Now from the power efficiency property it follows

$$\begin{aligned} S &\leq \sum_{i=1}^{\infty} 20c^2\beta^2 (d_i)^2 \#F(P_i, G_{d_i}) = 20c^2\beta^2 \sum_{i=1}^{\infty} (d_i)^2 F_i = 20c^2\beta^2 \sum_{i=1}^{\infty} A_i \\ &\leq 180c^2\beta^4 \sum_{i=1}^{\infty} E_i \leq 720\, c^2\beta^4 L^2 \leq 720\, c^4\beta^4 (|s-t|)^2 = \mathcal{O}(c^8(|s-t|)^2) . \end{aligned}$$

This lemma completes the proof of the theorem. ■ ■

3.3.3 Weak Spanners are not always Power Spanners for $\delta < 2$

In this subsection we show that there exist weak c-spanners that are not (C, δ)-power spanners for any constant C and $\delta < 2$. We introduce a new fractal curve that is similar to the HILBERT Curve (see Figure 3.9) to prove this claim.

Theorem 3.6 *To any $\delta < 2$, there exists a family of geometric graphs $\mathcal{G} = (V, E)$ with $V \subseteq \mathbb{R}^2$ which are weak c-spanners for a constant c but not (C, δ)-power spanners for any fixed C.*

Proof: As $\delta < 2$, there is a $k \in \mathbb{R}$ such that $2 < k < 4^{1/\delta}$. We present a recursive construction (see Figure 3.8). Fix $u^1 = (1/2, 1/2) \in \mathbb{R}^2$. In each following recursion step j, we replace every existing vertex $u^i = (u_x^i, u_y^i)$ by four new vertices $u^{4i-3} = (u_x^i - d, u_y^i + d)$, $u^{4i-2} = (u_x^i + d, u_y^i + d)$, $u^{4i-1} = (u_x^i + d, u_y^i - d)$, and $u^{4i} = (u_x^i - d, u_y^i - d)$ where $d := 1/(2k^j)$. Finally, we consider the graph $G_j := (V_j, E_j)$ with $V_j := \{u^i \mid i \in \{1, \ldots, 4^j\}\}$ and $E_j := \{(u^i, u^{i+1}) \mid i \in \{1, \ldots, 4^j - 1\}\}$. The resulting graph after 4 recursion steps with $k = 2.1$ is given in Figure 3.8(b). Let $u = u^1$ and $v = u^{4^j}$.

Lemma 3.6 *The graph G_j is a weak c-spanner for $c := \frac{\sqrt{2}k(k-1)}{k-2}$ independent of j.*

Proof: We prove the claim by induction over j. For $j = 1$ the weak stretch factor is dominated by the path between u and v. The distance between u and v is $1/k$. The farthest vertex on the path from u to v is u^3. It holds that $|u - u^3| \leq \sqrt{2}/k$. Hence, we get the weak stretch factor $\sqrt{2} \leq \frac{\sqrt{2}k(k-1)}{k-2} = c$. Now we consider G_j for any j. We can divide the graph G_j into four parts $G_j^1, \ldots, G_j^4$. By the definition of our recursive construction each part equals the graph G_{j-1}. For two vertices in one part the required weak c-spanner property holds by induction. We have to

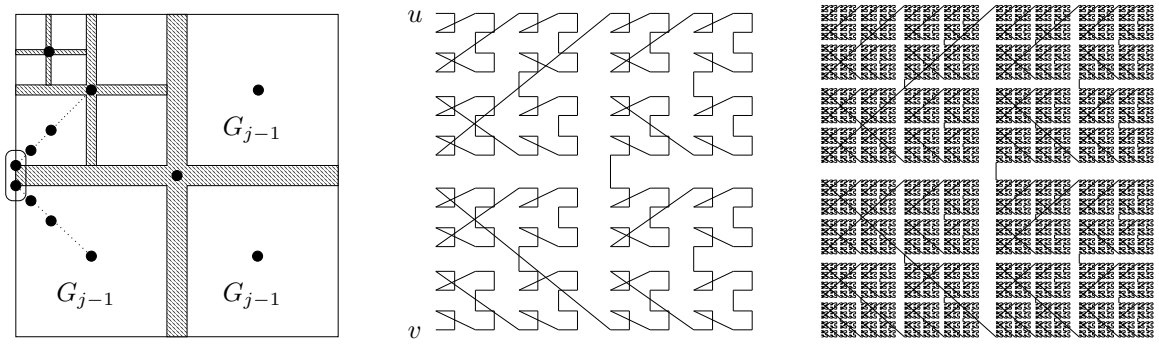

(a) Idea (b) After 4 steps (c) After 7 steps

Figure 3.8: Recursive construction: the underlying idea and two examples for $k = 2.1$

concentrate on two vertices which are chosen from two different parts. Since G_j^i is connected to G_j^{i+1} it is sufficient to consider a vertex from G_j^1 and a vertex from G_j^4. On the one hand, the weak stretch factor is affected by the shortest distance between such chosen vertices. On the other hand, this distance is given by (see also Figure 3.8(a))

$$\Big(\frac{1}{2}\cdot\big(1+\frac{1}{k}-\sum_{i=2}^{j}(\tfrac{1}{k})^i\big)-\frac{1}{2}\Big)\cdot 2=\frac{1}{k}-\sum_{i=2}^{j}(\tfrac{1}{k})^i\geq\frac{k-2}{k(k-1)}$$

The entire construction lies in a bounded square of side length 1, and hence we get a weak stretch factor of at most $\frac{\sqrt{2}k(k-1)}{k-2}=c$. ∎

Lemma 3.7 *The graphs G_j are not (C,δ)-power spanners for any fixed C.*

Proof: It suffices to consider the δ-cost of the path from u to v. The direct link from u to v has δ-cost at most 1. For any path P from u to v in G, it holds that

$$\|P\|^\delta \quad\geq\quad 3\cdot 4^j\cdot\big((\tfrac{1}{k})^j\big)^\delta \quad=\quad 3\cdot\left(\frac{4}{k^\delta}\right)^j$$

which goes to infinity if $j\to\infty$ for $k<4^{1/\delta}$. ∎

Combining Lemma 3.6 and Lemma 3.7 proves Theorem 3.6. ∎

3.3.4 Fractal Dimension

In this subsection we generalize the analysis used in Lemma 3.7. For this purpose we consider a self-similar polygonal fractal curve Γ as the result of repeated application of some generator K being a polygonal chain with starting point u and end point v. This is illustrated in Figure 3.2 showing a generator (left) and the resulting fractal curve (right part); see also [Tri95, Epp05]. But there are plenty of other examples: the KOCH Snowflake, SIERPINSKI's Arrowhead Curve

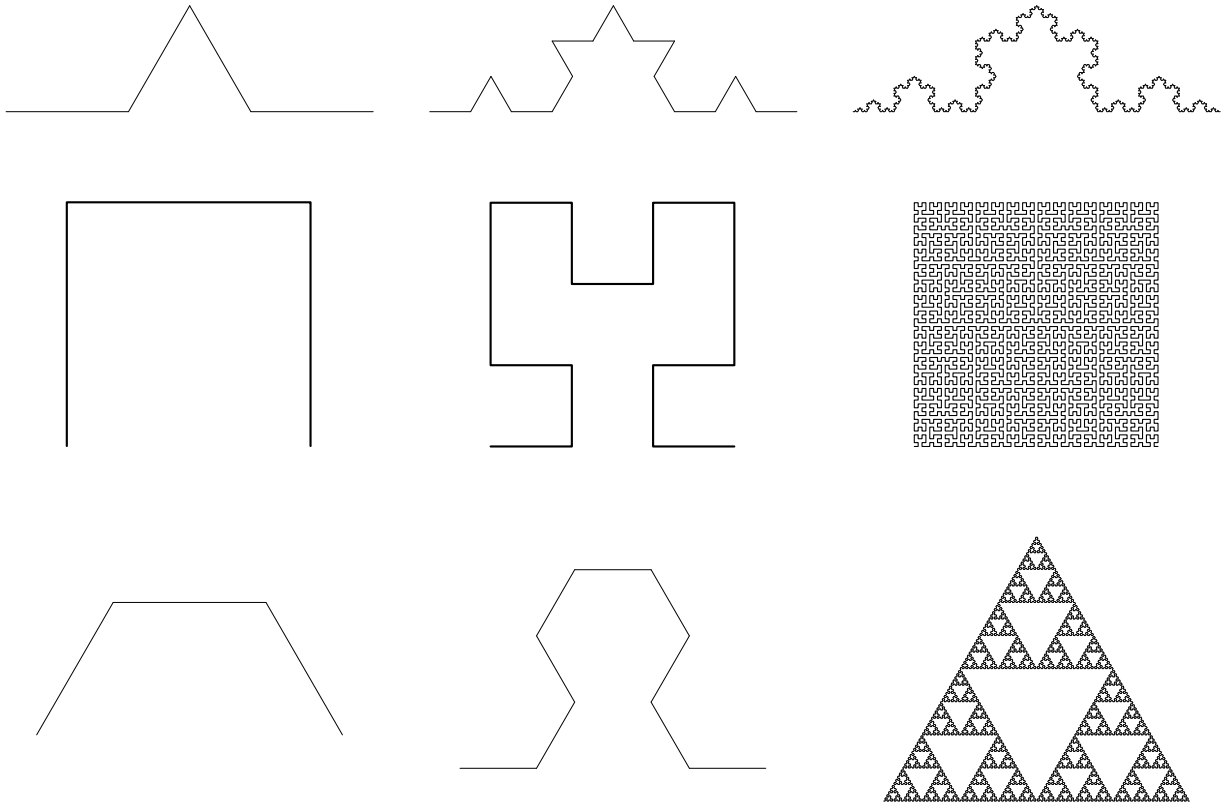

Figure 3.9: Three generators and the fractal curves they induce due to KOCH, HILBERT and SIERPINSKI

or the space filling HILBERT Curve (see Figure 3.9). Recall that the fractal dimension of Γ is defined as

$$\frac{\log(\text{number of self-similar pieces})}{\log(\text{magnification factor})}$$

Theorem 3.7 *Let K be a polygonal chain, Γ_n the result of n-fold application of K, and Γ the final self-similar polygonal fractal curve with dimension $\mathcal{D}_f$. Then, for all $\delta < \mathcal{D}_f$, there is no fixed C such that Γ_n is a (C, δ)-power spanner for all n.*

Proof: Let p denote the number of self-similar pieces in Γ_n and m the magnification factor. Then by definition, we have $\mathcal{D}_f = \log(p)/\log(m)$. Now consider the δ-cost of the (unique) path P in Γ_n from u to v. Since Γ_n is constructed recursively we get in the n-th step:

$$\|P\|^\delta \quad = \quad p^n \cdot \left(\left(\tfrac{1}{m}\right)^n\right)^\delta \quad = \quad \left(\frac{p}{m^\delta}\right)^n$$

Note that $\|P\|^\delta$ is unbounded iff $p/m^\delta > 1$, that is, iff $\delta < \log(p)/\log(m) = \mathcal{D}_f$. ∎

The fractal dimensions of KOCH's, SIERPINSKI's and HILBERT's Curves are well-known. Therefore by virtue of Theorem 3.7, the KOCH Curve is not a (c, δ)-power spanner for any c and $\delta < \log(4)/\log(3) \approx 1.26$; similarly, SIERPINSKI's Arrowhead Curve is not a (c, δ)-power

spanner for any c and $\delta < \log(3)/\log(2) \approx 1.58$; and HILBERT's Curve is not a (c,δ)-power spanner for any c and $\delta < 2$. One can show that KOCH's Curve is a weak spanner (the proof is analogously to Theorem 3.1). However, both SIERPINSKI's and HILBERT's Curves are not weak spanners as their inner vertices come arbitrarily close to each other. Further examples for self-similar polygonal curves can be found in [Tri95, Epp05].

3.4 Power Spanner Hierarchy

In the following we show that for $\Delta > \delta > 0$, a (c,δ)-power spanner is also a (C,Δ)-power spanner with C depending only on c and Δ/δ. Then we show that the converse is not true, in general, by presenting to each $\Delta > \delta > 0$ a family of graphs which are (c,Δ)-power spanners for some constant c but not (C,δ)-power spanners for any fixed C.

Theorem 3.8 *Let $G = (V,E)$ be a (c,δ)-power spanner with $V \subseteq \mathbb{R}^2$, $0 < \delta < \Delta$. Then G is also a (C,Δ)-power spanner for $C := c^{\Delta/\delta}$.*

Proof: Let $u, v \in V$ be two arbitrary vertices. Since G is a (c,δ)-power spanner there exists a path $P = (u = u_1, \ldots, u_\ell = v)$ with $\|P\|^\delta = \sum_{i=1}^{\ell-1} |u_i - u_{i+1}|^\delta \le c \cdot |u-v|^\delta$. The function $f(x) = x^{\Delta/\delta}$ is convex on $[0,\infty[$, hence we can apply JENSEN's inequality and get

$$\|P\|^\Delta = \sum_{i=1}^{\ell-1} |u_i - u_{i+1}|^\Delta = \sum_{i=1}^{\ell-1} \left(|u_i - u_{i+1}|^\delta\right)^{\Delta/\delta} \le \left(\sum_{i=1}^{\ell-1} |u_i - u_{i+1}|^\delta\right)^{\Delta/\delta} \le c^{\Delta/\delta} \cdot |u-v|^\Delta .$$

■

Theorem 3.9 *Let $0 < \delta < \Delta$. There is a family of geometric graphs which are (c,Δ)-power spanners but not (C,δ)-power spanners for any fixed C.*

Proof: We slightly modify the construction from the proof of Theorem 3.3 by placing n vertices $u = u_1, \ldots, u_n = v$ on an appropriately scaled circle such that the Euclidean distance between u and v is 1 and $|v_i - v_{i+1}| = (1/i)^{1/\delta}$ for all $i = 1, \ldots, n-1$. Now in the graph $G = (V,E)$ with edges (v_i, v_{i+1}), the unique path P from u to v has Δ-cost

$$\|P\|^\Delta \quad = \quad \sum_{i=1}^{n-1} (1/i)^{\Delta/\delta} \quad \le \quad \sum_{i=1}^{\infty} (1/i)^{\Delta/\delta} \quad =: \quad c$$

a convergent series since $\Delta/\delta > 1$. This has to be compared to the Δ-cost and/or to the δ-cost of the direct link from u to v which amount both to 1. On the other hand, the δ-cost of P is given by the harmonic series $\sum_{i=1}^{n-1} (1/i)^{\delta/\delta} = \Theta(\log n)$ and thus cannot be bounded by any constant C. ■

3.5 Higher-Dimensional Case

For simplicity, most results in this chapter have been formulated for the case of (not necessarily planar) geometric graphs in the plane. In this section, we show that our results will also hold in higher dimensions. The results of Section 3.1, Section 3.2 and Section 3.4 can be immediately applied to higher dimensions as well. The analysis of the relations concerning weak spanners requires an extended definition for higher dimensions. Now let $V \subseteq \mathbb{R}^{\mathcal{D}}$ for any constant $\mathcal{D}$. Mainly, we consider $\mathcal{D}$-dimensional spheres instead of disks. So, in a weak c-spanner, there is a path between any two vertices which remains within a ($\mathcal{D}$-dimensional) sphere of radius c-times the Euclidean distance between the vertices.

Corollary 3.1 *Let $G = (V, E)$ be a weak c-spanner with $V \subseteq \mathbb{R}^{\mathcal{D}}$. Then G is a (C, δ)-power spanner for $\delta > \mathcal{D}$ where $C := (8c+1)^{\mathcal{D}} \cdot \frac{(2c)^{\delta}}{1-2^{\mathcal{D}-\delta}}$*

Proof: Let $k_{\mathcal{D}} := \frac{\pi^{\mathcal{D}/2}}{(\mathcal{D}/2)!}$, then $k_{\mathcal{D}} r^{\mathcal{D}}$ is the volume of a $\mathcal{D}$-dimensional sphere of radius r. In the proofs of Lemma 3.1, Lemma 3.2 and Theorem 3.4 we replace disks by spheres and see that Lemma 3.1 still holds. In Lemma 3.2 we get the following new bound for the number m_k of edges of length between $c/2^k$ and $2c/2^k$:

$$m_k \leq \frac{k_{\mathcal{D}}(2c+\frac{1}{4})^{\mathcal{D}}}{k_{\mathcal{D}}(\frac{1}{4})^{\mathcal{D}}} \cdot \left(2^{\mathcal{D}}\right)^k = (8c+1)^{\mathcal{D}} \cdot (2^{\mathcal{D}})^k \, .$$

Applying the same facts given in Theorem 3.4 gives the upper bound for the δ-cost:

$$\|P\|^{\delta} \quad \leq \quad \sum_{k=0}^{\infty} (8c+1)^{\mathcal{D}} \cdot (2^{\mathcal{D}})^k \cdot \left(\frac{2c}{2^k}\right)^{\delta} \quad = \quad (8c+1)^{\mathcal{D}} \cdot \frac{(2c)^{\delta}}{1-2^{\mathcal{D}-\delta}}$$

■

Corollary 3.2 *Let $G = (V, E)$ be a weak c-spanner with $V \subseteq \mathbb{R}^{\mathcal{D}}$. Then G is a $(C, \mathcal{D})$-power spanner for $C := \mathcal{O}(c^{4\mathcal{D}})$.*

Proof: Now we extend the proof of Theorem 3.5 to the higher-dimensional case and replace disks by $\mathcal{D}$-dimensional spheres and, in addition, squares and cells by $\mathcal{D}$-dimensional cubes. Both, the **contract** and the **clean-up** procedure, remain unmodified. Remember that we have parameters $L, d, D \in \mathbb{R}^+$ fulfilling some requirements (see Theorem 3.5). It is easy to see that the parameters of the following four properties increase and depend on $\mathcal{D}$. At first, we must ensure that $D \geq 3(2c\sqrt{\mathcal{D}+3}+2)d$.

1. **Locality** For all vertices $u \in V(P')$ there exists $v \in V(P)$ such that

$$|u - v| \;\leq\; (\sqrt{\mathcal{D}} + \sqrt{\mathcal{D}+3}) \cdot c \cdot d \, .$$

2. **Continuity of long edges** For all edges $e \in E(P')$ with $|e| > 2c\sqrt{\mathcal{D}+3}d$ it holds $e \in E(P)$.

3. **Power efficiency** For all $k > 2c\sqrt{\mathcal{D}+3}$:

$$\sum_{e \in E(P'): 2c\sqrt{\mathcal{D}+3}d < |e| \leq kd} |e|^{\mathcal{D}} \;\leq\; k^{\mathcal{D}}\, d^{\mathcal{D}}\, \#F(P, G_d)\,,$$

where $\#F(P, G_d)$ denotes the number of grid cubes of G_d where at least one vertex of P lies which is the end point of an edge of minimum length $2c\sqrt{\mathcal{D}+3}d$.

4. **Empty space** For all grid cubes C of G_D we have at least one sub-cube of G_D within C without a vertex of P'.

Next we apply Lemma 3.5 with $\beta = 3(2c\sqrt{\mathcal{D}+3}+2)$ and get the following sum S as an upper bound on the power of the constructed path.

$$S = \sum_{i=1}^{\infty} \sum_{\substack{e \in E(P_i): \\ 2c\sqrt{\mathcal{D}+3}d_i \leq |e| < 2c\sqrt{\mathcal{D}+3}\beta d_i}} |e|^{\mathcal{D}}\,.$$

Again from the power efficiency property it follows ($E_i \geq F_i \cdot (\frac{1}{3})^{\mathcal{D}} \cdot (\frac{1}{\beta})^{\mathcal{D}}$)

$$\begin{aligned}
S \quad &\leq \quad \sum_{i=1}^{\infty} 2^{\mathcal{D}} c^{\mathcal{D}} (\mathcal{D}+3)^{\mathcal{D}/2} \beta^{\mathcal{D}} (d_i)^{\mathcal{D}} \#F(P_i, G_{d_i}) \\
&= \quad 2^{\mathcal{D}} c^{\mathcal{D}} (\mathcal{D}+3)^{\mathcal{D}/2} \beta^{\mathcal{D}} \sum_{i=1}^{\infty} (d_i)^{\mathcal{D}} F_i \quad = \quad 2^{\mathcal{D}} c^{\mathcal{D}} (\mathcal{D}+3)^{\mathcal{D}/2} \beta^{\mathcal{D}} \sum_{i=1}^{\infty} V_i \\
&\leq \quad 2^{\mathcal{D}} 3^{\mathcal{D}} c^{\mathcal{D}} (\mathcal{D}+3)^{\mathcal{D}/2} \beta^{2\mathcal{D}} \sum_{i=1}^{\infty} E_i \quad \leq \quad 2^{\mathcal{D}} 3^{\mathcal{D}} c^{\mathcal{D}} (\mathcal{D}+3)^{\mathcal{D}/2} \beta^{2\mathcal{D}} L^{\mathcal{D}} \\
&\leq \quad 2^{\mathcal{D}} 3^{\mathcal{D}} c^{2\mathcal{D}} (\mathcal{D}+3)^{\mathcal{D}/2} \beta^{2\mathcal{D}} (|s-t|)^{\mathcal{D}} \quad = \quad \mathcal{O}(c^{4\mathcal{D}} (|s-t|)^{\mathcal{D}})
\end{aligned}$$

■

Finally, we can also show that a weak spanner is not a power spanner for $\delta < \mathcal{D}$. We extend our recursive construction to the higher dimensional case.

Corollary 3.3 *To any $\delta < \mathcal{D}$, there exists a family of geometric graphs $\mathcal{G} = (V, E)$ with $V \subseteq \mathbb{R}^{\mathcal{D}}$ which are weak c-spanners for a constant c but not (C, δ)-power spanners for any fixed C.*

Proof: We choose similar parameters as in the proof of Theorem 3.6. The extension is that our recursive construction now grows in $\mathcal{D}$ dimensions in the same way as given in the proof for two dimensions. An example of the resulting graph in three dimensions is given in Figure 3.10.

The first corollary is that the resulting graph G_j is a weak c-spanner for $c := \frac{\sqrt{\mathcal{D}}k(k-1)}{k-2}$ independent of j. The second is that there exists a path which has δ-cost of at least

$$(2^{\mathcal{D}}-1) \cdot (2^{\mathcal{D}})^j \cdot \left((\tfrac{1}{k})^j\right)^{\delta} \quad = \quad (2^{\mathcal{D}}-1) \cdot \left(\frac{2^{\mathcal{D}}}{k^{\delta}}\right)^j$$

which goes to infinity if $j \to \infty$ for $k < 2^{\mathcal{D}/\delta}$. ■

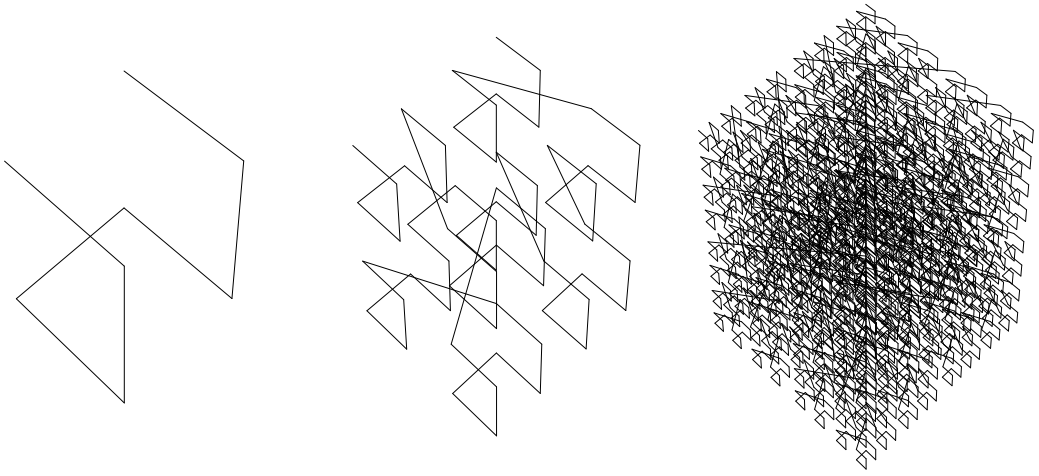

Figure 3.10: Our recursive construction in three dimensions for $k = 2.1$

3.6 Conclusions

In this chapter we investigated the relations between spanners, weak spanners, and power spanners for $V \subseteq \mathbb{R}^{\mathcal{D}}$ for any constant $\mathcal{D}$. The results are summarized in Table 3.1. An entry in the table should be read from left to right downwards, e.g., every c-spanner is a (c^{δ}, δ)-power spanner). For $\delta \geq \mathcal{D}$ it turns out that being a spanner is the strongest property, followed by being a weak spanner and finally being a (c, δ)-power spanner. For $1 < \delta < \mathcal{D}$, spanner is still strongest whereas weak spanner and (c, δ)-power spanner are not related to each other. For $0 < \delta < 1$ finally, (c, δ)-power spanners are both spanners and weak spanners. All stretch factors in these relations are constant and are pairwise polynomially bounded.

c-**spanner**	c	c	(c^{δ}, δ)
weak c-**spanner**	(unbounded)	c	$\Big(\mathcal{O}\big(c^{2\mathcal{D}+\epsilon}/(1-2^{-\epsilon})\big), \mathcal{D}+\epsilon\Big)$ $\big(\mathcal{O}(c^{4\mathcal{D}}), \mathcal{D}\big)$ $\big(\text{unbounded}, \mathcal{D}-\epsilon\big)$
(c, δ)-**power spanner**	(unbounded)	(unbounded)	for $\Delta > \delta$: $(c^{\Delta/\delta}, \Delta)$ for $\Delta < \delta$: (unbounded, Δ)
$\Rightarrow$	**-spanner**	**-weak spanner**	**-power spanner**

Table 3.1: Our results on the relations between spanners, weak spanners and power spanners

Although our results are exhaustive with respect to the different kinds of geometric graphs and in terms of δ, one might wonder about the optimality of the bounds obtained for C's dependence on c; for instance: any c-spanner is a (C, δ)-power spanner for $C = c^{\delta}$, $\delta > 1$; and

this bound is optimal. But is there some $C = o(c^{2\mathcal{D}})$ such that any weak c-spanner is a (C, δ)-power spanner as long as $\delta > \mathcal{D}$? Is there some $C = o(c^{4\mathcal{D}})$ such that any weak c-spanner is a (C, δ)-power spanner ?

Chapter 4

Static and Dynamic Ad Hoc Networks

In this chapter we investigate static and dynamic ad hoc networks and present solutions concerning the problem of point-to-point communication for a set of n radio stations. We concentrate on single frequency *power-variable* ad hoc networks, i.e. networks in which every station is allowed to adjust its transmission range to decrease energy consumption and to avoid interference. Furthermore, we distinguish between omnidirectional (radio, Section 4.1) and directional (beam radio or infrared, Section 4.2) communication. In both communication models we first investigate static vertex sets, before we extend our considerations to dynamic vertex sets.

A main result of Section 4.1 is that every weak c-spanner allows us to approximate an energy-optimal path system by a constant factor and a congestion-optimal path system by a factor of $\mathcal{O}(g(V))$ where $g(V)$ denotes the diversity of a vertex set $V \subseteq \mathbb{R}^{\mathcal{D}}$ for any constant $\mathcal{D}$. In real-world applications, the diversity can be regarded as $\Theta(\log n)$. In general, the diversity can only be upper bounded by $\mathcal{O}(n)$. We introduce the Hierarchical Layer Graph (HL-graph) and show that this graph is a c-spanner for a constant c. For the HL-graph, the (bidirectional) interference number, which we define as a measure for the amount of interference, can be upper bounded by $\mathcal{O}(g(V))$. Hence, the HL-graph allows us an $\mathcal{O}((\log n)^2)$ approximation of a congestion optimal path system in real-world applications. Furthermore, we investigate trade-offs and show that it is not possible to optimize more than one measure at the same time, in general. The relation between congestion and energy is even worse.

In Section 4.2 we show that we can construct better topologies using the directional communication model than using the omnidirectional one. We introduce the unidirectional interference number and present a sectorized, theoretically interference-free topology, the so-called sparsified Yao-graph (SparsY-graph), which allows us to approximate an energy-optimal path system by a constant factor and a congestion-optimal path system by a factor of $\mathcal{O}(g(V))$, i.e. by $\mathcal{O}(\log n)$ in realistic settings. A main result is that we prove that the SparsY-graph is a weak c-spanner for a constant c. Hence, we can apply our results of Chapter 3 to show that the SparsY-graph is a C-power spanner for some constant C depending only on c. We compare the SparsY-graph with other sectorized topologies, known as the Yao-graph and the SymmY-graph, and investigate degree and spanner properties as well as communication features with regard to interference. In general, we show that the SymmY-graph is neither a weak spanner nor a power spanner, but nevertheless it is connected. Note that some of these results require an appropriate number of

sectors/senders per node. But most of our results hold already if this number is greater than 6.

In Section 4.3 we discuss the handling of interference in a distributed wireless setting and, finally, in Section 4.4 we focus on the question how to maintain our basic network topologies under dynamic changes when stations appear and disappear, i.e. wireless devices enter and/or leave the network. For this we measure the number of radio stations involved and present distributed algorithms for repairing the network structure. We show that linear time algorithms are necessary in the worst case to repair the Yao-graph and its variants when a station appears or disappears. In this case the number of involved stations can be linear in the number of nodes. For the HL-graph we present algorithms that need time linear in the diversity. Hence, under realistic placements, the HL-graph can be updated in logarithmic time.

In our proofs we make use of the results of the last chapter, Chapter 3. These results can be seen as the theoretical fundament on which the following investigations are based. In this chapter we develop and analyze wireless network topologies for static vertex sets. Results concerning mobile vertex sets are presented in Chapter 5. The outcome of our extensive experimental analyses can be found in Chapter 6.

4.1 Omnidirectional Communication

In this section we consider ad hoc networks based on omnidirectional communication. In such a *radio network*, every station is equipped with a power-variable omnidirectional antenna. Our assumption is that only one frequency can be used for wireless transmission. We investigate the problem of path selection in radio networks for a given static set of n nodes in two- and three-dimensional space. For static point-to-point communication, we define measures for congestion, dilation, and energy consumption that take interference among communication links into account. Furthermore, we introduce the (bidirectional) interference number and show that energy-optimal path selection for static ad hoc networks can be computed in polynomial time. Then we introduce the diversity $g(V)$ of a set $V \subseteq \mathbb{R}^{\mathcal{D}}$ for any constant $\mathcal{D}$. It can be used to upper bound the number of interfering edges. For real-world applications, it can be regarded as $\Theta(\log n)$. A main result is that a weak c-spanner construction as a communication network allows one to approximate the congestion-optimal path system by a factor of $\mathcal{O}(g(V)^2)$.

Furthermore, we show that there are vertex sets where only one of the performance parameters congestion, dilation, and energy can be optimized at a time. We show trade-offs lower bounding congestion $\times$ dilation and dilation $\times$ energy. The trade-off between congestion and dilation increases with switching from two-dimensional to three-dimensional space. For congestion and energy, the situation is even worse. It is only possible to find a reasonable approximation for either congestion or energy minimization, while the other parameter is at least a polynomial factor worse than in the optimal path system.

In Subsection 4.1.1 we introduce our model of radio networks, and define and motivate our notions of congestion, dilation, and energy. Then, in Subsection 4.1.2, we relate congestion and dilation to the routing time in radio networks and present upper and lower bounds for the routing time. In Subsection 4.1.3 and in Subsection 4.1.4, we present strategies for path selection that provably optimize energy consumption and give an $\mathcal{O}(g(V)^2)$-factor approximation of con-

gestion where $g(V)$ is defined as the diversity that describes the number of magnitudes of all node-to-node distances. Two distances d_1, d_2 are in the same magnitude if $\lfloor \log d_1 \rfloor = \lfloor \log d_2 \rfloor$. In Subsection 4.1.5, as a main insight, we can conclude that no two of these measures can be minimized simultaneously. Trade-offs between two measures are unavoidable.

4.1.1 Modeling Radio Networks

We consider a set $V \subseteq \mathbb{R}^{\mathcal{D}}$ of n radio stations (or vertices, or nodes) for $\mathcal{D} \in \{2, 3\}$. In order to transmit a message from a radio station u to a radio station v, u is able to adjust its *transmission radius* to $|u - v|$, the Euclidean distance between u and v (see Section 2.2). We say that u establishes the *communication link* $e = \{u, v\}$. Instead of sending the packet directly from u to v, multi-hop communication is also possible by using a path $(u = u_1, \ldots, u_\ell = v)$ of stations. In order to deliver a packet from u to v, the communication links $\{u_i, u_{i+1}\}$, $i = 1, \ldots, \ell - 1$, have to be established.

Consider now a *routing problem* $f : V \times V \to \mathbb{N}_0$, where $f(u, v)$ packets have to be sent from u to v, for all $u, v \in V$. A collection of paths, one for each packet, forms a *path system* $\mathcal{P}$ for f. In this section we assume (as in [MBH01]) that each transmission along a link $\{u_i, u_{i+1}\}$ has to be acknowledged, so that the communication from u_{i+1} to u_i also has to be established. Thus the edges of the paths have to be used in both directions. The undirected graph on V defined by the undirected edges of the paths in $\mathcal{P}$ is the *communication network* N defined by $\mathcal{P}$. In one *communication step* exactly one packet can be transmitted along an edge $e = \{u, v\} \in N$. The *routing time* of a network N defined by the path system $\mathcal{P}$ is the minimum number of communication steps that are necessary to guarantee that all packets defined by the routing problem have reached their destinations. We define the *dilation* of $\mathcal{P}$ analogously to its well-known definition in wired networks, see [Lei92], i.e. the dilation is the maximum of the lengths of all paths in $\mathcal{P}$. In order to define congestion, we have to look at the specific properties of radio networks. For wired networks, the *load* $\ell(e)$ of an edge $e = \{u, v\}$ of the communication network N is defined as the number of packets to be forwarded along e. This load is often called congestion of e in a wired network, see [Lei92]; we will use the notion "load" to distinguish it from our notion of congestion for radio networks, to be described below.

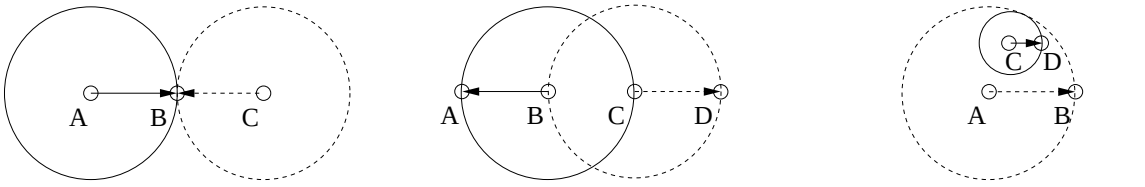

(a) Hidden terminals (b) Exposed terminals (c) Asymmetric interference

Figure 4.1: Interference problems in radio networks

A major problem in radio networks is the effect of interfering radio signals. If two nodes A and C are in range of a third listening node B, but cannot hear each other, a collision occurs at B if A and C transmit simultaneously. This is the *hidden terminal* problem [Bha98] (see

Figure 4.1(a)). Solutions exist that reduce this effect. In the IEEE 802.11 standard, see [IEE97], sender A and receiver C reserve the channel by sending request-to-send (RTS) and clear-to-send (CTS) packets prior to the data communication (similar to MACA and MACAW [Tan96]). Other nodes, also the nodes that cannot hear the sender, hear at least one of these packets and suspend all transmissions until the channel is free. However, this also reduces the network capacity since any node C that hears the CTS of B cannot start a transmission even if A is outside of C's range and thus no collision would occur. This is the *exposed terminal* problem [Bha98] (see Figure 4.1(b)). Since we allow each node to adjust its transmission power for sending data, a third interference problem can occur due to the fact that a short communication link between two nodes C and D cannot be heard by nodes A and B establishing a long communication link. This is the *asymmetric interference* problem (see Figure 4.1(c)).

In our radio model we allow the stations only one radio frequency. Now, if two packets are transmitted at the same time, we may experience a *radio interference*. Hence at a given time step only one or none packet can be received. The area covered by sending and acknowledging a packet from u to v along an edge $e = \{u, v\}$ is $D(e) := D_r(u) \cup D_r(v)$, where $D_r(u)$ denotes a disk with center u and radius $r := |e|$ (see Figure 4.2). Now, if another packet q has to be sent or received by a node within $D(e)$, the radio interference prevents the successful transmission of q. Since nodes adjust their transmission powers for sending packets, interference may not be symmetric.

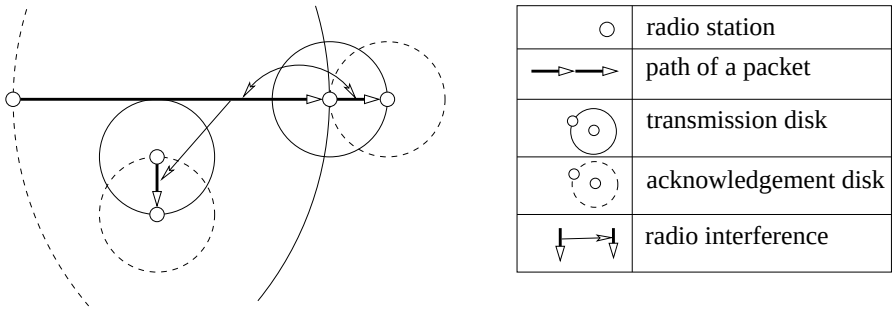

Figure 4.2: Stations, packet paths, and induced radio interference

As mentioned before, for radio networks we need to reflect the impact of radio interference on the delay of a packet. Therefore, we define the set of edges (bidirectionally) interfering with an edge $e = \{u, v\}$ of N as

$$\text{BInt}(e) := \{e' \in E(N) \setminus \{e\} \mid u \in D(e') \text{ or } v \in D(e')\} .$$

Thus, sending a packet along e is successful only if no other edges from $\text{BInt}(e)$ are sending concurrently. We define the *(bidirectional) interference number* of a communication link by $|\text{BInt}(e)|$. The *(bidirectional) interference number* of the network N is the maximum (bidirectional) interference number of all edges denoted by $\text{BInt}(N)$. Now we define the *congestion of the edge* e of $N = (V, E_{\mathcal{P}})$ defined by the path system $\mathcal{P}$ by

$$C_{\mathcal{P}}(e) := \ell(e) + \sum_{e' \in \text{BInt}(e)} \ell(e') .$$

The *congestion of the path system* $\mathcal{P}$ for V is defined by

$$C_{\mathcal{P}}(V) := \max_{e \in E_{\mathcal{P}}} \{C_{\mathcal{P}}(e)\} .$$

The variable choice of the transmission power allows us to reduce the energy consumption, saving on the tight resources of batteries in portable radio stations and reducing interference. The energy needed to send over a distance of d is given by d^2. It turns out that in practice the energy consumption goes up to $\mathcal{O}(d^6)$ or even $\mathcal{O}(d^8)$. However, all results besides Theorem 4.5 can be easily transferred to higher exponents.

We distinguish two energy models reflecting the power consumption by link maintenance and packet transmission. In the first model, called the *unit energy model*, we assume that maintaining a communication link e is proportional to $|e|^2$, where $|e|$ denotes its Euclidean length. We completely neglect any impact of power consumption by packet delivery. Therefore, the unit energy *U-Energy* used by radio network $N = (V, E_{\mathcal{P}})$ defined by the path system $\mathcal{P}$ is given by

$$\text{U-Energy}_{\mathcal{P}}(V) := \sum_{e \in E_{\mathcal{P}}} |e|^2 .$$

The *flow energy model* of a radio network $N = (V, E_{\mathcal{P}})$ defined by the path system $\mathcal{P}$ reflects the energy actually consumed by transmitting all packets of a routing problem f. We neglect any power consumption by link maintenance. Here, the power consumption of a communication link e is weighted by its load $\ell(e)$:

$$\text{F-Energy}_{\mathcal{P}}(V) := \sum_{e \in E_{\mathcal{P}}} \ell(e)|e|^2 .$$

We subdivide the design of a routing strategy for f into the following three steps:

- *Path selection*: select a path system $\mathcal{P}$ for f.
- *Interference handling*: design a strategy, that realizes the transmission of a packet along a link in the presence of interference.
- *Packet switching*: decide when and in which order packets are sent along a link.

4.1.2 Upper and Lower Bounds for Routing Time

It is easy to see, and is well known, that both the dilation and the maximum load $\max_{e \in E}\{\ell(e)\}$ lower bound the routing time, even in wired networks. In this subsection we show that the routing time in radio networks can also be lower bounded in terms of our extended notion of congestion (Theorem 4.1). We further present an upper bound for the routing time (Theorem 4.3).

Theorem 4.1 *Consider a radio network $N = (V, E_{\mathcal{P}})$ in $\mathcal{D}$-dimensional space for $\mathcal{D} \in \{2, 3\}$ defined by the path system $\mathcal{P}$ for a routing problem f with congestion C and dilation D. Let T be its routing time. Then it holds for $c_2 = 6$ and $c_3 = 20$ that*

$$T \;\geq\; \max\left\{\frac{C}{2c_{\mathcal{D}}}, D\right\} = \Omega(C + D) .$$

Proof: Let $e = \{u, v\} \in N$ be an edge with maximum congestion C. Now we try to calculate the number of edges along which successful transmissions can take place simultaneously to e. We partition the $\mathcal{D}$-dimensional space into regions $R_1, \ldots, R_{c_\mathcal{D}}$ (see Figure 4.3).

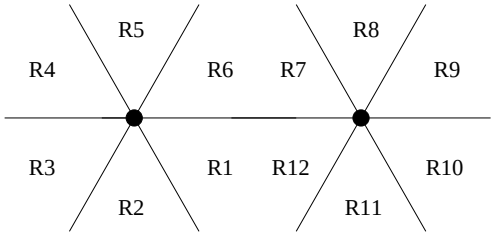

Figure 4.3: Partitioning the two-dimensional space into regions $R_1, \ldots, R_{12}$

The main property of these regions is that, for every pair of points $r, s \in R_i$ for all i, the angle between $\overline{ur}$ and $\overline{us}$ is less than or equal to $\frac{\pi}{3}$. Clearly, for two-dimensional space we have $c_2 = 6$. In [HSS97] it has been shown that $c_3 \leq 20$. Similarly we consider the analogous partitioning $R_{c_\mathcal{D}+1}, \ldots, R_{2c_\mathcal{D}}$ with v as the corner point of angles. Define

$$E_i := \{\{p, q\} \mid (p \in R_i \vee q \in R_i) \wedge \{p, q\} \in \text{BInt}(e)\} .$$

Note that by a straightforward geometric argument, for two edges $e', e'' \in E_i$, it holds that either $e' \in \text{BInt}(e'')$ or $e'' \in \text{BInt}(e')$. Therefore, all transmissions over edges in $E_i \cup \{e\}$ have to be done sequentially. Let $\ell_i := \ell(e) + \sum_{e' \in E_i} \ell(e')$. Then $\sum_{i=1}^{2c_\mathcal{D}} \ell_i \geq C$. Hence,

$$T \;\geq\; \max_{i \in [2c_\mathcal{D}]} \{\ell_i\} \;\geq\; \frac{1}{2c_\mathcal{D}} \sum_{i=1}^{2c_\mathcal{D}} \ell_i \;\geq\; \frac{C}{2c_\mathcal{D}} .$$

■

We now turn to upper bounding the routing time. Consider a communication network $N = (V, E_\mathcal{P})$ defined by the path system $\mathcal{P}$ with congestion $C_\mathcal{P}(V)$. Following the approach of local probabilistic control protocols for the MAC layer (also called *LPC schemes* , see [AS98]), we use the following protocol for handling interference. If u wants to send a packet (or an acknowledgement) along link e to v, u proceeds as follows. The link e is activated with probability $\varphi(e)$ and so, in each step, it decides with probability $\varphi(e)$ to send a packet. We choose $\varphi(e) := \min\{\frac{1}{2}, \frac{\ell(e)}{C_\mathcal{P}(V)}\}$. Then it holds that $\varphi(e) + \sum_{e' \in \text{BInt}(e)} \varphi(e') \leq 1$. We have the following for a transmission between two nodes:

Lemma 4.1 *The probability of a successful transmission on a link e is at least $\frac{1}{4}\varphi(e)$. Therefore, the expected time for a successful transmission is at most $\frac{4}{\varphi(e)}$. Furthermore, if u has decided to send a message to v, this transmission attempt has a success probability of at least $1/4$.*

Proof: Note that $1 - p \geq \frac{1}{4^p}$ for $p \in [0, \frac{1}{2}]$. Let BInt(e) be defined as $\{e_1, ..., e_m\}$. Then the following holds:

$$\begin{aligned} \text{Prob[Transmission on link } e \text{ is successful]} &= \varphi(e) \prod_{i=1}^{m} (1 - \varphi(e_i)) \\ &\geq \varphi(e) \prod_{i=1}^{m} 4^{-\varphi(e_i)} = \varphi(e) 4^{-\sum_{i=1}^{m} \varphi(e_i)} \geq \frac{1}{4}\varphi(e) \,. \end{aligned}$$

The bounds for the expected transmission time and the constant success probability follow directly. ∎

Definition 4.1 ([AS98], Definition 2.2) *Let the* probabilistic communication graph *(or PCG in short)* $G = (V, \tilde{\varphi})$ *be defined as a complete directed graph with node set* V *and edge labels determined by the function* $\tilde{\varphi} : V \times V \to [0, 1]$. *Every edge* e *can forward a packet in one time step, but only succeeds in doing this with probability* $\tilde{\varphi}(e)$.

The authors of [AS98] transform the problem of routing in wireless networks to routing in PCGs. Since we have a constant success probability, we can use the same technique to transform the problem of routing in our graphs to routing in PCGs.

We adopt the following result, but we need some other notation from [AS98]. Let the *maximum edge latency* $\tilde{L}$ of a PCG G be defined as the maximum expected time and the *minimum edge latency* $\tilde{l}$ as the minimum expected time needed to successfully transmit a packet along an edge in G. Note that our interference handling guarantees: $\tilde{L} \leq \infty$ and $\tilde{l} \geq 2$, since $1/2 \geq \varphi(e) \geq c$ for all $e \in E$ and a constant $c \in \mathbb{R}$. Given a collection $\mathcal{P}$ of simple paths in some PCG G, the *PCG-dilation* $\tilde{D}$ of $\mathcal{P}$ is defined as the maximum over all paths in $\mathcal{P}$ of the sum of $1/\tilde{\varphi}(e)$ over all edges e used by it (that is, $\tilde{D}$ denotes the maximum expected time a packet needs to traverse a path in $\mathcal{P}$), and the *PCG-congestion* $\tilde{C}$ of $\mathcal{P}$ is defined as the maximum over all edges e of $1/\tilde{\varphi}(e)$ times the number of paths in $\mathcal{P}$ that cross it (that is, $\tilde{C}$ denotes the maximum expected time spent at an edge e to forward all packets which contain e in their path). The size m of an arbitrary path collection is defined as the number of packets given by the routing problem.

Theorem 4.2 ([AS98], Theorem 2.12) *There is an online protocol for sending packets along an arbitrary path collection of size* m *with PCG-dilation* $\tilde{D}$*, PCG-congestion* $\tilde{C}$*, maximum edge latency* $\tilde{L}$*, and minimum edge latency* $\tilde{l}$ *in time* $\mathcal{O}(\tilde{C} + \tilde{D} \log(m \cdot \tilde{L}/\tilde{l}))$ *with probability at least* $1 - m^{-c}$ *for any constant* c.

Applying this to our model yields:

Theorem 4.3 *Consider a radio network* $N = (V, E_{\mathcal{P}})$ *defined by the path system* $\mathcal{P}$ *of size* m *for some routing problem* f *with maximum interference number* I*, congestion* C*, and dilation* D*. There is an online routing protocol that needs routing time* $\mathcal{O}(C + D \cdot I \cdot \log(m \cdot I))$*, with probability at least* $1 - m^{-c}$ *for any constant* c.

Proof: By definition we have that $1/\varphi(e) \leq I$ for all $e \in E$. This implies directly that $\tilde{D} \leq D \cdot I$ and by definition we have $\tilde{C} = C$. The maximum edge latency $\tilde{L}$ is given by $max_{e \in E}\{1/\varphi(e)\} = \mathcal{O}(I)$. The minimum edge latency $\tilde{l}$ is at least 2, by definition of $\varphi(e)$. Now we consider the PCG $G = (V, \varphi)$ and use Theorem 4.2 to complete the proof. ∎

4.1.3 Minimizing Energy

In this subsection we try to minimize unit energy and flow energy. We show that energy-optimal path selection for radio networks can be computed in polynomial time.

The unit energy of a radio network given by a path system is defined as the energy consumption necessary to deliver one packet on each communication link. It turns out that the paths of a minimum spanning tree (MST(V)) optimize unit energy, i.e., power consumption for maintaining links while neglecting all additional energy consumption for packet delivery. Note that the hardness results shown in [KKKP00, CPS04] do not apply because in our model the transmission radii are adjusted for each packet.

Theorem 4.4 *The unique paths defined by a minimum spanning tree result in an optimal path system for a radio network $N = (V, E), V \subseteq \mathbb{R}^{\mathcal{D}}$ for any $\mathcal{D}$, with respect to the unit energy.*

Proof: Consider the complete graph on V, where each edge e gets weight $|e|^2$. The minimum energy network can be constructed using Prim's or Kruskal's algorithm for minimum spanning tree. Note that the decisions in this algorithm are based on comparison of the length of some edges e and e', i.e. $|e| \leq |e'|$. Thus, the minimal network for energy is also the minimum spanning tree for Euclidean distances. ■

For the flow energy model, the best network is not necessarily a tree. However, one can compute the minimal flow energy network in polynomial time. In consideration of the flow energy we use the *Gabriel Graph* (GG(V)) introduced in [GS69]. It consists of all edges $\{u, v\}$ such that the open sphere using the line from u to v as diameter does not contain any other node from $V \subseteq \mathbb{R}^{\mathcal{D}}, \mathcal{D} \in \{2, 3\}$. It turns out that MST$(V) \subseteq$ GG(V). Let $\tilde{GG}(V)$ denote the weighted version of $GG(V)$ where each edge e has weight $|e|^{\mathcal{D}}$. The following holds:

Theorem 4.5 *For a given vertex set V and a routing problem f, the shortest paths between vertices $u, v \in V$ with $f(u, v) \neq 0$ of $\tilde{GG}(V)$ form an optimal path system for a radio network with respect to the flow energy.*

Proof: By the Theorem of Thales, the flow-optimal path between two nodes u and v only contains edges of $GG(V)$ (see Fig. 4.4). Thus, it is a shortest path in $GG(V)$, where each edge e has weight $|e|^{\mathcal{D}}$, i.e., in $\tilde{GG}(V)$. By definition of flow energy of a path system, the collection of all flow-optimal paths for packets of the routing problem f form a flow-optimal path system. ■

Note that a flow-optimal path system can easily be computed in polynomial time by an all-pairs-shortest-paths algorithm. There are situations where edges of the Gabriel Graph can be replaced by less energy-consuming paths, even if no node lies inside the disk described by the edge. In this case, the edge of the Gabriel Graph is not part of any energy optimal route.

4.1.4 Optimizing Congestion and Dilation

In this subsection we try to minimize the routing time in terms of congestion and dilation. i.e. we try to find nearly optimal path systems for a given vertex set V and a routing problem f. It is clear that the complete network is the optimal choice for dilation. So we only have to focus

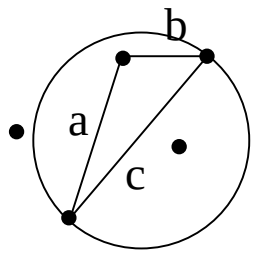

Figure 4.4: Communication on an edge c is more expensive with regard to unit energy than communication on the edges a and b ($a^2 + b^2 < c^2$)

on congestion. We present an approximation of a congestion-optimal path system. But first, we begin with the introduction of the diversity $g(V)$ of a set V that can be used to upper bound the number of interfering edges. After this we present a data structure that approximates the congestion-optimal communication network by a factor of $\mathcal{O}(g(V)^2)$.

Diversity of a Vertex Set

Sometimes the location of the radio stations does not allow us any routing without incurring high congestion. Consider a vertex set $V = \{v_1, \ldots, v_n\}$ on a line, with distances $|v_i - v_{i+1}| = 2^{i-1}$. The edge $\{v_i, v_{i+1}\}$ interferes with all edges $\{v_j, v_{j+1}\}$ for $j \leq i$, see Figure 4.5. Therefore the interference number of the network is $n - 2 = \mathcal{O}(n)$. Suppose only v_1 and v_n want to communicate, then the better solution for congestion is to disconnect all interior nodes and to realize only the edge $\{v_1, v_n\}$. Of course this is not an option when interior nodes need to communicate.

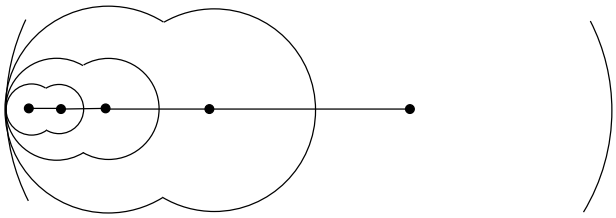

Figure 4.5: The high diversity of the vertex set causes high interference, resulting in high congestion

It turns out that a determining parameter for the realization of optimal communication networks for radio networks is the number of magnitudes of distances. Distances have different magnitudes if they differ by more than a factor of 2.

Definition 4.2 *The diversity $g(V)$ of a point set V in Euclidean space is defined by $g(V) := |Q(V)|$, where $Q(V) := \{m \in \mathbb{Z} \mid \exists u, v \in V : \lfloor \log |u - v| \rfloor = m\}$ denotes the levels of different magnitudes of all distances.*

Note that in the scenario of Figure 4.5 we observe almost maximum diversity of n (and a high interference number). We first show the close connection between interference number and diversity for vertices on a line.

Theorem 4.6 *The interference number of a line graph $G = (V, E)$ with edges between direct neighbors, i.e. $V = \{v_1, \ldots, v_n\} \subseteq \mathbb{R}$ and $E = \{\{v_i, v_{i+1}\} \mid i \in [n-1]\}$, is at most $6 \cdot g(V)$.*

Proof: For $q \in \mathbb{N}_0$ at most six edges of a length in a distance in the range $[2^q, 2^{q+1})$ can exist with an endpoint within distance 2^{q+1} of a given edge e. Three edges left and three edges right of e. These are the only edges of this length that possibly can interfere with e. Hence, the overall number of interfering edges is at most $6 \cdot |Q(V)|$. ∎

Because of this relationship between interference of radio networks and the diversity of vertex sets, we take a closer look at the possible range of the diversity. It is upper bounded by $\binom{n}{2} = \mathcal{O}(n^2)$, because it is defined over all possible distances. A divide-and-conquer argument, however, gives an upper bound of $\mathcal{O}(n \log n)$. With a randomization technique we will show that the diversity grows at most linear in the number of nodes. Such a worst case is depicted in Figure 4.5.

On the other hand, the diversity is at least logarithmic in the number of nodes. Such small diversity can be observed for equidistant nodes on a line or an $m \times m$ grid.

In the following we present results concerning the diversity $g(V)$ of n nodes $V \subseteq \mathbb{R}^{\mathcal{D}}$. By $r_0 := \min_{u,v \in V, u \neq v} |u - v|$ we denote the minimum distance of two different points u and v.

Lemma 4.2 $g(V) = \Omega\left(\frac{\log n}{\mathcal{D}}\right)$.

Proof: Note that all pairs of points $u \neq v$ have a minimum distance $|u - v| \geq r_0$. For a point u we consider all points W which are at most $2r_0$-distant to u. Now observe that all spheres with a center of W and radius $r_0/2$ do not intersect (yet may be tangent) and are included in the sphere with center u and radius $\frac{5}{2}r_0$ (This results from distance $2r_0$ between center points and u plus $\frac{r_0}{2}$ for the rest of the spheres). Hence, the sum of volumes of all the spheres with radius $r_0/2$ is at most the volume of the larger sphere. Note that the volume of a $\mathcal{D}$-dimensional sphere with radius r is given by $k_{\mathcal{D}} r^{\mathcal{D}}$, where $k_{\mathcal{D}} := \frac{\pi^{\mathcal{D}/2}}{(\mathcal{D}/2)!}$. This leads to the following inequality:

$$|W| \cdot k_{\mathcal{D}} \left(\frac{r_0}{2}\right)^{\mathcal{D}} \leq k_{\mathcal{D}} \left(\frac{5r_0}{2}\right)^{\mathcal{D}}$$

This yields:

$$|W| \ \leq \ 5^{\mathcal{D}} \, .$$

Now pick an arbitrary point of V, erase all points of V that are closer than $2r_0$ to this point, and reiterate this step until all points in the resulting set V' have a minimum distance $2r_0$. The above observation implies $|V'| \geq \frac{|V|}{5^{\mathcal{D}}}$, since every point has at most $5^{\mathcal{D}}$ other points in its $2r_0$-neighborhood.

Now we iterate this process on the reduced point set V', with $r_0' = \min_{u,v \in V' : u \neq v} |u - v|$, until only one point is left. This process takes at least $\lceil \log_{5^{\mathcal{D}}} |V| \rceil = \Omega\left(\frac{\log n}{\mathcal{D}}\right)$ iterations. In every

iteration step we find at least one new element of $Q(V)$, since the minimum distance after each reduction of the point set is at least twice as large as before.

Therefore, the number of rounds of this process gives a lower bound on the diversity of V. ■

Lemma 4.3 *For $\mathcal{D} = 1$, i.e., $V \subseteq \mathbb{R}$, we have $g(V) = \mathcal{O}(n)$.*

Proof: The main difficulty for the proof of this statement arises from side effects due to the rounding in the definition of the diversity. We overcome this problem by randomization, in particular we multiply each number of $V = \{v_1, \ldots, v_n\}$, where $v_1 < v_2 < \ldots < v_n$, by the same factor $k = 2^R$ yielding $v'_i = kv_i$, where R is a continuous uniform random variable over $[0, 1]$. Let $V_R = \{v'_1, \ldots, v'_n\}$ be the resulting set of real numbers and define for all $i \in [n]$: $Q_i := Q(\{v'_1, \ldots, v'_i\})$. We will prove for $i \in \{2, \ldots, n\}$:

$$\mathbf{E}[|Q_i \setminus Q_{i-1}|] \;\leq\; 5\,. \tag{4.1}$$

We concentrate on elements in the set S_i defined by

$$S_i := \{m \in \mathbb{Z} \mid \exists j \in [i-1] :\; m = \lfloor \log(kv_i - kv_j) \rfloor\}\,,$$

because $Q_i \setminus Q_{i-1} \subseteq S_i \setminus S_{i-1}$. We give a short proof that this inclusion is valid: $m \in Q_i \setminus Q_{i-1}$ holds if and only if

$$\exists j \in [i-1] :\; m = \lfloor \log(kv_i - kv_j) \rfloor \wedge\; \forall \ell \in [i-1], \forall j \in [\ell - 1] :\; m \neq \lfloor \log(kv_\ell - kv_j) \rfloor$$

This implies

$$\exists j \in [i-1] :\; m = \lfloor \log(kv_i - kv_j) \rfloor \wedge\; \forall j \in [i-2] :\; m \neq \lfloor \log(kv_{i-1} - kv_j) \rfloor$$

which holds if and only if $m \in S_i \setminus S_{i-1}$.

For fixed $i \in [2..n]$ let $x := v_i - v_{i-1}$, $y_j := v_{i-1} - v_j$, and $z_j := v_i - v_j$. Analogously, we define $x' := v'_i - v'_{i-1} = kx$, $y'_j := v'_{i-1} - v'_j = ky_j$, and $z'_j := v'_i - v'_j = kz_j$. In this notation we have

$$S_i = \{m \in \mathbb{Z} \mid \exists j \in [i-1] :\; m = \lfloor \log z'_j \rfloor\}\,.$$

If we observe $y_j \leq 2y_{j+1}$ in an interval $j \in [a..b-1]$, we can conclude that $z_j \leq 2z_{j+1}$, since $x + y_j = z_j$. A further implication is that $y'_j \leq 2y'_{j+1}$ and $z'_j \leq 2z'_{j+1}$. The consequence of $y_j \leq 2y_{j+1}$ is that the rounded logarithms $\lfloor \log y'_j \rfloor \in S_{i-1}$ form a consecutive interval of integer values

$$\{\lfloor \log y'_a \rfloor, \lfloor \log y'_{a+1} \rfloor, \ldots, \lfloor \log y'_b \rfloor\} \;=\; [\lfloor \log y'_a \rfloor .. \lfloor \log y'_b \rfloor] \;\subseteq\; S_{i-1}\,.$$

Yet, the same is true for S_i:

$$\{\lfloor \log z'_a \rfloor, \lfloor \log z'_{a+1} \rfloor, \ldots, \lfloor \log z'_b \rfloor\} \;=\; [\lfloor \log z'_a \rfloor .. \lfloor \log z'_b \rfloor] \subseteq S_i\,.$$

If $x \leq y_b$ we have $z'_b = x' + y'_b \leq 2y'_b$. Thus, $\log z'_b \leq 1 + \log y'_b$ and therefore the only contribution of the set $\{\lfloor \log z'_j \rfloor \mid j \in [a..b]\}$ to $S_i \setminus S_{i-1}$ is one element at the most, namely $\lfloor \log z'_b \rfloor$.

Furthermore, the probability that this element occurs decreases proportionally to $1/z_b$ as we will see now. For this, we estimate the probability that $\lfloor \log z'_b \rfloor \neq \lfloor \log y'_b \rfloor$. An equivalent representation of this inequality is

$$\lfloor R + \delta + \log y_b \rfloor \neq \lfloor R + \log y_b \rfloor \ ,$$

where $\delta = \log z_b - \log y_b = -\log \frac{z_b - x}{z_b} = -\log(1 - \frac{x}{z_b})$. Clearly, the probability for satisfying this inequality is given by $\max\{\delta, 1\}$, since R is chosen uniformly from $[0, 1]$. Note that for $r \in [0, \frac{1}{2}]$ it holds that $\log(1-r) \geq -2r$. Substituting $r = \frac{x}{z_b}$ we can conclude $\delta \leq \frac{2x}{z_b}$ if $z_b \geq 2x$.

Putting it all together, we see that if $z_j \leq 2x$ we have

$$\log z'_j \leq 1 + \log z_j \leq 2 + \log x$$

and hence at most the elements $q := \lfloor x \rfloor$, $q + 1$ and $q + 2$ might be added to $S_i \setminus S_{i-1}$.

For all $z_j > 2x$ we partition $[i - 1]$ into intervals $I_k = [a_k..b_k]$ with $a_k \leq b_k < a_{k+1}$ such that for all $j \in I_k \setminus \{b_k\}$ we have $y_i \leq 2y_{i+1}$ and $y_{b_k} > 2y_{a_{k+1}} > 2y_{b_{k+1}}$. The probability for $\lfloor \log z'_{b_k} \rfloor \in S_i \setminus S_{i-1}$ is at most $\frac{2x}{z_b}$. Since $\frac{2x}{z_{b_1}} \leq 1$, and $z_{b_{k+1}} \geq 2z_{b_k}$, the expected number of such elements is bounded by $\sum_{k=1}^{\infty} 2^{k-1} \leq 2$. Since $Q_i \setminus Q_{i-1} \subseteq S_i \setminus S_{i-1}$, this proves equation (4.1).

As a consequence of equation (4.1) it follows (note that $Q_1 = \emptyset$)

$$\mathbf{E}[|Q(V_R)|] \ = \ \mathbf{E}\left[\sum_{i=2}^{n} |Q_i \setminus Q_{i-1}|\right] \ = \ \sum_{i=2}^{n} \mathbf{E}[|Q_i \setminus Q_{i-1}|] \ \leq \ 5(n-1) \ .$$

Now we derandomize: if for the random variable $R \in [0, 1]$ the expected value is bounded by $\mathbf{E}[|Q(V_R)|] \leq 5(n-1)$, there exists a concrete choice $r \in [0, 1]$ such that $|Q(V_r)| \leq 5(n-1)$.

The relationship between $Q(V_r)$ and the diversity is the following. If $\ell \in Q(V_r)$, then either $\ell \in Q(V)$ or $\ell - 1 \in Q(V)$. Therefore $|Q(V)| \leq 2|Q(V_r)|$, which shows that

$$g(V) \ = \ |Q(V)| \ \leq \ 2Q(V_r) \ \leq \ 10(n-1) \ .$$

■

Lemma 4.4 *$g(V) = \mathcal{O}(\mathcal{D}(\log \mathcal{D})\, n)$ for $\mathcal{D} > 1$.*

Proof: For every point u let $u_1, \ldots, u_{\mathcal{D}} \in \mathbb{R}$ denote its coordinates in $\mathbb{R}^{\mathcal{D}}$. It holds for any points $u, v \in V$, $u \neq v$, that

$$|u - v| = \sqrt{\sum_{i=1}^{\mathcal{D}} (u_i - v_i)^2} \leq \sqrt{\mathcal{D} \cdot (\max_{i \in [\mathcal{D}]} |u_i - v_i|)^2} = \sqrt{\mathcal{D}} \max_{i \in [\mathcal{D}]} |u_i - v_i| \ .$$

We get

$$\frac{|u - v|}{\sqrt{\mathcal{D}}} \ \leq \ \max_{i \in [\mathcal{D}]} |u_i - v_i| \ \leq \ |u - v| \ .$$

This implies

$$\lfloor \log |u-v| \rfloor - \frac{1}{2}\log \mathcal{D} \;\leq\; \max_{i\in[\mathcal{D}]} \lfloor \log |u_i - v_i| \rfloor \;\leq\; \lfloor \log |u-v| \rfloor \; .$$

Now we consider all different values for $\lfloor \log |u_i - v_i| \rfloor$. These include also the values for $\max_{i\in[\mathcal{D}]} \lfloor \log |u_i - v_i| \rfloor$ which in combination with the last inequality allow us an estimation of the different values for $\lfloor \log |u-v| \rfloor$. Hence, let m be the number of different values for $\lfloor \log |u_i - v_i| \rfloor$ for all $i \in \{1,\ldots,\mathcal{D}\}$ and $u, v \in V$, then the number of different values for $\lfloor \log |u-v| \rfloor$ is bounded by $m(\frac{1}{2}\log \mathcal{D} + 1)$.

Note that for a fixed i the set $\{\lfloor \log |u_i - v_i| \rfloor \mid u, v \in V\}$ describes the diversity levels of a one-dimensional point set und thus has at most $10(n-1)$ elements. Summing over all $\mathcal{D}$ dimensions gives $m \leq 10\mathcal{D}(n-1)$ bounding the diversity of V by $g(V) \leq 10\ \mathcal{D}(n-1)(\frac{1}{2}\log \mathcal{D} + 1) = \mathcal{O}(\mathcal{D}(\log \mathcal{D})\ n)$. ∎

Lemma 4.5 $g(V) \leq 2 + \log \frac{\max_{u,v\in V} |u-v|}{\min_{u,v\in V \wedge u\neq v} |u-v|}$

Proof: It holds by definition that $\min(Q) > (\log \min_{u,v\in V: u\neq v} |u-v|) - 1$ and $\max(Q) \leq \log \max_{u,v\in V} |u-v|$. Therefore

$$\begin{aligned} g(V) &\leq \max(Q) - \min(Q) + 1 \\ &\leq 2 + \log \max_{u,v\in V} |u-v| - \log \min_{u,v\in V: u\neq v} |u-v| \\ &= 2 + \log \frac{\max_{u,v\in V} |u-v|}{\min_{u,v\in V: u\neq v} |u-v|} \; . \end{aligned}$$

∎

Lemma 4.6 *For a point set V randomly chosen from $[0,1]^{\mathcal{D}}$ the diversity is at most $\mathcal{O}(\log n) + \frac{1}{2}\log \mathcal{D}$ with probability $1 - n^{-c}$, for any constant $c > 0$.*

Proof: The maximum distance between two points in $[0,1]^{\mathcal{D}}$ is $\max_{u,v\in[0,1]^{\mathcal{D}}} |u-v| \leq \sqrt{\mathcal{D}}$. Now we try to estimate the minimum distance. There exist constants c and c' such that the probability that two random coordinates u_i, v_i are closer than $\frac{1}{n^{c'}}$ is at most $\frac{1}{n^c}$. Since $|u-v| \geq |u_i - v_i|$ we get $|u-v| \geq \frac{1}{n^{c'}}$ with probability $1 - n^{-c}$. We apply Lemma 4.5 and get the bound for the diversity, i.e. $g(V) \leq 2 + \log(n^{c'}\sqrt{d}) \leq 2 + c' \log n + \frac{1}{2}\log \mathcal{D} = \mathcal{O}(\log n) + \frac{1}{2}\log \mathcal{D}$. ∎

We summarize the results for the diversity $g(V)$ of n points $V \subseteq \mathbb{R}^{\mathcal{D}}$:

$$\begin{aligned} g(V) &= \Omega\left(\frac{\log n}{\mathcal{D}}\right), \\ g(V) &= \mathcal{O}(n) \text{ for } \mathcal{D} = 1, \text{ i.e. } V \subseteq \mathbb{R}, \\ g(V) &= \mathcal{O}(\mathcal{D}(\log \mathcal{D})\ n) \text{ for } \mathcal{D} > 1, \\ g(V) &\leq 2 + \log \frac{\max_{u,v\in V} |u-v|}{\min_{u,v\in V\wedge u\neq v} |u-v|}\ , \\ g(V) &= \mathcal{O}(\log n) + \frac{1}{2}\log \mathcal{D} \text{ with probability } 1 - n^{-c} \text{ for any constant } c > 0, \\ &\quad \text{if the point set } V \text{ is randomly chosen from } [0,1]^{\mathcal{D}} \end{aligned}$$

There are many reasons why for real-world scenarios the diversity can always be assumed to be bounded by $\mathcal{O}(\log n)$. Radio stations must be positioned with high accuracy such that most radio stations are closer than any polynomial fraction of the largest distance to achieve a high diversity. Note that assuming a polynomial bound on the fraction between the largest and smallest distance of radio stations implies logarithmic diversity, compare Figure 4.5. A further reason may be that there are not many orders of magnitude between the transmission range of a radio station and the physical size of the antenna the radio station is equipped with. A commonly used model for radio networks are civilized graphs [WL02, HBHMR$^+$98] satisfying the property that the distance between any two nodes in this graph is larger than a positive constant λ.

Approximating Congestion with the Hierarchical Layer Graph

Now we try to approximate congestion-optimal path systems for radio networks. For this purpose we introduce the *Hierarchical Layer Graph* (HL-graph) with bounded degree, see Figure 4.6. Adopting ideas from clustering [GGH$^+$01a, GGH$^+$01b] and generalizing an approach of [AS98] we present a graph consisting of w layers $L_1, L_2 \ldots, L_w$. The union of all these layers gives the HL-graph. The lowest layer L_1 contains all vertices V. The vertex set of a higher layer is a subset of the vertex set of a lower layer until in the highest layer there is only one vertex, i.e.

$$\{v_0\} = V(L_w) \subseteq \cdots \subseteq V(L_2) \subseteq V(L_1) = V \ .$$

The crucial property of these layers is that in each layer L_i vertices obey a minimum distance: $\forall u, v \in V(L_i) \ : \ |u - v| \ \geq \ r_i$. Furthermore, all nodes in the next-lower layer must be covered by this distance: $\forall u \in V(L_i) \ \exists v \in V(L_{i+1}) \ : \ |u - v| \ \leq \ r_{i+1}$. Our construction uses parameters $\alpha \geq \beta > 1$, where for some $r_0 < \min_{u,v \in V : u \neq v} |u - v|$ we use radii $r_i := \beta^i \cdot r_0$ and we define in layer L_i the edge set by $E(L_i) := \{(u, v) \mid u, v \in V(L_i) \ \wedge \ |u - v| \ \leq \ \alpha \cdot r_i\}$.

Note that if $V(L_i) = V(L_j)$ for $i < j$, then all edges of L_i are also in L_j, i.e. $E(L_i) \subseteq E(L_j)$. Hence, we omit the lower layer and consider only layers $i_1 < i_2 < \ldots < i_w$ that form a strict hierarchy, i.e. that $V(L_{i_j}) \subset V(L_{i_k})$ and for all $k \in [i_{j-1}+1, \ldots, i_j]$: $V(L_k) = V(L_{i_j})$. The only exception to this rule is the uppermost layer with $|V(L_{i_w})| = 1$, where we choose the minimum i_w with $|V(L_{i_w})| = 1$.

Using this subset of layers $L'_j := L_{i_j}$ we extend the indices of the layers also to negative values, i.e. $i_j \in \mathbb{Z}$. As a side effect, we avoid any dependency between the parameter r_0 and the minimum distance of two points.

Figure 4.6 shows the idea behind the HL-graph. Note that the highest layer is omitted. The graph is comparable to a map. For example, to drive from one city to another you can choose different ways. You could use small streets and drive from hickstown to hickstown, in our case this path would optimize energy consumption, or you drive via highways through big towns, this is a good solution concerning hop minimization, or you use a combination of both to optimize congestion. In the following we will more formalize these observations. It turns out that the number of layers grows linear with the diversity of the point set.

Lemma 4.7 *The number of layers of the HL-graph of a point set of n nodes is bounded by $g(V)(2 + \frac{1}{\log \beta}) + \mathcal{O}(1)$. If the orders of magnitudes of all distances $Q(V)$ form a consecutive interval, then the number of layers is bounded by $\frac{g(V)}{\log \beta} + \mathcal{O}(1)$.*

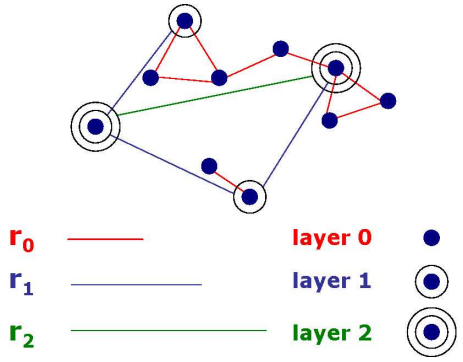

Figure 4.6: The idea of the Hierarchical Layer Graph

Proof: We start with the case that $Q(V)$ is consecutive, i.e. $Q(V) = \{q_0, \ldots, q_{\max}\}$, where $q_{\max} > q_0$. Then there are no vertices $u, v \in V$ with $|u - v| < 2^{q_0}$. For all layers L_i with $r_i < 2^{q_0}$ we have $V(L_i) = V$. Therefore, the first layer of the HL-graph is $i_1 := \lfloor \frac{q_0}{\log \beta} \rfloor$.

For $q_{\max} = \max\{Q(V)\}$ we observe that all vertices $u, v \in V$ satisfy $|u - v| < 2^{q_{\max}+1}$. Hence, in the layer L_i with $r_i \geq 2^{q_{\max}+1}$ there is exactly one vertex. The index of this layer is $i_w = \lceil \frac{q_{\max}+1}{\log \beta} \rceil$.

So, we get the following maximum number of layers.

$$\begin{aligned} w \;=\; i_w - i_1 + 1 \;&\leq\; \left\lceil \frac{q_{\max}+1}{\log \beta} \right\rceil - \left\lfloor \frac{q_0}{\log \beta} \right\rfloor + 1 \\ &=\; \left\lceil \frac{q_0}{\log \beta} + \frac{g(V)}{\log \beta} \right\rceil - \left\lfloor \frac{q_0}{\log \beta} \right\rfloor + 1 \\ &\leq\; \left\lceil \frac{g(V)}{\log \beta} \right\rceil + 2\,. \end{aligned}$$

If $Q(V)$ is non-consecutive, there are m sets $\{q'_i, \ldots, q'_i + \delta_i\} \subseteq \{q_0, \ldots, q_{\max}\}$ such that $\{q'_i, \ldots, q'_i + \delta_i\} \cap Q(V) = \emptyset$. Note that $q_{\max} - q_0 + 1 - \sum_{i=1}^{m} \delta_i = g(V)$. For all $i \in [m]$ there exists no pair $u, v \in V$ such that $2^{q'_i} \leq |u - v| < 2^{q'_i+\delta_i+1}$. Hence, no points $u, v \in V$ exist with distance $\beta^{\frac{q'_i}{\log \beta}} \leq |u - v| < \beta^{\frac{q'_i+\delta_i+1}{\log \beta}}$, which implies that layers L_j with $j \in \{1 + \lceil q'_i / \log \beta \rceil, \ldots, \lfloor (q'_i + \delta_i + 1)/\log \beta \rfloor - 1\}$ are omitted in the HL-graph. The number S of all omitted layers can be lower bounded as follows using $m \leq g(V)$.

$$\begin{aligned} S \;&\geq\; \sum_{i=1}^{m} \left\lfloor \frac{q'_i + \delta_i + 1}{\log \beta} \right\rfloor - \left\lceil \frac{q'_i}{\log \beta} \right\rceil - 1 \\ &\geq\; \left\lfloor \frac{m + \sum_{i=1}^{m} \delta_i}{\log \beta} \right\rfloor - 2m \\ &\geq\; \frac{\sum_{i=1}^{m} \delta_i}{\log \beta} - 2g(V)\,. \end{aligned}$$

Subtracting S from the number of layers in the consecutive case with lowest level q_0 and upper-

most level $q_{\max}$ we obtain the following for the number of layers w by using $m \leq g(V)$.

$$\begin{aligned} w &\leq \left\lceil \frac{q_{\max} - q_0}{\log \beta} + 2 \right\rceil - \frac{\sum_{i=1}^{m} \delta_i}{\log \beta} + 2g(V) \\ &\leq \frac{q_{\max} - q_0}{\log \beta} + 3 - \frac{q_{\max} - q_0 + g(V) - 1}{\log \beta} + 2g(V) \\ &\leq 2g(V) + \frac{g(V)}{\log \beta} + 3 \end{aligned}$$

■

In the following, we will see that the weak c-spanner property has implications for minimizing congestion. First, we show that the Hierarchical Layer Graph is a spanner which implies that it is also a weak spanner.

Theorem 4.7 *If $\alpha > 2\frac{\beta}{\beta-1}$ the HL-graph is a c-spanner for $c = \beta\frac{\alpha(\beta-1)+2\beta}{\alpha(\beta-1)-2\beta}$.*

Proof: In the following we define a directed tree T on the vertex set $V \times [w]$ where w is the number of layers. The leafs of T are all pairs $V \times \{1\}$. If $u \in V(L_i)$, then (u, i) is a vertex of T. T consists of the following edges: for $i \geq 2$ if $u \in V(L_i)$, then $\{(u, i-1), (u, i)\} \in E(T)$. If $u \in V(L_i) \setminus V(L_{i+1})$ then choose arbitrary $v \in V(L_{i+1})$ with $\{u, v\} \in E(L_i)$ and add $\{(u, i), (v, i+1)\}$ to the edge set of the tree T. The tree has depth w and the root is (v_0, w).

Now for two vertices $u, v \in V$ we define a *clamp* of height j, which is a path connecting u and v. The clamp consists of two paths

$$P_u^j := (u, p(u), p^2(u), \ldots, p^j(u)) \quad \text{and} \quad P_v^j := (v, p(v), p^2(v), \ldots, p^j(v))$$

of length $j-1$, where $p^i(w)$ denotes the ancestor of height i of a vertex w in the tree T. These two paths are connected by the edge $\{p^j(u), p^j(v)\}$.

Lemma 4.8 *If for vertices u, v the distance is bounded by $|u - v| \leq f_j$, where*

$$f_j = r_j \left(\alpha - 2\frac{\beta - \frac{1}{\beta^j}}{\beta - 1} \right) ,$$

then a clamp of height at most j is contained in the HL-graph.

Proof: First, it holds that

$$\sum_{i=0}^{j} r_i = \sum_{i=0}^{j} \beta^i \cdot r_o = r_o \cdot \frac{\beta^{j+1} - 1}{\beta - 1} = \frac{r_{j+1} - r_0}{\beta - 1} = r_j \left(\frac{\beta - \frac{1}{\beta^j}}{\beta - 1} \right) .$$

Hence we have

$$|u - v| \;\leq\; f_j \;=\; \alpha r_j - 2\sum_{i=0}^{j} r_i \, .$$

Consider the paths $(u, p(u), p^2(u), \ldots, p^j(u))$ and $(v, p(v), p^2(v), \ldots, p^j(v))$. They are contained in the HL-graph, since $|p^i(u) - p^{i+1}(u)| \leq r_{i+1}$ and $|p^i(v) - p^{i+1}(v)| \leq r_{i+1}$. Furthermore, the edge $\{p^j(u), p^j(v)\}$ is in the HL-graph since $|p^j(u) - p^j(v)| \leq |u - v| + 2\sum_{i=0}^{j} r_i \leq \alpha r_j$. Hence, a clamp of height j is contained in G. ■

Lemma 4.9 *A clamp of height j has maximum length g_j, where*

$$g_j = r_j \left(\alpha + 2\frac{\beta - \frac{1}{\beta^j}}{\beta - 1} \right) .$$

Proof: Recall that the length of the paths P_u^j and P_v^j is bounded by $2\sum_{i=1}^{j} r_i$, the edge $\{p^j(u), p^j(v)\}$ has length of at most αr_j and $\sum_{i=0}^{j} r_i = r_j \left(\frac{\beta - \frac{1}{\beta^j}}{\beta - 1} \right)$. This gives

$$||C|| \;\leq\; \alpha r_j + 2\sum_{i=0}^{j} r_i \;=\; g_j \; .$$

■

For any pair of vertices u, v with $f_{j-1} < |u - v| \leq f_j$ there is a clamp of height j and length g_j. Hence, the stretch factor c can be upper bounded by $c \leq \frac{g_j}{|u-v|} \leq \frac{g_j}{f_{j-1}}$.

$$\begin{aligned} c \;&\leq\; \frac{g_j}{f_{j-1}} \quad = \frac{g_j}{f_j} \cdot \frac{f_j}{f_{j-1}} \quad = \frac{g_j}{f_j} \cdot \beta \cdot \frac{\alpha(\beta-1) - 2\beta + 2\beta^{-j}}{\alpha(\beta-1) - 2\beta + 2\beta^{-j+1}} \\ &\leq\; \beta \cdot \frac{g_j}{f_j} \quad = \beta \cdot \frac{\alpha(\beta-1) + 2\beta - 2\beta^{-j}}{\alpha(\beta-1) - 2\beta + 2\beta^{-j}} \quad \leq \beta \cdot \frac{\alpha(\beta-1) + 2\beta}{\alpha(\beta-1) - 2\beta} \; . \end{aligned}$$

■

In Figure 4.7 the stretch factors of the HL-graph are given. We varied the parameter β and computed the required value for α and the length stretch factor c.

Lemma 4.10 *For any finite point set $V \subset \mathbb{R}^{\mathcal{D}}$ and every layer L_i of a HL-graph with parameters $\alpha \geq \beta > 1$ we have the following.*

1. *For any $u \in \mathbb{R}^{\mathcal{D}}$, the number of points $v \in V(L_i)$ with $|u - v| \leq c r_i$ is at most $(2c+1)^{\mathcal{D}}$.*
2. *The degree of the sub-graph L_i is at most $(2\alpha + 1)^{\mathcal{D}}$.*
3. *The interference number of L_i is bounded by $(2\alpha + 1)^{2\mathcal{D}}$.*

Proof: Recall that $k_{\mathcal{D}} := \frac{\pi^{\mathcal{D}/2}}{(\mathcal{D}/2)!}$ where $k_{\mathcal{D}} r^{\mathcal{D}}$ is the volume of a $\mathcal{D}$-dimensional sphere with radius r.

1. For all $u, v \in V(L_i)$ we have $|u - v| \geq r_i$. Hence, all spheres with radii $\frac{r_i}{2}$ and center points $u \in V(L_i)$ do not intersect. If $|u - v| \leq c r_i$ then the sphere with center u and radius $\frac{r_i}{2}$ lies inside a sphere with center v and radius $(c + \frac{1}{2}) r_i$. Let m be the number of the smaller spheres inside this larger one. Then it follows

$$m k_{\mathcal{D}} \left(\frac{r_i}{2} \right)^{\mathcal{D}} \leq k_{\mathcal{D}} \left(\left(c + \frac{1}{2} \right) r_i \right)^{\mathcal{D}} \quad \Longrightarrow \quad m \leq (2c+1)^{\mathcal{D}} \; .$$

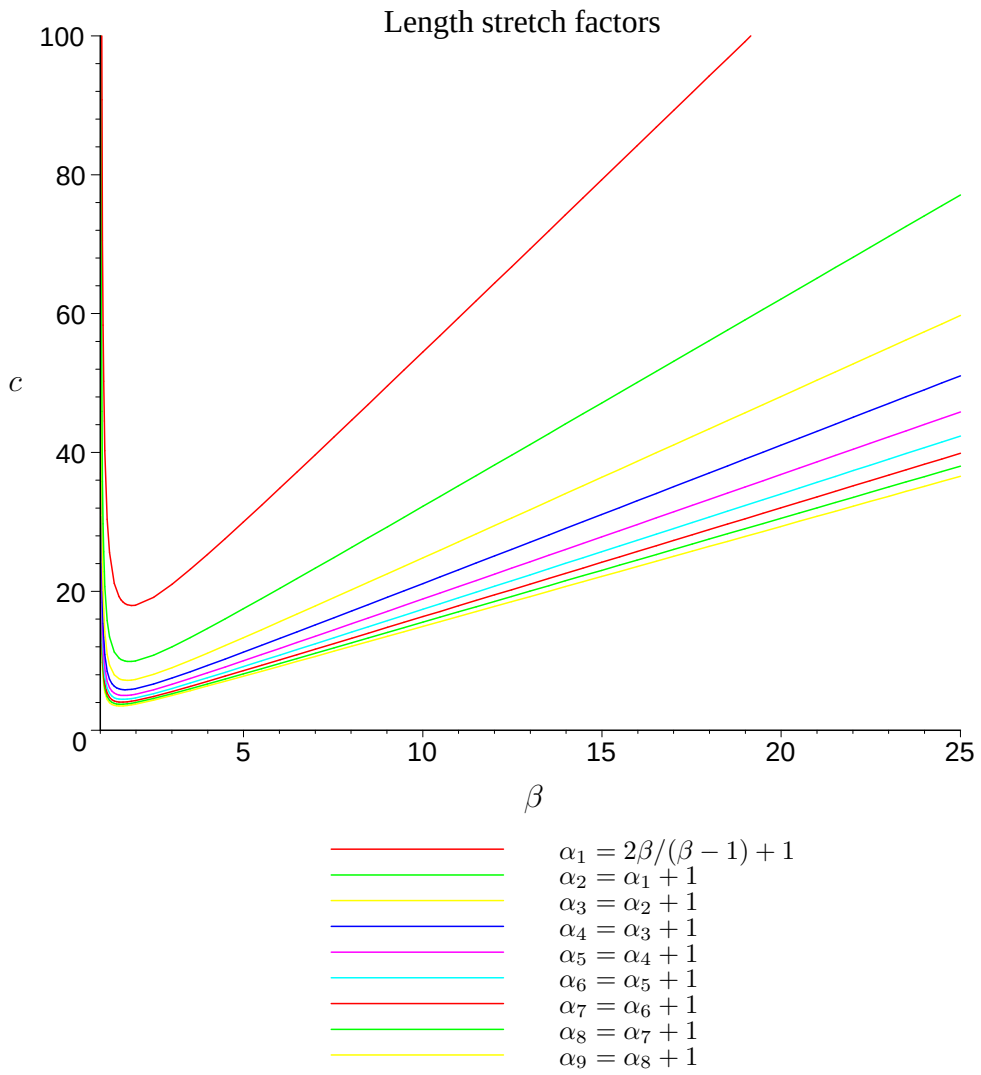

Figure 4.7: Length stretch factors of the HL-graph for different parameters α and β.

2. Follows by combining the preceding with the fact that the edge $\{u, v\} \in E(L_i)$ if $u, v \in V(L_i)$ and $|u - v| \leq \alpha r_i$.

3. Two edges each of length αr_i can only interfere if their end points have at most distance αr_i. For each layer the number of such points of the same layer is bounded by $(2\alpha + 1)^{\mathcal{D}}$. Every of these points is adjacent to at most $(2\alpha + 1)^{\mathcal{D}}$ edges of L_i. Hence, the interference number in L_i is bounded by $(2\alpha + 1)^{2\mathcal{D}}$.

■

Theorem 4.8 *For a vertex set V with diversity $g(V)$ the degree of the HL-graph is at most $g(V)(2 + \frac{1}{\log \beta})(2\alpha + 1)^{\mathcal{D}} + \mathcal{O}(1)$. The interference number is at most $g(V)(2 + \frac{1}{\log \beta})(2\alpha +$*

$1)^{2\mathcal{D}} + \mathcal{O}(1)$. *If $Q(V)$ is consecutive, the degree is bounded by $g(V)\frac{(2\alpha+1)^{\mathcal{D}}}{\log\beta} + \mathcal{O}(1)$ and the interference number is at most $g(V)\frac{(2\alpha+1)^{2\mathcal{D}}}{\log\beta} + \mathcal{O}(1)$.*

Proof: We apply Lemma 4.7, bounded number of layers in the HL-graph, and Lemma 4.10, bounded number of neighbors and egdes of a node in the HL-graph. For each point we observe that there are at most $(2\alpha+1)^{\mathcal{D}}$ vertices in a layer L_i with distance αr_i. Each of these nodes has at most $(2\alpha+1)^{\mathcal{D}}$ edges of length at most αr_i. Therefore, a vertex may suffer under at most $(2\alpha+1)^{2\mathcal{D}}$ interfering edges per layer. Summing up over all layers this observation proves the upper bound of the interference number of the HL-graph. ■

A typical feature of radio communication is that transmitting information blocks a region for other transmissions. We formalize this observation and define the capacity of a region following a similar approach presented in [GK00]. Let $A(R)$ denote the area of a geometric region R.

Definition 4.3 *Given a network $G = (V, E)$ and a load $\ell : E \to \mathbb{R}_0^+$ we define the interference function of an edge $e \in E$ and a point $x \in \mathbb{R}^{\mathcal{D}}$ as*

$$f_\ell(e, x) := \begin{cases} \ell(e)\,, & \text{if } x \in D(e)\,, \\ 0\,, & \text{elsewhere.} \end{cases}$$

The communication load $\kappa_{G,\ell}$ of a point x and a bounded geometric region $R \subseteq \mathbb{R}^+$ for a given network G and load ℓ is defined as follows.

$$\kappa_{G,\ell}(x) := \sum_{e \in E(G)} f_\ell(e, x) \qquad \text{and} \qquad \kappa_{G,\ell}(R) := \int_R \kappa_{G,\ell}(x)\, dx\,.$$

An equivalent description of the communication load can be done by partitioning the region R into elementary regions, where the same subset of edges interfere. For such an elementary region R' we observe

$$\kappa_{G,\ell}(R') = \sum_{e \in E(G): R' \subseteq D(e)} \ell(e) \cdot A(R')\,,$$

where $A(R')$ denotes the area or volume of R'.

For a non-elementary bounded region R we consider a partitioning into elementary regions $R_1, \ldots, R_m$ and get $\kappa_{G,\ell}(R) := \sum_{i=1}^m \kappa_{G,\ell}(R_i)$.

The following lemma will help to understand the relationship between the communication load of an elementary area and the congestion.

Lemma 4.11 *For a graph $G = (V, E)$ with $V \subset \mathbb{R}^{\mathcal{D}}$, load ℓ and a point $x \in \mathbb{R}^{\mathcal{D}}$ it holds for $\mathcal{D} \in \{2, 3\}$*

$$\kappa_{G,\ell}(x) \;\le\; c_{\mathcal{D}} \cdot \max_{e \in E(G)} \sum_{e' \in \mathrm{BInt}(e)} \ell(e')\,,$$

where $c_2 = 6$ and $c_3 = 20$.

Proof: For the point x we partition the space into $c_{\mathcal{D}}$ disjoint sub-spaces $A_1, \ldots, A_{c_{\mathcal{D}}}$ such that for all $u, v \in A_i$ $|u - x| \leq |v - x|$, then $|u - v| \leq |v - x|$. Then the angle between $\overline{xu}$ and $\overline{xv}$ is at most $\pi/3$. Clearly, for two dimensions the optimal choice is $c_{\mathcal{D}} = 6$, which resembles six sectors centered at x. For three dimensions, one can show that $c_3 = 20$ cones starting at x suffice. Therefor, one has to cover the surface of a sphere with disks whose diameter equals the radius of the sphere. In [HSS97] it is shown that 20 such disks cover a sphere.

Now choose for each non-empty sub-space A_i a vertex $u_i \in A_i$ that minimizes the distance $|x - u_i|$. For every edge $\{v, w\}$ with $x \in D(\{v, w\})$ we show that there exists a vertex u_i with $u_i \in D(\{v, w\})$. Assume w.l.o.g. that $x \in D_{|v-w|}(v)$ and let u_i be in the sub-space where v lies. Since $|u_i - x| \leq |x - v|$ we have $|u_i - v| \leq |x - v| \leq |v - w|$. Therefore we have

$$\kappa_{G,\ell}(x) \leq \sum_{i=1}^{c_{\mathcal{D}}} \sum_{e \in E(G): u_i \in D(e)} \ell(e) \leq c_{\mathcal{D}} \cdot \max_{u \in V(G)} \sum_{e \in E(G): u_i \in D(e)} \ell(e) \leq c_{\mathcal{D}} \cdot \max_{e \in E(G)} \sum_{e' \in \mathrm{BInt}(e)} \ell(e) \; .$$

■

We get the following relationship between capacity, area, and congestion.

Lemma 4.12 *Let R be a bounded region of area or volume $A(R)$ and $C_{\mathcal{P}}$ the congestion of a path system $\mathcal{P}$. Then the communication load of R is bounded by $\kappa(R) \leq c_{\mathcal{D}} \cdot A(R) \cdot C_{\mathcal{P}}$, where $c_2 = 6$ and $c_3 = 20$.*

Proof:

$$\kappa_{G,\ell}(R) = \int_R \kappa_{G,\ell}(z) \, dz \; = \int_R \sum_{e \in E(G)} \sum_{e': z \in D(e)} \ell(e') dz \; \leq \int_R c_{\mathcal{D}} \cdot C_{\mathcal{P}} \, dz \; = c_{\mathcal{D}} \cdot C_{\mathcal{P}} \cdot A(R) \; .$$

■

Every edge e with load $\ell(e)$ has a certain impact on the capacity of the area covered by the radio network. The following lemma claims that an edge e with load $\ell(e)$ induces at least communication load $k_{\mathcal{D}} \ell(e) |e|^{\mathcal{D}}$ into a region R with $D(e) \subseteq R$.

Lemma 4.13 *Consider an edge e in a region R, i.e. $D(e) \subseteq R$. Let K be the communication load of R without any load on e and K' be the communication load of R with load $\ell(e)$ on e without any load change on the other edges. Then we observe*

$$K' - K \; \geq \; k_{\mathcal{D}} \ell(e) |e|^{\mathcal{D}} \; .$$

Proof: The proof follows from the definition of $f_\ell(e, x)$ and the fact that the volume of $D(e)$ for $e = \{u, v\}$ is at least $V(D_{|u-v|}(u)) = k_{\mathcal{D}} |u - v|^{\mathcal{D}}$. ■

Lemma 4.14 *Let C^* be the congestion of the congestion-optimal path system $\mathcal{P}^*$ under an optimal network N^* for a vertex set V. Then every weak c-spanner N can host a path system $\mathcal{P}'$ such that the induced load $\ell(e)$ in N is bounded by $\ell(e) \leq c' g(V) \, C^*$ for a positive constant c'.*

Proof: Given a path P of the path system $\mathcal{P}^*$, we replace every edge $e = \{u, v\}$ of N^* that does not exist in the weak c-spanner N with a path $P(u, v)$ from u to v in N such that the new route lies completely inside a disk of radius $(c - \frac{1}{2})|u - v|$ and center $\frac{1}{2}(u + v)$. The existence of such a path follows from the weak spanner property, since we consider undirected edges. In the case of directed edges there is a new route which lies completely inside a disk of radius $(c + \frac{1}{2})|u - v|$ and center $\frac{1}{2}(u + v)$, see Observation 3.1 in Chapter 3. As you can see, in this case we would get $c + \frac{1}{2}$ instead of c.

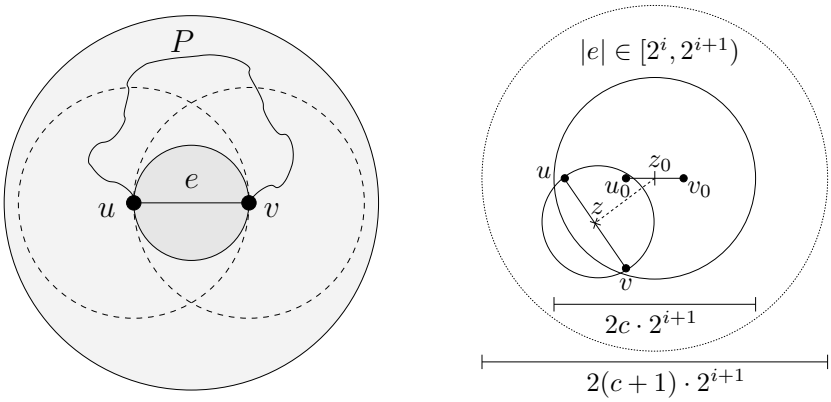

Figure 4.8: Left: the edge e interferes with other edges (at least) within the central disk. Its information is rerouted on P, lying completely within the outer-disk with radius $(c - \frac{1}{2})|e|$. Right: the idea behind the upper bound for the rerouting. The traffic of the edge $e = (u, v)$ is rerouted to the edge $e_0 = (u_0, v_0)$. The disk or sphere around z reduces the capacity of the area around z_0.

For the path system $\mathcal{P}^*$ there may have been interference between e and other edges. For simplicity we underestimate the area where e can interfere with other communication by the disk $D_1(e)$ with center $\frac{1}{2}(u + v)$ and radius $\frac{1}{2}|u - v|$ (see Figure 4.8 (left)).

We want to describe the impact of rerouting of all edges in $E(N^*)$ to a specific edge $e_0 \in E(N)$ in the weak c-spanner N. If such an edge $e_0 = \{u_0, v_0\} \in E(N)$ transmits the traffic of a detour for an edge $e = \{u, v\} \in E(N^*)$ of length $|e|$, then the distance between u as well as v and any point of the tour is at most $c|e|$. Hence, also for the center $z_0 := \frac{1}{2}(u_0 + v_0)$ of e_0 and $z := \frac{1}{2}(u + v)$ we observe $|z_0 - z| \leq c|e|$.

Now consider the edge set $E_{i,e_0} \subseteq E(N^*)$ of edges e with length $|e| \in [2^i, 2^{i+1})$ for $i \in \mathbb{Z}$ which reroute their traffic to e_0. Their center points are located inside a sphere with radius $c2^{i+1}$ and center z_0. The region where e interferes has been defined by $D(e)$. $D(e)$ has volume of at least $k_{\mathcal{D}} 2^{\mathcal{D}i - \mathcal{D}}$ and lies completely inside the sphere D with radius $2^{i+1}(c+1)$ and center z_0. The volume of D is $k_{\mathcal{D}} 2^{\mathcal{D}(i+1)}(c + 1)^{\mathcal{D}}$ (see Figure 4.8 (right)).

Lemma 4.13 shows that every edge e reduces the capacity in D by at least $k_{\mathcal{D}} \ell(e) 2^{\mathcal{D}i - \mathcal{D}}$. Because of Lemma 4.12, the overall capacity is at most

$$\kappa_{G,\ell}(D) \;\leq\; c_{\mathcal{D}} k_{\mathcal{D}} 2^{\mathcal{D}(i+1)}(c + 1)^{\mathcal{D}} C^* \; .$$

This implies the following

$$\begin{aligned} \sum_{e \in E_{i,e_0}} \ell(e) k_{\mathcal{D}} 2^{\mathcal{D}i-\mathcal{D}} &\leq c_{\mathcal{D}} k_{\mathcal{D}} 2^{\mathcal{D}(i+1)} (c+1)^{\mathcal{D}} C^* \\ \Longrightarrow \sum_{e \in E_{i,e_0}} \ell(e) &\leq c_{\mathcal{D}} 2^{2\mathcal{D}} (c+1)^{\mathcal{D}} C^* \, . \end{aligned}$$

There are at most $g(V)$ non-empty sets E_{i,e_0}. This implies for the sum of loads $\ell(e)$ of the set $E_{e_0} := \bigcup_i E_{i,e_0} \subseteq E(N^*)$:

$$\sum_{e \in E_{e_0}} \ell(e) \leq c_{\mathcal{D}} 2^{2\mathcal{D}} (c+1)^{\mathcal{D}} g(V) C^* \, .$$

■

Theorem 4.9 *Let $\mathcal{P}^*$ be the congestion optimal path system for the vertex set V. Then the HL-graph contains a path system $\mathcal{P}$ with congestion $\mathcal{O}(g(V)^2 C_{\mathcal{P}^*}(V))$.*

Proof: From Theorem 4.7 we know that the HL-graph is a c-spanner with $c = \beta \frac{\alpha(\beta-1)+2\beta}{\alpha(\beta-1)-2\beta}$ for $\alpha > 2\beta \frac{\beta}{\beta-1}$. Since a c-spanner is also a weak c-spanner, we can use Lemma 4.14 to show that there exists a routing such that the load of an edge e is bounded by $\ell(e) \leq 2^{\mathcal{D}}(c+1)^{\mathcal{D}} g(V) C_{\mathcal{P}^*}(V)$. Theorem 4.8 shows that the interference number of the network is bounded by $\mathcal{O}(g(V))$. Hence we get that $C_{\mathcal{P}}(V) = \mathcal{O}(g(V)^2 C_{\mathcal{P}^*}(V))$. ■

In practical scenarios the diversity can be seen as a logarithmic term (e.g., because the ratio between longest and shortest distance is polynomial in the number of vertices, or the points are chosen according to some uniform probability distribution). In these cases the HL-graph provides a $\mathcal{O}((\log n)^2)$-approximation for congestion.

4.1.5 Trade-Offs

We have seen efficient ways for selecting paths to optimize energy and approximate congestion. One might wonder whether an algorithm can compute a path system for a radio network optimizing congestion, dilation, and energy at the same time. It turns out that this is not the case.

Congestion versus Dilation

Let $n \in \mathbb{N}$ and $W = c \cdot n^2$ for any constant $c \in \mathbb{N}$. For a vertex set G_n given by a $\sqrt{n} \times \sqrt{n}$-grid with unit grid distance the best choice to minimize congestion is to connect grid points only to their neighbors given the demand $f(u,v) = W/n^2$ for all pairs of vertices (see Figure 4.9). Then the congestion is $\mathcal{O}(W/\sqrt{n})$ and the dilation is given by $\mathcal{O}(\sqrt{n})$. In [GK00] it is shown that such a congestion is best possible in a radio network. A fast realization is given by a tree featuring a hop-distance of $\mathcal{O}(\log n)$ and congestion $\mathcal{O}(W)$. Such a tree-construction for the Cost-distance problem is presented in [SW01]. In both cases we observe $C_{\mathcal{P}}(G_n) D_{\mathcal{P}}(G_n) = \Omega(W)$. This also is true for any other path selection.

In 3-dimensional space we place the vertices on a $\sqrt[3]{n} \times \sqrt[3]{n} \times \sqrt[3]{n}$-grid and experience minimal congestion of $\mathcal{O}(W n^{-2/3})$ with dilation $\mathcal{O}(n^{1/3})$.

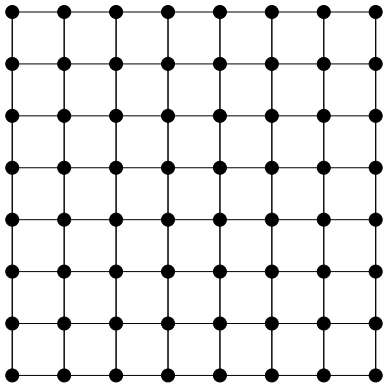

Figure 4.9: The grid G_n

Theorem 4.10 *Given the grid vertex set G_n in $\mathcal{D}$-dimensional space for $\mathcal{D} \in \{2,3\}$ with traffic W then for every path system $\mathcal{P}$ the following trade-off between congestion $C_{\mathcal{P}}(G_n)$ and dilation $D_{\mathcal{P}}(G_n)$ exists:*

$$C_{\mathcal{P}}(G_n) \cdot (D_{\mathcal{P}}(G_n))^{\mathcal{D}-1} = \Omega(W) \ .$$

Proof: For $n = (3p)^{\mathcal{D}}$ we partition the 2-dimensional grid into three $p \times 3p$ rectangle shaped vertex sets V_1, V_2, V_3, such that V_1 contains all left vertices, V_3 all right vertices and V_2 the vertices in the middle. Similarly, we partition the 3-dimensional grid into three $p \times 3p \times 3p$ cubicle shaped vertex sets V_1, V_2, V_3.

In both cases G denotes the complete graph with vertex set G_n and $\mathcal{P}$ denotes a path system for the demand f. We concentrate on $\frac{1}{9}$th of the demand starting at V_1 heading for vertices in V_3. We define by $p_{i,j}$ the route from vertex v_i to vertex v_j. Let $\ell(p_{i,j}) := f(u_i, u_j) := W/n^2$ denote the information flow on path $p_{i,j}$.

Consider two vertices $v_i \in V_1$ and $v_j \in V_3$. Then the path $p_{i,j}$ has at most $D_{\mathcal{P}}(G)$ edges. It follows from Lemma 4.13 that the induced communication load $\kappa_{G,\ell}(p_{i,j})$ of the path $p_{i,j}$ is at least $\kappa_{G,\ell}(p_{i,j}) \geq k_{\mathcal{D}} \ell(p_{i,j}) \sum_{e \in p_{i,j}} |e|^{\mathcal{D}} = k_{\mathcal{D}} \frac{W}{n^2} \sum_{e \in p_{i,j}} |e|^{\mathcal{D}}$. This term is minimized if the path uses the maximum possible number $D_{\mathcal{P}}(G)$ of edges and all edges have equal length of $|e| = \frac{|u_i - v_j|}{D_{\mathcal{P}}(G)}$. Since $|u_i - v_j| \geq p = \frac{1}{3} \sqrt[\mathcal{D}]{n}$, this implies $\kappa_{G,\ell}(p_{i,j}) \geq \frac{k_{\mathcal{D}} W}{3^{\mathcal{D}} n D_{\mathcal{P}}(G)^{\mathcal{D}-1}}$.

The length of the diagonal of the grid can be upper bounded by $\sqrt{\mathcal{D}} \sqrt[\mathcal{D}]{n}$ (a side of the grid has length $3p = \sqrt[\mathcal{D}]{n}$). Hence, all points with non-zero communication load reside in a square S with edge length $3\sqrt{\mathcal{D}} \sqrt[\mathcal{D}]{n}$. Lemma 4.12 states that the communication load of S with area $A(S) = (3\sqrt{\mathcal{D}})^{\mathcal{D}} n$ is bounded by

$$\kappa(G, \ell)(S) \ \leq \ c_{\mathcal{D}} \cdot C_{\mathcal{P}}(G) A(S) \ = \ c_{\mathcal{D}} \cdot C_{\mathcal{P}}(G) \cdot (3\sqrt{\mathcal{D}})^{\mathcal{D}} n \ .$$

The sum of the communication load induced by all paths $p_{i,j}$ cannot extend the communication load of S.

$$\sum_{v_i \in V_1} \sum_{v_j \in V_3} \kappa_{G,\ell}(p_{i,j}) \leq \kappa_{G,\ell}(S) \ .$$

Combining the inequalities we get

$$\frac{n^2}{9}\frac{k_{\mathcal{D}}W}{3^{\mathcal{D}}nD_{\mathcal{P}}(G)^{\mathcal{D}-1}} \leq \sum_{v_i\in V_1}\sum_{v_j\in V_3}\kappa_{G,\ell}(p_{i,j}) \leq \kappa_{G,\ell}(S) \;\leq\; c_{\mathcal{D}}\cdot C_{\mathcal{P}}(G)\cdot(3\sqrt{\mathcal{D}})^{\mathcal{D}}n\;.$$

This states the claim, since

$$C_{\mathcal{P}}(G)(D_{\mathcal{P}}(G))^{\mathcal{D}-1} \;\geq\; \frac{k_{\mathcal{D}}W}{c_{\mathcal{D}}9^{\mathcal{D}+1}\sqrt{\mathcal{D}}^{\mathcal{D}}}\;.$$

■

Dilation versus Energy

The simplest location of nodes is the line vertex set L_n as investigated in [KKKP00], see Figure 4.10. Here all vertices $L_n = \{v_1,\ldots,v_n\}$ are placed on a line of length Δ with equal distances $|v_i - v_{i+1}| = \frac{\Delta}{n-1}$ for $i \in \{1,\ldots,n\}$. Only the leftmost and the rightmost node want to exchange messages, i.e. $f(v_1,v_n) = W$ and $f(v,w) = 0$ for all other pairs (v,w). The energy-optimal network for unit and flow energy is the path $(v_1,v_2,\ldots,v_n)$, given the unit energy U-Energy$_{\mathcal{P}}(L_n) = (n-1)\frac{\Delta^2}{(n-1)^2} = \frac{\Delta^2}{n-1}$, the flow energy F-Energy$_{\mathcal{P}}(L_n) = \frac{\Delta^2 W}{n-1}$ and the dilation n.

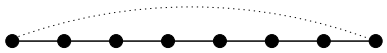

Figure 4.10: The line L_n

The fastest network realizes only the edge $\{v_1,v_n\}$ with hop-distance 1 and unit energy Δ^2 (and flow energy $W\Delta^2$). There are path systems that can give a compromise between these extremes. However, it turns out that the product of dilation and energy cannot be decreased:

Theorem 4.11 *Given the vertex set L_n with diameter Δ then for every path system $\mathcal{P}$ the following trade-offs between dilation D and unit energy* U-Energy *(resp. flow energy* F-Energy*) exist:*

$$\begin{aligned} D_{\mathcal{P}}(L_n)\cdot \textit{U-Energy}_{\mathcal{P}}(L_n) &= \Omega(\Delta^2)\;,\\ D_{\mathcal{P}}(L_n)\cdot \textit{F-Energy}_{\mathcal{P}}(L_n) &= \Omega(\Delta^2 W)\;. \end{aligned}$$

Proof: Let m be the hop length, i.e. the number of edges on the longest path of $\mathcal{P}$ (w.l.o.g. we assume that there are only edges with non-zero information flow $\ell(e) > 0$). For the unit energy model we can assume that there is only a path P from v_1 to v_n, since introducing more edges needs additional energy without decreasing the dilation. We have to minimize U-Energy$_{\mathcal{P}}(p) := \sum_{i=1}^{m}(L_i)^2$ defined by the edge lengths $L_1,\ldots,L_m$, where $\sum_{i=1}^{m} L_i = \Delta$. Clearly, the energy sum is minimal for $L_1 = L_2 = \cdots = L_m = \frac{\Delta}{m}$ giving U-Energy$_{\mathcal{P}}(p)\cdot D_{\mathcal{P}}(p) \;\geq\; \Delta^2$. The bound for the flow energy follows analogously. ■

The Incompatibility of Congestion and Energy

We show that for some vertex sets congestion and energy are incompatible. This is a worst case trade-off-situation since there is no possible compromise between congestion and energy.

The vertex set $U_{\alpha,n}$ for $\alpha \in [0, \frac{1}{2}]$ consists of two horizontal parallel line graphs L_{n^α} and contains n vertices. Neighbored (and opposing) vertices have distance $\frac{\Delta}{n^\alpha}$ for any Δ. There is only demand W/n^α between the vertical pairs of opposing vertices of the line graphs. The rest of the $n - n^\alpha$ vertices are equidistantly placed between the vertices of each line graph and the leftmost vertical pair of vertices (see Figure 4.11).

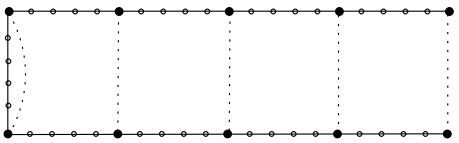

Figure 4.11: Vertex set U_α, n

The minimum spanning tree consists of n vertices and $n - 1$ edges where all edges have length $\Theta(\Delta/n)$. This results in a total unit energy of

$$\text{U-Energy}_{\text{MST}}(U_{\alpha,n}) = \mathcal{O}(\Delta^2 n^{-1})$$

and flow energy of

$$\text{F-Energy}_{\text{MST}}(U_{\alpha,n}) = \mathcal{O}(W\Delta^2 n^{-1}) \, .$$

The congestion of the same network is given by

$$C_{\text{MST}}(U_{\alpha,n}) = \mathcal{O}(W) \, .$$

The congestion optimal path system $\mathcal{P}'$ connects only vertices with non-zero demand. Its congestion is

$$C_{\mathcal{P}'}(U_{\alpha,n}) = \mathcal{O}(Wn^{-\alpha})$$

and its unit energy is

$$\text{U-Energy}_{\mathcal{P}'}(U_{\alpha,n}) = \mathcal{O}(\Delta^2 n^{-\alpha}) \, .$$

The flow energy is given by

$$\text{F-Energy}_{\mathcal{P}'}(U_{\alpha,n}) = \mathcal{O}(Wn^{-\alpha}\Delta^2) \, .$$

Lemma 4.15 *For $\alpha \in [0, \frac{1}{2})$ and the vertex set $U_{\alpha,n}$ with diameter Δ let $x \in \{0, \ldots, n^\alpha\}$ be the number of edges of length at least $\Delta n^{-\alpha}$ of a path system for the radio network and let $r \in [0, W]$ be the information flow on these edges. Then we have for the congestion C, unit energy and flow*

energy:

$$\begin{aligned} \textit{U-Energy}_{\mathcal{P}}(U_{\alpha,n}) &\geq \max\left\{\frac{\Delta^2}{4n}, \frac{x\Delta^2}{n^{2\alpha}}\right\}, && (4.2)\\ C_{\mathcal{P}}(U_{\alpha,n}) &\geq \frac{W}{x+1}, && (4.3)\\ \textit{F-Energy}_{\mathcal{P}}(U_{\alpha,n}) &\geq \max\left\{W\frac{\Delta^2}{4n}, r\frac{\Delta^2}{n^{2\alpha}}\right\}, && (4.4)\\ C_{\mathcal{P}}(U_{\alpha,n}) &\geq \max\left\{\frac{r}{12n^{\alpha}}, W-r\right\}. && (4.5) \end{aligned}$$

Proof: The energy consumption of the minimum unit energy network is given by the U-shaped path (MST). The minimum hop-distance between the half of the communication partners is at least $n/2$. Hence, the minimum energy is at least $\frac{\Delta^2}{2n}$. For x edges of length Δ/n^{α} the unit energy cost of theses edges alone is $\frac{x\Delta^2}{n^{2\alpha}}$. In the case of flow energy, we get the additional factors.

For simplicity we call an edge with minimum length Δ/n^{α} a long edge. Note that every long edge $\{u, v\}$ that connects two points on the same horizontal line or one of the leftmost vertical pair and a horizontal line does not reduce the congestion of any point that lies between u and v according to the minimum unit energy network. So, let x denote the number of edges connecting nodes of the lower row with the upper row. Using these x edges the minimum cut of the path system between upper row and the lower row is $x + 1$. Hence, the minimum load on every edge of this cat is $\frac{W}{x+1}$. If we optimistically assume that these edges do not interfere we obtain the lower bound.

Now let r denote the number of messages that are delivered on long edges connecting the lower with the upper row. Now consider the rectangular region R between the rows. The communication load of each of these long edges e induced into this region R of area $A(R) = \frac{\Delta^2}{n^{\alpha}}$ is at least $\frac{\Delta^2}{2n^{2\alpha}}\ell(e)$. Therefore the communication load induced by all these edges is at least $r\frac{\Delta^2}{2n^{2\alpha}}$ and at most $c_2 C_{\mathcal{P}}(U_{\alpha,n})A(R) = 6\frac{\Delta^2}{n^{\alpha}}C_{\mathcal{P}}(U_{\alpha,n})$. This implies

$$C_{\mathcal{P}}(U_{\alpha,n}) \geq \frac{r}{12n^{\alpha}}.$$

The residual $W - r$ packets need to be routed between the shorter edges of the leftmost vertices. Even without radio interference at least congestion W_r will occur. ∎

Theorem 4.12 *There exists a vertex set V with a path system minimizing congestion to C^*, and another path system optimizing unit energy by U-Energy* and minimal flow energy by F-Energy* such that we have for any path system $\mathcal{P}$ on this vertex set V*

$$\begin{aligned} C_{\mathcal{P}}(V) &= \Omega(n^{1/3}C^*) \quad \textit{or}\\ \textit{U-Energy}_{\mathcal{P}}(V) &= \Omega(n^{1/3}\textit{U-Energy}^*),\\ C_{\mathcal{P}}(V) &= \Omega(n^{1/3}C^*) \quad \textit{or}\\ \textit{F-Energy}_{\mathcal{P}}(V) &= \Omega(n^{1/3}\textit{F-Energy}^*). \end{aligned}$$

Proof: The claim follows directly by Lemma 4.15 using the graph $V = U_{1/3,n}$. ∎

Hence, it is not possible to optimize more than one parameter at the same time. The wireless network designer has to decide in favor of small congestion or low energy consumption.

4.2 Directional Communication

In this section, we focus on *directional* single frequency, power-variable ad hoc networks. We assume that every station is equipped with a fixed number k of wireless transmitters and can send and receive radio signals independently and in parallel in k (disjoint) sectors or cones. Every node is allowed to adjust the transmission power in each of its sectors.

In comparison with the traditional use of omnidirectional transmitters, we show improvements in efficiency and capacity of ad hoc networks due to directional communications which can also be described as one kind of space multiplexing. In the following subsections, we compare different network topologies for basic networks, i.e. the Yao-graph (or θ-graph or sector graph or YG) and some also known related topologies, which will be called the SparsY-graph (or sparsified Yao-graph or YY) and the SymmY-graph (or symmetric Yao-graph or YS).

We compare elementary graph properties and consider the communication features. Especially, we investigate how these network topologies bound the amount of (unidirectional and bidirectional) interference and whether these basic networks allow us to approximate energy- and/or congestion-optimal path systems. It turns out that in a worst case scenario, the SparsY-graph combines good performance in terms of interference, congestion, and energy: for energy it allows us a constant factor approximation and a $\mathcal{O}(\log n)$ approximation of congestion using realistic settings.

In cooperation with electrical engineers, we have developed an infrared communication module for the mini-robot Khepera [MFG99, KTe00] that can transmit and receive data in eight sectors using infrared light with variable transmission distances up to one meter (see Figure 4.12). We have used a colony of Khepera robots, each equipped with such a module, to show that the directional approach is also suitable in practical situations. Besides our simulations, see Chapter 6, this has been very helpful to evaluate our results using realistic settings. Our hardware model allows us sector-independent directional communication, adjustable transmission power, one frequency, and interference detection. Nowadays communication techniques make it also possible to build up such a wireless network using directional antennae, adaptive antennae, or beam-forming antennae. There exists a lot of works concerning wireless networks using directional antennae, e.g., [HP96, BGLA02, Oka98, Ram01, TMBR02, CYVR02, GY04, KSV00].

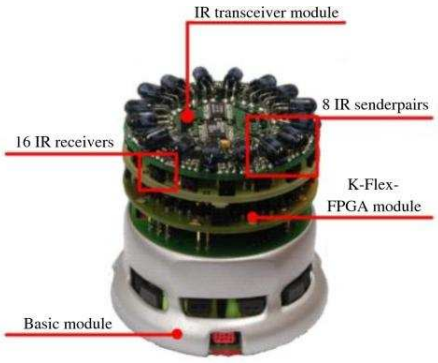

Figure 4.12: The mini-robot Khepera equipped with an infrared communication module

To the best of our knowledge we are one of the first who combined theoretical algorithmic research and prototypical realization of the directional communication model. On the one hand, we present mathematical analyses and prove interesting properties. On the other hand, we have implemented our algorithms in testbeds as well as in prototypical environments in cooperation with electrical engineers and show that they perform well in realistic szenarios. In the meantime, similar algorithmic approaches using a directional or a cone-based or a sectorized modeling can be found, e.g., in [WLWF02, LWW01, WL02, ALW+03, LHB+01, SWL04, WL03]. But all works differ in assumptions. In some works the knowledge of coordinates is assumed given by a GPS module or there is some centralized administration necessary, e.g., in [CJBM01, XHE01], or sectorized topologies are used in an omnidirectional communication model to approximate the unit disk graph. In the last case the omnidirectional antennae have to be equipped with additional functionalities like the detection of the angle of incoming signals to get a rough estimation in which sector a signal is received. Excellent surveys of applications of computational geometry in ad hoc networks, especially with focus on topology control and routing, are presented by X.-Y. Li [Li03b, Li03a, Li03c] and R. Rajaraman [Raj02].

The remainder of this section is organized as follows. In Subsection 4.2.1 we introduce our communication and our hardware model in which we allow each node to transmit data in parallel in a fixed number of (non-overlapping) sectors. In addition, we discuss assumptions concerning the location of nodes. In Subsection 4.2.2 we present three different sectorized topologies, namely the Yao-graph, the SparsY-graph, and the SymmY-graph. In Subsection 4.2.3 we prove that the SparsY-graph is a weak c-spanner for a constant c if more than 6 sectors/senders per node are available. Hence, we can apply our results of Chapter 3 to show that the SparsY-graph is a C-power spanner for some constant C depending only on c. This implies directly that the SparsY-graph allows us to approximate an energy-optimal path system by a constant factor. Furthermore, we show that the SymmY-graph is neither a weak spanner nor a power spanner, in general. Nevertheless, we prove that it is connected if every station is equipped with more than 6 transmitters. In Subsection 4.2.4, we introduce the unidirectional interference number and compare network properties. Since a weak spanner as a communication network allows us an approximation of a congestion optimal path system by a factor of $\mathcal{O}(g(V))$, where $g(V)$ denotes the diversity of V (see Section 4.1), we prove that the Yao-graph gives an $\mathcal{O}(n \cdot g(V))$ approximation in consideration of bidirectional interference which can be regarded as $\mathcal{O}(n \log n)$ in real-world applications. For the SparsY-graph this approximation factor is given by $\mathcal{O}(g(V))$ resp. $\mathcal{O}(\log n)$ taken unidirectional interference into account.

4.2.1 Modeling Directional Communication

One aim of this thesis was to design, to analyze, and to implement algorithms for ad hoc networks based on the directional communication model. Besides the traditional use of omnidirectional antennae, we wanted to investigate the effect of space multiplexing techniques and variable transmission powers on the efficiency and capacity of ad hoc networks. Therefore our stations can send and receive radio signals independently in k sectors of angle $\theta = 2\pi/k$ using one frequency. Furthermore, our radio stations can regulate its transmission power for each transmitted signal. As mentioned already in Section 4.1 a major problem in wireless networks is the effect of inter-

fering (radio) signals. Analogously to the interference problems in the omnidirectional communication model, see Figure 4.1, we have directed hidden and exposed terminals as well as directed asymmetric interference in the directional communication model, see Figure 4.13. Solutions exist that reduce the negative outcome of these problems. For example, in [KSV00, CYVR02] the authors attempt to design new MAC protocols suitable for ad hoc networks based on directional antennae, i.e. directional MAC (D-MAC) schemes that combine the use of omnidirectional and directional control packets to reserve the channel.

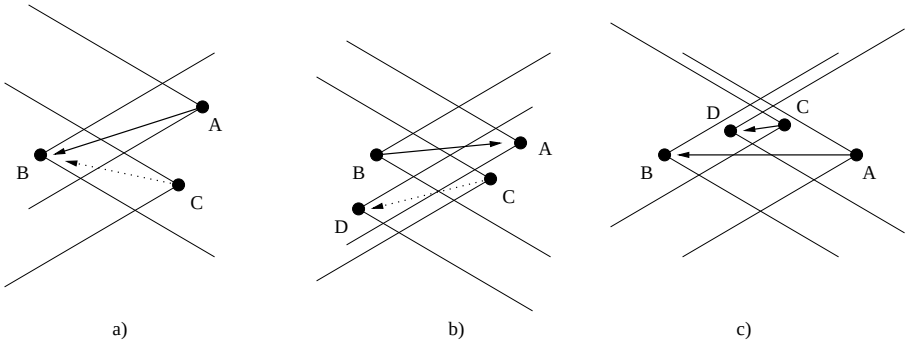

Figure 4.13: Directed hidden and exposed terminals: a) Node A is transmitting to node B. When C listens, C does not receive the signal from A, starts transmitting and the signals will interfere, b) B is transmitting to A. C listens (the sector in which D lies). Since it seemed to be busy, C does not start transmitting and throughput is decreased. Asymmetric interference: c) C is transmitting to D, the transmission power had been adjusted. For A the channel to B seems to be free and A also begins to send data. The shorter link breaks down.

We assume that most of the time the ad hoc network is stable and performs a communication protocol according to a given routing problem. In Section 4.1 we showed that the quality of the routing depends on the choice of the underlying network that we call the (basic) communication network or the topology. We want to investigate a distributed network model where the only information available is given by incoming radio signals and in which sector it is received. This gives a rough estimation of the direction to the sender.

In our **communication model**, we assume that a radio station u is able to detect three types of incoming signals: *no signal* indicates that no radio signal is transmitted at all or that all radio stations in distance d send with some transmission distance $d' < d$. The *interference signal* indicates that at least one radio station v transmits to a station w in this time step in a sector in which u lies and $|v - u| \leq |v - u|$. A *clear signal* is received by u if one radio signal with appropriated transmission power to cancel out weaker incoming signals is reaching u's antenna. Then u can read the transmitted information $m \in \{0,1\}^p$ of some length p. A communication round is the time necessary to send one packet of length p, where p is large enough to carry some elementary information like the sending station, the addressed stations (if specified), the transmission distance, and some control information.

We assume that there is a timing schedule adapted to the topology that allows the stations in a static time period to transmit and acknowledge packets over the network routes with only

small number of interfering packets. During such a phase we can neglect the interfering impact of acknowledgment signals. In [GRSV03] it is shown that assuming such a phase is realistic.

However when a connection is established the sending and answering signal have the same small length, because only control information needs to be transmitted. Then the impact of answering signals is the same as those of sending signals. Therefore, we consider two types of interference: the *unidirectional interference* in the routing mode and the *bidirectional interference* when connections are established or network changes are compensated.

In our **hardware model**, every node can choose the transmission power according to s discrete choices $p_1, \ldots, p_s$. The energy to send over distance d is given by d^δ for some constant $\delta \geq 2$, see Section 2.1. This defines the transmission distances $d_i = (p_i)^{1/\delta}$ for all $i \in \{1, \ldots, s\}$. Every node u has k sending and receiving devices which are located such that they can communicate in parallel within each of its k disjoint sectors with angle $\theta = 2\pi/k$. Every node u has been rotated by an angle $\alpha_u \in [0, 2\pi/k)$ which is unknown to u. Note that the radio stations have different offset angles α_u. If u sends a signal in the sector i for $i \in \{0, \ldots, k-1\}$ it actually sends into a direction described by the interval $R = [\alpha_u + i\theta, \alpha_u + (i+1)\theta)$ and can be received by the node v in sector j for $j \in \{0, \ldots, k-1\}$ if $R \cap [(\alpha_v + j\theta + \pi) \bmod 2\pi, (\alpha_v + (j+1)\theta + \pi) \bmod 2\pi) \neq \emptyset$. Of course v receives the packet from u only if in addition u sends this signal with transmission distance $d_i \geq |u - v|$.

Furthermore, we allow the radio stations to measure distances only by sending messages with varying transmission power. Then the receiving party can only decide whether the signal arrives or not. This restricts transmission distances to the set $S = \{d_1, \ldots, d_s\}$. Define $\tilde{D} : \mathbb{R} \to \{\varnothing, 1, \ldots, s\}$ as the minimum discrete choice of transmission power to send over a given distance by

$$\tilde{D}(x) := \begin{cases} \min\{i \mid d_i \geq x\} & \text{if } x \leq d_s \\ \varnothing & \text{if } x > d_s \end{cases}$$

Define $\sphericalangle(u, v)$ as the number of u's sector containing the edge (u, v) (note that $\theta = 2\pi/k$), i.e.

$$\sphericalangle(u, v) := \left\lfloor \frac{[\measuredangle(v - u) - \alpha_u]}{\theta} \right\rfloor \bmod k \,,$$

where $\measuredangle(x)$ denotes the angle of a vector x in $\mathbb{R}^2$.

One of the most delimiting properties is that radio stations do not know their locations. In the following we want to clarify some assumptions concerning the **location of nodes**. As mentioned in Section 2.3 we search for a good subgraph of the complete geometric graph or of the unit disk graph which fulfills specific properties. In this section every node can choose from a set of transmission distances, such that the maximum transmission range is bounded, i.e. it is not always possible to build up a complete graph, if it is wished, but we get a graph which is comparable with a unit disk graph. Here, it makes no sense to consider wireless networks where nodes take abnormal positions. We want to neglect problems occurring when the maximum transmission distance is shorter than distances between nodes. Therefore, in our practical setting, we assume a nice and normal vertex set. This particularly means that there is always only one nearest neighbor in each sector.

Definition 4.4 *A vertex set V is in* **general position***, if there are no vertices $u, v, w \in V$ with $v \neq w$ and $|u-v| = |u-w|$. We call a vertex set* **normal***, if for a fixed polynomial $p(n)$ we have*

$$\frac{\max_{u,v \in V} |u-v|}{\min_{u,v \in V, u \neq v} |u-v|} \leq p(n) \ .$$

Because of the discrete model for the transmission distances we cannot distinguish distances within $[d_i, d_{i+1})$. However, we assume that these distances form a fine granular scale.

Definition 4.5 *We call the locations of radio stations* **nice***, if we have $\tilde{D}(|u-v|) \neq \varnothing$ for all $u, v, w \in V$ and*

$$v = w \qquad \Longleftrightarrow \qquad \sphericalangle(u,v) = \sphericalangle(u,w) \wedge \tilde{D}(|u-v|) = \tilde{D}(|u-w|) \ .$$

Note that we do not need nice and normal vertex sets for our mathematical analyses. We need only the assumption that the node set V is not degenerated, i.e. no point in V is placed on the boundary of a sector of another point in V, and we assume unlimited transmission ranges.

4.2.2 Directional Topologies

We consider a set of n nodes distributed in the Euclidean plane. Since every node has $k \in \mathbb{N}$ transmission devices that allow each node sending data in *sectors*, we divide the area around a node into k equal non-overlapping sectors of angle $2\pi/k$, see Figure 4.14. This is an idealized assumption because we assume that these sectors do not overlap and have fixed borders. In reality, sectors overlap, borders are not fixed, and physical effects like areas with no reception occur. In Chapter 6 we present the results of our simulations using realistic propagation models.

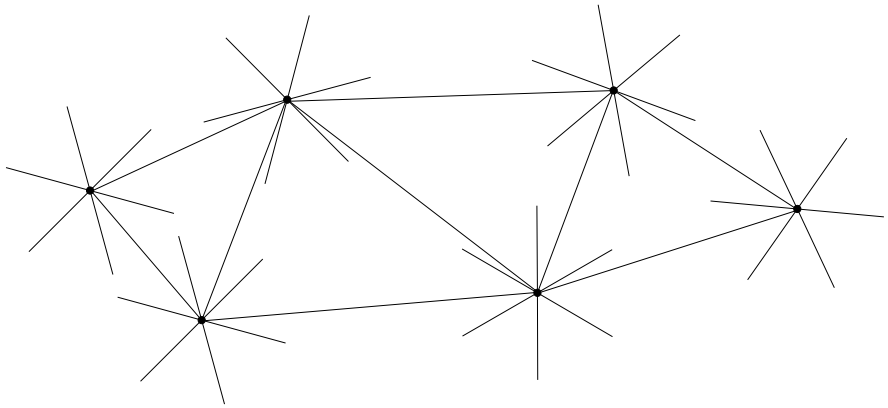

Figure 4.14: The area around a node is divided into a fixed number of sectors, in this case 6. In each of its sectors a node can establish communication links.

Since our underlying hardware model allows a node to communicate in k (disjoint) sectors in parallel, a straight-forward approach is to choose as a communication partner the nearest neighbor in a sector. This leads directly to the definition of the Yao-graph. Here, in each sector a

node establishes a communication link to the nearest node in this sector. Note that the definition of nearest neighbor differs in some approaches because of additional side conditions. We use the definition where the nearest node in a sector is given by the node with the shortest Euclidean distance. Furthermore, we assume that a nearest neighbor is unique, i.e. we do not consider the case of degenerated vertex sets or in the case of more than one nearest neighbor in a sector we choose the one with the lowest identification (see [WL02]) respectively. Hence, the out-degree of the Yao-graph is bounded by k, but a node can be the nearest neighbor of many nodes. To overcome this problem of high in-degree resulting time-consuming interference resolution schemes (high interference), we present further Yao-graph based topologies. In the SparsY-graph (or sparsified Yao-graph or YY) every node accepts only the shortest incoming communication link. Finally, in the SymmY-graph (or symmetric Yao-graph or YS) only links are established that are symmetric. More formally, we get the following definitions (note that we have investigated these structures in parallel to the authors of [LWW01, WLWF02]):

Definition 4.6 *Let $V \subseteq \mathbb{R}^2, k \in \mathbb{N}$ and $G = (V, E)$ be a geometric graph. The area around a node $u \in V$ is divided into k non-overlapping sectors or cones of angle $\theta = 2\pi/k$. We denote the sector of u in which a node $v \in V$ lies by $\sphericalangle(u, v)$.*

- *G is the* Yao-graph (Yao(V)) *of V, if $E := \{(u, v) \mid \forall w \neq u : \sphericalangle(u, v) = \sphericalangle(u, w) \Rightarrow |u - v| < |u - w|\}$.*
- *G is the* SparsY-graph (SparsY(V)) *of V, if $E := \{(u, v) \in E(\overline{G}) \mid \forall w \neq u : ((w, v) \in E(\overline{G})$ and $\sphericalangle(v, w) = \sphericalangle(v, u)) \Rightarrow |u - v| < |w - v|\}$ where $\overline{G}$ denotes the Yao-graph of V.*
- *G is the* SymmY-graph (SymmY(V)) *of V, if $E := \{(u, v) \in E(\overline{G}) \mid (v, u) \in E(\overline{G})\}$ where $\overline{G}$ denotes the SparsY-graph of V.*

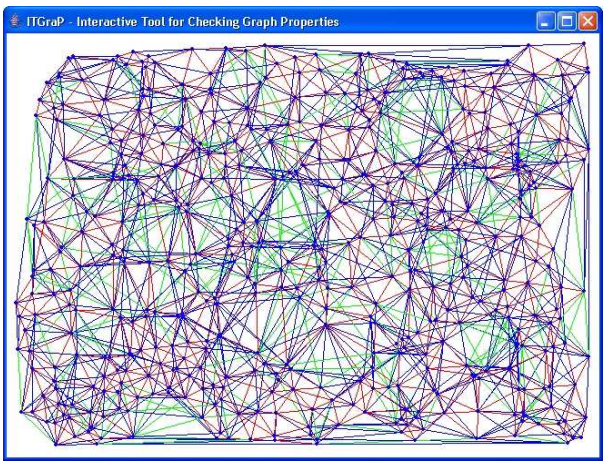

Figure 4.15: Yao(V) of a random vertex set V of 500 nodes with 8 sectors.

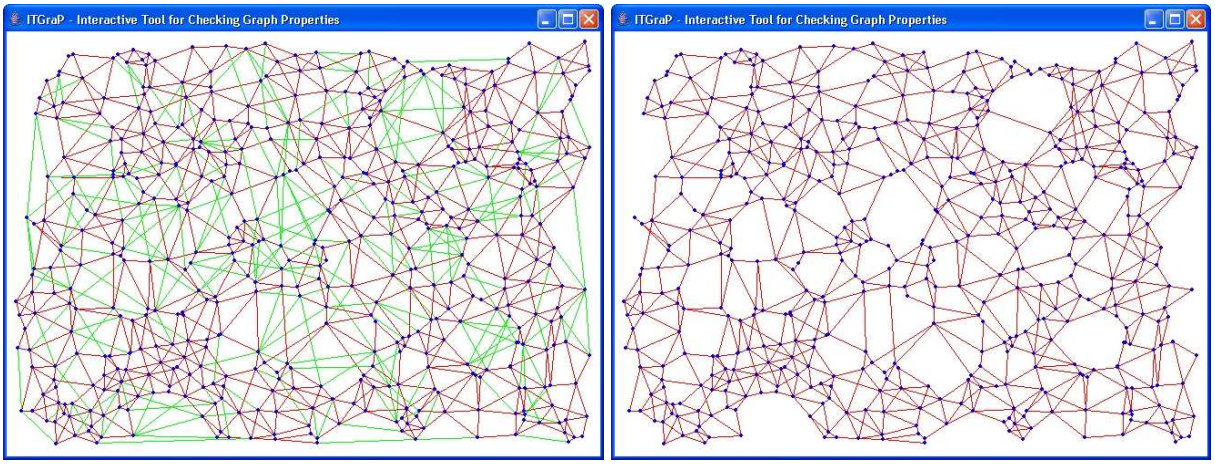

Figure 4.16: SparsY(V) and SymmY(V) of a random vertex set V of 500 nodes with 8 sectors.

All three topologies or graphs are sparse graphs, i.e. the number of edges in a graph is upper bounded by $\mathcal{O}(|V|)$, in this case even exactly by $k \cdot |V|$. Examples of the Yao-graph and its variants are given in Figure 4.15 and Figure 4.16. We used our tool presented in Section 6.2 to generate the three graphs of a random vertex set V of 500 nodes in wich every node is equipped with 8 sectors/senders. The reader should observe the decreasing edge density from the first to the third picture. Brighter edges indicate edges which appear in the SparsY-graph but not in the SymmY-graph. Clearly, the SparsY-graph and the SymmY-graph are graphs with bounded in- and out-degree. Definition 4.6 directly implies that the SymmY-graph is a subgraph of the SparsY-graph, and that the SparsY-graph is a subgraph of the Yao-graph. The figures point out this relation. It is known that all three graphs can be constructed locally, e.g., using a sweepline algorithm in time $\mathcal{O}(n \log n)$ if the orientation of the sectors on the nodes is fixed and equal on all nodes (see [FLZ98, FMS97]).

4.2.3 Elementary Graph Properties

The Yao-graph [Yao82] was first introduced to computational geometry for constructing minimum spanning trees in k-dimensional space and related problems. In [FLZ98] it was proven that Yao(V) is a weak $\left(\sqrt{3+\sqrt{5}}\right)$-spanner for $k = 4$. In [FMS97], the authors showed that Yao(V) is a weak $\max\left\{\sqrt{1+48\sin^4(\pi/k)}, \sqrt{5-4\cos(2\pi/k)}\right\}$-spanner for $k \geq 6$. Furthermore, it is known that Yao(V) is a $1/(1-2\sin(\pi/k))$-spanner for $k > 6$ [RS91].

It is easy to construct examples for $k \leq 3$ such that the Yao-graph with k sectors is not connected when the orientation of the sectors on the nodes is fixed and equal on all nodes. In this case Yao-graphs are provably connected for $k \geq 4$. There exist placings such that the Yao-graph, the SparsY-graph, and the SymmY-graph are not connected using less than 6 sectors when we assume an offset angle α_u for each node (see Figure 4.17). Later on, we show that SymmY-graphs are always connected for $k > 6$, i.e. all three variants guarantee connectivity for $k > 6$. The case $k = 6$ depends on assumptions: if we assume non-degenerated vertex sets, i.e. no point

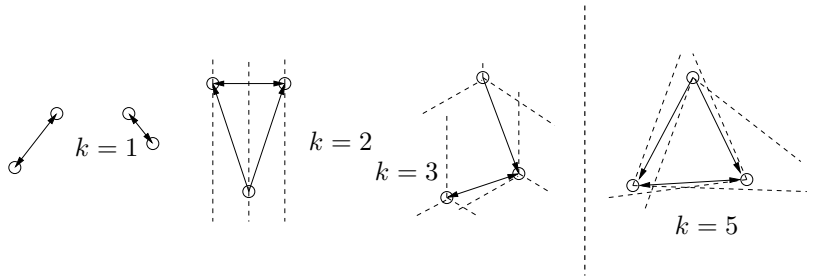

Figure 4.17: Yao-graphs are not always connected for $k \leq 3$ when the orientation of the sectors on the nodes is fixed and equal on all nodes (left). In our model we assume an arbitrary offset angel α_u for each node u, such that all three graphs are not always connected for $k \leq 5$ (right).

in V is placed on the boundary of a sector of another point in V, all the following results for $k > 6$ hold also for $k = 6$. In real-world applications we can assume non-degenerated node placements due to technical inaccuracies, e.g., very small differences in the size of the hosts or in the alignment of transmitters etc.

Observation 4.1 *Let $V \subseteq \mathbb{R}^2$ and n:=$|V|$. Then SymmY$(V) \subseteq$ SparsY$(V) \subseteq$ Yao(V) and*

Topology	*Yao(V)*	*SymmY(V)*	*SparsY(V)*
in-degree	$n-1$	k	k
out-degree	k	k	k
degree	$n-1$	k	$2k$

Now we show that the Yao-graph is a c-power spanner for some constant c.

Theorem 4.13 *Let $V \subseteq \mathbb{R}^2$ and $k > 6$. Then Yao(V) is a $\left(\left(\frac{1}{1-2\sin(\pi/k)}\right)^{\delta}, \delta\right)$-power spanner.*

Proof: Since Yao(V) is a c-spanner for $k > 6$ and $c = 1/(1 - 2\sin(\pi/k))$, we apply Theorem 3.2: every c-spanner is (c^{δ}, δ)-power spanner and the claim follows directly. ■

Theorem 4.14 shows a stronger result proven in [LWW01].

Theorem 4.14 *[LWW01] Let $V \subseteq \mathbb{R}^2$ and $k > 6$. Then Yao(V) is a $\left(\frac{1}{1-(2\sin(\pi/k))^{\delta}}, \delta\right)$-power spanner.*

It is an open problem whether all SparsY-graphs are c-spanners, i.e. the shortest path between vertices in the network is at most c-times longer than the Euclidean distance. It was proven in [WL02] that SparsY-graphs are c-spanners for a constant c in civilized graphs. In a civilized graph the distance between any two nodes is larger than a positive constant λ. The power spanner property follows analogously in civilized graphs. In the following we show that SparsY-graphs are weak c-spanners for a constant c, in general. But first, we need a technical lemma.

Lemma 4.16 *Let $V \subseteq \mathbb{R}^2$ and $k > 6$. Consider two vertices u, v, then for all $w \in V$ with $|u-w| \leq |u-v|$ and $\sphericalangle(u,w) = \sphericalangle(u,v)$ it holds that $|u-w|+|w-v| < |u-v|+2\sin(\pi/k)|u-v|$.*

Proof: Let w' be the point on the line segment uv with $|u-w'| = |u-w|$. Then $|w'-v| = |u-v| - |u-w'| = |u-v| - |u-w|$ and therefore $|u-w| = |u-v| - |w'-v|$. Furthermore, we have $|w-w'| < 2\sin(\pi/k)|u-v|$ and $|w-v| \leq |w-w'| + |w'-v|$. Combining the facts yields the claim. ■

Now we are ready to prove that every SparsY-graph is a weak spanner if more than 6 sectors/senders per node are available.

Theorem 4.15 *Let $V \subseteq \mathbb{R}^2$ and $k > 6$. Then SparsY(V) is a weak c-spanner for $c = \frac{1}{1-2\sin(\pi/k)}$.*

Proof: Let $G = (V, E)$ be the SparsY-graph and $G_Y = (V, E_Y)$ be the underlying Yao-graph. For any two vertices $u, v \in V$ we will show how to find a directed path from u to v in the SparsY-graph that is inside a disk with center u and radius $|u-v|/(1-2\sin(\pi/k))$.

For a sector i, define the Yao-neighbor w of the vertex u as the (unique) vertex w with $(u,w) \in E_Y$. Now if u has no directed edge in a sector i in G, then either the sector is empty, i.e. there is no edge in the Yao-graph, or there is a Yao-neighbor w in sector i, i.e. $(u,w) \in E_Y$. In the second case there must be another vertex w' in another sector of u, but in the same sector of w as u, with $(w',w) \in E$ and $|w'-w| < |u-w|$ and $|u-w'| < |u-w|$ since $k > 6$, see Figure 4.18 (left). Note that u has at least one nearest neighbor w'' in a sector, i.e. $\exists w'' \in V : (u,w'') \in E$. This is the vertex $w'' \in V$ with the shortest Euclidean distance to u.

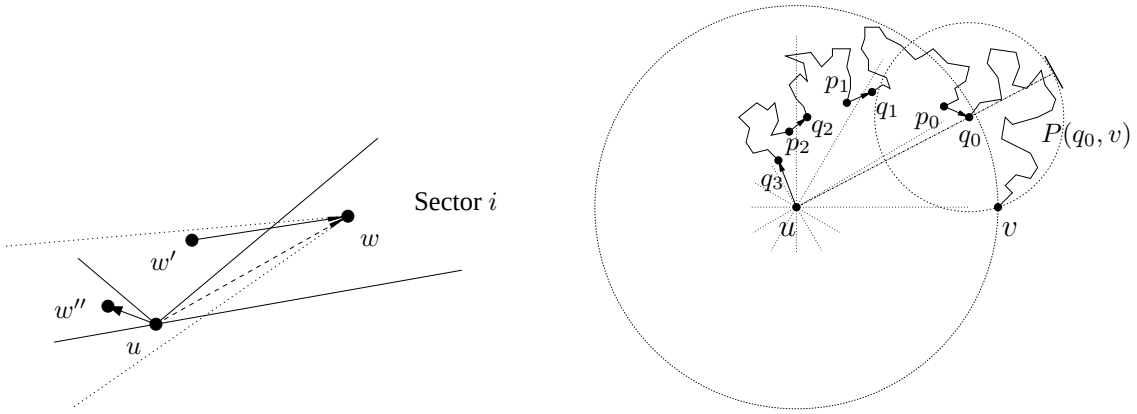

Figure 4.18: Weak spanner property of the SparsY-graph

Now we recursively construct the path $P(u,v)$ from u to v using some of the Yao-neighbors of u. An example of such a path is given in Figure 4.18 (right). If $(u,v) \in E$ then $P(u,v) = (u,v)$, if $u = v$ then $P(u,v) = (u = v)$. If in sector $i = \sphericalangle(u,v)$ the Yao-neighbor, called q_0, is not directly connected to u. Then we know that there exists an edge $(p_0, q_0) \in E$, where p_0 is in a sector $i_1 \neq i_0$ of u and $|u-p_0| < |u-q_0|$ since $k > 6$. Furthermore, we have that $|u-q_0| \leq |u-v|$. Then we repeat this consideration for the sector i_1 and replace p_0 by v.

This iteration ends when a Yao-neighbor q_m or p_m is directly connected to u, i.e. $(u, q_m) \in E$ or $(u, p_m) \in E$. Because every node has at least one neighbor in E this process terminates.

Now we recursively define the path $P(u, v)$ from u to v that terminates at node q_m by

$$P(u, v) = (u, q_m) \circ P(q_m, p_{m-1}) \circ (p_{m-1}, q_{m-1}) \circ \ldots \circ P(q_1, p_0) \circ (p_0, q_0) \circ P(q_0, v).$$

For p_m the path can be defined analogously: we replace (u, q_m) by $(u, p_m) \circ (p_m, q_m)$. Note that all nodes p_i, q_i are inside the disk with center u and radius $|u - v|$, see Figure 4.18 (right). Furthermore, we have $|q_i - p_{i-1}| < |u - v|$. In the next recursion step, i.e. if we assume that the same construction works for all $P(q_i, p_{i-1})$, vertices of the path may lie outside of this disk. However Lemma 4.16 implies that the maximum disk amplification of this recursion step can be bounded by $2\sin(\frac{\pi}{k})\,|u - v|$. Now let r be the depth of the recursion, then by

$$\sum_{i=0}^{r} \left(2\sin\left(\frac{\pi}{k}\right)\right)^i |u - v| \leq \frac{1}{(1 - 2\sin(\frac{\pi}{k}))} \cdot |u - v|$$

it follows, that the path $P(u, v)$ from u to v lies completely inside the disk with center u and radius $|u - v|/(1 - 2\sin(\frac{\pi}{k}))$. ■

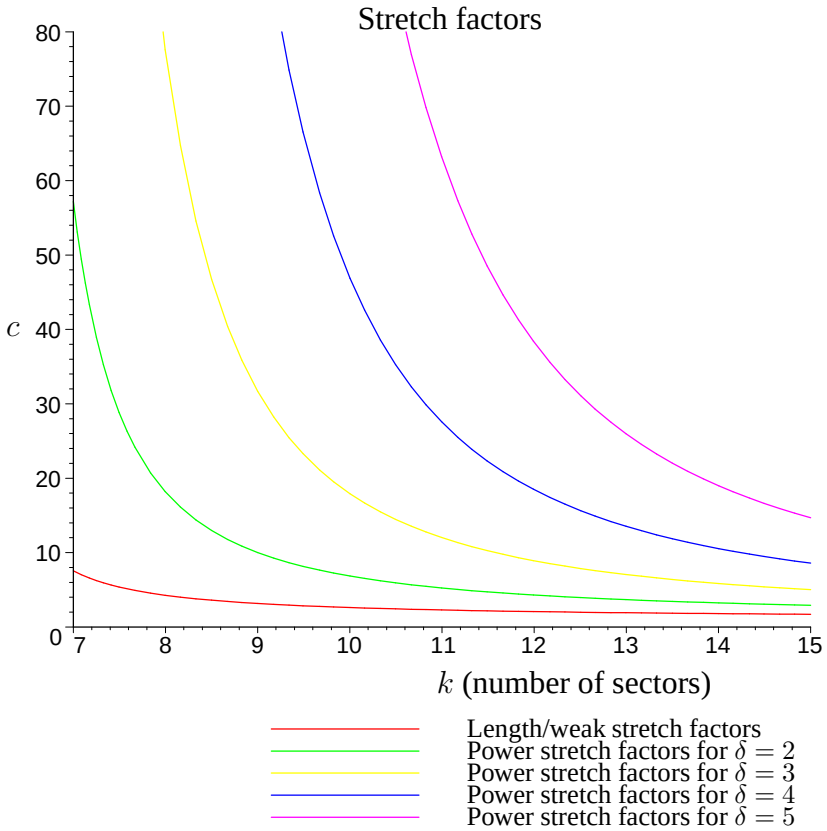

Figure 4.19: Stretch factors of the Yao-graph and the SparsY-graph.

Figure 4.19 gives an overview of the stretch factors of the Yao-graph and the SparsY-graph. The length and the weak stretch factors are given respectively. Furthermore, the power stretch factors of the Yao-graph given by Theorem 4.14 are presented for different values of δ. In the following we present an upper bound for the δ-cost of the path constructed in Theorem 4.15. If we assume that in a recursion step all k sectors are used as specified in Theorem 4.15 then there is only one edge of length at most $|u-v|$ in the first step, see Figure 4.18 (right), and in step i there are at most k^i new edges of length at most $(2\sin(\pi/k))^i|u-v|$. Hence, the δ-cost of the path $P(u,v)$ from u to v is given by

$$||P(u,v)||^\delta \leq \sum_{i=0}^{\infty}(k\cdot(2\sin(\pi/k)^\delta)^i|u-v|^\delta \leq \frac{1}{1-k\cdot(2\sin(\pi/k))^\delta}\cdot|u-v|^\delta$$

for $k\cdot(2\sin(\pi/k))^\delta < 1$. If we assume that $\sin\frac{1}{k}\approx\frac{1}{k}$, we get: $k > (2\pi)^{\frac{\delta}{\delta-1}}$. In the case that this upper bound is also an upper bound for the δ-cost of any path between u and v we could directly follow that SparsY(V) is a (c,δ)-power spanner for $k > (2\pi)^{\frac{\delta}{\delta-1}}$ where $c = \frac{1}{1-k\cdot(2\sin\frac{\pi}{k})^\delta}$. This means that SparsY(V) would be a power spanner for $k > 4\pi^2$, i.e. at least 40 sectors are necessary to fulfill the power spanner property for $\delta = 2$. Of course, this is not a proof but in the following we show a better result: SparsY(V) is already a power spanner for $k > 6$.

The SparsY-graph was investigated experimentally in [LWW01, WLWF02, Vol04a], see also Section 6.2 of Chapter 6, on uniformly and randomly distributed vertex sets. One conclusion was that the SparsY-graph might be a spanner and also a power spanner. The first conjecture is still open, while the latter was independently investigated in [JRS03] and [GLSV02]. In [GLSV02] we presented only the idea of a proof. The authors of [JRS03] presented a technical proof with lots of different cases and assumed further that $\theta \leq \pi/60$, i.e. when at least $k \geq 120$ sectors are present. Combining our results on the relation between weak spanners and power spanners and Theorem 4.15 we can show that the SparsY-graph is already a power spanner for $k > 6$ sectors.

Corollary 4.1 *Let $V \subseteq \mathbb{R}^2$ and $k > 6$. Then SparsY(V) is a c-power spanner for a constant c.*

Proof: We combine Theorem 4.15 and Theorem 3.5 and the claim follows directly. ∎

Now we solve the open problem stated in [WL02], whether the SymmY-graph is a c-spanner, or a power spanner by giving a negative answer:

Theorem 4.16 *Let $V \subseteq \mathbb{R}^2$ and $k = 6$. Then SymmY(V) is neither a weak c-spanner for any constant $c \in \mathbb{R}$, nor a (c,δ)-power spanner for any constant $c \in \mathbb{R}$ and $\delta > 1$.*

Proof: We present a construction (see Figure 4.20) for n points in the plane, such that the SymmY-graph of these points is not a weak c-spanner for any constant c and not a (c,δ)-power spanner for any constant c and $\delta > 1$.

Let ℓ_1 and ℓ_2 be two vertical lines of unit distance from each other, such that ℓ_2 is right to ℓ_1. Rotate ℓ_1 clockwise around its intersection point with the x-axis by a very small angle γ_c, and rotate ℓ_2 counter clockwise around its intersection point with the x-axis by an angle

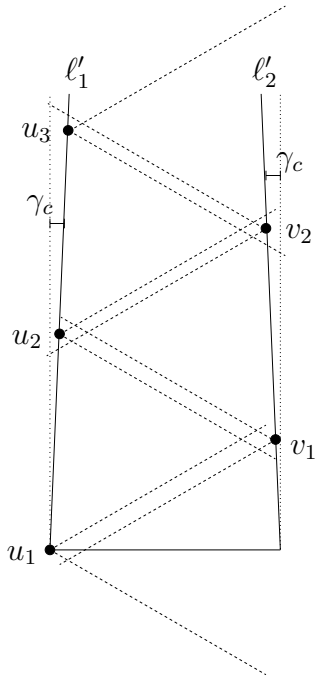

Figure 4.20: SymmY(V) for $k = 6$: construction with large stretch factors

γ_c. We denote the rotated lines by ℓ'_1 and ℓ'_2. Consider the vertex sets $U = \{u_1, \ldots, u_m\}$ and $V = \{v_1, \ldots, v_m\}$, $m = n/2$, placed on ℓ'_1 and ℓ'_2, respectively, as follows. Assume that for each point $u \in U$, the half-line, halving the ith sector of u is horizontal and directed in positive x-direction, and for $v \in V$, the half-line, halving the i'th sector of v is horizontal and directed in negative x-direction. The vertex u_1 is placed on the intersection point of ℓ_1 and the x-axis. We place v_1 on ℓ'_2 such that v_1 is in the ith sector of u_1 and it is very close to the upper boundary of the ith sector of u_1. The vertex u_2 is placed on ℓ'_1 in the i'th sector of v_1 close to the upper boundary of that sector. The vertex v_2 is placed on ℓ'_2 in the ith sector of u_2 close to the upper boundary of that sector and so on. Then the SymmY-graph does not contain any edge (u, v) such that $u \in U \setminus \{u_m\}$ and $v \in V \setminus \{v_m\}$. The nearest neighbor of u_1 in sector i is v_1, while v_1 has u_1 and u_2 also in sector i', where u_2 is nearer, etc. Only the last link u_m, v_m will be established. Therefore, even if there is a path from u_1 to v_1 in the SymmY-graph, its length is at least $|u_1 - u_m| + |u_m - v_m| + |v_m - v_1|$. For any given c we can choose γ_c appropriately small, in order to get $|u_1 - u_m|, |v_m - v_1| \geq c/2$. Analogous arguments hold if we look at the δ-cost of this path. ■

Now we extend the result of Theorem 4.16 to $k > 6$. Note that we have to modify the construction, since it does not work for $k > 6$. An important observation is that the construction for $k = 6$ does not change its characteristics if the placed nodes are not close to the boundaries of the sectors. All the arguments for $k = 6$ still hold for arbitrary distances between u_i and u_{i+1} if it is ensured that v_i is placed on ℓ'_2 in the middle between u_i and u_{i+1}.

In the following we discuss the problem for $k > 6$. First, we consider the case for even $k > 6$. As you can see in Figure 4.21 (left) we have not only to look at neighboring sectors but also in

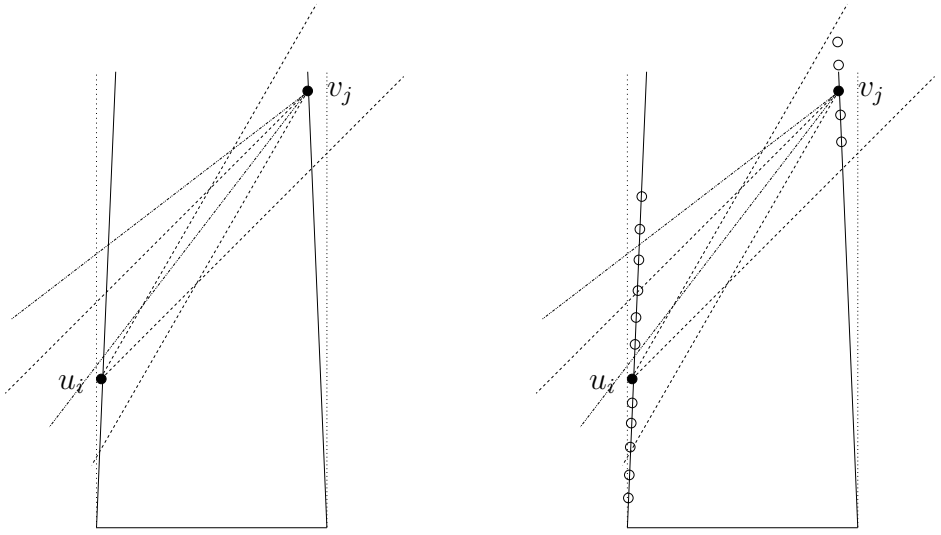

Figure 4.21: SymmY(V) for even $k > 6$: a lot of transverse edges may appear

sectors that lie crossways in the construction. These sectors are empty by construction for $k = 6$. In some of these sectors symmetric links will be established, e.g., between u_i and v_j, and hence the length of the path is shortened. A first try to avoid these links could be to place some new points, for example, the white points in Figure 4.21 (right), but this does not help. The nearest neighbor of the point u_i is given by the lowest white point in this sector, if γ_c is appropriately small. The nearest neighbor of the lowest white point in its corresponding sector is always u_i or the highest white point above u_i in its sector. Anyway, we get a symmetric link. We can solve the problem by adjusting the orientation of the sectors of all nodes on the line ℓ_2' by an angle of π/k. Then, always, the nearest neighbor of a node on the left line is not the nearest neighbor of a node on the right line (see also Figure 4.21), if the number of placed nodes on the lines is large enough. With this modification we can use the same arguments as done in Theorem 4.16. Finally, note that now the case odd $k > 6$ is obvious, since the orientation of the nodes placed on the line ℓ_1' differs by an angle of π/k from that of the nodes on line ℓ_2', since the number of sectors is odd. Hence, we get the following corollary.

Corollary 4.2 *Let $V \subseteq \mathbb{R}^2$, $k > 6$ and we can adjust the orientations of the sectors. Then SymmY(V) is neither a weak c-spanner for any constant $c \in \mathbb{R}$, nor a (c, δ)-power spanner for any constant c and $\delta > 1$.*

Note that in our robot scenario the adjustment of sectors is irrelevant since the robots have a fixed communication module and its orientation depends on the movement of a robot. Hence, such a worst case construction might be possible. We leave it as an open problem to show that SymmY(V) is a weak c-spanner or a c-power spanner for even $k > 6$ using fixed sector orientations for all vertex sets V and a constant c or to construct a counter-example. Nevertheless, we can prove the following positive property of SymmY(V).

Theorem 4.17 *Let $V \subseteq \mathbb{R}^2$ and $k > 6$. Then SymmY(V) is connected.*

Proof: We prove this by an induction over the distance of vertices $|u - v|$. First, note that the closest pair of vertices forms an edge in Symmy(V). Now assume two vertices u, v: either there is an edge from u to v or there is a vertex w with $\sphericalangle(u, v) = \sphericalangle(u, w)$ and $|u-w| < |u-v|$. Since $k > 6$ we have $|v - w| < |u - v|$. By induction there is a path from u to w and a path from w to v which implies the claim that there is a path from u to v. ∎

4.2.4 Network Properties

In Subsection 4.1.1 we modeled radio networks, formulated routing problems, and introduced the network parameters (bidirectional) interference number, congestion, dilation, and energy for the omnidirectional communication model. In this subsection we extend these notions to the directional communication model in which we allow the nodes two communication modes: in the *packet routing mode* acknowledgement signals are very short and we can neglect its impact on the interference. Here, we account only for unidirectional interference. In the *control mode*, when control messages have to be exchanged, sending and answering signals are both short, then we have to consider also bidirectional interference and combinations thereof. The directed edge (u, v) interferes unidirectionally with an edge (r, s), if $|u - s| \leq |u - v|$ and $\sphericalangle(u, v) = \sphericalangle(u, s)$ as well as $\sphericalangle(s, r) = \sphericalangle(s, u)$ (see Figure 4.22 a)). We denote the set of of edges unidirectionally interfering with an edge (r, s) by UInt(r, s). The directed edge (u, v) interferes bidirectionally with an edge (r, s), if $(u, v) \in$ UInt(r, s) or $(u, v) \in$ UInt(s, r) or $(v, u) \in$ UInt(s, r) or $(v, u) \in$ UInt(r, s) (see Figure 4.22 b)). The set of edges birectionally interfering with an edge (r, s) is defined by BInt(r, s).

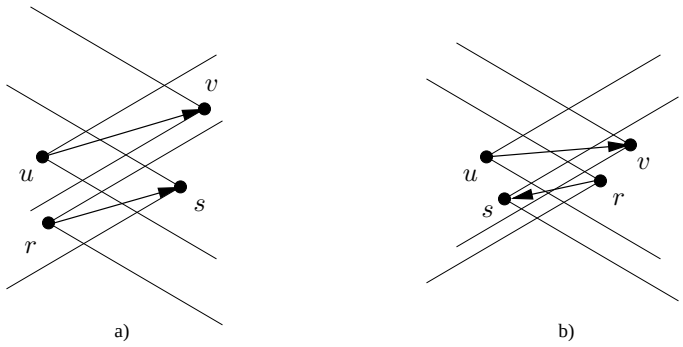

Figure 4.22: Directional interference: a) (u, v) unidirectionally interferes with (r, s), b) (u, v) bidirectionally interferes with (r, s),

We denote the (bidirectional) interference number of an edge e by $|\text{BInt}(e)|$ and the unidirectional interference number by $|\text{UInt}(e)|$. The (bidirectional) interference number of a graph G is the maximum (bidirectional) interference number of all edges, BInt(G). Analogously, we define the unidirectional interference number of a graph G by UInt(G).

Note that this definition of bidirectional interference matches the definition given in Subsection 4.1.1. The omnidirectional communication model is equal to the directional one with 1 sector/sender per node. Furthermore, both types of interference are asymmetric, i.e. $e \in \text{BInt}(f)$

does not imply that $f \in \text{BInt}(e)$ and also $e \in \text{UInt}(f)$ does not imply that $f \in \text{UInt}(e)$ for two edges e,f, since we allow the nodes adjustable transmission ranges (see also Section 2.1, asymmetric interference).

Observation 4.2 *Let $G_1 = (V_1, E_1)$ and $G_2 = (V_2, E_2)$ be two geometric graphs. It holds*

$$\begin{aligned} \text{UInt}(G_1) &\leq \text{BInt}(G_1)\ , \\ \text{UInt}(G_1 \cup G_2) &\leq \text{UInt}(G_1) + \text{UInt}(G_2)\ , \\ \text{BInt}(G_1 \cup G_2) &\leq \text{BInt}(G_1) + \text{BInt}(G_2)\ . \end{aligned}$$

Proof: Let $e \in E_1$ be an edge with maximum unidirectional interference number, i.e. $|\text{UInt}(e)| = \text{UInt}(G_1) = \max_{e' \in E_1}\{|\text{UInt}(e')|$. By definition at least $|\text{UInt}(e)|$ edges bidirectionally interfere with this edge. Hence, $\text{UInt}(G_1) = |\text{UInt}(e)| \leq |\text{BInt}(e)| \leq \text{BInt}(G_1)$. An edge e in $G_1 \cup G_2$ can be interfered by edges in G_1 and in G_2. Let u_1 the number of interfering edges from $E(G_1)$ and u_2 the number of $E(G_2)$. Then $u_1 + u_2$ gives an upper bound on $|\text{UInt}(e)|$ in $G_1 \cup G_2$. The proof for the bidirectional case works analogousy. ∎

With these types of interference we define the parameters congestion, dilation, and energy analogously to Subsection 4.1.1. We have already shown in Theorem 4.14 that the congestion of a network is connected to the weak spanner property in consideration of bidirectional interference. This result implies directly that both, the Yao-graph and the SparsY-graph, can host a path system that approximates a congestion optimal path system by a factor of $\mathcal{O}(n \cdot g(V))$ where $g(V)$ denotes the diversity of V. If we assume a nice and normal vertex set V the diversity is $g(V) = \mathcal{O}(\log n)$, i.e. we get an approximation factor of $\mathcal{O}(n \log n)$. Since there exists placements in which the unidirectional interference number of the Yao-graph can be $\Theta(n)$, this result for the Yao-graph also holds taken unidirectional interference into account. For the SparsY-graph we get an improved approximation factor of $\mathcal{O}(g(V))$ (resp. $\mathcal{O}(\log n)$ for nice and normal vertex sets), if we consider unidirectional interference, since Theorem 4.14 (a weak c-spanner allows us a good approximation of an optimal path system for congestion) still because the unidirectional interference number is smaller than the bidirectional interference number, see Observation 4.2. The second argument is that the unidirectional interference number of the SparsY-graph is given by a constant. Now, we clarify the relation between energy consumption in a wireless network and power spanners.

Theorem 4.18 *Let $V \subseteq \mathbb{R}^2$ and $G = (V, E)$ be the network formulated as a geometric graph. If G is a (c, δ)-power spanner, then G allows us a path system that approximates the energy-optimal path system by a constant factor c.*

Proof: Let Q denote some path $Q = (u = u_1, \ldots, u_\ell = v)$, not necessarily in G, from u to v of minimum δ-cost, i.e. an energy-optimal path from u to v. For each $i = 2, \ldots, \ell$ there exists by presumption a path P_i in G from u_{i-1} to u_i of δ-cost at most $c \cdot |u_i - u_{i-1}|^\delta$. The concatenation of all these paths yields a path P from u to v in G with δ-cost $\|P\|^\delta$ at most $c \cdot \|Q\|^\delta$. ∎

The following theorem summarizes the results concerning the Yao-graph and its variants.

Corollary 4.3 *Let $V \subseteq \mathbb{R}^2$ and $n := |V|$. Then in worst case it holds*

Topology	*unidirectional interference number*	*bidirectional interference number*	*Spanner*	*Energy approx. factor*	*Congestion approx. factor*
Yao(V)	$n-1$	$n-1$	*yes*	$\mathcal{O}(1)$	$\mathcal{O}(n \log n)$
SparsY(V)	1	$n-1$	*weak and power*	$\mathcal{O}(1)$	$\mathcal{O}(\log n)$[1]
SymmY(V)	1	1	*only connected*	—	—

4.3 Handling Interference

The standard mode of our ad hoc network is the packet routing mode. In the lucky case of SymmY-graphs there is no interference between messages and acknowledgements of different edges theoretically. For the SparsY-graph packets sent along the direction of the edges cannot interfere with other packets on different edges. However, acknowledgement signals of such edges can interfere. Since in the normal transportation mode data packets are long compared to the short acknowledgments, we neglect this interaction.

In the Yao-graph and the HL-graph we have to resolve (unidirectional) interference. Solutions exist that reduce the amount of interference, especially the effects of (directed) hidden and exposed terminals (see Section 4.1 and Section 4.2), e.g., using request-to-send (RTS) and clear-to-send (CTS) mechanisms. An overview of MAC-protocols for ad hoc networks, e.g., CSMA, CSMA/CA, MAC, MACAW, FAMA, IEEE 802.11 MAC DCF, DBTMA, D-MAC, and lots of other are given in [HS02]. Power control approaches suggest to use more than one transmission frequency, e.g., PAMAS [SR98]. Further details concerning medium access control can also be found in [Tan96].

Since we allow the nodes only one transmission frequency and consider power-variable ad hoc networks in which also asymmetric interference can occur, standard solutions can not be directly applied. There exist approaches for power control which propose, e.g., to transmit RTS and CTS packets with the maximum power level and DATA and ACK (acknowledgement) packets with the minimum necessary power level [JV02]. We want to completely avoid sending with the maximum power level and distinguish between two strategies: non-interfering deterministic schedules and interfering probabilistic schedules.

Non-interfering deterministic schedule

In general it is an NP-hard problem to compute a schedule that resolves all interference within optimal time, see [ET90, EGMT84, RP89, BGLA02]. However, in the HL-graph in each layer the bidirectional interference number is a constant, Lemma 4.10. Hence, it is easy to define a deterministic schedule that ensures each edge a time frame of $\frac{1}{c \log n}$, which in the worst case slows down communication only by this logarithmic factor. For the Yao-graph, both, the unidirectional interference number and the bidirectional interference number, are given by the in-degree. Hence

[1] Taking only unidirectional interference into account. Note that in consideration of bidirectional interference this factor is $\mathcal{O}(n \log n)$.

a straight-forward strategy is to assign each of these incoming senders a time frame of same size. Unlike as for the HL-graph this schedule is far away from being optimal, since it does not reflect the actual load on the edges.

The main advantage of such a non-interfering schedule is that collisions immediately indicate that dynamic changes have occurred.

Interfering probabilistic schedule

Following the ideas presented in [AS98] and already used in Section 4.1 every link e is activated with probability $\varphi(e)$ and, in each step, it decides with probability $\varphi(e)$ to send a packet. We can choose $\varphi(e) \leq \frac{1}{2}$ for all edges e, such that there is a constant probability of at least $\frac{1}{4}$ that a packet is transferred successfully without being interfered by another packet (see Lemma 4.1).

The detection of dynamic network changes may need more time than in non-interfering schedules. Here, since with probability of at least $\frac{1}{4}$ every receiver does not get an input signal, it suffices to repeat the dynamic change signal for some $\mathcal{O}(\log n)$ rounds. Then all nodes are informed with probability $1 - 1/p(n)$ for some polynomial $p(n)$.

The only information necessary to maintain such a probabilistic schedule is the local unidirectional interference number, or an approximation of that number. Therefore, a node has to inform all its m interfering nodes, that they interfere and how many of them interfere. A straightforward approach is that we contact all m interfering nodes directly and this takes time $\mathcal{O}(m)$. Note that this is only possible if all nodes have the same maximum transmission range and send its control messages with maximum power because of the problem of asymmetric interference (see Subsection 4.2.1).

4.4 Maintaining Networks

In this section we focus on the question how to maintain our basic network topologies under dynamic changes when stations appear and disappear, i.e. enter and/or leave the network. Here, it makes no sense to consider ad hoc networks where the nodes take abnormal positions. Therefore, we assume a nice and a normal vertex set, see Definition 4.4 and Definition 4.5 of Section 4.2. This implies that the diversity is given by $\Theta(\log n)$.

We assume that if a station enters the network it will send out control messages to stop normal packet routing for the (hopefully short) time needed to update the network structure. All packets are stored on the radio stations and delivered when the network structure has been restored. In contrast to this reactive approach, one can also take advantage of synchronized clocks if available. If a periodically time period is reserved that is known to all nodes (including new ones), the maintenance of the network can be done in this special maintenance period. Thus, no control packets are necessary to stop the packet routing mode and collisions caused by the control packets can be prevented.

We claim that a node entering a network knows this situation, e.g., because it is switched on or it eavesdrops on existing communication from the network. A node leaving the system is equivalent to a complete node failure. This means that it is not necessary that the leaving node informs the network. Such dynamic changes are the most frequent changes of a radio network besides the motion of radio stations, see Chapter 5.

In our view its very unlikely that all mobile radio station would start (or leave) at the same time. And even if this is enforced one can easily add a probabilistic strategy that prevents this situation. Then the establishment of the complete network turns out to be a series of single stations entering an existing network. This approach makes sense, since nobody expects that a radio connection to the network is instantly established and we will see that there exist network structures where entering and leaving will only need some logarithmic communication rounds.

In this chapter, we do not address the problem of moving radio stations. However, if the movement is not too fast, the moving node can reestablish the correct network by triggering a **leave**- and an **enter**-operation. Furthermore, we hope that the basic routines developed for this switching dynamics provide basic techniques for more sophisticated maintenance techniques of mobile ad hoc networks. We investigate two elementary dynamic operations necessary to maintain dynamic wireless networks:

- **Enter:** While the network is distributing some packets, one radio station wants to enter the network. It will send a special signal causing a special interference signature that will cause all radio stations in some specified distance to stop the packet routing communication mode and switch to a special enter mode. Then this part of the network devotes its communication to insert the new node into the network topology. After this, it will resume to the normal packet routing mode.

- **Leave:** A single station stops sending and receiving. At some time a neighboring node notices this failure and signals it to other nodes of the network. These nodes halt routing packets and rebuild the network.

The two important resources in these update processes are *time* and *number of involved stations*. If these parameters are minimized, then the impact of the network disturbance can be kept to a minimum.

Theorem 4.19 *Let $V \subseteq \mathbb{R}^2$ be nice and normal. Then rebuilding the Yao-graph, the SparsY-graph, and/or the SymmY-graph after an enter/leave operation affects $\Theta(|V|)$ edges. For the HL-graph this number is upper bounded by $\mathcal{O}(g(V))$, i.e. by $\mathcal{O}(\log n)$.*

Proof: We consider the following graph $G = (V, E)$ with $V = V_1 \cup V_2$ where $V_1 := \{u_1, \ldots, u_m\}$ and $V_2 := \{v_1, \ldots, v_m\}$ define two parallel lines, such that the edge (u_i, v_i) is orthogonal to (u_1, u_m) and (v_1, v_m) and all nodes in V_1 are in the same sector of a node in V_2 and vice versa, see Figure 4.23. In this situation we have $m = n/2$ edges in the Yao-graph and its variants, which all have to be erased if a node w pops up in the middle of the network. The inverse situation occurs if we switch off this node.

For the HL-graph the situation is not so bad. We consider each of the $\mathcal{O}(g(V))$ layers, Lemma 4.7, separately. If a station enters a layer, then at most a constant number of edges have to be added while no edges have to be erased, see Lemma 4.10. When a node disappears in a layer, we might have to determine only a constant number of replacement nodes. These are chosen from the lower layer. In both cases only a constant number of edges is involved. ■

Clearly, this worst case behavior is not the typical situation. Therefore, we introduce the number of involved vertices m as an additional parameter into the analysis of the time behavior

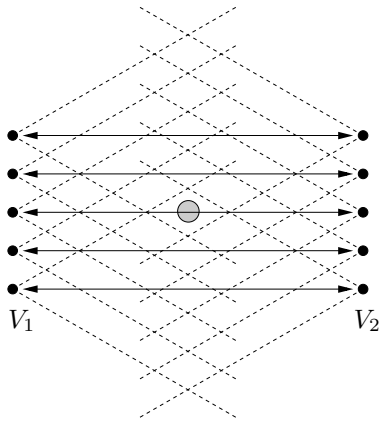

Figure 4.23: A bad situation for the Yao-graph and its variants, if the node in the middle appears. Here, all nodes are placed on a line. When we assume nice and normal vertex sets we must replace the points a bit but we will get the same result.

of the enter/leave algorithms. Remember, that our hardware model supports s discrete choices for transmission powers (see Subsection 4.2.1). Our analysis also uses this parameter.

Theorem 4.20 *Let $V \subseteq \mathbb{R}^2$ be nice and normal and m be defined as the number of involved edges when a node enters and/or leaves the network. Then the Yao-graph and its variants can be updated in time $\mathcal{O}(m \log s)$. For the HL-graph the time is bounded by $\mathcal{O}(g(V) + \log s)$, i.e. by $\mathcal{O}(\log n + \log s)$.*

Proof: First, we show how to reconstruct the Yao-graph and its variants in time $\mathcal{O}(m \log s)$ after an enter and/or leave operation.

Enter: Let us assume that a node u_0 appears in the network. The node u_0 informs all neighbors by sending out control messages in all sectors. Theoretically, this can be done in parallel but practically no two neighboring sectors should be used at the same time because of physical effects like overlapping radio/infrared waves. All informed nodes immediately halt normal packet transportation. This needs only a constant number of rounds. Afterwards u_0 searchs for nearest neighbors in each of its sectors. This can be accomplished in time $\mathcal{O}(\log s)$ using a binary search algorithm. Note that since other communication is inhibited, we can interpret interference signals as answers. Then every informed node starts searching for a nearest neighbor in each of its empty sectors in the same way in time $\mathcal{O}(\log s)$ per node and hence in time $\mathcal{O}(m \log s)$. Finally, for each sector all nodes u who had already a nearest neighbor v in a sector are asked to test whether u_0 is closer than this neighbor by sending with transmission distance $d_{\tilde{D}(|u-v|)-1}$. If u_0 now receives a signal it can successively determine all these m nodes and establish all the links in time $\mathcal{O}(m \log s)$.

In the case the SymmY-graph or the SparsY-graph is established, we have to extend the algorithm. Then a control message contains the transmission distance d_i with that it has been transmitted. After establishing all edges of the Yao-graph, every involved node checks the number of ingoing edges in its sectors. If there is a sector in which more then one node is connected,

then it sends back one control message to the farthest node in this sector with the transmission distance of the shortest ingoing edge. All nodes receiving this message now know forbidden edges and interference also indicates that there is a forbidden edge. This extension builds up only edges which are part of the SparsY-graph. Finally, to construct only edges of the SymmY-graph we check not only the distance but also the node identification. It follows that all three graphs can be rebuild in time $\mathcal{O}(m \log s)$.

Leave: Let us assume that a node u_0 leaves the network. If u_0 has no neighbors, nothing has to be done. In the other case let u' be a neighbor of u_0. During the normal packet routing scheme u' notices that u_0 has left. Then u' informs interfering nodes by sending a control message to immediately halt packet transportation and to switch to the control mode. All informed nodes immediately halt packet transportation and this needs only constant rounds. Afterwards u_0 starts to determine new nearest neighbors. For this u_0 can use a reduced version of the enter-algorithm and starts a binary search starting with the known transmission distance of the lost node. This costs $\mathcal{O}(\log s)$ rounds per node and sector. Hence, after $\mathcal{O}(m \log s)$ rounds all new links can be established, since m is the number of involved edges.

Now we show how to rebuild the HL-graph in time $\mathcal{O}(g(V) + \log s)$ after an enter and/or leave operation.

Enter: Let us assume that a node u_0 appears in the network. The node u_0 switches to the control mode and informs the nodes in a layer by sending a control message. This needs $\mathcal{O}(\log s)$ steps, since the minimum distance in the network is unknown. All informed nodes immediately halt packet transportation and establisch a connection. Lemma 4.10 shows that the degree of a layer is constant such that this update is possible in constant time. Since we have to check at most $\mathcal{O}(g(V))$ different layers the rebuilding is possible in $\mathcal{O}(g(V) + \log s)$ rounds.

Leave: Let us assume that a node u_0 leaves the network. Again, if u_0 has no neighbors, nothing has to be done. The other case is more difficult, since possibly replacement nodes have to be assigned in the layers where u_0 was present. To overcome this problem nodes which notice that u_0 is down send out a control message and inform neighboring nodes. These nodes perform iteratively the enter operation. Since u_0 has only a constant number of neighbors in each layer and the informed nodes also have only a constant number of neighbors, this update process is also possible in time $\mathcal{O}(g(V))$. ■

In Chapter 6 we present implementations of these algorithms in more detail. Furthermore, we present the results of our extensive simulations.

4.5 Further Geometric Structures and Works

In Section 4.1 and Section 4.2 we distinguished between omnidirectional and directional wireless transmission. In both communication models we have designed and analyzed basic network topologies to approximate a complete topology, e.g., a complete graph or a unit disk graph, that can be used for higher tasks like routing, selecting routing paths, and forwarding routing packets. We have also implemented most of these topologies and present the results of our experimental evaluations in Chapter 6. The directional approach has the advantage that we can theoretically build interference-free topologies. In realistic environments we could see that a lot of practical problems coming with directional senders exist. We will also discuss some of them also in

Chapter 6. As already mentioned, it is also possible to use the sectorized or cone-based topologies using the omnidirectional communication model if additional communication features are given (e.g., angle detecting of incoming signals). In this case, the Yao-graph and its geometric variants can be used to build a sparse communication network for a set of nodes where each node is equipped with an omnidirectional antenna which can detect the angle of incoming signals. Several other geometrical structures (e.g., unit disk graphs, relative neighborhood graphs, combinations between Yao-graphs and gabriel graphs, local delaunay graphs, topologies based on connected dominating sets, topologies based on mobile k-centers, etc.) have been studied recently by computational geometry scientists as well as by network engineers. Overviews of main concepts and structures with applications in computational geometry in wireless networks and in sensor networks are given by X.-Y. Li [Li03b, Li03a, Li03c] and R. Rajaraman [Raj02].

4.6 Conclusions

In this chapter we have developed and investigated static and dynamic single frequency power-variable ad hoc networks using two different communication models. We have introduced the diversity $g(V)$ of a vertex set V as an important parameter regarding the amount of interference. A high diversity indicates high interference. In real-world applications or if we assume nice and normal vertex sets, it can be regarded as $\Theta(\log n)$.

The results achieved for a communication network N defined by the path system $\mathcal{P}$ for a vertex set V of n vertices using the omnidirectional communication model are summarized in Table 4.1 and Table 4.2. Table 4.3 describes the network properties of the topologies considered in this chapter. Let k be defined as the number of sectors/senders per node then in Table 4.4 we give an overview of elementary graph properties of the sectorized topologies in whiconsidered for the directional communication model and the Hierarchical Layer Graph.

	Congestion	Dilation	Unit Energy	Flow Energy
Structure	HL(V)	Complete Network	MST	Gabriel Sub-Graph
Approx.-factor	$\mathcal{O}(\log^2 n)$	optimal	optimal	optimal

Table 4.1: Approximation results for logarithmic diversity

One can see an overview of the trade-offs between congestion and dilation as well as between dilation and energy. Furthermore, we showed that the relation between congestion and energy is even worse. It is only possible to find a reasonable approximation for either congestion or energy, while the other parameter is at least a polynomial factor worse than in an optimal network.

It turns out that the best dynamic behavior can be achieved by the HL-graph, if $g(V) = \mathcal{O}(\log n)$ which can be assumed for real-world applications. Comparing the HL-graph with the Yao-graph and its variants shows that the SparsY-graph outperforms the HL-graph with regard to congestion approximation. The SymmY-graph gives the worst impression in this worst case consideration. Nevertheless, it allows us a connected interference-free topology. Therefore, for a small number of radio stations or average locations, it may outperform all the other graph

	Dilation	Congestion
Congestion	$C_{\mathcal{P}}(V) \cdot D_{\mathcal{P}}(V) = \Omega(W)$	—
Unit Energy	$D_{\mathcal{P}}(V) \cdot \mathrm{UE}_{\mathcal{P}}(V) = \Omega(d^2)$	$C_{\mathcal{P}}(V) = \Omega(n^{1/3} C^*_{\mathcal{P}}(V))$ or $\mathrm{UE}_{\mathcal{P}}(V) = \Omega(n^{1/3} \mathrm{UE}^*_{\mathcal{P}}(V))$
Flow Energy	$D_{\mathcal{P}}(V) \cdot \mathrm{FE}_{\mathcal{P}}(V) = \Omega(d^2 W)$	$C_{\mathcal{P}}(V) = \Omega(n^{1/3} C^*_{\mathcal{P}}(V))$ or $\mathrm{FE}_{\mathcal{P}}(V) = \Omega(n^{1/3} \mathrm{FE}^*_{\mathcal{P}}(V))$

Table 4.2: Trade-offs and incompatibilities on network parameters

types. In Chapter 6 the results of our extensive experimental analyses using realistic assumptions support this statement.

Topology	Congestion approx. factor	Energy approx. factor	time for enter/leave	enter/leave involved nodes
Yao(V)	$\mathcal{O}(n \log n)$	$\mathcal{O}(1)$	$\mathcal{O}(n \log s)$	$\Theta(n)$
SparsY(V)	$\mathcal{O}(\log n)$[1]	$\mathcal{O}(1)$	$\mathcal{O}(n \log s)$	$\Theta(n)$
SymmY(V)	—	—	$\mathcal{O}(n \log s)$	$\Theta(n)$
HL(V)	$\mathcal{O}(\log^2 n)$	$\mathcal{O}(1)$	$\mathcal{O}(\log n + \log s)$	$\mathcal{O}(\log n)$

Table 4.3: Network properties for logarithmic diversity and dynamic operations for nice and normal vertex sets

The Yao-graph and the HL-graph fulfill all of the spanner properties. It is still an open problem whether all SparsY-graphs are spanners or not. It turns out that the SymmY-graph is not a good choice for a power-efficient topology in general, but it allows us theoretically interference-free communications. In Chapter 6 we show experimentally that all three sectorized graphs are spanners on random vertex sets where the nodes are placed uniformly at random.

Topology	Connected	Power Spanner	Weak Spanner	Spanner
Yao(V)	$k \geq 4$	$k > 6, c = \left(\frac{1}{1-2\sin\frac{\pi}{k}}\right)^{\delta}$ $k > 6, c = \frac{1}{1-(2\sin\frac{\pi}{k})^{\delta}}$	$k = 4, c = \sqrt{3+\sqrt{5}}$ $k \geq 6, c = \max\{ \sqrt{1+48\sin^4(\pi/k)}, \sqrt{5-4\cos(2\pi/k)}\ \}$	$k > 6, c = \frac{1}{1-2\sin\frac{\pi}{k}}$
SparsY(V)	$k > 6$	c exists for $k > 6$	$k > 6$, $c = \frac{1}{1-2\sin\frac{\pi}{k}}$	***Open***
SymmY(V)	$k > 6$	—	—	—
HL(V)	$\alpha > 2\frac{\beta}{\beta-1}$	$\alpha > 2\frac{\beta}{\beta-1}$, $c = \left(\beta\frac{\alpha(\beta-1)+2\beta}{\alpha(\beta-1)-2\beta}\right)^{\delta}$	$\alpha > 2\frac{\beta}{\beta-1}$, $c = \beta\frac{\alpha(\beta-1)+2\beta}{\alpha(\beta-1)-2\beta}$	$\alpha > 2\frac{\beta}{\beta-1}$, $c = \beta\frac{\alpha(\beta-1)+2\beta}{\alpha(\beta-1)-2\beta}$

Table 4.4: Elementary graph properties of omnidirectional and directional topologies

[1]Taking only unidirectional interference into account. Note that, in consideration of bidirectional interference, this factor is $\mathcal{O}(n \log n)$.

Chapter 5

Mobile Ad Hoc Networks

In this chapter we investigate distributed algorithms for power-variable mobile ad hoc networks in a worst case scenario. We consider two models to find a reasonable restriction on the worst case mobility. In the *pedestrian model* we assume a maximum speed $v_{\max}$ of the radio devices, while in the *vehicular model* we assume a maximum acceleration $a_{\max}$ of the hosts.

Our goal is to maintain persistent routes with good communication network properties like small diameter, low energy-consumption, low congestion, and low interference. A route is persistent, if we can guarantee that all edges of this route can be upheld for a given time span Δ, which is a parameter denoting the minimum time the mobile network needs to adopt changes, i.e. update routing tables, change directory entries, etc. This Δ can be used as the length of an update interval for a proactive routing scheme.

We extend the notions transmission range, interference, spanner, weak spanner, power spanner, and congestion introduced in Chapter 4 for static and dynamic ad hoc networks to both mobility models and introduce a new parameter called *crowdedness* that states a lower bound for the amount of radio interference. Then we prove that a mobile weak spanner hosts a path system that polylogarithmically approximates the optimal congestion.

We present distributed algorithms based on a grid clustering technique and a high-dimensional representation of the dynamic start situation which constructs mobile spanners with low congestion, low interference, low energy-consumption, and low degree. We measure the optimality of the output of our algorithm by comparing it to the optimal choice of persistent routes under the same circumstances with respect to pedestrian or vehicular worst case movements. Finally, we present solutions for dynamic position information management under our mobility models.

5.1 Motivation

We investigate the problem of constructing a wireless ad hoc network under a worst case assumption for mobility. We consider two different models for the movement of n mobile stations or hosts in the Euclidean plane, the **velocity bounded** and the **acceleration bounded** model.

For the first model, the **velocity bounded**, we picture to ourselves a large number of **pedestrians** using mobile, wireless communication devices in a rather small area. Clearly, the maximum

speed is bounded by a small constant. The standard approach in a static ad hoc network scenario is to build up connections between nearest neighbors, see Chapter 4. If the mobility is very high, like on a crowded sidewalk, this leads to short communication links, that survive for only short time periods. Although it is possible to build up these connections and transmit some data, it is nearly impossible to maintain packet routes or maintain directories for efficient localization of users. Therefore, we need communication links to sustain for some time span Δ to enable the routing layer to keep up with the dynamic changes. We can guarantee that a communication link between two moving stations sustains for this period if we adjust the transmission range to a value, which covers all possible distances the communication partners can reach in time Δ. Since, we know the maximum speed, this implies that the transmission power must be chosen such that the transmission range is at least an additive term $2v_{\max}\Delta$ larger than the distance at the beginning of the time interval. The task is now to appropriately build up the basic communication links such that the routing algorithm can choose routes with low energy or low congestion, while the number of edges and interfering edges is small.

A motivating example for the **acceleration bounded** model is given by **vehicles** of high speed, like cars, trains, or aircrafts. For example, we have in mind trains where each wagon carries a mobile radio station. Now consider a scenario, where two such trains pass each other in opposite directions, as shown in Figure 5.1. If we take a snapshot of this moment and build a static ad hoc network using the temporary positions, then this static approach may lead to a ladder-like network which can also be seen in Figure 5.1. But the communication links forming the rungs of the ladder can be upheld only for a short time period since the trains move with high speed. After a short period all rung links need to be replaced by new ones. Therefore this static network design is not a good choice.

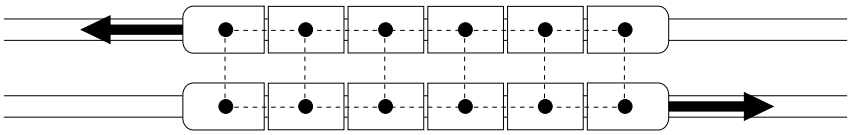

Figure 5.1: Two trains passing each other in opposite directions.

We allow all nodes to accelerate by some maximum amount of $a_{\max}$ to generalize from linear movements to some worst case settings. Let $s_i(t)$ be the coordinates of a mobile station s_i at time t, $s_i'(t)$ the velocity vector and $s_i''(t)$ the vector describing the acceleration, then $|s_i''(t)| \leq a_{\max}$. Now, if we try to adjust the transmission range r of a connection such that the moving communication partners s_i and s_j of known relative speed $v = s_i'(t) - s_j'(t)$ and distance vector $d = s_i(t) - s_j(t)$ sustain for a time span Δ, we need a transmission distance that covers at least the distance d at the beginning and the distance at the end stretched by a possible acceleration, i.e. $r = \max\{|d|, |d+v\Delta| + a_{\max}\Delta^2\}$. In the train example this implies that the communication links between the passing trains are more expensive than one expects looking only at a snapshot. If we add to the two position coordinates the vertical and horizontal speed coordinates, we map the dynamic aspect of the scenario into four dimensions, as shown in Figure 5.2 (vertical speed and location coordinates are left out). In this setting the speed difference separates the trains. Hence,

rung links between the trains add radio interference with other edges. It is straightforward that a small number of rung connections between the trains improve the mobile network, while the edges inside should follow a static ad hoc network policy.

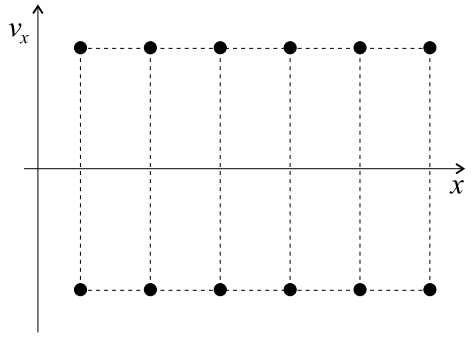

Figure 5.2: Horizontal speed and directions in the train example. Each point represents a wagon.

Our goal is to build up a mobile ad hoc network that is stable and prefers short links. In a high-speed scenario one cannot provide both features at the same time. We will try to present a reasonable compromise. We allow the nodes any movement within these restrictions and will compare the performance of our network solutions with the best offline solution for this dynamic scenario.

In the following we mainly extend our results on congestion, dilation, and energy in radio networks presented in Section 4.1 of Chapter 4 to mobile ad hoc networks considering two worst case mobility models. The remainder of this chapter is organized as follows. In Section 5.2 we first present some basic known mobility models. We review models used in simulations as well as models considered in theoretical analyses like kinetic data structures. In Section 5.3 we introduce our network model. Assuming that a fixed time interval of length Δ is given, we describe how we construct the mobile ad hoc network for a set of stations to solve routing problems. Furthermore, we innovate the pedestrian and the vehicular mobility as two worst case mobility models. In Section 5.4 we define some network parameters which partly extend measures and definitions like transmission range, interference number, spanner, power spanner, and congestion to mobile networks. Furthermore, we introduce a measure called crowdedness that states a lower bound on the amount of radio interference. We concentrate on the distributed computation of the network at MAC and physical layer, see Figure 6.1 in Chapter 6 concerning the ISO OSI reference model, and show the main result that a mobile weak spanner hosts a path system that polylogarithmically approximates the optimal congestion. In Section 5.5 we give techniques how to construct such mobile (weak) spanners with small congestion, small interference number, small energy-consumption, and small degree. We present the Hierarchical Grid, an extension of the Hierarchical Layer Graph, based on a grid-cluster technique and prove that its interference number can be upper bounded by a logarithmic term if we assume the crowdedness to be logarithmic. One assumption in this chapter is that all positioning information is available to all nodes. We discuss this problem in Section 5.6 and present two solutions: the first is based on a positioning system and the second uses distances as location information. This yields to a very

dynamic data structure, the so-called Mobile Hierarchical Layer graph that fulfills all our requirements. We conclude this chapter with an overview of the results and discuss open questions in Section 5.7.

5.2 Related Mobility Models

Many mobility models have been proposed as a basis for simulation of cellular and ad hoc networks. Most of them use a random process to vary speed or direction of the moving objects, like the *random walk* model and its variants. The most common model for simulations of cellular networks is a random walk model which describes mobility as a stop-and-go motion between cells. According to the *fluid flow* model every object moves with a randomly chosen speed and direction for a predefined time interval. In contrast to the random walk the motion is more predictable. The *Gauss-Markov* model [LH99] is a bit of both the random walk and the fluid flow model: speed and direction are changed with an adjustable amount of randomness, ranging from completely random to predictable, linear motion.

In the *random waypoint* model [JM96] the objects move between randomly chosen positions where they pause for a certain time interval. Their speed is uniformly distributed between zero and a maximum. The speed chosen for the next motion period does not depend on the speed of the previous period. Thus sharp turns and sudden stops are possible, i.e. the acceleration is not bounded.

Besides these models, in which the movement of each object is independent from others, there are mobility models that regard mobility of a group of objects, e.g., the *reference point group mobility* model [HGPC99] that defines for groups of objects a logical center that determines direction, speed, and acceleration of each object. Other examples are the *column* model, the *pursue* model, and the *nomadic community* model. These models are less suitable to model worst case mobility as they provide some kind of smoothed or uniform mobility pattern.

Surveys of mobility models are [CBD02, Bet01b, Bet01a, BH04]. In [Bet04] C. Bettstetter gives an overview of mobility modeling, tries to classify known models for mobility in wireless networks, and presents simulation-based studies.

In the network model of Chatzigiannakis et al. [CNS01] the nodes are allowed to move arbitrarily while the *support* (a set of nodes controlled by the protocol that form a virtual backbone) moves randomly. The authors abstract from the geometric properties of this movement and divide the motion space into cubes that approximate a sphere that is given by a predefined transmission range. These cubes are represented by the nodes of a motion graph, adjacent cubes are connected by an edge. Then mobility of the support is modeled by a random walk on this motion graph.

Another way to deal with mobility in ad hoc networks is to consider what happens to the underlying topology when the nodes are moving. This leads to the *adversarial network model* [ABBS01] in which all communication links are under control of an adversary. A worst case for mobility corresponds with the topological changes the adversary may perform within some predefined restrictions.

Recently, a novel general technique, based on renewal theory, for analyzing mobility models in ad hoc networks were proposed in [LNR04]. A technique is presented that enables an accu-

rate derivation of the steady state distribution functions for node movement parameters such as distance and speed. The main contribution is a new methodology for simulating mobility which guarantees steady state for node movement distributions from the start of the simulation. The authors give formal proofs as well as extensive simulations.

Further models like the contraction, the expansion model, and combinations thereof have been investigated by simulations, see [LLGH04]. The contraction model emulates movement of mobile nodes toward a logical center from all directions. The expansion has the opposite effect of movement pattern compared to the contraction model. Nodes in the area will move toward the edges away from the center on a line.

An intrinsic property of mobile ad hoc networks is the mobility of the nodes. Despite of this fact the network topology is mostly designed for quasi-static nodes. Then according to some events, a new network topology is computed.

In the context of computational geometry Basch et al. introduced the concept of *kinetic data structures* (KDS) [BGH99] that describes a framework for analyzing algorithms on mobile objects. In their model the mobility of objects is described by pseudo-algebraic functions of time and fully or partially predictable. The analysis of a KDS is done by counting the combinatorial changes of the geometric structure that is maintained by the KDS. Therefore the worst case mobility depends on the specific application for which the KDS is designed. Another approach that captures unpredictable mobility is the concept of *soft kinetic data structures* (SKDS) [CS01]. These data structures maintain an approximate geometric structure that is updated by property testing and reorganization. SKDS are evaluated with respect to the dynamics of the system, which is measured by the number of errors the data structure contains due to the mobility of objects. Worst case mobility is rather described as number of changes that violate the internal structure than as a random process. The mobility is regarded with respect to the specific purpose of the SKDS. It is not characterized in terms of velocity and direction.

The idea of kinetic data structures is also used in [GGH$^+$01a] to maintain a clustering of moving objects. This approach is used in [GGH$^+$01b] to determine the head of each cluster in a mobile network. In each cluster the nodes are directly connected to the head. The heads and some intermediate gateway nodes are connected by a Delaunay graph with restricted edge lengths that forms a backbone network. In this network routing can be performed by a geometric forwarding scheme. The clustering is updated by an event-based kinetic data structure.

In [BV05] a generic mobility model and a framework to analyze it is presented. The framework provides a rich set of well understood models that can be used to simulate mobile networks with independent node movements.

5.3 The Model

In our model we consider a fixed set S of n mobile stations $s_1, \ldots, s_n$ in the Euclidean plane. We denote by $s_i(t)$ the coordinates of a mobile station s_i at time point t and by $s_i'(t) = ds_i(t)/dt$ its speed vector. Furthermore, $s_i''(t) = ds_i'(t)/dt$ denotes the acceleration of s_i at time t, i.e. the change of the speed.

All mobile stations remain active all the time. We allow the nodes adjustable transmission

power for each connection, which is high enough such that all mobile stations never leave the maximum transmission range of a mobile station. The mobile stations use omnidirectional radio antennae, i.e. all mobile stations inside a disk with the sender as center and the transmission distance as radius can receive the message or will be disturbed while receiving data on a different connection. We assume bidirectional communication on a single frequency with time-multiplexing, i.e. using different time slots. Data need to be acknowledged and for simplicity we assume that the impact of acknowledgments is similar to the impact of sent data, compare Section 4.1.

5.3.1 The Mobile Ad Hoc Network

We try to keep all connections alive for at least a fixed time interval of length Δ. This parameter is an over-all network parameter which induces some stability into the network. It should be chosen sufficiently large to set up the communication links between neighbors, to update routing tables, and deliver some amount of data. For a practical realization it may not be necessary to adopt a synchronous round model as we will do now.

We assume that all nodes work synchronized in subsequent time intervals of length Δ. Then during each time interval of length Δ every mobile station of the mobile ad hoc network performs the following operations.

1. Compute new positions and speed vectors of reasonable communication partners
2. Establish communication links to selected neighbors
3. Update routing information, e.g., routing tables
4. Deliver data packets of higher layers, e.g., of applications

Note that this approach embodies the concept of a network protocol stack. The first phase refers to the physical layer, where physical data like transmission power and the change of the incoming signal can be used to estimate relative distances and relative speed. The second phase describes the task of the Medium Access Layer (MAC). Note that the specific routing requests are not known in this layer. Its task is to build up a general-purpose network which allows us efficient routing, while the network graph is pruned such that the number of interfering edges is small.

In the third phase the routing algorithm can rely on a stable communication network for some time span Δ. Then the routing in the mobile network is reduced to routing in a (temporary) static network and standard techniques are applicable. The packet routes are chosen to minimize latency, traffic-induced congestions, and, typically for mobile devices, to reduce the transmission energy. In Section 4.1 we showed that even in the static case it is not possible to optimize more than one of these parameters at the same time. However, in the static case it is possible to build up a general-purpose-network which enables the routing algorithm to choose its optimization policy afterwards. The fourth phase of our model describes the activity induced by the upper-most layer of the network protocol stack, the application layer.

In this chapter we concentrate on the distributed computation of the interconnection network by the MAC layer and the problem of distributing location information in the physical layer.

5.3.2 Pedestrian Mobility

The **pedestrian mobility** model is a worst case approach relying on all mobile stations obeying a speed limit of $v_{\max}$. In this **velocity bounded** model the starting position $s_i := s_i(0)$ is known and for the speed vector $s_i'(t) = ds_i(t)/dt$ it holds $|s_i'(t)| \leq v_{\max}$. This implies for the relevant time interval Δ that all mobile stations remain in a disk with radius $v_{\max} \cdot \Delta$ around the starting position s_i, i.e.

$$\text{for } t \in [0, \Delta] \ : \ |s_i(t) - s_i| \ \leq \ v_{\max}\, \Delta.$$

As a technical condition we require a polynomial bound on the maximum distances, i.e. for some constant k we claim $|s_i - s_j| = \mathcal{O}((v_{\max}\Delta)^k)$.

5.3.3 Vehicular Mobility

The **vehicular mobility** model describes the movement of n stations with **bounded acceleration** $a_{\max}$. It refers to transportation vehicles which can operate at high speeds, where the limitation by the change of speed has a higher impact on the movement than the maximum possible speed, e.g., cars, trains, aircrafts. Let $s_i''(t) = ds_i'(t)/dt$ denote the acceleration vector of a mobile station s_i, then we claim that for all mobile stations $|s_i''(t)| \leq a_{\max}$. Now the starting speed vector $s_i' := s_i'(0)$ at the beginning of the time interval Δ can be arbitrarily large. Yet, we assume that at the beginning of the time interval $[0, \Delta]$ we know all locations $s_1, \ldots, s_n$ and all speed vectors $s_1', \ldots, s_n'$. Then we can estimate the position of station i at time point $t \in [0, \Delta]$ by

$$|s_i(t) - ts_i' - s_i| \ \leq \ \frac{1}{2} a_{\max} t^2 \ \leq \ \frac{1}{2} a_{\max} \Delta^2 \ .$$

As a technical condition we require a polynomial bound on the maximum distances and relative speed differences, i.e. for some constant k we claim $|s_i - s_j| + |s_i' - s_j'| = \mathcal{O}((a_{\max}\Delta)^k)$.

5.4 Mobility and Network Parameters

In our worst case approach scenarios may appear where even optimal networks have bad performance. We introduce a network independent measure, called **crowdedness**, to identify such scenarios. We will see that it states a lower bound on the amount of radio interference and the maximum degree of reasonable connection networks. In the **velocity bounded** model we define the crowd of a node u by

$$\mathrm{Crowd}_{\mathsf{v}}(u) := \{w \mid w \in S \setminus \{u\} \text{ and } |u - w| \leq 2v_{\max}\Delta\} \ .$$

Its cardinality defines $\mathrm{crowd}_{\mathsf{v}}(u)$, the crowdedness of u. In the **acceleration bounded** model we define the crowd of a node u by

$$\mathrm{Crowd}_{\mathsf{a}}(u) := \{w \mid w \in S \setminus \{u\}, |u - w| \leq \frac{1}{2} a_{\max}\Delta^2 \text{ and } |u' - w'| \leq \frac{1}{2} a_{\max}\Delta\} \ ,$$

where u, w denote the starting positions, and u', w' the starting speed vector of mobile stations for the time interval $[0, \Delta]$. The crowdedness $\mathrm{crowd}_{\mathsf{a}}(u)$ is defined by its cardinality. It can be interpreted as the number of nodes that can approach u with maximum acceleration $a_{\max}$ in time Δ such that $s_i(\Delta) = s_j(\Delta)$ and $s'_i(\Delta) = s'_j(\Delta)$.

The overall crowdedness of a set of stations S is given by the maximum crowdedness for $\alpha \in \{\mathsf{a}, \mathsf{v}\}$:

$$\mathrm{crowd}_{\alpha}(S) := \max_{u \in S}\{\mathrm{crowd}_{\alpha}(u)\} \ .$$

Transmission Range One crucial property of our mobile network approach is to build up persistent links for the time interval $[0, \Delta]$. The only method to ensure this property for a communication link is to increase the transmission radius such that the maximum distance that two stations can reach is covered. In the velocity bounded **pedestrian model** we therefore redefine the transmission distance of two stations $u, w \in S$ by (see Figure 5.3)

$$|u - w|_{\mathsf{v}} := 2v_{\max}\Delta + |u - w| \ .$$

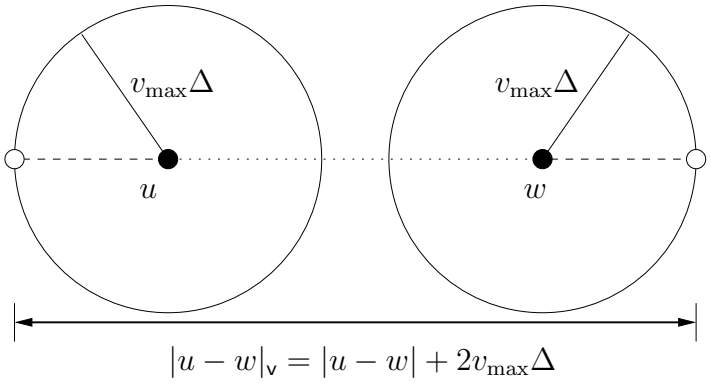

Figure 5.3: Transmission range using pedestrian mobility

In the **vehicular model** the necessary transmission range is described by (see Figure 5.4)

$$|u - w|_{\mathsf{a}} := |(u, u') - (w, w')|_{\mathsf{a}} := \max\{|u - w|, |u - w + (u' - w')\Delta| + a_{\max}\Delta^2\} \ .$$

Lemma 5.1 shows that both definitions are symmetric and fulfill the triangle inequality. For a shorter notation we denote the tuple (u, u'), which represents a quadruple (u_x, u_y, u'_x, u'_y) for $u, u' \in \mathbb{R}^2$, simply by u. Note that $|u - u|_{\alpha} \neq 0$ for $\alpha \in \{\mathsf{a}, \mathsf{v}\}$.

Lemma 5.1 *The distance measures $|u - w|_{\mathsf{v}}$ and $|u - w|_{\mathsf{a}}$ are symmetric and fulfill the triangle inequality.*

Proof: For the **velocity bounded** model the symmetry and the triangle inequality of the distance measure follows from the symmetry and triangle inequality of the Euclidean metric. For

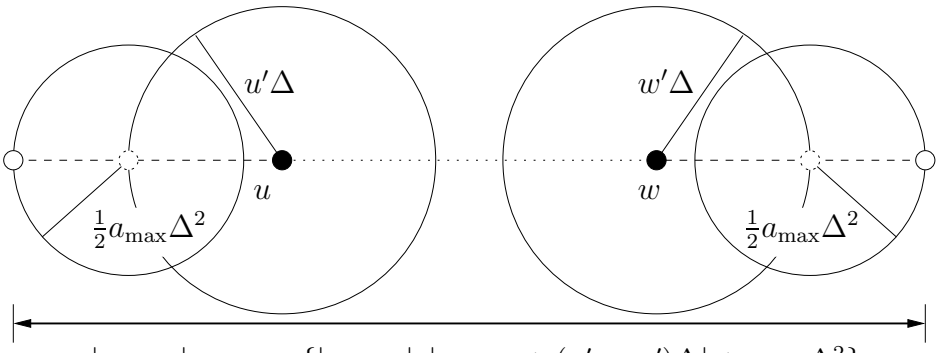

Figure 5.4: Transmission range using vehicular mobility

the **acceleration bounded** model the symmetry of the distance measure also follows from the symmetry of Euclidean metric. We prove the triangle inequality:

Let $|u-w|^*_{\mathsf{a}}$ be defined as $|u-w+(u'-w')\Delta| + a_{\max}\Delta^2$. Then we get

$$\begin{aligned}
|u-w|^*_{\mathsf{a}} &= |u-w+(u'-w')\Delta| + a_{\max}\Delta^2 \\
&= |u-v+v-w+(u'-v'+v'-w')\Delta| + a_{\max}\Delta^2 \\
&\leq |u-v+(u'-v')\Delta| + |v-w+(v'-w')\Delta| + a_{\max}\Delta^2 \\
&\leq |u-v+(u'-v')\Delta| + a_{\max}\Delta^2 + |v-w+(v'-w')\Delta| + a_{\max}\Delta^2 \\
&= |u-v|^*_{\mathsf{a}} + |v-w|^*_{\mathsf{a}}
\end{aligned}$$

Now we can prove the triangle inequality for $|u-w|_{\mathsf{a}}$. Note that $\max\{a,b\} = \frac{1}{2}|a+b| + \frac{1}{2}|a-b|\ \forall a,b \in \mathbb{N}_0$.

$$\begin{aligned}
|u-w|_{\mathsf{a}} &= \max\{|u-w|, |u-w|^*_{\mathsf{a}}\} \\
&= \max\{|u-v+v-w|, |u-v+v-w|^*_{\mathsf{a}}\} \\
&\leq \max\{|u-v|+|v-w|, |u-v|^*_{\mathsf{a}} + |v-w|^*_{\mathsf{a}}\} \\
&= \frac{1}{2}\Big||u-v|+|v-w|+|u-v|^*_{\mathsf{a}}+|v-w|^*_{\mathsf{a}}\Big| \\
&\quad + \frac{1}{2}\Big||u-v|+|v-w|-|u-v|^*_{\mathsf{a}}-|v-w|^*_{\mathsf{a}}\Big| \\
&\leq \frac{1}{2}\Big||u-v|+|u-v|^*_{\mathsf{a}}\Big| + \frac{1}{2}\Big||v-w|+|v-w|^*_{\mathsf{a}}\Big| \\
&\quad + \frac{1}{2}\Big||u-v|-|u-v|^*_{\mathsf{a}}\Big| + \frac{1}{2}\Big||v-w|-|v-w|^*_{\mathsf{a}}\Big| \\
&= \max\{|u-v|, |u-v|^*_{\mathsf{a}}\} + \max\{|v-w|, |v-w|^*_{\mathsf{a}}\} \\
&= |u-v|_{\mathsf{a}} + |v-w|_{\mathsf{a}}
\end{aligned}$$

■

Diameter and Degree The union of all (bidirectional) communication links E describes the mobile ad hoc network. The **diameter** $\mathrm{diam}(G)$ of this undirected graph G is described by the

maximum hop-distance between a pair of nodes. The **degree** $\deg(v)$ of a node v is the number of established communication links at v.

Interference Modern communication networks use many frequencies and sophisticated spread spectrum techniques, that allow many senders to share the same medium. However, in most systems the bandwidth of the medium can be outnumbered by the communication load of the participants. For a theoretical approach we assume that such spread spectrum systems behave like a single frequency network with a probabilistic time schedule.

In our single frequency model with adjustable transmission distances edges interfere if a mobile station is inside the transmission area of an edge and messages are sent simultaneously, see Section 4.1. Because of our little knowledge about the movement of the mobile stations, we cannot exactly predict interference. For an accurate analysis one has to take into account the sending time of a message, the movements of senders and receivers, their transmission radii, the impact of control data induced by distance measurements and acknowledgments.

For a theoretical approach we need a simple definition that allows us to classify mobile networks. Radio interference result from a combination of bad timing, bad locations, and large transmission radii. We want to concentrate on the geographical cause of interference and count all communication links that could interfere at some time. In the static wireless network scenario this can be described by deciding, whether a node resides in the transmission area of a communication link. In our worst case mobility scenario the situation is more difficult.

We do not know in advance whether the mobile station could move into the transmission area of a link. If we consider the worst case motion for radio interference we encounter numerous such interdependencies. This approach would lead to a definition where small local changes of positions can influence the radio interference of all other mobile stations. We would like to use a practical local definition for radio interference, which only uses knowledge from the mobile stations of the interfering and interfered links. Furthermore, we want to exclude the timing of the movement from the definition of radio interference.

We took several alternative models for interference into consideration. One of the possible approaches is to count every radio interference that **could** happen for some time under every allowed movement. But this turns out being too pessimistic. We also considered a too optimistic model where we only count interfering links that **must** interfere under every possible movement. For a reasonable compromise between these two extreme models assuming a certain adversarial or friendly behavior of the mobile stations, we consider a compromise assuming that we only count interfering edges of mobile stations using the average route. In the pedestrian model the **average route** is to remain on the starting position, while in the vehicular model it describes the unaccelerated floating with the original speed.

So, we define interference as if the distance between two interfering stations is not stretched by the additional constant that is given by the velocity bound in the pedestrian model and the acceleration bound in the vehicular model. Thus, in our pedestrian model we count interfering links as if the radio stations are not moving at all. For the vehicular model we count only interfering links as if the interfering mobile stations are not accelerating (yet using an oversized transmission radius to compensate for worst case movements). Furthermore, we count only interfering links if they interfere for the complete time span Δ.

In this interference model two edges do not interfere even if they pass each other at a close

distance with high relative speed. One may argue that in this case the interaction between the links is so short that it can be neglected. Of course we are aware of worst case scenarios of passing mobile clusters giving a counter-example. As a physical argument, the large relative speed difference may be large enough to cause a frequency shift, known as Doppler-effect, which prevents radio interference.

In the **velocity bounded** model an edge $g = \{p_1, p_2\}$ interferes with an edge $e = \{q_1, q_2\}$ if

$$\exists p_i \in g : \exists q_j \in e \ : \ |p_i - q_j| \leq |p_1 - p_2|_{\mathsf{v}} \ .$$

In the **acceleration bounded** model we model interference only between edges which interfere for the complete interval $[0, \Delta]$, if the velocity vectors of their nodes remain the same. Formally we define that an edge $g = \{p_1, p_2\}$ interferes with an edge $e = \{q_1, q_2\}$ if

$$\exists p_i \in g : \exists q_j \in e \ : \ |p_i - q_j| \leq |p_1 - p_2|_{\mathsf{a}} \quad \text{and} \quad |\tilde{p}_i - \tilde{q}_j| \leq |p_1 - p_2|_{\mathsf{a}} \ ,$$

where $\tilde{u} := u + \Delta u'$ denotes the position of u at time point Δ if the speed vector of u remained unchanged during $[0, \Delta]$.

For $\alpha \in \{\mathsf{a}, \mathsf{v}\}$, i.e. in both mobility models, we define $\mathrm{BInt}_\alpha(e)$ as the set of edges that interfere with the edge e. The interference number $\mathrm{BInt}_\alpha(G)$ of a mobile network G is given by the maximum interfered set of edges:

$$\mathrm{BInt}_\alpha(G) := \max_{e \in E(G)} \{|\mathrm{BInt}_\alpha(e)|\} \ .$$

Now the crowdedness of the underlying set of mobile stations states a lower bound on the amount of interference every connected mobile network produces.

Theorem 5.1 *For $\alpha \in \{\mathsf{a}, \mathsf{v}\}$ we observe for all connected graphs $G = (S, E)$*

$$\mathrm{BInt}_\alpha(G) \ \geq \ \mathrm{crowd}_\alpha(S) - 1 \ .$$

Proof: Let $u \in S$ be a node for which $\mathrm{crowd}_\alpha(u)$ is maximal in G, i.e. $\mathrm{crowd}_\alpha(u) = \mathrm{crowd}_\alpha(S)$, and let e be an arbitrary edge incident to u. Such an edge exists, because G is connected. We define the set $E(\mathrm{Crowd}_\alpha(u))$ as the set of edges incident to a node from $\mathrm{Crowd}_\alpha(u)$, i.e. $E(\mathrm{Crowd}_\alpha(u)) := \{g = \{w, z\} : w \in \mathrm{Crowd}_\alpha(u)\}$. Consider the Graph $\hat{G}$ which is obtained from G by substituting each node of $S \setminus \mathrm{Crowd}_\alpha(u)$ by the new node $\hat{u}$. (The position of $\hat{u}$ is irrelevant.) The edges which are incident to a node from $S \setminus \mathrm{Crowd}_\alpha(u)$ in G become incident to $\hat{u}$ in $\hat{G}$ (multiple edges are deleted). Note that $u \in S \setminus \mathrm{Crowd}_\alpha(u)$, so $S \setminus \mathrm{Crowd}_\alpha(u)$ is not empty. Therefore the number of nodes in $\hat{G}$ is $\mathrm{crowd}_\alpha(u) + 1$. Furthermore, each edge in $\hat{G}$ is incident to a node of $\mathrm{Crowd}_\alpha(u)$ and so contained in $E(\mathrm{Crowd}_\alpha(u))$. Since G is connected, the graph $\hat{G}$ is also connected. Hence, the number of edges of $E(\mathrm{Crowd}_\alpha(u))$ in $\hat{G}$ is at least $\mathrm{crowd}_\alpha(u)$. Since each edge in $\hat{G}$ is incident to a node of $\mathrm{Crowd}_\alpha(u)$, it is contained in $E(\mathrm{Crowd}_\alpha(u))$. Hence $|E(\mathrm{Crowd}_\alpha(u))| \geq \mathrm{crowd}_\alpha(u)$. We show that each of the edges in $E(\mathrm{Crowd}_\alpha(u)) \setminus \{e\}$ is interfering with e. This will imply that $\mathrm{BInt}_\alpha(G) \geq \mathrm{crowd}_\alpha(u) - 1 = \mathrm{crowd}_\alpha(S) - 1$.

In the **velocity bounded** model $\mathrm{Crowd}_{\mathsf{v}}(u)$ is defined as the set $\{w \in S \mid |u - w| \leq 2v_{\max}\Delta \text{ and } w \neq u\}$. Then each edge $g = \{w, z\} \in G$ incident to a node $w \in \mathrm{Crowd}_{\mathsf{v}}(u)$

interferes with e, because $|u-w| \leq 2v_{\max}\Delta \leq |w-z| + 2v_{\max}\Delta = |w-z|_{\mathsf{v}}$ holds. Therefore, $E(\mathrm{Crowd}_{\mathsf{v}}(u)) \setminus \{e\} \subseteq \mathrm{BInt}_{\mathsf{v}}(e)$.

In the **acceleration bounded** model the set $\mathrm{Crowd}_{\mathsf{a}}(u)$ is defined as $\{w \in S \mid |u-w| \leq \frac{1}{2}a_{\max}\Delta^2$ and $|u'-w'| \leq \frac{1}{2}a_{\max}\Delta$ and $w \neq u\}$. Every edge $g = \{w,z\} \in G$ incident to a node $w \in \mathrm{Crowd}_{\mathsf{a}}(u)$ interferes with e, because $|u-w| + |u'-w'| \leq a_{\max}\Delta^2 \leq \max\{|w-z|, |w-z+(w'-z')\Delta| + a_{\max}\Delta^2\} = |w-z|_{\mathsf{a}}$ holds. Hence $E(\mathrm{Crowd}_{\mathsf{a}}(u)) \setminus \{e\} \subseteq \mathrm{BInt}_{\mathsf{a}}(e)$. ∎

Mobile Spanner Analogously to Section 2.4 a graph $G = (S,E)$ is called a **mobile c-spanner** according to pedestrian or vehicular mobility, i.e. for $\alpha \in \{\mathsf{a},\mathsf{v}\}$, if for all nodes $u, w \in S$ there is a path $P = (u = u_1, \ldots, u_\ell = w)$ in G such that

$$\sum_{i=2}^{\ell} |u_{i-1} - u_i|_\alpha \;\leq\; c \cdot |u-w|_\alpha \,,$$

for some constant c. In a **mobile weak c-spanner** the radius of this path is at most $c \cdot |u-w|_\alpha$, i.e.

$$\max_{u_i \in P, i=1,\ldots,\ell} |u-u_i|_\alpha \leq c \cdot |u-w|_\alpha \,.$$

The definitions imply directly that every mobile c-spanner is also a mobile weak c-spanner. For the optimization of energy consumption we use again the model that transmission power for sending to a distance d increases as a function d^δ, where $\delta \geq 2$ (see Section 2.1). Therefore, in a **mobile (c,δ)-power spanner** there is a path $P = (u = u_1, \ldots, u_\ell = w)$ in G such that

$$\sum_{i=2}^{\ell} (|u_{i-1} - u_i|_\alpha)^\delta \;\leq\; c \cdot (|u-w|_\alpha)^\delta \,,$$

for some constant c. G is a **mobile c-power spanner**, if G is a **mobile $(c,2)$-power spanner**.

Lemma 5.2 *For $\alpha \in \{\mathsf{a},\mathsf{v}\}$ every mobile c-spanner is a mobile (c^δ,δ)-power spanner.*

Proof: Consider a mobile c-spanner G and a path $(u = u_1, \ldots, u_\ell = w)$ in G from u to w.

$$\begin{aligned}\sum_{i=2}^{\ell} (|u_{i-1} - u_i|_\alpha)^\delta \;&\leq\; \left(\sum_{i=2}^{\ell} |u_{i-1} - u_i|_\alpha\right)^\delta \\ &\leq\; (c \cdot |u-w|_\alpha)^\delta = \; c^\delta \cdot (|u-w|_\alpha)^\delta\end{aligned}$$

∎

Congestion Following our approach in Section 4.1 we observe on each communication link e some packet **load** $\ell(e)$, which will be delivered in time interval $[0,\Delta]$. This load is caused by packets following routes (also called paths) which include e. The union of all these paths is called a path system $\mathcal{P}$.

As a worst case estimation on the number of packets that cause a congestion at link e we have to count all packets $\ell(e)$ as well as all packets being transported on interfering edges, which

leads to the following definition of congestion $C_{\alpha,\mathcal{P}}(e)$ of an edge e with respect to a path system $\mathcal{P}$ for $\alpha \in \{\mathsf{a}, \mathsf{v}\}$:

$$C_{\alpha,\mathcal{P}}(e) \ := \ \ell(e) + \sum_{e' \in \mathrm{BInt}_\alpha(e)} \ell(e') \ .$$

We describe the mobile network congestion by

$$C_{\alpha,\mathcal{P}}(G) := \max_{e \in E(G)} C_{\alpha,\mathcal{P}}(e) \ .$$

If we know the optimal path system $\mathcal{P}$ in advance, the definition of the underlying optimal network is given by all edges used in the path system. However, because of the structure of the protocol stack we have to determine the network before knowing a path system or even routing requests. We solve this problem by showing that a mobile weak spanner hosts a path system that polylogarithmically approximates the optimal congestion.

Theorem 5.2 *Given a mobile weak c-spanner G then for every optimal path system $\mathcal{P}$ on a complete network N there exists a path system $\mathcal{P}'$ on G such that for $\alpha \in \{\mathsf{v}, \mathsf{a}\}$*

$$C_{\alpha,\mathcal{P}'}(G) \ = \ \mathcal{O}(C_{\alpha,\mathcal{P}}(N) \ \cdot \ \mathrm{BInt}_\alpha(G) \cdot \log n) \ .$$

Proof: We apply the techniques of Subsection 4.1.4 used for approximating congestion in static ad hoc networks. Remember Lemma 4.11, Lemma 4.12, Lemma 4.13, and Lemma 4.14.

Now let $K_\mathsf{v} := 2v_{\max}\Delta$ and $K_\mathsf{a} := a_{\max}\Delta^2$. Let $\mathcal{D}(\mathsf{v}) = 2$ and $\mathcal{D}(\mathsf{a}) = 4$. In the **pedestrian model** the relationship between the L_2 norm and the transmission distance is

$$|u - w|_\mathsf{v} = |u - w| + K_\mathsf{v} \ .$$

In the **vehicular model** we define the distance $|u - w|_\mathsf{am}$ by

$$|u - w|_\mathsf{am} := \max\{|u - w|, |u - w + (u' - w')\Delta|\} \ .$$

Note that $\mathrm{dist}(u, w) = |u - w|_\mathsf{am}$ now defines a metric. Since we have $|u - w|_\mathsf{a} = \max\{|u - w|, |u - w + (u' - w')\Delta| + K_\mathsf{a}\}$, we get

$$|u - w|_\mathsf{a} - K_\mathsf{a} \leq |u - w|_\mathsf{am} \leq |u - w|_\mathsf{a} \ .$$

Define the interference region $D_\alpha(e)$ of an edge $e = \{u, w\}$ as the set of points, which can be interfered by an edge e, i.e.

$$\begin{aligned} D_\mathsf{v}(e) \ &:= \ \{x \in \mathbb{R}^2 \mid \exists p \in e \ : \ |x - p| \leq |u - w|_\mathsf{v}\} \ , \\ D_\mathsf{a}(e) \ &:= \ \{x \in \mathbb{R}^4 \mid \exists p \in e \ : \ |x - p|_\mathsf{am} \leq |u - w|_\mathsf{a} \ \} \ . \end{aligned}$$

For the vehicular distance measure we need the following Lemma.

Lemma 5.3 *There are $c_\mathsf{a} \leq 72$ disjoint sub-spaces $A_1, \ldots, A_{c_\mathsf{a}} \subset \mathbb{R}^4$ such that $\forall i \in \{1, \ldots, c_\mathsf{a}\}$:* $\forall u, p, w \in A_i \ : \ |u - w|_\mathsf{am} \leq |u - p|_\mathsf{am} \Longrightarrow \ |p - w|_\mathsf{am} \leq |u - p|_\mathsf{am}$.

Proof: W.l.o.g. let $u = (0,0,0,0)$. For $k, j \in \{0,\ldots,5\}$ we define

$$\begin{aligned} A_{6j+k+1} &:= \Big\{ x \in \mathbb{R}^4 \mid \measuredangle(x_1,x_2) \in \Big[k\frac{\pi}{3},(k+1)\frac{\pi}{3}\Big) \\ &\qquad \text{and } \measuredangle(x_3,x_4) \in \Big[j\frac{\pi}{3},(j+1)\frac{\pi}{3}\Big) \\ &\qquad \text{and } |x_1-x_2| \geq |x_3-x_4| \Big\}, \\ A_{36+6j+k+1} &:= \Big\{ x \in \mathbb{R}^4 \mid \measuredangle(x_1,x_2) \in \Big[k\frac{\pi}{3},(k+1)\frac{\pi}{3}\Big) \\ &\qquad \text{and } \measuredangle(x_3,x_4) \in \Big[j\frac{\pi}{3},(j+1)\frac{\pi}{3}\Big) \\ &\qquad \text{and } |x_1-x_2| < |x_3-x_4| \Big\}. \end{aligned}$$

where $\measuredangle(a,b)$ denotes the angle between the vector (a,b) and the vector $(1,0)$. Furthermore, let $p = (p_1,p_2,p_3,p_4), w = (w_1,w_2,w_3,w_4) \in A_{6j+k+1}$ for $k,j \in \{0,\ldots,5\}$. Then $|0-w|_{\mathsf{am}} = |(w_1,w_2)|$ and $|0-p|_{\mathsf{am}} = |(p_1,p_2)|$. By assumption we have $|u-w|_{\mathsf{am}} \leq |u-p|_{\mathsf{am}}$, i.e. $|(w_1,w_2)| \leq |(p_1,p_2)|$. Note that the angle between the vector (p_1,p_2) and the vector (w_1,w_2) is smaller than $\frac{\pi}{3}$. This implies that $|(p_1,p_2)-(w_1,w_2)| \leq |(p_1,p_2)|$.

Since $|(w_3,w_4)| \leq |(w_1,w_2)| \leq |(p_1,p_2)|$ and $|(p_3,p_4)| \leq |(p_1,p_2)|$ it follows that $|(p_3,p_4)-(w_3,w_4)| \leq |(p_1,p_2)|$. This implies $|p-w|_{\mathsf{am}} = \max\{|(p_1,p_2)-(w_1,w_2)|, |(p_3,p_4)-(w_3,w_4)|\} \leq |(p_1,p_2)|$.

Now, let $p = (p_1,p_2,p_3,p_4), w = (w_1,w_2,w_3,w_4) \in A_{36+6j+k+1}$ for $k,j \in \{0,\ldots,5\}$. Then $|0-w|_{\mathsf{am}} = |(w_3,w_4)|$ and $|0-p|_{\mathsf{am}} = |(p_3,p_4)|$. By assumption we have $|u-w|_{\mathsf{am}} \leq |u-p|_{\mathsf{am}}$, i.e. $|(w_3,w_4)| \leq |(p_3,p_4)|$. Note that the angle between the vector (p_3,p_4) and the vector (w_3,w_4) is smaller than $\frac{\pi}{3}$. This implies that $|(p_3,p_4)-(w_3,w_4)| \leq |(p_3,p_4)|$.

Since $|(w_1,w_2)| < |(w_3,w_4)| \leq |(p_3,p_4)|$ and $|(p_1,p_2)| < |(p_3,p_4)|$ it follows that $|(p_1,p_2)-(w_1,w_2)| \leq |(p_3,p_4)|$. This implies $|p-w|_{\mathsf{am}} = \max\{|(p_1,p_2)-(w_1,w_2)|, |(p_3,p_4)-(w_3,w_4)|\} \leq |(p_1,p_2)|$. ■

We extend the notion of congestion to nodes by counting all traffic which send out radio interference to the location of the point:

$$C_{\alpha,\mathcal{P}}(x) := \sum_{e \in E(\mathcal{P}): x \in D_\alpha(e)} \ell(e) .$$

$C_{\alpha,\mathcal{P}}(x)$ defines the capacity of the point x. For an edge $e = \{u,w\}$ the following relationship is valid.

$$\max\{C_{\alpha,\mathcal{P}}(u), C_{\alpha,\mathcal{P}}(w)\} \;\leq\; C_{\alpha,\mathcal{P}}(e) \;\leq\; C_{\alpha,\mathcal{P}}(u) + C_{\alpha,\mathcal{P}}(w) .$$

Lemma 5.4 shows that the maximum congestion of any point in $\mathbb{R}^{\mathcal{D}}$ is linearly bounded by the congestion of the network.

Lemma 5.4 *For all graphs $G = (V,E)$ with $V \subset \mathbb{R}^{\mathcal{D}(\alpha)}$, all path systems $\mathcal{P}$ and all points $x \in \mathbb{R}^{\mathcal{D}(\alpha)}$:*

$$C_{\alpha,\mathcal{P}}(x) = \sum_{e \in E: x \in D_\alpha(e)} \ell(e) \leq\; c_\alpha \cdot \max_{e \in E} \sum_{e' \in \mathrm{BInt}(e)} \ell(e') = c_\alpha C_{\alpha,\mathcal{P}}(G) ,$$

for constants $c_\alpha > 1$. In the **pedestrian model** *we have $c_{\mathsf{v}} = 6$ and in the* **vehicular model** *we get $c_{\mathsf{a}} \leq 72$.*

Proof: Let $k_{\mathsf{v}} := 2$ and $k_{\mathsf{a}} := \mathsf{am}$. For the point x we partition the space into c_α disjoint sub-spaces $A_1, \ldots, A_{c_\alpha}$ such that for all $u, v \in A_i$ $|x-u|_{k_\alpha} \leq |x-v|_{k_\alpha}$ implies $|v-u|_{k_\alpha} \leq |x-v|_{k_\alpha}$.Then for the **pedestrian mobility model** the angle between $\overline{xu}$ and $\overline{xv}$ is less or equal than $\pi/3$. Clearly, the optimal choice is $c_{\mathsf{v}} = 6$, which resembles six sectors centered at x. For the **vehicular model** it follows by Lemma 5.3 that $c_{\mathsf{a}} \leq 72$ suffices.

Now choose for each non-empty sub-space A_i a vertex $u_i \in A_i$ that minimizes the distance $|x-u_i|_{k_\alpha}$. For every edge $e = \{v, w\}$ with $x \in D_\alpha(e)$ we now show that there exists a vertex u_i with $u_i \in D_\alpha(e)$. Assume that $x \in D_\alpha(e)$ and let A_i be the sub-space where v lies in. Since $|u_i - x|_{k_\alpha} \leq |x-v|_{k_\alpha}$ we have $|u_i - v|_{k_\alpha} \leq |x-v|_{k_\alpha} \leq |v-w|_\alpha$. This implies

$$\begin{aligned} C_{\alpha,\mathcal{P}}(x) = \sum_{e \in E : x \in D_\alpha(e)} \ell(e) &\leq \sum_{i=1}^{c_\alpha} \sum_{e \in E : u_i \in D_\alpha(e)} \ell(e) \\ &\leq c_\alpha \cdot \max_{u \in V(G)} \sum_{e \in E : u \in D_\alpha(e)} \ell(e) \\ &\leq c_\alpha \cdot \max_{e \in E} \sum_{e' \in \mathrm{BInt}(e)} \ell(e') \leq c_\alpha C_{\alpha,\mathcal{P}}(G) \; . \end{aligned}$$

■

Lemma 5.5 *Let $C^*_{\alpha,\mathcal{P}}$ be the congestion of a given congestion-optimal path system $\mathcal{P}^*$ for a vertex set V and $\alpha \in \{\mathsf{a}, \mathsf{v}\}$. Then every mobile weak c-spanner N can host a path system $\mathcal{P}'$ such that the induced load $\ell(e)$ in N is bounded by $\ell(e) \leq \tilde{c}\, C^*_{\alpha,\mathcal{P}} \log n$ for a constant $\tilde{c} > 0$.*

Proof: Note that $|u-w|_\alpha \geq K_\alpha$ for all u, w. Now we replace every edge $e = \{u, w\}$ of the optimal path system $\mathcal{P}^*$ by the path $P(u, w) = (u = u_0, \ldots, u_\ell = w)$ from u to w in N with $|u - u_i|_\alpha \leq c \cdot |u-w|_\alpha$ and $|w - u_i|_\alpha \leq c \cdot |u-w|_\alpha$ (we consider only bidirectional edges). Analogously to Lemma 4.14 we consider the edge set $E_{\alpha,i,e_0} \subseteq E(\mathcal{P}^*)$ of edges $e = \{u, w\}$ with length $|u-w|_\alpha \in [2^i K_\alpha, 2^{i+1} K_\alpha)$ for $i \in \mathbb{N}_0$ which reroute their traffic to $e_0 = \{u_0, w_0\}$. The region where e interferes has been defined by $D_\alpha(e)$. Now we use the same arguments with regard to capacity, area, and congestion, applied in Section 4.1.

In the **pedestrian model** $D_{\mathsf{v}}(e)$ is a sphere with volume of at least $\pi 2^{2i+2} v^2_{\max} \Delta^2$ and lies completely inside the sphere D_{v} with radius $(c+1)2^{i+2} v_{\max} \Delta$. The volume of D_{v} is $\pi(c+1)^2 2^{2i+4} v^2_{\max} \Delta^2$. We apply Lemma 4.12 and Lemma 4.13 in the same way and get

$$\sum_{e \in E_{\mathsf{v},i,e_0}} \ell(e) \leq 4 c_{\mathsf{v}} (c+1)^2 C^*_{\mathsf{v},\mathcal{P}}(G) \; .$$

In the **vehicular model** we try to underestimate the volume of $D_{\mathsf{a}}(e)$ denoted by $\mathrm{vol}(D_{\mathsf{a}}(e))$. First, we define $D_{\mathsf{a}}(u) := \{x \in \mathbb{R}^4 \mid |u-x|_{\mathsf{am}} \leq |u-w|_{\mathsf{a}}\}$. Clearly, $\mathrm{vol}(D_{\mathsf{a}}(u)) \leq \mathrm{vol}(D_{\mathsf{a}}(e))$. Note that

$$|u-x|_{\mathsf{am}} = \max\{|u-x|, |u-x+(u'-x')\Delta|\} \geq \max\{|u-x|_1, |u-x+(u'-x')\Delta|_1\} \; .$$

Hence the 4-dimensional parallelepiped with volume

$$(\sqrt{2}\cdot 2^i a_{\max}\Delta^2)\times(\sqrt{2}\cdot 2^i a_{\max}\Delta^2)\times(\sqrt{2}\cdot\frac{2^i a_{\max}\Delta^2}{\Delta})\times(\sqrt{2}\cdot\frac{2^i a_{\max}\Delta^2}{\Delta}) = 2^{4i+2}a_{\max}^4\Delta^6$$

lies completely inside $D_{\mathsf{a}}(u)$. Furthermore, we have

$$|u-x|_{\mathsf{am}} = \max\{|u-x|, |u-x+(u'-x')\Delta|\} \le \max\{|u-x|_\infty, |u-x+(u'-x')\Delta|_\infty\}\ .$$

Since $|p-q|_{\mathsf{a}} \le c\cdot|u_0-w_0|_{\mathsf{a}} \le c\cdot 2^{i+1}a_{\max}\Delta^2$ for $p\in\{u,w\}$ and $q\in\{u_0,w_0\}$, all volumes $\mathrm{vol}(D_{\mathsf{a}}(e))$ lie completely inside the 4-dimensional parallelepiped with volume

$$((c+1)2^{i+1}a_{\max}\Delta^2+\sqrt{2}\cdot 2^i a_{\max}\Delta^2)^4\ .$$

Note that $\Delta>0$ and $a_{\max}$ are constants. With the same arguments used in the pedestrian model, we can conclude that

$$\sum_{e\in E_{\mathsf{a},i,e_0}}\ell(e) \le c_{\mathsf{a}}\frac{((c+1)2^{i+1}+\sqrt{2}\cdot 2^i)^4 a_{\max}^4\Delta^8}{2^{4i+2}a_{\max}^4\Delta^6} = \mathcal{O}(C^*_{\mathsf{a},\mathcal{P}}(G))\ .$$

For all mobile stations, we assume that $|s_i-s_j| = \mathcal{O}((v_{\max}\Delta)^k)$ in the **pedestrian model** and $|s_i-s_j|+|s'_i-s'_j| = \mathcal{O}((a_{\max}\Delta)^k)$ in the **vehicular model** for some constant k. This implies that there are at most $\mathcal{O}(\log n)$ different intervals $[2^iK_\alpha, 2^{i+1}K_\alpha)$. For the sum of loads $\ell(e)$ of the set $E_{\alpha,e_0} := \bigcup_i E_{\alpha,i,e_0} \subseteq E(\mathcal{P}^*)$ we get:

$$\sum_{e\in E_{\alpha,e_0}}\ell(e) = \mathcal{O}(c_\alpha\cdot\log n\cdot C^*_{\alpha,\mathcal{P}}) = \mathcal{O}(\log n\cdot C^*_{\alpha,\mathcal{P}})\ .$$

■

Lemma 5.5 shows that the number of packets transfered on detours is at most $\mathcal{O}(\log n)$ higher than the congestion in the optimal network. We denote by $\mathrm{BInt}_\alpha(G)$ the maximum interference number in the mobile weak c-spanner G. If the loads of all interfering edges can be bounded by m, then the overall congestion is at most $m\cdot\mathrm{BInt}_\alpha(G)$, which proves Theorem 5.2. ■

5.5 Constructing Mobile Networks

Now we present techniques to construct mobile (weak) spanners with low interference. We use a **grid-cluster** technique which adopts ideas of [AS98] for static ad hoc networks. We have already used such techniques in Chapter 4 to approximate static congestion optimal path systems with the Hierarchical Layer Graph.

In the **pedestrian model** we consider a grid of cell size $v_{\max}\Delta$. For every grid cell, where at least one mobile station resides at the beginning of the time interval $[0,\Delta]$, we elect one of them as a cluster head u_c. All other mobile stations in this cell have a communication link to the cluster head forming a star for each cell. The set of cluster heads S_c will be connected by a (static) spanner, e.g., the HL-graph.

In the **vehicular model** we consider a 4-dimensional grid $G_{j,k,\ell,m}$, where each cell forms a 4-dimensional box. A mobile station s_i with coordinates $(p_1, \ldots, p_4) = (s_{i,x}, s_{i,y}, s'_{i,x}, s'_{i,y})$ is in the grid cell $q = (q_1, \ldots, q_4) \in \mathbb{Z}^4$, i.e. $s_i \in G_q$, if $q_{\hat{\imath}} = \lfloor \mathrm{g}(p)_{\hat{\imath}} \rfloor$, where

$$\mathrm{g}(x, y, v_x, v_y) := \left(\frac{x}{6a_{\max}\Delta^2}, \frac{y}{6a_{\max}\Delta^2}, \frac{v_x}{2a_{\max}\Delta}, \frac{v_y}{2a_{\max}\Delta} \right).$$

Like in the pedestrian model we elect a cluster head for each cell and a star-like communication network in each cell. All cluster heads will be connected by a (static) four-dimensional spanner.

Lemma 5.6 *The grid-cluster-technique constructs mobile spanners for both mobility models.*

Proof: For a given mobile station u let $h(u)$ denote the cluster head of the cell where u is located. We choose as a path for two given nodes u, w the shortest path between $h(u)$ and $h(w)$ using only cluster heads combined with the edges $(u, h(u))$ and $(h(w), w)$.

For the **velocity bounded mobility** model the transmission distance between a node and its cluster head is at most $\sqrt{2}v_{\max}\Delta + 2v_{\max}\Delta = (\sqrt{2} + 2)v_{\max}\Delta$.

For the **acceleration bounded mobility** model the transmission distance between a node and its cluster head is at most $\sqrt{72\Delta^2 + 4\Delta}a_{\max}\Delta^2 + a_{\max}\Delta^2$.

The number of hops h between the cluster heads is linearly bounded by the Manhattan-distance between u and w according to the grid.

Hence, the additional impact of every hop of the path is linearly bounded by the distance. In the case that the two nodes are very near, i.e. $|u - w| < K_\alpha$, one uses that $|u - w|_\alpha \geq K_\alpha$. Because of the nearness of the cluster heads, there is only a constant number of hops and a linear long detour with respect to $K_\alpha \leq |u - w|_\alpha$. ∎

Note that the spanner property does not imply a bound on the interference number. For this, we can use the Hierarchical Layer Graph construction presented in Section 4.1 as a spanner. Here, we use a simplified approach, called **Hierarchical Grid** (because of the knowledge of absolute coordinates). An example of the resulting Hierarchical Grid Graph for pedestrians is given in Figure 5.5.

We start with the grid $G^0 = G$ introduced above and the set of all stations $S_0 := S$, and promote for each cell one mobile station for being cluster head. The set of these cluster heads form the set S_1. In this level only cluster heads may communicate with nodes in their cell. Besides these links, cluster heads have communication links with all cluster heads in neighboring cells sharing at least a corner of the grid.

We iterate this extended grid-cluster-technique until only one point is left. Formally, in the i-th level of the network structure, we start with a set of stations S_i and consider the grid G^i, with grid coordinates $\mathrm{g}^i(s_j)$.

$$\mathrm{g}^i(s_j) = \mathrm{g}^i(s_{j,x}, s_{j,y}, s'_{j,x}, s'_{j,y}) := \left(\frac{s_{j,x}2^{-i}}{6a_{\max}\Delta^2}, \frac{s_{j,y}2^{-i}}{6a_{\max}\Delta^2}, \frac{s'_{j,x}2^{-i}}{2a_{\max}\Delta}, \frac{s'_{j,y}2^{-i}}{2a_{\max}\Delta} \right).$$

A cell $q \in \mathbb{Z}^4$ contains all points p with $\lfloor \mathrm{g}^i(p)_\ell \rfloor = q_\ell$. We assign for each cell a cluster head and add it to the set S_{i+1}. We connect each of the cluster heads to all nodes of rank i in its cell.

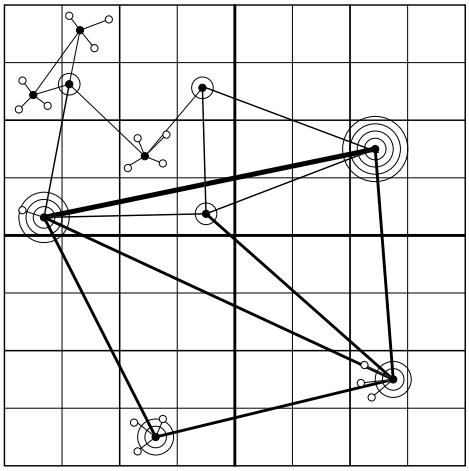

Figure 5.5: The hierarchical grid graph for pedestrians

Then we connect all cluster heads to all cluster heads of neighboring cells. For the pedestrian model we use an analogous construction based on the two-dimensional grid cell size $2v_{\max}\Delta$.

Theorem 5.3 *For both mobility models, i.e. for $\alpha \in \{\mathsf{v}, \mathsf{a}\}$, the Hierarchical Grid Graph constitutes a mobile spanner with interference number of at most $\mathcal{O}(\mathrm{crowd}_\alpha(V) + \log n)$.*

Proof: We start with the proof that the Hierarchical Grid Graph is a mobile spanner. If two nodes lie in the same grid cell of G^0, then they have hop-distance of at most 2, since both of them are connected with the cluster head. Since $|u-w|_{\mathsf{a}} \geq a_{\max}\Delta^2$ and $|u-w|_{\mathsf{v}} \geq 2v_{\max}\Delta$ for each pair of nodes u, w and the cell size is linear in this distance, this case is settled. Note that $|u-u|_{\mathsf{a}} = a_{\max}\Delta^2$ and $|u-u|_{\mathsf{v}} = 2v_{\max}\Delta$ hold for each node u.

We now prove that the mobile spanner property holds with respective to the grid distance measure $|\mathrm{g}^0(u) - \mathrm{g}^0(w)|$. We recursively define a path $P(u,w)$ from u to w. Let i be the lowest level of the hierarchical grid, where the ancestor u^* of u and the ancestor w^* of w are in neighboring grid cells, i.e. the cell of u^* and the cell of w^* are sharing at least one corner, where the ancestor of a node is defined recursively as its cluster-head and an ancestor of its cluster-head. Such a level exists, since at the second highest level each pair of cells are neighbors of each other. The nodes u^* and w^* are connected in level i by an edge $\{u^*, w^*\}$ per definition. We add the edge $\{u^*, w^*\}$ to $P(u,w)$. Now we must construct a path $P(u,u^*)$ and $P(w,w^*)$. This paths consist of the edges from a node to its cluster-head. Then the path $P(u,w)$ is defined as $P(u,u^*) \cup \{u^*, w^*\} \cup P(w,w^*)$.

Now we give a bound on the length of $P(u,w)$. Let x be the side length of the cells at level i. Then $|u-w| \geq x/2$, since the ancestor of u and w are not in neighboring cells at level $i-1$, otherwise they would be still connected by an edge at this level. The Euclidean length of the edge $\{u^*, w^*\}$ is at most two times the length of the diagonal of a cell at level i, i.e. it is at most $2x\sqrt{\mathcal{D}} \leq 4x$, where $\mathcal{D}$ is the dimension of the grid. The length of $P(u,u^*)$ is the sum of the lengths of the edges in $P(u,u^*)$, which is at most $x\sqrt{\mathcal{D}}\sum_{j=0}^{i} 2^{-j} \leq 4x$. Similarly, the length of

$P(w, w^*)$ is at most $4x$, and therefore the length of $P(u, w)$ is at most $12x$. This implies that the Euclidean stretch factor is at most 24.

We assume that Δ, $a_{\max}$, and $v_{\max}$ are constants. Then it remains to show that for each pair of nodes u and w

$$|\mathrm{g}^0(u) - \mathrm{g}^0(w)| = \Theta(|u - w|_\alpha) \,, \quad \text{for } |\mathrm{g}^0(u) - \mathrm{g}^0(w)| \geq 1 \tag{5.1}$$

This follows immediately from the definition of the cell size.

For the interference number, it is essential that every edge e connecting neighboring cells in G^i only interferes with an edge e', if for a node u of e and w of e' it holds $|\mathrm{g}^i(u) - \mathrm{g}^i(w)| = \mathcal{O}(1)$. This follows directly from (5.1). Hence, most of the interfering occur at the lowest level of the grid G^0, where a mobile station can suffer under the amount of radio interference of at most $\mathcal{O}(\mathrm{crowd}_\alpha(S))$ mobile stations in some constant number of near cells. In every higher grid level this amount reduces to a constant interference number, because only one cluster head resides in a cell and the number of connections with cluster heads of next lower or same level is constant. We assume that $|s_i - s_j| = \mathcal{O}((v_{\max}\Delta)^k)$ in the pedestrian model and $|s_i - s_j| + |s'_i - s'_j| = \mathcal{O}((a_{\max}\Delta)^k)$ in the vehicular model for some constant k. This implies that we have at most $\mathcal{O}(\log n)$ grid levels, which completes the proof. ∎

5.6 Position Information Management

In the previous sections, we have assumed that all positioning information is available to all nodes. But distributing this information is a non-trivial task. This process has to be done in the physical layer, where routing is not available. But the physical layer may use a positioning system (e.g., GPS [DJ96]) which enables every mobile station to learn its position and absolute speed. Then it can use short radio broadcast messages, called beacons, to inform all neighbors in the transmission range.

Another solution is to measure the distances between mobile stations by comparing the transmission power (which the sender may write in a data packet) with the received power. At first sight this looks similar to the position beacon model. However, using only distance information it is impossible to compute the relative speed of the communication partner.

We dedicate this section to present ideas for dynamic position information management using the **vehicular mobility model** which can be also applied to the **pedestrian mobility model** as well.

5.6.1 Coordinating Location Beacons

If the mobile stations can determine their absolute coordinates (and thus can compute absolute speed vectors), we suggest to broadcast this information in the physical layer in order to construct the basic network of the next round (of time span Δ).

A straightforward solution is sending special beacon signals carrying location and identification information. One can assign special time slots for these beacon signals, which are not propagated by other nodes. However, if all nodes send these beacons at maximum transmission

range, then n beacon signals would interfere at each node. It turns out that a data structure as the Hierarchical Grid helps to reduce the necessary transmission range and the size for the beacon time slot. For this, we use the following observation.

Lemma 5.7 *Let s_i, s_j be mobile stations using vehicular mobility and let $\tilde{s}_i := s_i(\Delta)$, $\tilde{s}_j := s_j(\Delta)$. Then for $k > 0$*

$$\frac{2}{3}|\mathrm{g}^k(s_i) - \mathrm{g}^k(s_j)|_\infty - 2^{-k} \leq |\mathrm{g}^k(\tilde{s}_i) - \mathrm{g}^k(\tilde{s}_j)|_\infty \leq \frac{4}{3}|\mathrm{g}^k(s_i) - \mathrm{g}^k(s_j)|_\infty + \frac{1}{6}2^{-k} .$$

Proof Sketch: The relative change of the position coordinates $x(s_i) - x(\tilde{s}_i)$ is bounded by at most $\pm(\Delta \cdot |(x(s_i') - x(s_j')| + a_{\max}\Delta^2)$, while the relative change of the velocity coordinate $x(s_i') - x(\tilde{s}_i')$ is bounded by $\pm 2a_{\max}\Delta$ and analogously for the y-coordinates. The rest of the proof follows straightforward by a case distinction. ∎

This observation helps to bound the dynamic changes of the Hierarchical Grid Graph. If a node u has rank $i > 1$ in round t, then the number of nodes of equal rank in the same cell as u is bounded by 9 in the **pedestrian model** and by 81 in the **vehicular model**.

5.6.2 Distances as Location Information

There is a number of reasons why absolute coordinates in mobile stations are not available, e.g., size and cost of GPS subsystems, reachability, accurateness. However, we will show that little relative distance information is sufficient to maintain a good mobile network structure. We assume, that a mobile station can measure the distance to another station by measuring the receiving transmission power. Such measurements can be performed in the physical layer of the protocol stack and we reduce the number of measurements, while still maintaining a mobile network similar to a grid-cluster network. Define $\delta_{i,j}(t) = |s_i(t) - s_j(t)|$.

Lemma 5.8 *Given distances $\delta_{i,j}(-\Delta)$ and $\delta_{i,j}(0)$ it is possible to approximate the transmission distance $|s_i - s_j|_{\mathsf{a}}$ by a factor of 5.*

Proof: We use

$$\tilde{\delta} := \max\{\delta_{i,j}(0), |2\,\delta_{i,j}(0) - \delta_{i,j}(-\Delta)|, a_{\max}\Delta^2\}$$

as an approximation for $|s_i - s_j|_{\mathsf{a}}$ and show that $\tilde{\delta} \leq |s_i - s_j|_{\mathsf{a}} \leq 5\tilde{\delta}$. Assume s_i measures the distance to $s_j(-\Delta)$ and $s_j(0)$. Let $d := s_i(0) - s_j(0)$ the distance at time 0 and $v(t) := s_i'(t) - s_j'(t)$ the relative velocity. Since both stations may accelerate we assume that s_i is fixed and s_j may accelerate with $2a_{\max}$.

First we prove that $\tilde{\delta} \leq |s_i - s_j|_{\mathsf{a}}$. Because $\delta_{i,j}(0) = |s_i - s_j|$ we only have to show that $|2\delta_{i,j}(0) - \delta_{i,j}(-\Delta)| \leq |d + v\Delta| + a_{\max}\Delta^2$. The term $|\delta_{i,j}(0) - \delta_{i,j}(-\Delta)|$ represents the estimated average velocity during $[-\Delta, 0]$. If s_i lies in the middle between $s_j(-\Delta)$ and $s_j(0)$, the measured velocity is 0 and thus underestimated. Apart from this exceptional case, the true relative velocity at time 0 may differ from the estimated average value by an error of $\pm a_{\max}\Delta$ because s_j may accelerate/decelerate with $2a_{\max}$. Thus $|2\delta_{i,j}(0) - \delta_{i,j}(-\Delta)| = |d + v\Delta \pm a_{\max}\Delta|$ and $\tilde{\delta} \leq |s_i - s_j|_{\mathsf{a}}$.

Now we show that $|s_i - s_j|_{\mathsf{a}} \leq 5\tilde{\delta}$. We can minimize $\tilde{\delta}$ if we position s_i in the middle of $s_j(-\Delta)$ and $s_j(0)$. $|d + v\Delta|$ can be maximized if s_j accelerates with $2a_{\max}$ during $[-\Delta, 0]$ (The acceleration in $[0, \Delta]$ is irrelevant). For the distance estimation $\delta_{i,j}(0) = \frac{1}{2}(|v(-\Delta)|\Delta + a_{\max}\Delta^2) =: r$. The estimation yields $\tilde{\delta} = \max\{r, 2r - r, a_{\max}\Delta^2\}$. At time 0 the velocity $v(0) = v(-\Delta) + 2a_{\max}\Delta$ and thus $|s_i - s_j|_{\mathsf{a}} = r + |v(-\Delta)|\Delta + 3a_{\max}\Delta^2 = 3r + 2a_{\max}\Delta^2$. If we choose $v(-\Delta) = a_{\max}\Delta$ so that $r = a_{\max}\Delta^2$, then the ratio $|s_i - s_j|_{\mathsf{a}}/\tilde{\delta}$ is maximized and at most 5. ■

Based on the physical restriction on the movements of mobile stations, we have found a dynamic data structure, called **Mobile Hierarchical Layer graph** (MHL-graph). Essentially, it uses the same ideas as the Hierarchical Grid graph if one replaces the grid distance measure with the Euclidean L_2-norm. Again, one can show that this distance measure can be approximated by two distance measurements at different time points. The notion of cells will be replaced with a disk around nodes of certain rank. These MHL-graphs are mobile spanners and approximate the minimum amount of mobile interference by a constant factor.

5.7 Conclusions

The main contribution of this chapter is the model of worst case mobility which was defined in a formal way. We have discussed two worst case models for mobility. In the first pedestrian motivated model, we bound the speed by a speed limit of $v_{\max}$. In the other model designed for the special mobility induced by high-speed vehicles, we assume that the acceleration of all nodes is bounded by a constant $a_{\max}$. Our idea is to adjust the transmission range of senders such that we can guarantee the persistence of all communication links for at least a time period of length Δ to ensure some elementary stability in a wireless ad hoc network.

For network construction we concentrate on the medium access layer, which builds up communication links without known routing tasks. We have presented a distributed algorithm to build such an elementary mobile network, which allows us low congestion, low interference, low energy data routes, small degree, and small diameter as summarized in the following corollary.

Corollary 5.1 *There exist distributed algorithms that construct mobile ad hoc networks for the* **velocity bounded** *and the* **acceleration bounded** *mobility model with the following properties:*

1. *The mobile network allows us data routes on this mobile network inducing a congestion of at most $\mathcal{O}(\log^2 n)$ times the congestion of the optimal routing.*
2. *The interference number of the mobile network approximates the optimal interference number by a factor of $\mathcal{O}(\log n)$.*
3. *Energy-optimal routes can be approximated by a constant factor.*
4. *The degree is bounded by $\mathcal{O}(\mathrm{crowd}_\alpha(V) + \log n)$ and the diameter is at most $\mathcal{O}(\log n)$.*

For the routing problem, this does not imply that low congestion, low energy, and short routes can be optimized using the same routing policy. Already for the static case of wireless networks,

one experiences trade-offs between any two of these measures, see Section 4.1. However, the algorithms presented here, build up a general-purpose communication network which performs well for all kinds of routing requests and has reasonable approximation ratios for any routing policy with regard to congestion, energy or dilation.

As a side effect of our network construction for the vehicular mobility model, we achieve a data structure, where clustering takes locality of positions and movement into account. E.g., consider a highway of two lanes in each direction, see Figure 5.6. All algorithms and data structures, neglecting the impact of relative speed, build up too many communication links between the opposing lanes. However, these links are very unstable and hence expensive. In our model, communication links along each direction are much more frequent and, if there is a choice, then the communication link across the middle of the highway will be established between slower moving vehicles (e.g., trucks) instead faster ones (and this is even the case if the fast vehicles are nearer to each other).

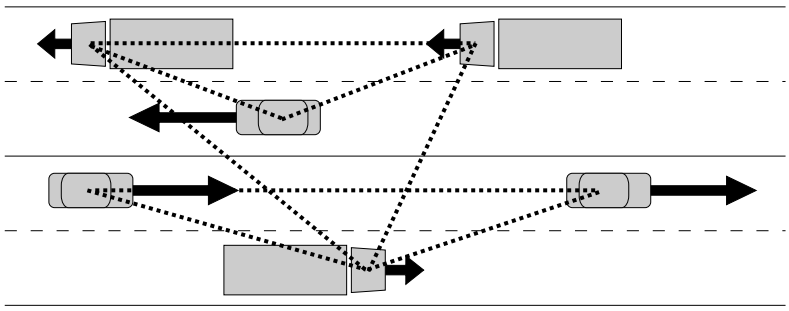

Figure 5.6: Vehicles on a highway with different speed vectors

Finally, we want to mention that there are some open questions concerning our first approach to velocity and acceleration bounded mobility. The modeling of the interference of moving edges presented here is only a rough estimation. It is not clear how a mobile network design may look for a more accurate model. The movements of the communication partners also affect the routing algorithms. We have neglected the problem of long routes which require an update time of length greater than Δ. Possibly, communication can be improved if for the communication paths those nodes are preferred that also move towards the receiver's direction.

The distributed measurement and computation of the relative locations and relative speed vectors states a problem. We have seen that a rough approximation can be deduced from the receiving transmission energy and its change in time. However, for the construction of a reasonable basic network, a direct implementation of previous approaches needs some interaction between location beacons and distance measurements.

Chapter 6

Experimental Analyses and Results

In this chapter we present the results of our extensive experimental evaluations. We have developed two different testbeds to perform a number of significant simulations that demonstrate the applicability of our algorithms and/or analyses using realistic settings.

In the first section, we describe our **s**imulation environment for mobile **a**d **h**oc **ne**tworks, SAHNE. We use SAHNE to close the gap between theoretical investigations of communication protocols in wireless networks and realistic wireless environments. For this purpose we have implemented realistic models for radio and infrared transmissions to test our algorithms using the omnidirectional as well as using the directional communication model presented in Chapter 4. Furthermore, we have developed and integrated an interface between mathematical modeling and prototypical realization that allows us to use the same source code of our algorithms, that we have implemented and successfully tested in our simulation environment, directly on the mini robot Khepera (see Subsection 4.2.1).

In the second section we present our **i**nteractive **t**ool for checking **gra**ph **p**roperties, ITGraP. Here, our aim was not to go into technical detail, but more to present a theoretical study of important graph properties on vertex sets where the nodes are placed uniformly at random. We have implemented the Yao-graph and its variants as well as the HL-graph to perform simulations and to find out about the performance of our topologies. In addition, we allow each node to adjust the orientation of its senders to improve the quality, especially the stretch factors, of the sectorized topologies. We show improvements experimentally and present algorithms to compute the stretch factors of a given graph exactly.

6.1 A Simulation Environment for Mobile Ad Hoc Networks

Modern computer networks are designed in a highly structured way. Most networks are organized as a series of layers, each one built upon its predecessor, to reduce their design complexity. The OSI model [Spo93, Tan96], shown in Figure 6.1, is based on a proposal developed by the International Standards Organisation (ISO) as a first step toward international standardization of the protocols used in the various layers. The model is called the ISO OSI (Open Systems Interconnection) reference model, shortly OSI model, and consists of seven layers. Note that the

OSI model just tells what each layer should do. It is not a network architecture, since it does not specify the exact services and protocols to be used in each layer.

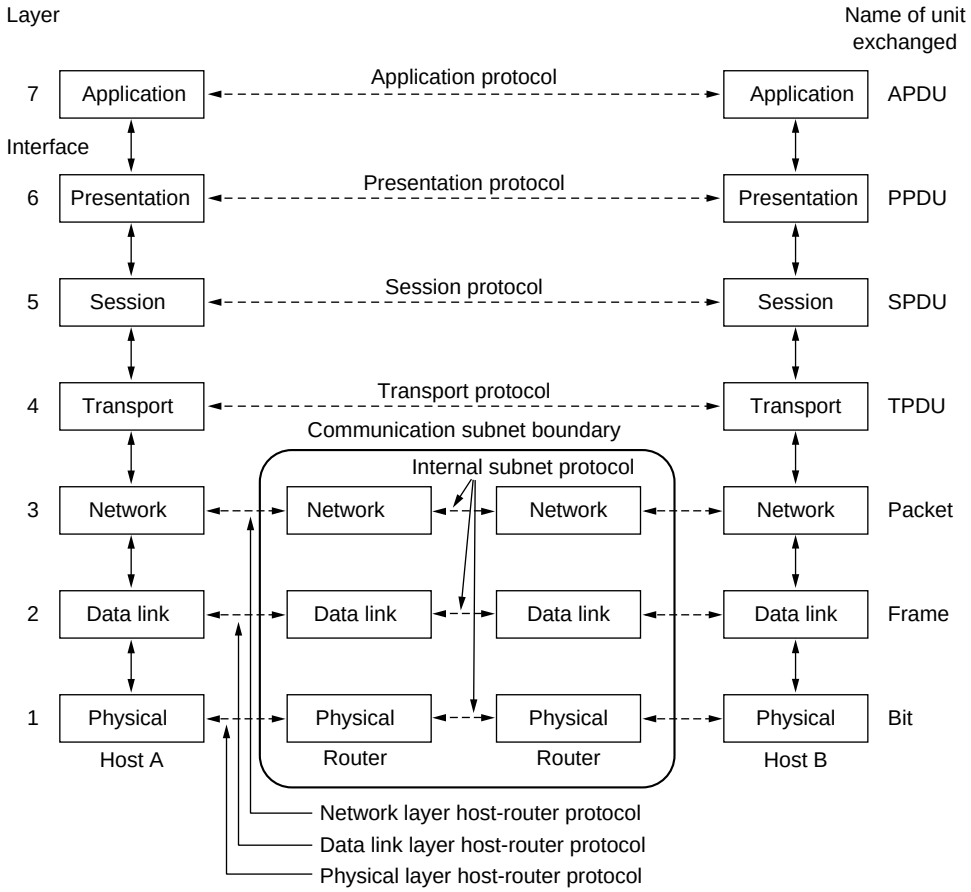

Figure 6.1: The OSI reference model minus the physical medium [Tan96]

For mathematical investigations the complexity of communication in networks is sometimes to difficult to handle. Therefore abstract models and simple, sometimes restricted, assumptions have to be used. Based on these models algorithms are developed and analyzed on a high level of abstraction. For example, in Chapter 4 we have investigated point-to-communication using two different types of wireless communication models and for our analyses we have introduced abstract models for interfering signals. In real-world applications interference appear in a different way. Furthermore, we have to consider other physical side-effects like overlapping of sectors and areas with no reception. The whole communication process between two nodes in a network including all communication overhead has to be taken into consideration.

We have developed a simulation environment for mobile ad hoc networks, SAHNE [Vol01, Vol02, Rüh02, RSVG03], for analyzing communication in MANETs based on the directional communication model to get realistic experimental results. The omnidirectional communication model in SAHNE can be simulated using the directional one with one sector/sender per node. Free existing simulation environments for MANETs, e.g., ns-2[FV98], GloMoSim[ZBG98, LL00], or OMNet++[Var01], are not specially designed for directional communications used in our sce-

nario. In addition, especially in ns-2, every communication layer is implemented in high detail and this has the disadvantage that only small sets of nodes can be simulated in a short time. In SAHNE it is possible to simulate hundreds of nodes in a wireless environment. But nevertheless we have also performed simulations of omnidirectional communication with ns-2. Here, we have implemented the Hierarchical Layer Graph.

One goal during the development of our simulation environment SAHNE has been to build up a flexible, well-expandable, and easy-to-use-environment, with which nearly every communication layer can be simulated. The focus of this thesis is on routing (multi-hop communication) and topology control in wireless networks. Hence, we have been interested in realistic implementations of some lower layers, i.e. especially the network and the data link layer, see Figure 6.1. Furthermore, SAHNE simulates effects like interference and uses realistic models for radio and infrared signal propagation.

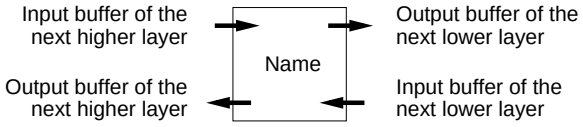

Figure 6.2: Layout of one communication unit

We have designed SAHNE with respect to the OSI model (see [Spo93, Tan96]) and the functionality of the nodes in SAHNE has been divided into several communication units (see Figures 6.2 and 6.3). The number of these units is not fixed and it is easy to integrate new units. The main functional units that are already implemented in SAHNE have the following tasks.

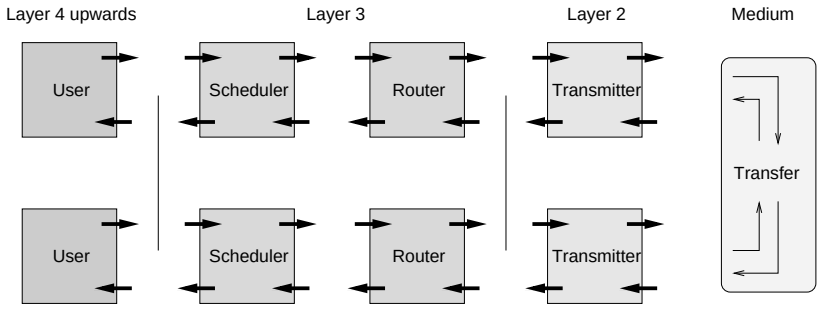

Figure 6.3: Most important communication units of SAHNE

The *user* is equivalent to the application layer and it is comparable with a data transfer service. In this unit data will be generated and destinations have to be chosen for the initiated packets. The user can be extended by new application services that are arranged in higher layers.

As the first part of the network layer the *scheduler* determines what should be done with packets received by the user. Packets will be scheduled (e.g., forwarding packets via a random target that acts as a stopover, or splitting packets into smaller packets and vice versa).

As the second part of the network layer the *router* forwards packets received by the scheduler to its targets. Especially, there will be created and chosen routes and it will be decided how

to transmit information along these routes. The router uses topology knowledge, e.g., it knows every node in the neighborhood.

The *transmitter* represents the MAC (Medium Access Control) layer of the data link layer. It is responsible for direct data transmissions between two neighboring nodes. In this layer, problems depending on the network architecture will be simulated such as the occurrence of interference in MANETs. The transmitter acquires direct neighbors, builds up topologies, and decides when to use established edges, e.g., using a probabilistic channel transmission protocol.

The *medium* models the communication channel. Data will be forwarded from its source to its target with consideration of physical channel properties.

Two nodes are able to communicate at every layer of this model. In general these functional units will be used in the following way to generate and to process network traffic. A user generates a packet with a target and forwards it to the scheduler of the same node. The scheduler decides whether to send the packet directly to the target, or via another node, or something like this, and forwards it to the router. The router knows where the target is and chooses a node that will get the packet next. The wireless transmission will be performed by the transmitter. The last two steps will be repeated until the packet arrives at the target. Then it goes again through the scheduler to another scheduler or directly to the user. In fact, this is a very simple example. In parallel, at every layer, other tasks can take place. For example, the transmitter transmits control packets beside data packets to establish communication links and to build up and to maintain a topology.

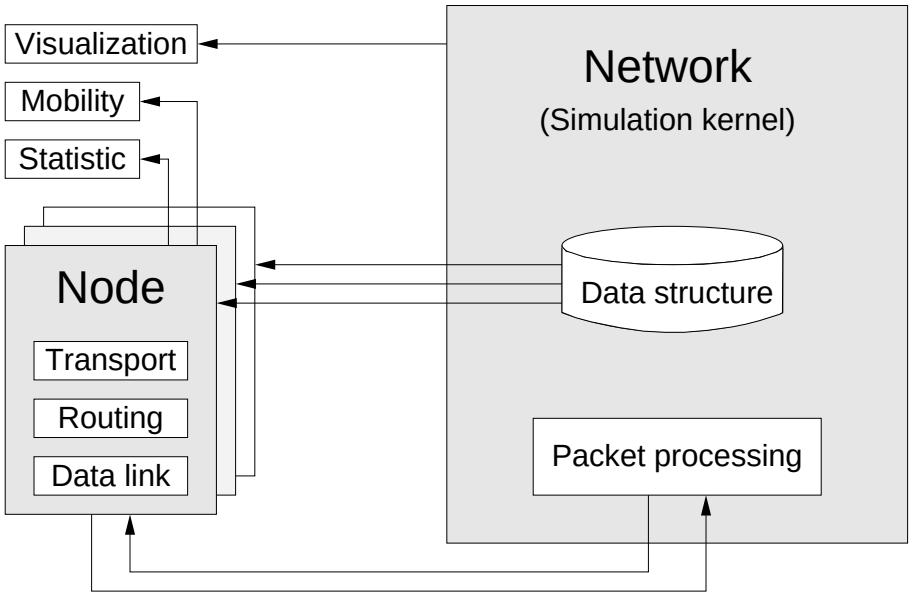

Figure 6.4: Internal structure of SAHNE

SAHNE has been implemented in C++ using various data structures and several advanced data types of LEDA [MN99]. The development has been done with great care to be platform independent (SAHNE was tested on several operating systems: Solaris, Linux, Windows). The units in SAHNE are realized as C++ classes and the whole environment is based on an object-

oriented model. SAHNE can be compiled in two different ways, either in textual mode or in interactive mode. In both cases simulation parameters will be read from a configuration file (e.g., a textfile called *sahne.cfg*). Additionally, in the interactive mode they can be edited interactively via a graphical user interface (GUI). In the textual mode the simulation runs until the number of simulation steps will be finished. In the interactive mode the user is able to change parameters, check nodes/edges, view statistics, and some others interactively. At the end of a simulation with SAHNE, local and global statistics will be given and some files will be generated that can be used directly as an input for the gnuplot tool [WK86] to produce statistics. In Figure 6.4 an overview of the internal structure of SAHNE is given. Beside the communication units there exist further classes. The network class is the most important one. Here, we have integrated the simulation kernel in which we have implemented our models for signal propagation. Main data structures for realizing fast range queries necessary for computing receiving nodes when signals are transmitted are also part of the network class. A link to a packet processing library connects simulation and prototypical realization. It is possible to use the same source code implemented in this library directly on the Khepera robot.

We have additional classes for visualization, mobility, and statistics. The visualization class is completely independent from other classes, i.e. it can be easily replaced by other libraries. The mobility class regulates motion patterns. Every node can move around without any restriction in a MANET and therefore motions have to be calculated at each simulation step. In SAHNE miscellaneous movement strategies have been implemented. The most known is the random waypoint model. In this model, a node chooses a destination with a uniform random distribution over the given area, moves there with a velocity, waits for some simulation steps, and then repeats this behaviour (see [JM96, Per01]). We have implemented this model and some extensions. More details about mobility models are given in Chapter 5. Known motion patterns such as the Brownian Motion Model, the Column Model, and the Pursue Motion Model [San98] are also available in SAHNE. For fixed motion sequences it is possible to define trajectories in SAHNE on which nodes have to move. This is very helpful to perform simulations using special (movement) szenarios, e.g., two trains passing each other.

During a simulation we assume that all nodes wishing to communicate with other nodes within the MANET are willing to participate fully in the protocols of the network. In particular, each node participating in the network should also be willing to forward packets for other nodes in the network. Information will be transmitted by *packets*. Every packet has a clear identification (ID), a source, and a target. Furthermore, it can contain additional information such as parameters or data like files, audio- or videodata, text, etc. A packet needs one *time step* to make a single hop in the network, regardless of the distance to the destination node. In many situations it is more time- and resource-efficient for a message to perform a sequence of hops, *multi-hop-communication*, instead of one single hop to its final destination. The sequence of nodes used for the hops is called route or path of a message. All nodes in SAHNE work in a synchronized way.

6.1.1 Communication Strategies using Idealized Assumptions

In this subsection we present routing and topology control algorithms and experimental results for the Yao-graph using idealized assumptions. Here, we assume that each node is equipped with

$k \in \mathbb{N}$ transmitting devices that allow a node sending data in sectors. We divide the area around a node in k equal non-overlapping sectors of angle $2\pi/k$ and use one transmitting device per sector. We assume that there is given only one frequency for transmissions and that each node can adjust the transmission power of its devices. The attentive reader might have observed that this matches exactly our assumptions in Section 4.2. In this subsection we perform simulations without a realistic model for signal propagation, i.e. we assume that the borders of a sector are straight, the senders on a node are fixed, and the nodes have always the same orientation (no rotation is possible). The visualization of such idealized data-transmissions is shown in Figure 6.5.

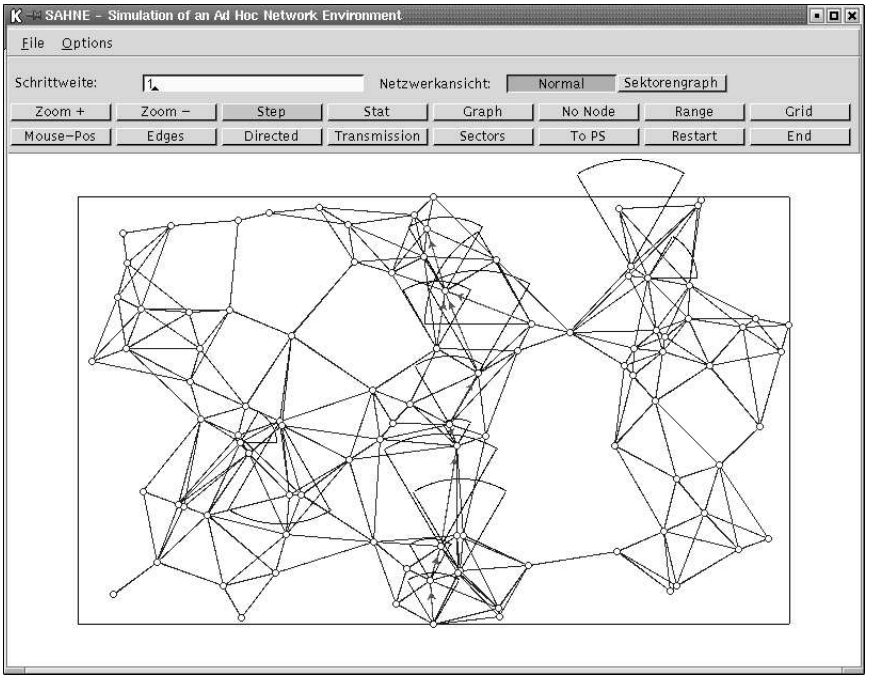

Figure 6.5: Visualization of data-transmissions in SAHNE

A transmission failure or an interference occurs, if and only if more than one signal is received in the same sector a the same time. Furthermore, a node can send out at most one packet at a time per sector. If a node v attempts to send a packet with transmission power t, then all nodes needing less than $\alpha \cdot t$ power to receive a packet from v are blocked, where $\alpha > 1$ is some fixed constant [AS98]. Any information transmitted to a blocked node is not received. Note that this means that it is possible that no transmission during a single time step was succesful. A transmission conflict caused by interference cannot be detected by the sending node. In Chapter 4 we have already discussed hidden and exposed terminals as well as asymmetric interference. We assume that every sender will be received only within its sector and nodes are only allowed to communicate with their neighbors in these particular sectors.

We have implemented in SAHNE several strategies for routing and topology control using different assumptions. These algorithms can be regarded as exemplary implementations. SAHNE can easily be extended by other strategies. In the following we will describe first, simple algorithms for the most important communication units of SAHNE, see also Figure 6.3.

The *transmitter* is responsible for construction and maintenance of the Yao-graph. In this subsection we assume that every node is equipped with a GPS-module [DJ96] to get its physical location. In reality, position information provided by GPS includes some amount of error, which is the difference between GPS-calculated coordinates and the real coordinates. In this case we assume that each node knows its current location precisely. The transmitter collects the following information about each of its k neighbors: name (ID), physical location, distance, and the time, at which the last information update by a packet took place.

If in a sector of a node more than one packet is received, then all the packets are removed. Otherwise the packet is received correctly. The transmitter processes only received packets and uses these to collect necessary information about directly connected neighbors. Every transmitter periodically transmits neighbor-control-packets (NNP) in each sector with some constant probability to produce neighbor information. The transmission range of such a message can be chosen randomly from a fixed interval or is fixed. In this manner edges of the Yao-graph will be established. Transmitters may have random transmission breaks to reduce the number of collisions in a time step. Packets to higher layers will be forwarded as soon as they will be received completely. Packets from higher layers will be split before being forwarded if they are oversized. The maximum size of a packet and other values can be set by the simulation parameters.

The *routing unit* handles and forwards packets in the order of their arrivals: First-In-First-Out (FIFO). Other packet switching schemes can easily be integrated. At the beginning of a simulation, the user is able to choose whether packets should be sent with acknowledgments or not. Some other parameters can also be adjusted. In the following, we distinguish between two routing schemes: *pq-routing* and *hop-minimization*. Both algorithms use the information collected by the transmitter to route packets.

The *pq-routing* works as follows: assume a packet p arrives at node u. Let the target of p be the node w and i the sector of u in which w lies. Then p will be forwarded over a neighboring node v in sector i. We call sector i the *target-sector*. In this way p will be transmitted until the destination is reached. A precondition is that the targets of the packets are known. Remember the proof that the Yao-graph is a c-spanner for a constant c. The proof is constructive and pq-routing exactly uses the idea given in the proof to find a path from a source to its destination. Such routing protocols are called localized routing since the decision to which node a packet is forwarded is based only on the information in the packet header and the local information gathered by the node from a small neighborhood [Li03b, Li03a, Li03c].

We assume that the underlying wireless network is connected, but since the maximum transmission range in a MANET is bounded, it might be possible that we get empty sectors. Sectors in which no connection to a nearest neighbor is possible. Then the pq-routing will not work correctly. Known solutions to this kind of problems use simple heuristics like compass routing, right hand rule, face, or greedy routing (see [Li03b, Li03a, Li03c]). We consider a very simple strategy to investigate the problem of empty sectors. If there is no connection to a node in the target-sector possible, we will forward the packet to a node in the sector on the left/on the right, each with probability of $1/2$, until we will find a node to forward the packet.

The *hop-minimization* is a distance-vector algorithm that operates like the Destination Sequenced Distance Vector protocol (DSDV, [Per01]). Every node creates a routing table that includes the destination's address (e.g., the node number), the number of hops required to reach the

destination, the neighbor required to reach the destination with a minimal number of hops, and the creation time of the information received regarding that destination, as originally stamped by the destination. Every node periodically broadcasts to all of its neighbors its current estimation of the shortest distance to every other node in the network without the information about the neighboring node (to avoid loops) to keep the data up to date. The router looks in its routing table at the entry regarding the destination of p to forward a packet p, and if it is not empty, p will be transmitted via the located neighbor. Otherwise the packet will be held. Storing of the routing table requires $\mathcal{O}(n)$ space per node for a network with n nodes.

The *scheduler* is responsible for the scheduling of packets. All the packets should have a limited size that is much smaller than the maximum size of a TCP/IP packet to transmit packets error free and to reduce the number of collisions. For this purpose the scheduler can split data packets into many several packets. These smaller packets will be forwarded and routed separately. The scheduler forwards packets either directly or via a randomly selected node that acts as a stopover which sometimes improves network parameters, see Valiant's trick [Val82].

Finally, in the *node unit*, network traffic will be generated. Several selected nodes create data packets, choose destinations for them, and forward them to the scheduler. The creation of packets will take place in one simulation step with some constant probability which gives the injection rate, if packets are generated asynchronously. In case of synchronous creation packets will be injected after a fixed number of simulation steps. The size of packets can be chosen randomly or it can be fixed.

Parameter	*Value(s)*
Simulation area:	500 m × 300 m
Max. transm. range:	200 m
Number of nodes:	60 (2 fi xed)
Simulation time:	10 s (= 100,000 simulation steps)
Bandwidth:	2 MBit/s (≈ 209 Bit/simulation step)
Link utilization:	80 %
Fixed packet size:	512 Byte
Injection:	100 packets/s (= exp. every 1,000 simulation steps)
Motion pattern:	random motion pattern, 15 km/h
Pause time:	2 s (= 20,000 simulation steps)
Number of sectors:	6
Upd. of routing inf.:	10 updates/s
Every node of the network creates data packets. The destinations for these packets will be chosen randomly. The transfers are similar to a permutation routing.	

Table 6.1: Simulation parameters

Simulation Results using Idealized Assumptions

We carried out a number of experiments modeling different possible situations. The results presented in the following are based on parts of the diploma thesis of the author of this work. We have chosen only a very small choice from all results and want to refer to the diploma thesis for more details, see [Vol01]. The most important parameters of our simulations are listed in Table 6.1. At the beginning of a simulation the nodes will be placed over the given simulation

area uniformly at random. We compare the algorithms with regard to the expected injection distance, the number of sectors of the Yao-graph, the transmission range, and the velocity of the nodes. Finally, the accessibility will be illustrated depending on the number of sectors and on the transmission range.

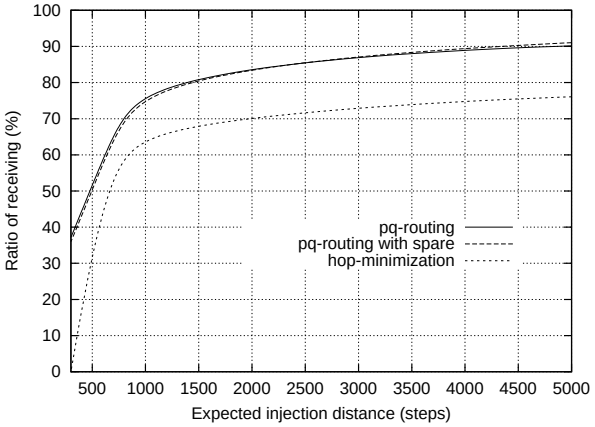

(a) The expected injection distance

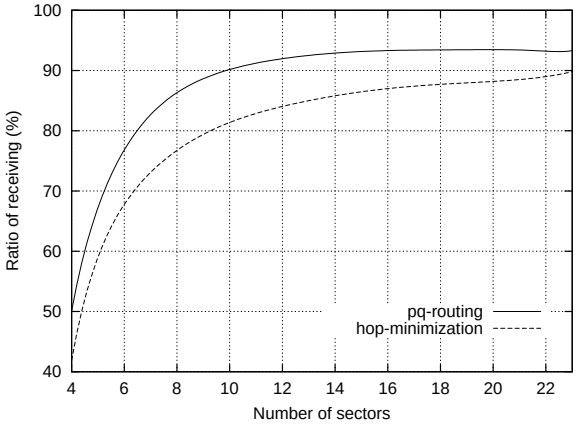

(b) The influence of sector number

Figure 6.6: Varying the injection distance and the number of sectors

In Figure 6.6(a) the exploration of the expected injection distance is illustrated. The rate of successfully received packets of the pq-routing as well as of the hop-minimization decreases with an increasing number of generated packets. The pq-routing is better than the hop-minimization, since no further overhead is needed for transmissions. The amount of interference of the pq-routing is reduced.

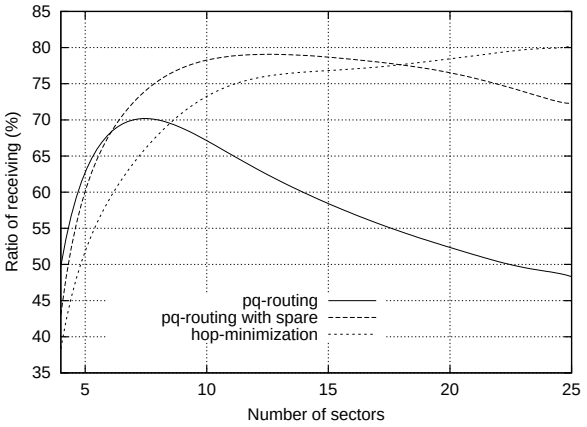

(a) The influence of sector number by using small transmission ranges

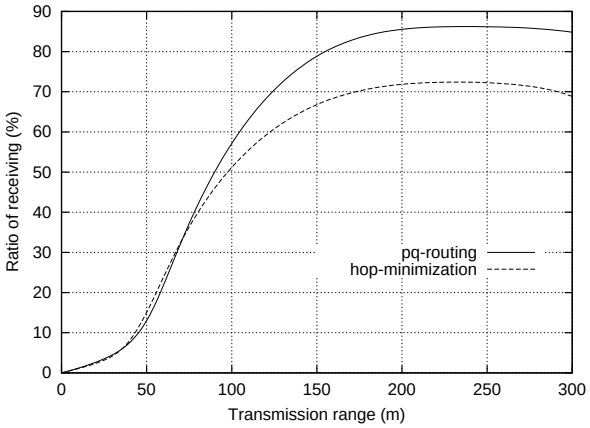

(b) The transmission range

Figure 6.7: Varying the number of sectors and the transmission range

The number of sectors in the directional communication model is a very interesting parame-

ter. In Figure 6.6(b) one can see that the ratio of receiving increases with an increasing number of sectors. But this conclusion is not always correct. Be careful, because in this simulation the transmission range is high (200 m).

In Figure 6.7(a), the expected result can be seen. The transmission range is low (100 m) and the pq-routing will be bad, if more than 7 sectors are available. The explanation is simple. The more sectors available the longer are the edges of the Yao-graph. Thus, many packets will be held at some nodes, if pq-routing is used. In this case, a spare strategy gives better results. But the hop-minimization will be the best, because it only uses edges that exist (pq-routing possibly tries to use sectors in which no edges are available).

A simple assumption is that the ratio of receiving will be better, if the transmission power is very high. Figure 6.7(b) shows that this is correct, but beginning with a certain transmission range the best ratio cannot be exceeded. If the transmission range is too high, the ratio will be worse because of the high number of collisions.

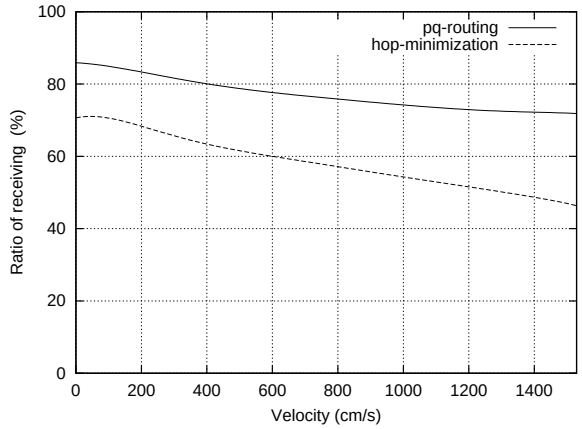

(a) The influence of motion

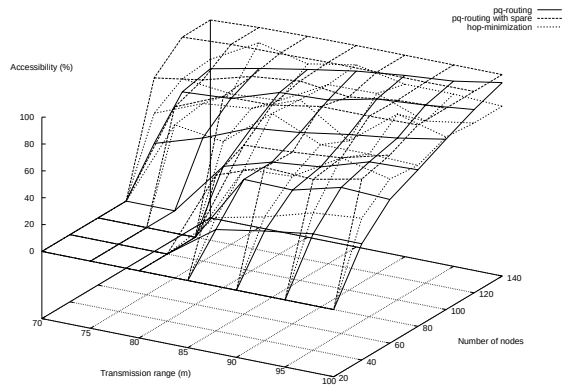

(b) The accessibility

Figure 6.8: Varying the velocity and both, the transmission range and the number of nodes

The exploration of the influence of motion in Figure 6.8(a) clarifies that a higher velocity entails a worse ratio of receiving. The hop-minimization is more concerned as the pq-routing. The necessary information to update the routing tables cannot arrive in time.

The last Figure 6.8(b) gives an overview of the accessibility in the simulated MANETs. A node v will be accessible, if all other nodes can send v a packet. The number of correct routes was counted and compared to the number of all possible routes.

6.1.2 Topology Control using Realistic Propagation Models

Now we try to close the gap between our theoretical investigations of wireless network topologies and realistic wireless environments. For point-to-point communication, we examine the Yao-graph, the SparsY-graph, the SymmY-graph (see Section 4.2), and the HL-graph (see Section 4.1). We present distributed algorithms that can be used to build up the Yao-graph and its

variants in time $\mathcal{O}(\log n)$ per node without the use of any geographical positioning system. Our algorithms are based only on local knowledge and local decisions and make use of power control to establish communication links with low energy-cost. We compare these algorithms with respect to congestion, dilation, and energy. For congestion we introduce different measures that allow us to investigate the difference between real-world wireless networks and our models for wireless communication at a high level of abstraction. For more realistic simulations we have extended our simulation environment SAHNE, see Figure 6.9. We use a realistic transmission model for directional communication that uses sector subdivision. Finally, our experimental results show that our topologies and algorithms work well in a distributed environment and we give some recommendations for topology control based on our simulations. The experiments presented in this subsection were performed by Stefan Rührup in the context of his diploma thesis [Rüh02] under the supervision of the author of this work. We present some selected results.

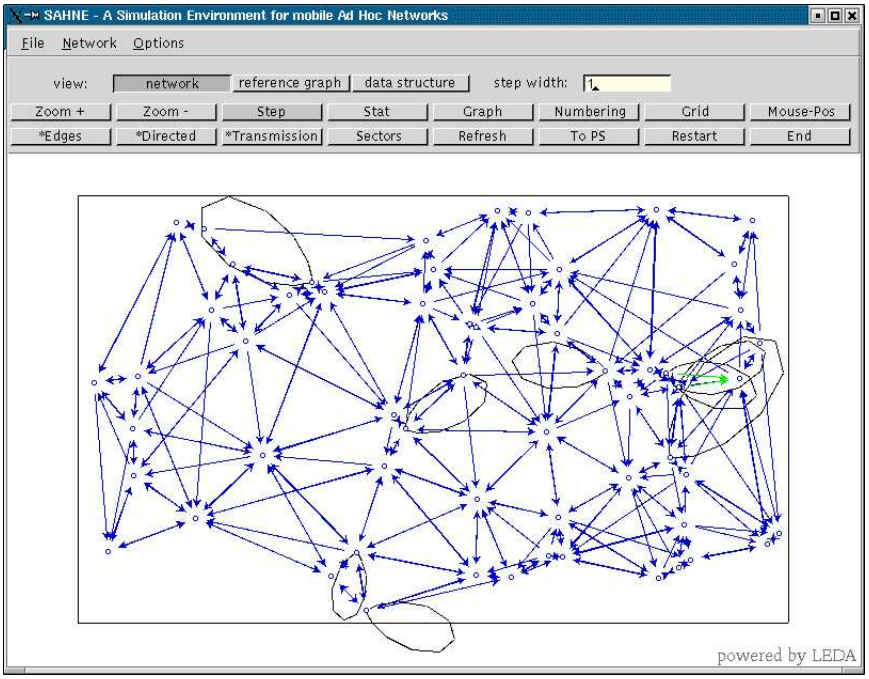

Figure 6.9: SAHNE - A simulation environment for mobile ad hoc networks

As already mentioned, we investigate topology control at the medium access layer (MAC) in wireless ad hoc networks and our research aims at the implementation of such a network based on distributed robust communication protocols. Here, we want to show how the (sparse) graphs with promising network and graph properties, presented in Chapter 4, perform in practice. We use space multiplexing techniques and variable transmission powers to realize the topologies. Therefore, the network nodes, e.g., a colony of robots equipped with a suitable communication device, can send and receive radio or infrared signals independently in k disjoint sectors of angle θ using one communication channel. We call this ability sector subdivision or directional communication model or sectorized approach, compare Section 4.2. Furthermore, every device is able to regulate its transmission power for each transmitted signal.

On the one hand, a number of distributed topology control algorithms [WLBW01, RM98, RH00, LHB+01], proximity graphs [LWW01, WLWF02], and geometric spanner graphs [GLSV02, WL02, HP00, GGH+01b] have been proposed that model communication networks at a high level of abstraction, see also Subsection 4.2.2. On the other hand, we have developed a communication module for the mini robot Khepera [GRSV03] that can transmit and receive in eight sectors, using infrared light with variable transmission powers to show that these approaches are also suitable in practical situations. In this section, we try to investigate theoretical results using realistic conditions given by the Khepera robots. We want to close the gap between theoretical investigations of wireless network topologies and real-world wireless environments. For simulations we use our simulation environment for mobile ad hoc networks, SAHNE, presented in the previous section. As seen, SAHNE allows us to implement, test, and evaluate algorithms for communication in MANETs.

In the following we discuss known models for signal propagation and reception, present extensions for SAHNE that allow us more realistic simulations, and present algorithms and experimental results for power- and time-efficient topology control. We distinguish between the omnidirectional and the directional communication model.

Signal Propagation and Reception

In Section 2.1 we have already discussed some distinguishing features of radio transmissions that are important for designing and analyzing wireless network topologies. During wireless data transmissions between nodes, the bits have to be modulated in a waveform suitable for transmission over the air. The channel distorts the waveform in various ways. For example, the waveform can reach the receiver directly and via a reflection from an obstacle. The resulting two waves are phase-delayed and the superimposition of both waves is received by the destination node. Due to the phase-delay, *intersymbol interference* is observed at the receiver. This effect is called *multipath fading* and can be reduced by appropriate techniques at the receiver, e.g., maximum-likelihood sequence detection with the Viterbi algorithm [BB99, MMF98]. We assume that the physical layer solves this kind of problems. However, some aspects of the physical transmission have to be considered for performing realistic simulations suitable for developing medium access control algorithms. *Signal propagation* and *signal reception* are the most important ones. A model of the signal propagation is necessary since we want to adjust the transmission power dynamically. In wireless networks, several nodes can transmit signals simultaneously to one receiver, therefore the reception of signals has to be modeled to decide when interfering signals cause collisions.

We first describe the propagation models used. For omnidirectional communication, we apply the well-known *free space propagation* model:

$$P_r = \frac{P_t G_t G_r \lambda^2}{(4\pi d)^2 L} \tag{6.1}$$

where G_t and G_r are the gains of the transmitting and receiving antennae, λ is the wavelength of the radio signal, P_t the transmission and P_r the receiving power, d the distance between sender and receiver, and L the path loss due to the sender and receiver hardware [Kra88, Par92,

AZ03]. For directional communication, we adapt a well-known model from directed infrared (IR) communication, that shows the relation between the transmission power P_t and the received power P_r:

$$P_r = A_{\texttt{eff}}(\psi)\frac{1}{d^2}R_t(\varphi)P_t \tag{6.2}$$

where $A_{\texttt{eff}}(\psi)$ is the effective area of the IR sensor, d is the distance between sender and receiver, and $R_t(\varphi)$ is the radiant intensity of the IR transmitter [KB97]. The angular characteristics of the sensors and the diodes can be accurately modelled by

$$f(\alpha) = c[(m+1)/2\pi]\cos^m\alpha, \;\; m = -\ln 2/\ln(\cos\alpha_{1/2}) \tag{6.3}$$

where c accounts for the characteristics of the optical transducers (e.g., the area of the receiver) and $\alpha_{1/2}$ is the semi-angle at which half of the signal intensity is emitted/detected.

Signal reception depends on the received signal strength P_r of the data signal. If it is high enough compared to interfering signals and noise, the data signal can be extracted from the received superimposed signal. The *signal-to-interference-plus-noise-ratio* ($SINR$) expresses this relation [LP99]:

$$SINR = \frac{P_{r,d}}{\sum_{i=1}^{m} P_{r,i} + P_n} > SINR_{\texttt{min}} \tag{6.4}$$

where $P_{r,d}$ is the signal strength of the data signal, $P_{r,i}$ are the signal strengths of the m interfering signals and P_n is the noise power. If the $SINR$ exceeds the threshold $SINR_{\texttt{min}}$, the data signal can be decoded with a low *bit error rate* (BER). The threshold $SINR_{\texttt{min}}$ is usually chosen such that the BER is below 10^{-6}. The *signal-to-interference-ratio* is considered when no noise power is modeled:

$$SIR = \frac{P_{r,d}}{\sum_{i=1}^{m} P_{r,i}} > SIR_{\texttt{min}} \tag{6.5}$$

Hence, in our communication models we assume propagation in free space and without any obstacle and the quality of a channel is characterized by the signal-to-interference-plus-noise ratio (SINR) and the signal-to-interference ratio (SIR). When the radio waves reach close to an obstacle, we had to consider also other effects like reflection, diffraction and scattering [AZ03]. We have extended our simulation environment SAHNE accordingly. The propagation models are used to calculate the signal strength of transmitted data packets. The packet with the highest reception power is selected as the data packet and the SIR is computed. If it exceeds the threshold $SIR_{\texttt{min}}$, the packet has been correctly received. All other interfering packets are discarded. A collision is produced if equation 6.5 is not fulfilled.

SAHNE-Extensions for Realistic Simulations

We concentrate on algorithms for the medium access (MAC) layer, a sublayer of the data link layer (see Figure 6.1), that build up the Yao-graph and/or its variants using realistic propagation models. For this purpose we have modified the network- and the transmitter-unit of SAHNE. A first version was already presented in the last subsection. Furthermore, we have extended the simulation kernel with the described realistic signal propagation models. Table 6.10 shows new

SAHNE extensions and some differences between the former, idealized directional simulation model assumed in Subsection 6.1 and the newer, more realistic model. The main difference between the idealized omnidirectional simulation model and the more realistic one is the modeling of interference. In our analyses and in Subsection 6.1 we assumed that a packet gets lost when more than one transmitter is active at the same time on the same channel. Here, we use the SIR with a threshold to decide when packets get lost. As you can see, this model is not so strong, since sometimes it is possible to receive data correctly also when more then one transmitter use the channel. Theoretically, nothing is received error-free, but practically the packet with the highest reception power could be received correctly.

Idealized Model	*Realistic Model*
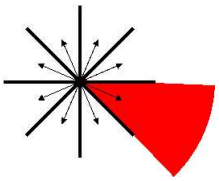	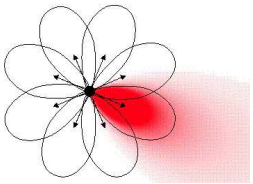
Sectors with fixed borders	Ellipsoidal transmission range
Fixed sector orientation	Variable sector orientation
Transmitted signals will be received in at most one sector	Transmitted signals will be received in different sectors depending on the receiver characteristic
Interference results always in complete data loss	Signal-to-interference-ratio (SIR)

Figure 6.10: Differences between idealized and more realistic modeling

The new simulation kernel allows us to simulate effects like interfering signals (SIR), overlapping of sectors, or rotation of senders (see Figure 6.11). Some special problems that only occur using the directional communication model are pointed out. You can see areas where no reception is possible, overlapping of signals when two neighboring senders transmit at the same time, and ellipsoidal signal propagation. At all points of the ellipse the same transmission power is received. Hence, estimate the distance to a (nearest) neighbor is not always possible. In the following we present algorithms that do not need it. Furthermore, the channel is non-reciprocal, i.e. even under free space propagation it could happen that a node can reach another node with a given transmission power but not viceversa with the same transmission power.

Distributed Algorithms

A main advantage of the Yao-graph and its variants is that they can be constructed locally without using any geographical positioning system. We have implemented a distributed algorithm for constructing these topologies: the Sector-Based Topology Control (SBTC)-Algorithm builds up

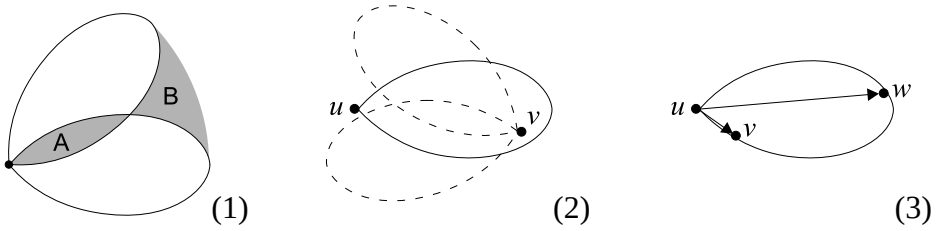

Figure 6.11: (1) Overlapping regions (A) and regions with no reception (B). The non-reciprocity of the channel (2): a node u can reach v but not vice versa, although both, u and v, use the same transmission power. (3) Node u can reach v and w with the same transmission power.

the Yao-graph. It takes interference into account and does not need a reciprocal channel. Transmissions with maximum power are avoided if possible. The algorithm can easily be extended with the capability to build up the SparsY- and/or the SymmY-graph.

According to our simulation model the algorithm must comply with the following preconditions: a node can transmit and receive messages in k sectors independently. It can vary the transmission power. There is a fixed number of power levels available. It can detect interference, but it cannot determine how many signals interfere. A node knows neither its position nor its orientation, see Section 4.2 for further details.

The SBTC-Algorithm, that builds up the Yao-graph, is presented in Figure 6.12. The main task of the algorithm is to find the nearest neighbor in each sector. The nearest neighbor is the node that can be reached with the minimal power level. It is determined by exchanging the so-called *control messages*. The algorithm consists of two phases:

During the **first phase** a node (called the *initiator*) searches for a neighbor independently in each sector: first it sends a "Hello"-message with the minimal power. If no one answers, it increases the power so that the range is doubled. This is repeated until an acknowledgement is received or the maximum power is reached. Interference between two or more acknowledgments, that are received simultaneously, are resolved by an exponential backoff algorithm. This is necessary because the initiator cannot distinguish if an interference is caused by nodes within the sector or nodes outside the sector. Acknowledgements are transmitted with the same power as the transmission power of the "Hello"-message. During the **second phase** the power is adapted to the neighbor found in the first phase (called the *responder*): with repeated transmission of power control messages the initiator performs a binary search. The upper bound is the power level from the first phase. The lower bound is the minimum power level. Acknowledgements from the responder are transmitted with the power of the last acknowledgement in the first phase. This is crucial for the reachability of the nodes, because the channel is not reciprocal.

After these two phases, the initiator can establish an edge to the responder. If a neighbor cannot receive a "Hello"-message due to interference, the initiator does not find him or establishes an edge to another node. Therefore the search is repeated. If the initiator finds the same neighbor again, the search interval is increased to reduce power consumption and interference. That way we obtain the Yao-graph. To avoid interference while searching neighbors the initiator must not start the search in adjacent sectors at the same time. After the neighbors have been found the

Preliminaries

CREATEEDGE(addr, p, s) establishes an edge to the node with the address addr, that can be used by sending a message in sector s with the transmission power p.
UPDATEEDGE(addr, p, s) updates the transmission power.
DELETEEDGE(addr, s) deletes an edge.
SEND(type, target, p, s) sends a message to the node with the address target in sector s with transmission power p.

$1/p_\delta$ is the expected length of an interval between updating a neighbor.
M is a list of messages a node receives.
$N[s]$ denotes information about the neighbor in sector s, containing the following data:
addr is the address of the neighbor.
p_{send} is the transmission power needed to reach the neighbor.
p_{recv} is the received power of a message received from the neighbor.

The Algorithm

```
SBTC()
 1  for t ← 1 to ∞
 2  do for s ← 1 to sectors
 3     do parallel
 4        with Probability p_δ
 5        do UPDATENEIGHBOR(s)

UPDATENEIGHBOR(s)
 1  N_old ← N[s]
 2  FINDYAONEIGHBOR(s)
 3  if N[s] ≠ NIL
 4     then if N_old = N[s]
 5             then UPDATEEDGE(N[s].addr, N[s].p_send, s)
 6                  decrease p_δ
 7             else CREATEEDGE(N[s].addr, N[s].p_send, s)
 8                  reset p_δ
 9                  if N_old ≠ NIL
10                    then DELETEEDGE(N_old.addr, s)
11     else if N_old ≠ NIL
12             then DELETEEDGE(N_old.addr, s)
13                  reset p_δ
```

```
FINDYAONEIGHBOR(s)
 1  p ← 1                                          // phase 1
 2  a ← 1
 3  while M = ∅ and p ≤ p_max
 4  do M ← ∅
 5     interference ← false
 6     SEND(Hello-Packet, undef, p, s)
 7     wait 2^a time steps
 8     and add received acknowledgements to M
 9     update interference
10     if M = ∅
11       then if interference
12                 then a ← a + 1
13                 else p ← 4 · p          // doubling the range
14                      a ← 1
15  if M = ∅
16    then ABORT
17  p_low ← 1                                      // phase 2
18  p_high ← p
19  a ← 1
20  while p_low + 1 ≤ p_high
21  do M ← ∅
22     interference ← false
23     SEND(Power-Control-Packet, undef, p, s)
24     wait 2^a time steps
25     and add received acknowledgements to M
26     update interference
27     if M = ∅
28       then if interference
29                 then a ← a + 1
30                 else p_low ← p
31                      a ← 1
32                      p ← (p_low + p_high)/2
33       else p_high ← p
34            a ← 1
35            p ← (p_low + p_high)/2
36  if M = ∅
37    then ABORT
38  msg ← message with the max. received power in M
39  if (p < N[s].p_send) or
40    (p = N[s].p_send and msg.p_recv > N[s].p_recv)
41    then N[s].no = msg.sender
42         N[s].p_send = p
43         N[s].p_recv = msg.p_recv
```

Figure 6.12: The sector-based topology control algorithm (SBTC)

transmission powers are adjusted, so data transmission in adjacent sectors is possible, unless the angular characteristics of the receiver does not allow it. If the opening angle of the receiver is high, a node has to schedule the communication on ingoing edges (this is a problem when using non-reciprocal channels) or it has to acknowledge every message. Furthermore, we want the algorithm to react on node failures and mobility so we infinitely repeat the search.

A modified version of this algorithm constructs the SparsY-graph and/or the SymmY-graph: for the SparsY-graph it is necessary that every node keeps track of its ingoing edges. If the initiator wishes to establish an edge to the responder, he first has to apply for this edge. If the responder knows no other ingoing edge in the corresponding sector that is “shorter", then the new edge is accepted. If the new edge replaces another ingoing edge, the responder has to inform the

owner of the old edge.

In the case of the SymmY-graph, the nodes also have to apply for an edge to a neighbor. If the initiator applies for an edge and if he is already known to the responder as a Yao-neighbor, then the requested edge can be established on both sides. So the nodes do not have to store information about ingoing edges.

Theorem 6.1 *For a vertex set V in general position with n nodes and s power levels per node the Yao-graph and its variants can be constructed in time $\mathcal{O}(\log n \cdot \log s)$ (the time one node needs to find its neighbors).*

Proof: Phase 1 uses power doubling and needs $\mathcal{O}(\log s)$ steps until some first nodes will be reached. The time needed for sending a successful acknowledgement can be bounded by $\mathcal{O}(\log n)$, since at most all nodes could answer and in this case we need the time to resolve the collisions by the binary exponential backoff algorithm. Phase 2 is just a binary search algorithm based on the number of power levels. In this phase we need at most $\mathcal{O}(\log s)$ steps to adjust the transmission power to the nearest neighbor and at each of these steps $\mathcal{O}(\log n)$ time slots to resolve collisons. ■

For omnidirectional communication we have also implemented a distributed algorithm for constructing the Hierarchical Layer Graph: the Hierarchical Layer Topology Control (HLTC)-Algorithm, presented in Figure 6.13.

The two main tasks of the HLTC-algorithm are the selection of nodes, i.e. to decide in which layer a node lies, and the establishing of connections inside the layers. We assume that the lowest radius r_0 or an approximation of that distance is known to all nodes.

Essentially, a node sends a claim for leadership (CFL) packet to appear in a next higher layer. If there is no other node having a higher rank given by its unique identification then the node climbs up to a next higher layer. In the case that there is another node with a higher rank, this node answers back sending a disagreement (DIS) packet. At the beginning, every node is only a member of layer L_0.

When a node is a member of a layer, it can send a neighbor notification packet (NNP) including the transmission power necessary in this layer to inform other nodes such that they can establish bidirectional connections if they are also member of the same layer. NNP packets are created and transmitted uniformly at random in the layers of a node. Control information are stored in the packets. A CFL packet in a new layer i is transmitted such that all nodes in distance r_i are able to receive this packet. An NNP packet in a layer i should achieve all nodes in distance $\alpha \cdot r_i$. The HLTC-algorithm uses an exponentiell backoff scheme to avoid interference. Furthermore, we have intregrated known algorithms for congestion control, e.g., additive increase and multiplicative decrease (AIMD), to increase the througput. Some more details can be found in Figure 6.13. Note that this is only one possible implementation of the HL-graph. Modified versions use other algorithms to decide in which layery a node lies.

Experimental Results

In Chapter 4 we have investigated the basic network parameters congestion (that takes interference into account), dilation, and energy. Here, we extend the definition of congestion to practical

Preliminaries

RANDOM($x_0, \ldots, x_i$) generates a random number uniformly chosen from $\{x_0, \ldots, x_i\} \subset \mathbb{N}$.
SEND(`type`, `target`, p, i) sends a message to the node with the address `target` in layer i with transmission power p.

r gives the highest layer in which a node currently lies, it can be regarded as a rank.
$1/p_\delta$ is the expected length of an interval between updating a neighbor.
M is a list of messages a node receives.
$p_\alpha[i]$ is the power necessary to achieve a node in distance $\alpha \cdot r_i$ in layer i
$p_\beta[i]$ is the power necessary to achieve a node in distance r_i in layer i

The Algorithm

```
HLTC()
 1  r ← 0
 2  for t ← 1 to ∞
 3  do with Probability p_δ
 4     do if RANDOM(0, 1) = 0
 5           then ℓ ← RANDOM(0, ..., r)
 6                SEND(NNP, undef, p_α[ℓ], ℓ)
 7           else a ← 1
 8                repeat
 9                     M ← ∅
10                     interference ← false
11                     SEND(CFL, undef, p_β[r + 1], r + 1)
12                     wait 2^a time steps
13                     and add received LVAL − Messages to M
14                     update interference
15                     a ← a + 1
16                   until interference = false or M ≠ ∅
17                if M = ∅
18                  then r = r + 1
```

Figure 6.13: The hierarchical layer topology control algorithm (HLTC)

environments where interference are modeled by the signal-to-interference-ratio (SIR) and the fact, that transmitted signals are received in more than one sector at a time. In our simulations we consider three types of congestions to measure the quality of topologies and algorithms. We begin each simulation with a set of nodes randomly placed in the simulation area. No edges are established at the beginning. Then we start an algorithm to build up one selected topology, e.g., the Yao-graph, the SparsY-graph, the SymmY-graph, or the HL-graph. At some time steps we stop the topology control and calculate network and communication properties. For our congestion values we construct a permutation routing problem: every node u creates one packet for each possible destination node v. Now we consider two path systems on the constructed topology. The path system $\mathcal{P}_d$ that optimizes **dilation**, which is given by the maximum of the lengths of all paths in $\mathcal{P}_d$, and the path system $\mathcal{P}_e$ that optimizes **flow energy**, which is defined by $\sum_{e \in E(\mathcal{P}_e)} \ell(e)|e|^2$. Both schemes can be computed in polynomial time. Now we simulate the transport of all packets and count the number of packets that go through an edge e and define it as the **load** $\ell(e)$ of e. This load is often called congestion in wired networks, compare [Lei92] and Section 4.1. We define the load L of a path system as $L := \max_{e \in E} \ell(e)$. In Chapter 4 we have extended this definition to an intuitive definition of congestion in wireless networks. Remember Section 4.1 that the **congestion** of an edge e of $N = (V, E_\mathcal{P})$ defined by a path system $\mathcal{P}$ is given

by

$$C(e) := \ell(e) + \sum_{e' \in \mathrm{BInt}(e)} \ell(e') \; .$$

The congestion C of the path system $\mathcal{P}$ for V is defined by $C := \max_{e \in E_{\mathcal{P}}} C(e)$. For our experimental results we modify this parameter further and introduce the **realistic congestion** C_r**.** The realistic congestion combines load, interference, power attenuation, and SIR. The definition is the same as for congestion, but for the definition of interference we take the realistic SIR into account. Let us assume, that transmissions take place on all edges. An edge interferes with another edge only if the receiver can not extract the transmitted signal from the received superimposed signal.

In our experiments we chose the following parameters: the nodes are placed uniformly at random in an area of size 50m $\times$ 30m and also the sector orientations of the nodes are chosen uniformly at random. Every node has 8 sectors (transceivers) and can change its transmission power at 256 power levels. The transmission range at maximum power is about 50m. The directional characteristic is based on the specification of the IR communication modules: the transmitter has a semi-angle of 20°, the receiver a semi-angle of 50°. The probability p_δ for repeating the UPDATENEIGHBOR procedure is initially set to $1/500$, see Figure 6.12.

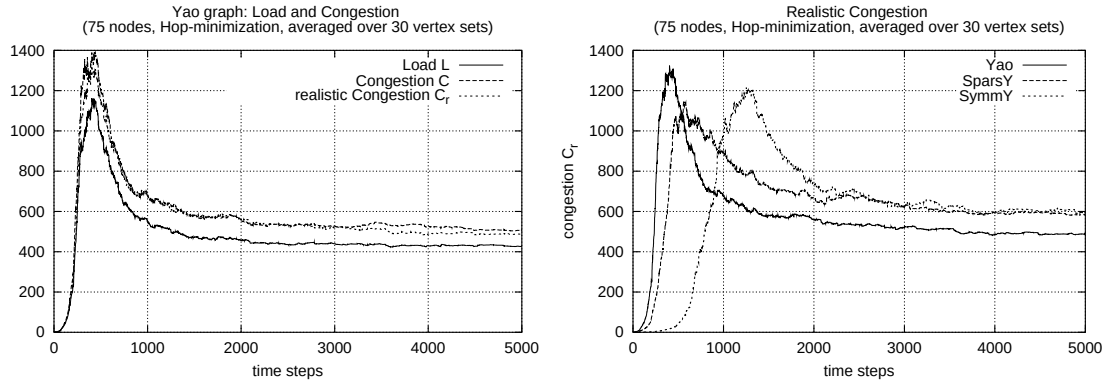

Figure 6.14: Load and congestion during network build-up

The left diagram in Figure 6.14 shows the progression of load and congestion during the build-up of the Yao-graph. In every time step we do an offline-computation of an all-pairs shortest-path algorithm to obtain a path system on which congestion is calculated. The path system is computed with either hop minimization or energy minimization. As hop minimization yields better congestion, we do not present the results of energy minimization. The resulting values are averaged over 30 vertex sets.

In the diagram all curves grow until a peak at 500 time steps is reached. One time step stands for the time needed to transmit one control packet. At this time the last edge that is necessary to make the network connected has been established. Then the major part of the load is allotted to this edge. When more edges are established, the load is distributed over more paths, so load and congestion decrease. Finally the curves balance out and the build-up process converges after

nearly 4000 simulation steps. The diagram also shows that the difference between idealized and realistic congestion is small.

The right diagram in Figure 6.14 compares the realistic congestion of the Yao-graph, the SparsY-graph, and the SymmY-graph during the network construction. It shows that the Yao-graph can be built up quickly. Constructing the SparsY-graph and the SymmY-graph takes longer, because the nodes have to apply for an edge and so additional messages have to be exchanged. The diagram also shows that the Yao-graph provides smaller congestion than the SparsY-graph and/or the SymmY-graph. There are two reasons: First, the load of the Yao-graph is usually lower than that of the SparsY-graph or SymmY-graph. Second, the SparsY-graph and the SymmY-graph do not prevent interference in our simulation model due to the angular characteristic of the receiver (in contrast to the idealized sector model)!

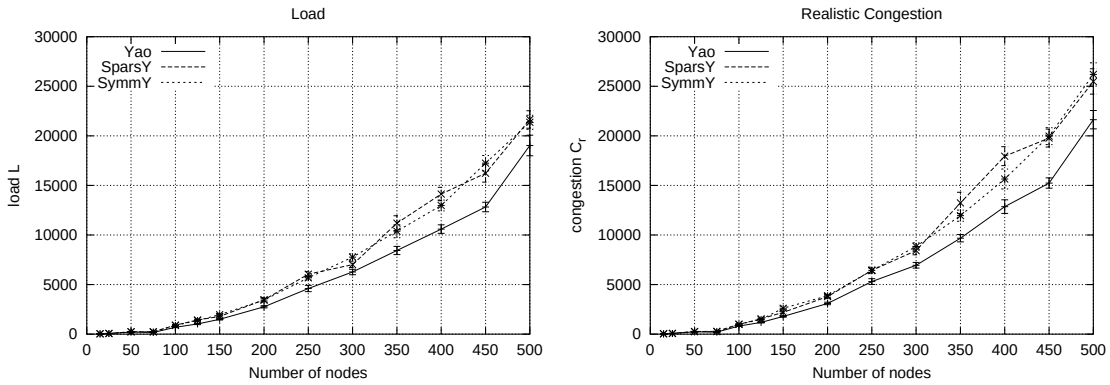

Figure 6.15: The relation of load, congestion, and number of nodes

Figure 6.15 also points out this behavior. It shows congestion and realistic congestion for different numbers of nodes. The values are averaged over 15 vertex sets and were taken after the network had been constructed. Note that the area has always the same size so that a growing number of nodes implies a growing density. If we compare the two diagrams, we can see that the congestion of the Yao-graph is similar to the load of the SparsY-graph and SymmY-graph.

Figure 6.16 shows dilation and flow energy for the Yao-graph and its variants, based on a hop-optimal path system. Flow energy is measured in standard energy which is defined as the energy needed to transmit 1 bit relative to the energy consumption of a transmission at maximum power, divided by the number of sectors. It turns out that the SparsY-graph and the SymmY-graph have similar dilation and flow energy values, because for randomly distributed vertex sets there are no significant differences between the SparsY-graph and the SymmY-graph. The edges in the Yao-graph that are not allowed in the SparsY-graph or the SymmY-graph are usually longer edges. So in the Yao-graph the distances can be spanned by a path over fewer hops than in the SparsY-graph or SymmY-graph. Thus dilation for the Yao-graph is smaller than for the SparsY-graph and SymmY-graph. Although paths that contain long edges are not energy efficient, the SparsY-graph and the SymmY-graph provide better values for flow energy in our simulation.

The Hierarchical Layer Graph of a vertex set V is defined by the parameters α and β, see Section 4.1. We performed a lot of simulations to find approriate values for these parameters.

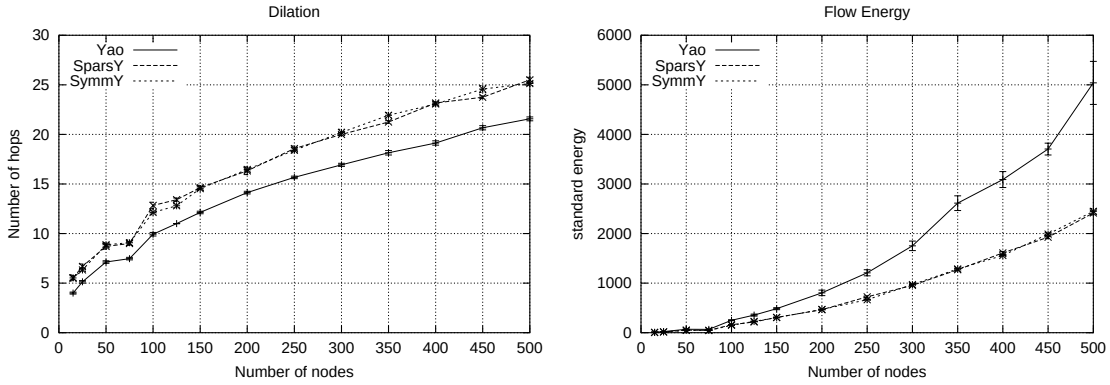

Figure 6.16: Dilation and flow energy

By definition it must hold that $\alpha \geq \beta > 1$. Theorem 4.7 shows that the HL-graph is a c-spanner for some constant c for $\alpha > 2\frac{\beta}{\beta-1}$. In the following we present only a small selection of our simulations concerning the HL-graph. The path system is computed with either hop minimization or energy minimization. We assumed at most 10 layers for each vertex set and varied the number of nodes from 15 up to 160. The propagation exponent δ is equal to 2. The resulting values are averaged over 15 vertex sets. The vertical bars depict the standard error.

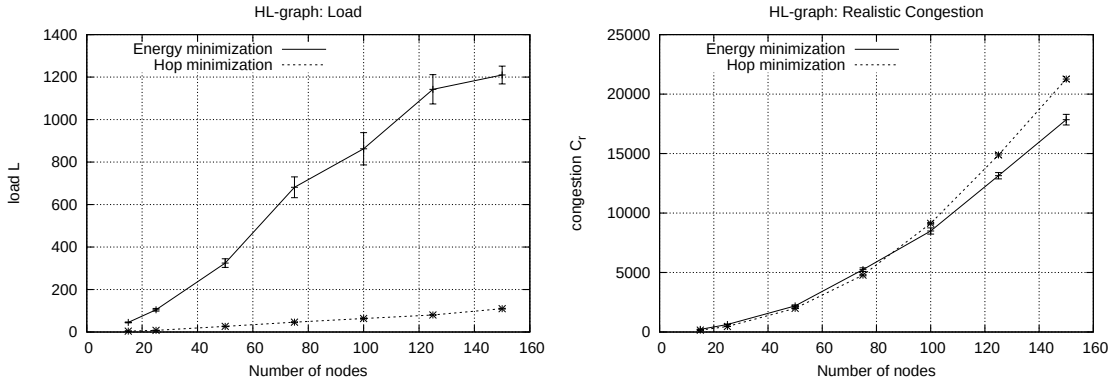

Figure 6.17: The relation of load, congestion, and number of nodes

Figure 6.17 shows the load and the realistic congestion of the HL-graph under energy and hop minimization varying the number of nodes. Be careful because of the different scaling. Note that the transmission power to send over a link e is not exactly adjusted to $|e|^\delta$ but to the distance required by the layer in which this link is established. This makes it more diffcult to compare energy and hop minimization. As you can see there is a big gap between the load and the realistic congestion. This is caused by high interference in the omnidirectional communication model. There was nearly no difference between congestion and realistic congestion.

Another interesting observation is that, on the one hand, there is a major difference between the loads of path systems that optimize energy and hop minimization. But, on the other hand, the curve progressions of the realistic congestions for both path systems are nearly the same.

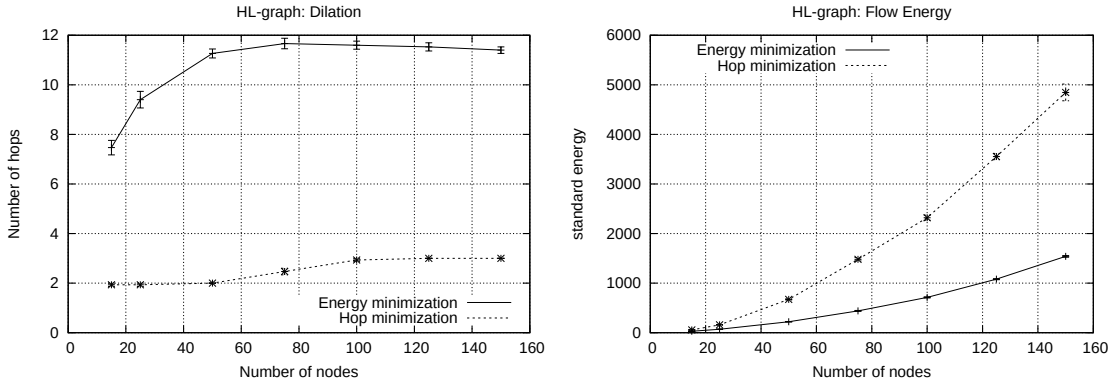

Figure 6.18: Dilation and flow energy

Figure 6.18 points out expected values for dilation and flow energy: the path system optimized for the energy yields better results than the path system optimized for the hop distance, if we look at the flow energy. We observe the converse if we look at the dilation.

6.1.3 Further Extensions and Simulations

In parallel to our investigations concerning topology control at the MAC layer, we have performed experiments at the network layer (see Figure 6.1). Here, our focus was not on deep mathematical analyses which we have performed already in Chapter 4 but more on the realization of distributed algorithms for path selection based on our implemented topologies. We have implemented and experimentally evaluated an algorithm proposed for fixed networks in [ABBS01] on our MANETs. Our simulations showed that the original version is only suitable for networks with symmetric edges. Furthermore, we have implemented the Dynamic Source Routing (DSR) protocol [JM96] in SAHNE and analyzed its performance on our integrated topologies based on the Yao-graph and its variants [Eik03]. Besides these implementations, we also tried to find first solutions to compute the required probability $\varphi(e)$ of an edge $e \in E$, see Lemma 4.1 of Section 4.1, in a communication network $N = (V, E)$ in a local and distributed manner using the directional communication model [Pos03].

6.2 Interactive Tool for Checking Graph Properties

In this section we present the results of our extensive experimental analysis of graph properties of the sectorized topologies considered in Section 4.2 on randomly generated vertex sets. Namely, we compare the Yao-graph, the SparsY-graph, and the SymmY-graph with regard to energy consumption, given by the power spanner property, and to congestion, given by the (weak) spanner property. We concentrate on sets of static devices that are randomly distributed over a given area.

In addition, we introduce in this section a new dimension and use this to improve known stretch factors experimentally. In general, it is assumed that the sectors of the nodes underlie a fixed orientation or that they are oriented as a result of the movement of nodes. We assume an

extended model and allow each node to adjust the orientation of its senders independently of any other conditions. We introduce new optimization tasks and present algorithms which improve the stretch factors of known sectorized topologies only by adjusting the orientation of some sectors of the nodes.

Furthermore, we present new algorithms to calculate the power stretch factor and the weak stretch factor of a graph $G = (V, E)$ in time $\mathcal{O}(|V|^2 \log |V| + |V||E|)$ exactly. Hence, we can determine these factors for sparse graphs in time $\mathcal{O}(|V|^2 \log |V|)$. Applying this yields a lower bound for an optimal orientation of all senders, e.g., with regard to energy consumption, that can be computed in polynomial time. We use this bound to analyze the simulation results.

Our extensive experimental evaluation of the three sectorized topologies on random vertex sets using different sector orientations show that we can improve the known stretch factors and that the considered topologies perform well on "normal" vertex sets where the nodes are placed uniformly at random.

6.2.1 Motivation

We assume directional communication (see Section 4.2) as the underlying communication model and compare the Yao-graph, the SparsY-graph, and the SymmY-graph experimentally on randomly generated vertex sets using a new extension. Note that in all existing theoretical works concerning topology control in wireless networks it is assumed that the orientation of the senders is fixed or it is affected by the movement of a node. In our Khepera test environment the orientation depends on the forefront of a Khepera-robot, see Section 4.2. We introduce a new dimension, since we allow each node to control the orientation of its sectors/senders to improve the energy consumption or to decrease the amount of interference. To the best of our knowledge, we are the first who study this additional freedom for the devices in wireless networks.

Our model also diverges from the standard model coming from computational geometry where the sectors on all nodes are fixed and equal oriented. We perform an extensive experimental evaluation of the Yao-graph, the SparsY-graph, and the SymmY-graph using the extended communication model. A fixed orientation of the sectors has the advantage that the construction of the Yao-graph and its variants is possible centrally in time $\mathcal{O}(n \log n)$, e.g., using a sweepline algorithm [FLZ98, FMS97], where n is the number of nodes. In our model, if the orientation can be arbitrary, there is only the naive algorithm which needs time $\mathcal{O}(n^2)$.

A challenge in wireless networks is to spare energy and to avoid congested communication links having the amount of interference so low as possible. From a graph theoretic point of view this means that we want to build up a graph that gives at least one path between two arbitrary nodes with low energy-cost, low interference, and low congestion. For this purpose we consider spanners, weak spanners, and power spanners (see Chapters 3 and 4). One aim of this section is to measure and compare the stretch factors given by the definitions of these structures. On the other hand we use the extended communication model to improve the stretch factors and show the improvement experimentally. We developed a testbed [Vol04b] which can also be used over the World Wide Web and we present new algorithms we used to perform our simulations.

The aim of this section is not to go into technical detail, but more to present first algorithms, ideas, and experimental results for the extended communication model. It is more a theoreti-

cal study on the question: assumed each node can adjust the orientation of its senders, what is possible concerning energy consumption? In contrast to the works investigating wireless networks using directional antennae we consider three known topologies using the extension that each node can adjust its sectors/senders. We want to evaluate the length stretch factor, the power stretch factor, and the weak stretch factor experimentally. In literature, there exist already experimental results concerning these graphs on random vertex sets, e.g., [WLWF02], but they are not comprehensive and there it is not allowed to adjust the orientation of the sectors.

In Subsection 6.2.2 we first present algorithms to determine the power stretch factor and the weak stretch factor of a given graph $G = (V, E)$ exactly. We show that this can be done, in general, in time $\mathcal{O}(|V|^2 \log |V| + |V||E|)$ and in time $\mathcal{O}(|V|^2 \log |V|)$ if we consider the Yao-graph and its variants. In Subsection 6.2.3 we introduce the extended communication model and present first algorithms to orientate sectors. We can improve the length stretch factor of the Yao-graph by a factor of 2 and the power stretch factor by a factor of 2^δ, where δ is a constant that depends on transmitting characteristics (see Section 2.1), if it is allowed to adjust the sectors for all nodes on a complete path from a source node to a destination node. In Subsection 6.2.4 we present a lower bound for an optimal orientation of the sectors. We construct a graph in which we can calculate lower bounds for the stretch factors of the Yao-graph using any orientation of the sectors in polynomial time. Finally, in Subsection 6.2.5 we present the results of our extensive experimental evaluation.

6.2.2 Calculating Stretch Factors

In this subsection we present new algorithms we need to efficiently compute the length stretch factor, the power stretch factor, and the weak stretch factor. In [NS00] algorithms are presented for approximating the length stretch factor, but in this work we want to compute the exact values. Let $G = (V, E)$ be a geometric graph and $n := |V|$ and $m := |E|$. The length stretch factor can be calculated by solving the all-pairs-shortest-path problem (APSP). We check all $n(n-1) = \mathcal{O}(n^2)$ directed shortest paths and determine the maximum length stretch factor. Hence, running Dijkstra's algorithm using Fibonacci heaps gives the length stretch factor of G in time $\mathcal{O}(n^2 \log n + nm)$ (see [CLSR01] for further details). The power stretch factor can be calculated in the same way if we use $|u - v|^\delta$ as the cost of an edge $e = (u, v)$ instead of $|u - v|$.

In Figure 6.19 you see the main part of our algorithms based on Dijkstra's algorithm. An exact calculation of the weak stretch factor seems to be more complicated since we know nothing about the length of a path in a weak spanner. Nevertheless, we can prove that we can also compute the weak stretch factor in the time needed by Dijkstra's algorithm for solving the APSP problem. The main idea of the algorithm is presented in Figure 6.19 b).

We run the algorithms for all n nodes and then calculate the maximum over these n stretch values. In the following we show that both algorithms terminate and calculate the required values correctly. We denote by dist(u) the δ-cost of a cheapest path found so far from s to u (power stretch) or the smallest radius found so far of a disk in which a path from s to u lies (weak stretch). Let $d(u)$ be the value of dist(u) at the time when u is dequeued. In the following we consider a) the power stretch factor and b) the weak stretch factor at the same time.

```
POWERSTRETCH(G = (V, E), V ⊆ ℝ^D, s ∈ V)
 1  for all v in V
 2  do dist(v) ← ∞, pre(v) ← ∅
 3  dist(s) ← 0, pre(s) ← s, Q ← V
 4  while Q ≠ ∅
 5  do u ← EXTRACTMIN(Q)
 6     for each v ∈ Adj[u]
 7     do if dist(u) + |u − v|^δ < dist(v)
 8           then dist(v) ← dist(u) + |u − v|^δ, pre(v) ← u
 9  power-stretch ← 0
10  for all v in V \ {s}
11  do if dist(v)/|s − v|^δ > power-stretch
12        then power-stretch ← dist(v)/|s − v|^δ
```

```
WEAKSTRETCH(G = (V, E), V ⊆ ℝ^D, s ∈ V)
 1  for all v in V
 2  do dist(v) ← ∞, pre(v) ← ∅
 3  dist(s) ← 0, pre(s) ← s, Q ← V
 4  while Q ≠ ∅
 5  do u ← EXTRACTMIN(Q)
 6     for each v ∈ Adj[u]
 7     do if max{dist(u), |s − v|} < dist(v)
 8           then dist(v) ← max{dist(u), |s − v|}, pre(v) ← u
 9  weak-stretch ← 0
10  for all v in V \ {s}
11  do if dist(v)/|s − v| > weak-stretch
12        then weak-stretch ← dist(v)/|s − v|
```

Figure 6.19: Calculating a) power stretch factor and b) weak stretch factor

Lemma 6.1 *If u is dequeued before v we have $d(u) \leq d(v)$.*

Proof: We assume that there exist two nodes u and v with u is dequeued before v and $d(u) > d(v)$. W.l.o.g. let v be the first such node. At the time u is dequeued, it holds that $d(u) = \text{dist}(u) \leq \text{dist}(v)$. By the definition $d(u)$ is never changed again and hence $\text{dist}(v)$ has to be decreased. This happens only if a node w is dequeued and a) $\text{dist}(v) = \text{dist}(w) + |w - v|^\delta$ or b) $\text{dist}(v) = \max\{\text{dist}(w), |s - v|\}$is set. W.l.o.g. let w be the last such node. Then we have a) $d(v) = d(w) + |w - v|^\delta$ or b) $d(v) = \max\{d(w), |s - v|\}$. By the choice of v it holds that $d(u) \leq d(w)$. Furthermore, a) $|w - v|^\delta \geq 0$ or b) $\max\{d(w), |s - v|\} \geq d(w)$. In both cases, we get a contradiction: $d(v) \geq d(u)$. ∎

Lemma 6.2 *Let Q be empty. Then a)* $\text{dist}(v) \leq \text{dist}(u) + |u - v|^\delta$ *or b)* $\text{dist}(v) \leq \max\{\text{dist}(u), |s - v|\}$ *for all $(u, v) \in E$.*

Proof: It is easy to see that in both cases the claim holds at the time u is dequeued. After this point of time the claim breaks only, if $\text{dist}(u)$ is decreased. Since $\text{dist}(v)$ is never increased, this can only happen when a node w is dequeued and a) $\text{dist}(u) = d(w) + |w - u|^\delta$ or b) $\text{dist}(u) = \max\{d(w), |s - u|\}$ is set. From Lemma 6.1 it follows that $d(w) \geq d(u)$. With a) $|w - u|^\delta \geq 0$ or b) $\max\{d(w), |s - u|\} \geq d(w)$ we get that $\text{dist}(u) \geq d(u)$ and this is a contradiction. ∎

Theorem 6.2 *a)* POWERSTRETCH(G, s) *calculates the maximum power stretch factor over all paths starting at s, b)* WEAKSTRETCH(G, s) *calculates the maximum weak stretch factor over all paths starting at s.*

Proof: We prove the claim by induction. Let $v \in V$ and $u := \text{pre}(v)$ be a predecessor of v on an optimal path from s to v concerning the a) δ-cost or b) radius of a disk. By induction we can assume that $\text{dist}(u)$ is the minimum a) δ-cost of a path from s to v or b) radius of a disk which contains the whole path from s to v. Since a) $\text{dist}(v) \leq \text{dist}(u) + |u - v|^\delta$ or b) $\text{dist}(v) \leq \max\{\text{dist}(u), |s - v|\}$ (Lemma 6.2) we get that $\text{dist}(v)$ is the a) δ-cost of a cheapest path from s to v or b) minimum required radius of a disk such that the whole path from s to v lies in this disk. The last operation gives the maximum over all stretch values. ∎

6.2.3 Adjusting Sector Orientations

In this subsection we present the extended communication model and present first heuristics to improve the length stretch factor, the power stretch factor, and the weak stretch factor of the Yao-graph and its variants. We consider a static ad hoc network consisting of n nodes given by $V \subseteq \mathbb{R}^2$. Furthermore, let $k \in \mathbb{N}$ be the number of senders with that a node is equipped. In general, it is assumed that the orientation of the senders on a node is fixed or that the orientation depends on node movements. We allow each node to adjust not only the transmission power of a sender but also the orientation. Therefore, the area around a node is subdivided into k sectors of equal size and each node can set an angle where the first sector begins. The orientation can be changed at any time or can be fixed, e.g., when an optimal orientation is computed for a static vertex set. The angle is given by a rotation function $r : V \to [0, 2\pi/k)$. Hence, e.g., sector i of a node $u \in V$ goes from $r(u) + (i-1) \cdot 2\pi/k$ to $r(u) + i \cdot 2\pi/k$. In a fixed model, assumed in computational geometry where, e.g., the Yao-graph is used as a data structure to calculate properties like nearest neighbors efficiently, we have $r(u) = 0$ for all $u \in V$. In Section 4.2 and in Subsection 6.1.2 $r(u)$ is defined by the forefront of the used robot and so depends on the movement of a robot (remember the offset angle α_u for a node u). Since we allow each node u to adjust $r(u)$, we got questions like

- What is the best orientation for which measure?
- How can we compute an optimal orientation concerning a specific stretch factor?
- What is the complexity of this problem?
- Is it possible to improve the stretch factors using simple algorithms?
- Is it possible to adjust the orientations such that the SparsY-graph will be a spanner?
- Is it possible to adjust some orientations such that the SymmY-graph will be a spanner, a weak spanner, or at least a power spanner?

Note that under fixed orientation it is still an open problem whether the SparsY-graph is a spanner or not. The aim of this subsection is not to answer all these questions, but to discuss some of them and to present the results of an extensive experimental evaluation of some new algorithms for the new communication model. We do not know how to find a best orientation for a node set with regard to a given measure in a time faster than the time needed by a naive approach trying all possible combinations which is possible in exponential time. Optimizing measures are, e.g., the stretch factors, the energy needed to keep up all network links, the number of links, or the in-degree of the nodes to reduce the amount of interference.

Now we show that it is possible to improve the stretch factors by adjusting orientations. We present first algorithms that use these results to improve all three stretch factors.

Lemma 6.3 *Let $G = (V, E)$ be the Yao-graph and $k \in \mathbb{N}$ the number of sectors per node. If it is allowed to adjust the orientation of the sectors on the nodes at any time and to establish a communication link between two nodes $u, v \in V$, then G is a c-spanner with length stretch factor $c = \frac{1}{1-\sin(\pi/k)}$ for $k > 3$.*

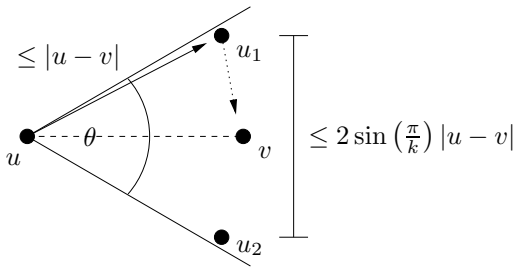

Figure 6.20: Adjusting a sector

Proof: We consider two nodes u and v and give a path construction for a path $P_G(u,v)$ from u to v. We rotate the sector of u in which v lies such that v is placed on the bisector. In the worst case there exist two further nodes u_1 and u_2 on the opposite boundaries of this sector and both are nearer to u than v (see Figure 6.20).

Now it is not possible to get an edge directly to v. From Lemma 4.16 it follows that this placement is the worst case (see also [RS91]). If we assume that the same construction works for the path from u_1 to v and for u_2 to v and so on recursively, we get an upper bound for the path length between u and v:

$$||P_G(u,v)|| \leq \sum_{i=0}^{\infty} \left(\sin\left(\frac{\pi}{k}\right)\right)^i |u-v| \leq \frac{1}{1-\sin(\pi/k)}|u-v|$$

■

As you can see, in the best case, we can improve the length stretch factor of the Yao-graph by a factor of 2. Applying this result to the power stretch factor of the Yao-graph, see Lemma 3.2 and Subsection 4.2.3, yields to a better power stretch of the Yao-graph of $\left(\frac{1}{1-\sin(\pi/k)}\right)^{\delta}$. It is possible to improve the power stretch factor of the Yao-graph to $\frac{1}{1-(\sin(\pi/k))^{\delta}}$ using the analysis of Li et al. [LWW01]. Hence, we can get an energy improvement by a factor of at most 2^{δ}.

Another interesting and helpful observation for the search for an orientation which improves stretch factors is that there is always a symmetric communication link to the nearest neighbor of a node (the nearest neighbor over all nearest neighbors in its sectors). This link exists in all possible orientations.

Lemma 6.4 *Let $G=(V,E)$ be the Yao-graph and $u,v \in V$ with $\forall w \in V : |u-w| \leq |u-v| \Rightarrow w = v$. Then $(u,v) \in E$ and $(v,u) \in E$ for $k \geq 6$.*

Proof: Let $u,v \in V$ with $\forall w \in V : |u-w| \leq |u-v| \Rightarrow w = v$. It follows directly that $(u,v) \in E$. Now we consider the sector of v in that u lies. For $k \geq 6$ the disk around u with radius $|u-v|$ contains the complete area of this sector of v up to the distance of $|u-v|$. If there would be a nearer neighbor of v then this node would also be a nearer neighbor of u. Hence, $(v,u) \in E$ and the claim follows. ■

Now we are ready to present algorithms that adjust the sectors of the nodes. Our main focus in the following is on the improvement of the maximum stretch factors. Lemma 6.4 shows that

it makes no sense to adjust the sectors to nearest node neighbors because they are connected by a symmetric link in all possible sector orientations. Mainly, we differ between four sector orientations:

- **Fixed Sector Orientation:** This is the assumption that comes with the definition of the Yao-graph from computational geometry. The orientation of the sectors is fixed and uniformly arranged on all nodes. Hence, in our definition we have $r(u) = 0$ for all $u \in V$.
- **Farthest Sector Orientation:** Here, we adjust the orientation of the sectors on a node to the farthest possible neighbor. In Section 6.2.4 we present an algorithm to compute all possible neighbors of all nodes in time $\mathcal{O}(n^2 \log n)$. We apply this algorithm to determine the farthest possible neighbors of all nodes in the same time (farthest possible neighbor of one node in time $\mathcal{O}(n \log n)$).
- **Random Sector Orientation:** Every node $u \in V$ chooses $r(u)$ uniformly at random from $[0, 2\pi/k)$.
- **Targeted Sector Orientation:** We begin with a fixed sector orientation and compute a specific stretch factor, i.e. the length, the weak or the power stretch factor. In addition to this stretch factor of the network, we get the source node s and the target node t which are responsible for this bad stretch factor. Now we use the result of Lemma 6.3 and adjust the sector of s in which t lies to t such that t is exactly on the bisector. Again, we compute the corresponding stretch factor and repeat the process until no improvement of the maximum stretch factor is achieved.

6.2.4 Lower Bound for an Optimal Adjustment

In this subsection we present algorithms to compute lower bounds for the stretch factors of the Yao-graph in the new model where each node can adjust the orientation of its senders. Let $G = (V, E)$ be the Yao-graph of V with k sectors and $n := |V|$. Now we construct the extended graph G^* which is defined by V and all anyhow possible Yao-edges denoted by E^*. Hence, $(u, v) \in E^*$ if there exists an orientation of the sectors of u such that (u, v) is an edge in the resulting Yao-graph of V. It is obvious that the stretch factors of this extended graph yield to lower bounds for the stretch factors in a Yao-graph in general and hence for an optimal adjustment with regard to a specific stretch factor. Our algorithm works as follows. Each node $u \in V$ determines all its possible neighbors. Therefore, u sorts all other $n - 1$ nodes according to their Euclidean distance. This needs time $\mathcal{O}(n \log n)$ per node. The nearest node v_1 and the second nearest node v_2 are always possible neighbors of u. It is possible to adjust the sectors such that v_1 and v_2 are nearest neighbors in two different sectors. We insert them into a sequence sorted by the angle, e.g., for v_1 the angle is given by the three points $(u(x) + 1, u(y)), u, v_1$. For a following node $v_i, i > 2$, we determine again the angle $(u(x) + 1, u(y)), u, v_i$ and look up the sequence for the node which builds the next smaller angle and for the node which builds the next greater angle. If the difference between these two angles is greater than $2\pi/k$ it is possible to build up an edge from u to v_i and we insert v_i with its angle into the sequence. In the other case there exists no

adjustment such that the link between u and v_i is also an edge of the Yao-graph. As you can see each node is inserted at most once into the sequence and so we need time $\mathcal{O}(n \log n)$. Altogether over all nodes we need time $\mathcal{O}(n^2 \log n)$ to calculate G^* centrally.

Corollary 6.1 *Let $G = (V, E)$ be the Yao-graph of G using any sector orientation with k sectors, c be its length (weak, power) stretch factor and c^* be the length (weak, power) stretch factor of G^* as defined before. Then $c^* \leq c$.*

6.2.5 Experimental Analysis

We have implemented an **i**nteractive **t**ool for checking **gra**ph **p**roperties, ITGraP, in Java. We use it to evaluate all variants of the sectorized topologies using different sector orientations [Vol04b]. In contrast to our simulation environment SAHNE, presented in Section 6.1, we do not simulate communication layers, physical effects, and signal propagation. ITGraP is a testbed that allows us to visualize the Yao-graph and its variants (see Figure 6.21) using variable, adjustable sector orientations. It is easy to construct random sectorized graphs as well as fixed arrangements. The sectors of every node can be arbitrarily rotated and functions to compute stretch factors, optimal orientations, and lower bounds were implemented.

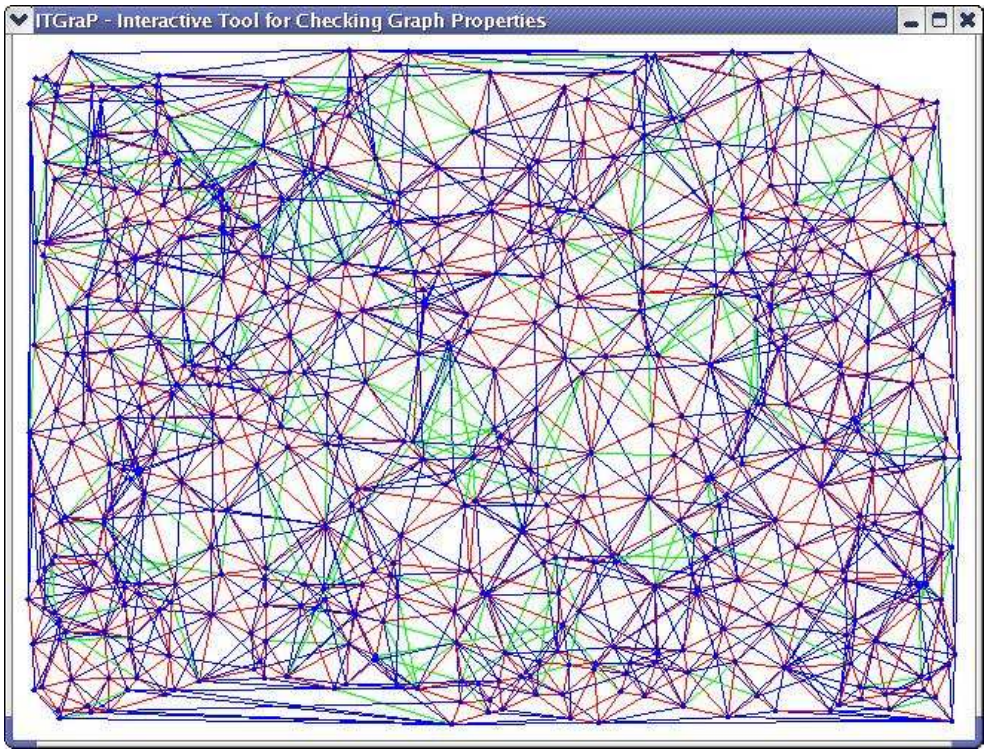

Figure 6.21: ITGraP - Interactive tool for checking graph properties

In Figure 6.21 the Yao-graph of a random vertex set V of 500 nodes in wich every node is equipped with 8 sectors/senders is illustrated. Brighter edges indicate edges which appear in the SparsY-graph but not in the SymmY-graph.

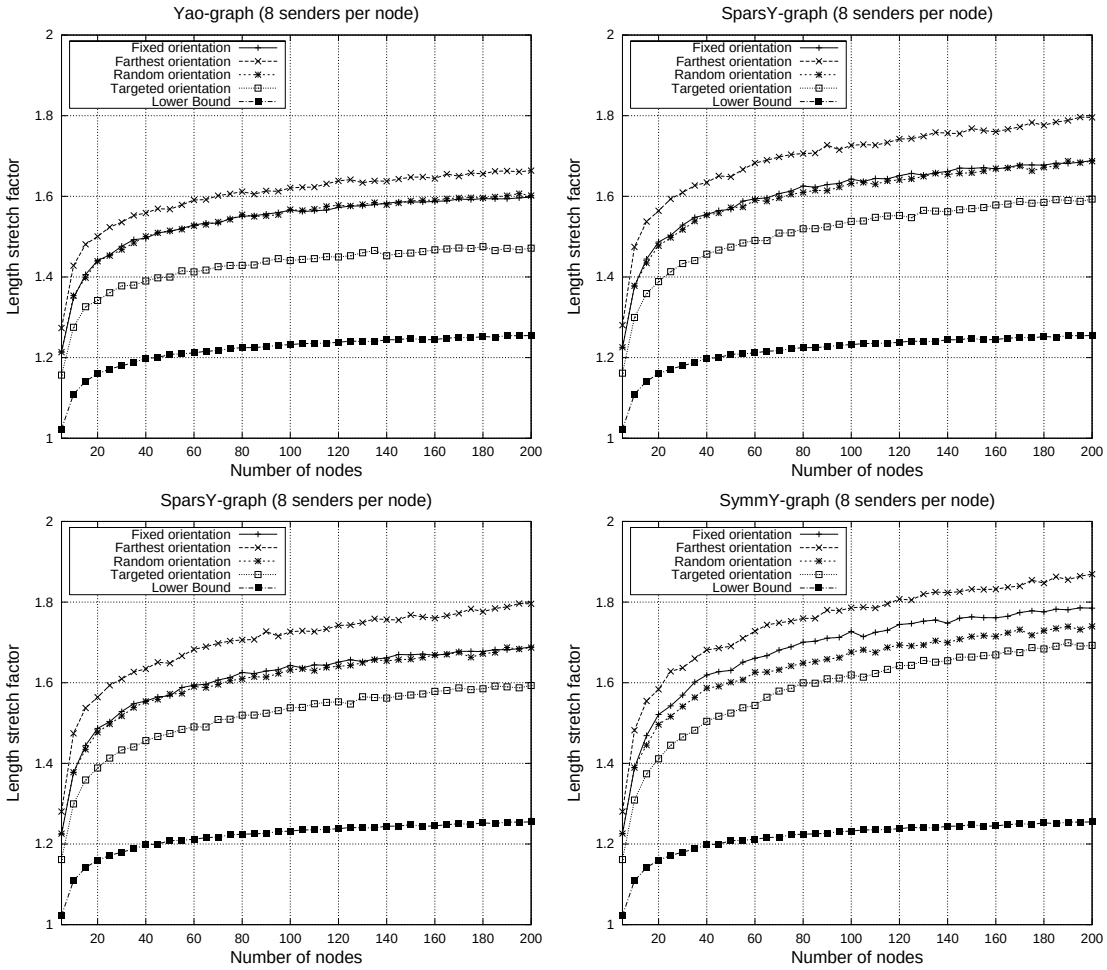

Figure 6.22: Maximum length stretch factors of Yao-graph, SparsY-graph and SymmY-graph

In the following we concentrate on sets of wireless devices given in the Euclidean plane and assume that the energy needed to transmit some data over a distance d is given by d^δ with propagation exponent $\delta = 2$, see Section 2.1.

Mainly, we compare stretch factors, number of edges, node degrees, edge lengths, and network energy consumption of the Yao-graph and its variants using fixed, farthest, random, and targeted sector orientation. We assume that there is given a static set of nodes and the number of nodes varies from 5 to 200. The number of senders per node goes from 6 to 11. All nodes are placed uniformly at random over the given area of size 652×476. For each measurement we performed 500 passes and computed the average and/or the maximum over all these 500 values to get significant simulation results. Our main focus is on improving the maximum stretch factors. We want to reduce energy consumption of the topology on which other tasks like selecting routing paths and forwarding packets take place. Furthermore, we want to give a complete overview of the properties of the Yao-graph and its variants using random vertex sets. In the following, we present our simulation results. Sometimes we placed four graphics in one figure then you should

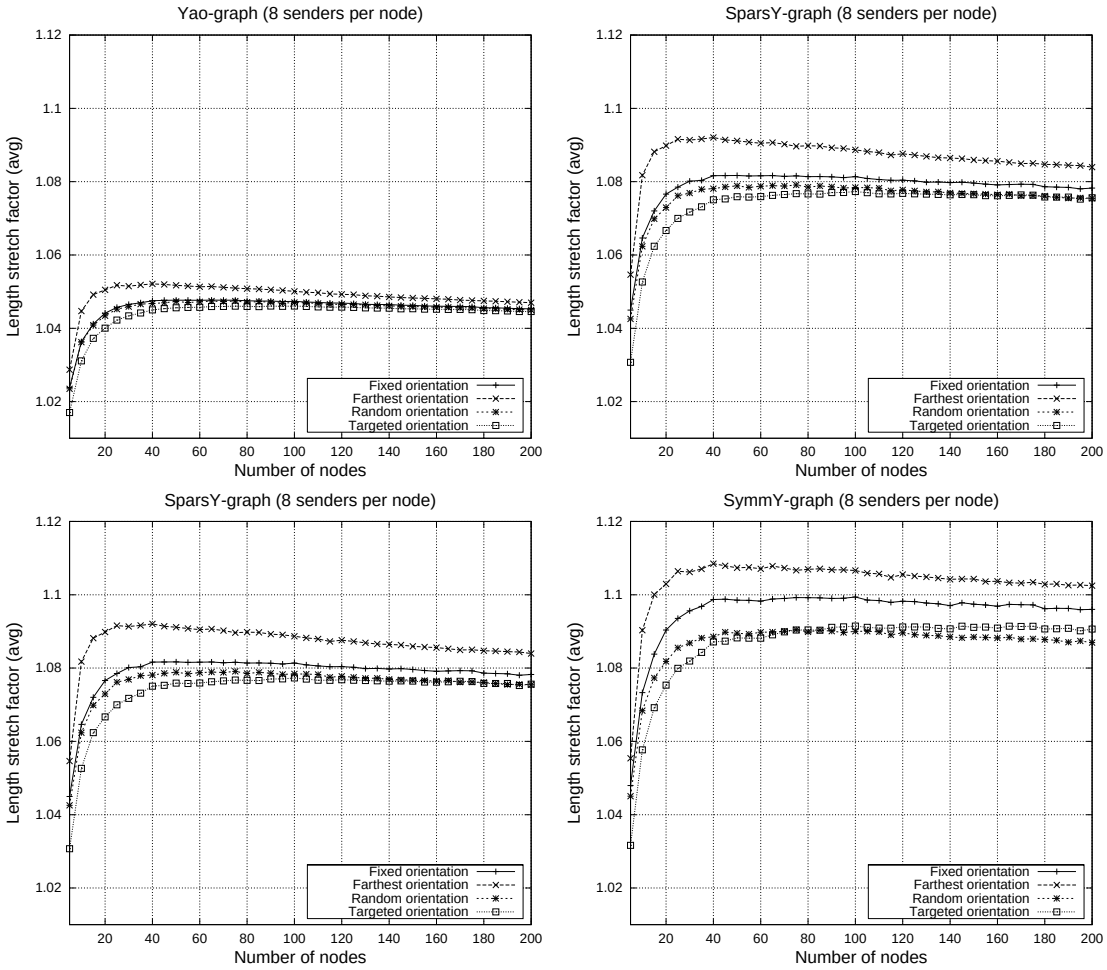

Figure 6.23: Average length stretch factors of Yao-graph, SparsY-graph and SymmY-graph

notice that one graphic occurs twice to see the differences between different measurements. This kind of top view is better than a view where three small graphics are placed side by side in one figure. In each illustration we have arranged the y-axes.

Stretch Factors The maximum stretch factors, especially the length and the power stretch factor, of a wireless network should be minimized since energy conservation is a critical issue for node and network lifetime.

In Figure 6.22 the maximum length stretch factors of the Yao-graph and its variants are presented. We compare them using different sector orientations with regard to the lower bound shown in Section 6.2.4. It is known that the length stretch factor of the Yao-graph and the weak stretch factor of the SparsY-graph can be upper bounded by $1/(1-2\sin(\pi/k))$, see Chapter 4. For 8 sectors this value is given by 4.262. The diagram shows that the maximum length stretch factor on random vertex sets is smaller and far away from this upper bound. The average length stretch factors, given in Figure 6.23, point out this behavior.

As expected the length stretch factor of the Yao-graph is the best, followed by the factor of the

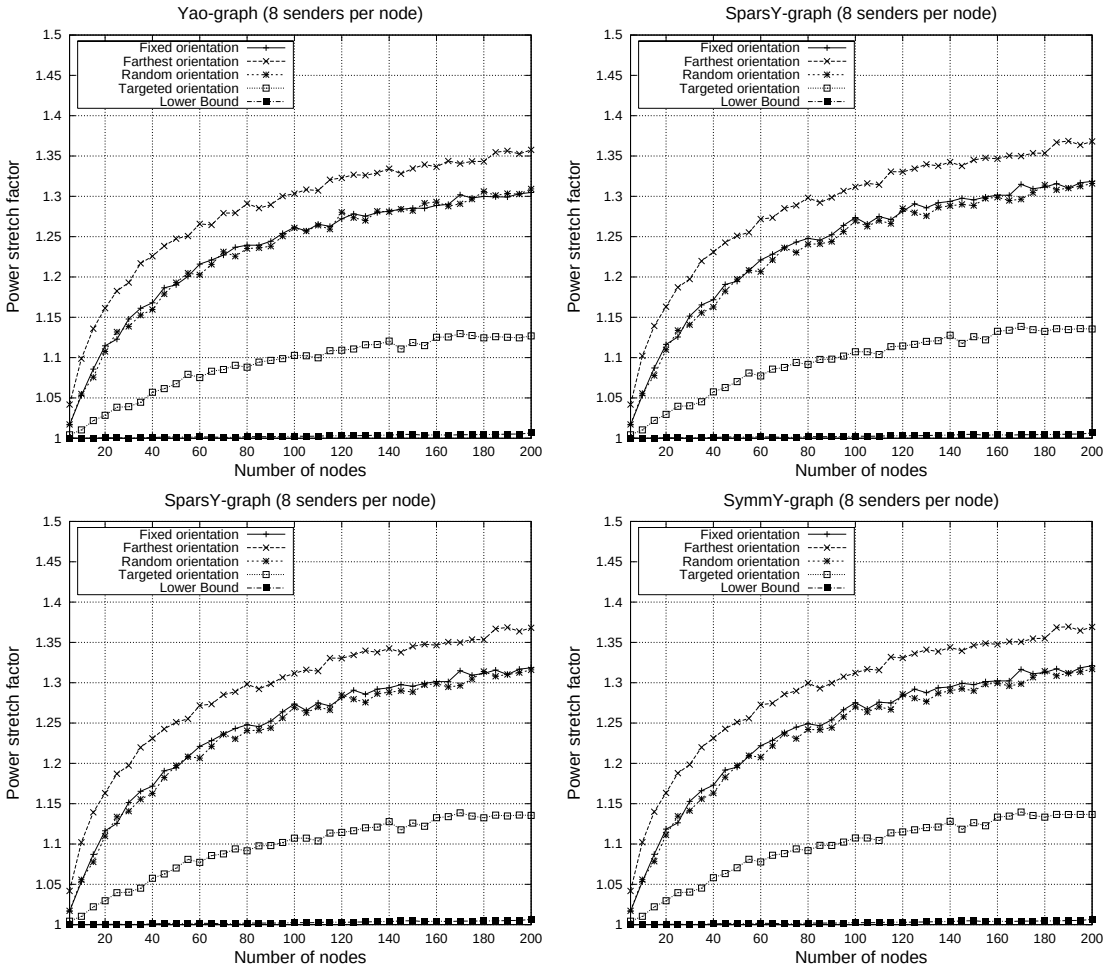

Figure 6.24: Maximum power stretch factors of Yao-graph, SparsY-graph and SymmY-graph

SparsY-graph and finally the factor of the SymmY-graph. Furthermore, it is shown that a farthest sector orientation yields to bad length stretch factors. A targeted sector orientation betters the length stretch factor of a fixed sector orientation in all three graphs. Hence, on random vertex sets it is very useful to adjust some sectors of the nodes to get better results concerning energy consumption.

Another very interesting observation, comparing the three diagrams in Figure 6.22, is that the quality of a random orientation increases with decreasing the number of edges. In the Yao-graph a random orientation gives nearly the same results as a fixed orientation. In the SparsY-graph there is already a relatively small difference between a fixed and a random orientation. But in the SymmY-graph it makes more sense to orientate the sectors at random instead of using a fixed orientation. Randomness helps improving the length stretch factor.

We got similar results for the maximum power stretch factors and for the maximum weak stretch factors (see Figure 6.24 and Figure 6.25). The diagrams concerning the power stretch factors show that there is only a small difference between the maximum power stretch factor

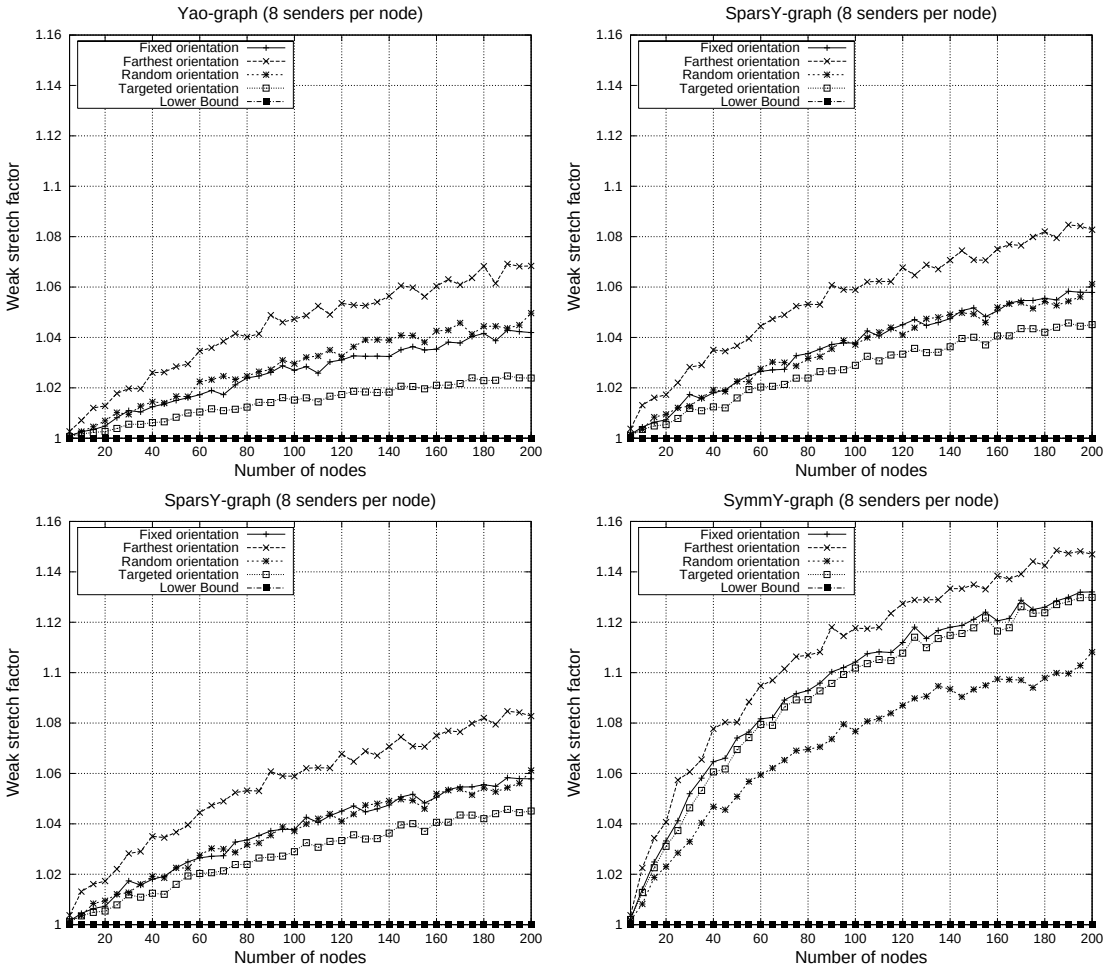

Figure 6.25: Maximum weak stretch factors of Yao-graph, SparsY-graph and SymmY-graph

of the Yao-graph and its variants. On random vertex sets they have nearly the same maximum power stretch factors. The difference between a random sector orientation and a fixed one is not so high as before.

Comparing the maximum weak stretch factors it stands out that in the Yao-graph a random sector orientation is worse than a fixed orientation, but in the SymmY-graph it is suddenly better than a fixed as well as a targeted orientation. All results show that for a given graph the weak stretch factors have the smallest values, followed by the power stretch factors and the highest values are given by the length stretch factors. But this behavior is not really amazing. We can argue that the Yao-graph and its variants on random vertex sets are spanners, weak spanners, and power spanners. Furthermore, our extended communication model allows us to improve their stretch factors.

Finally, we varied the number of sectors from 6 to 11 to investigate how this affects the behavior of the different sector orientations. The results of the SymmY-graph are given in Figure 6.26 and Figure 6.27. Again, best stretch factors are achieved using targeted orientation. It is known

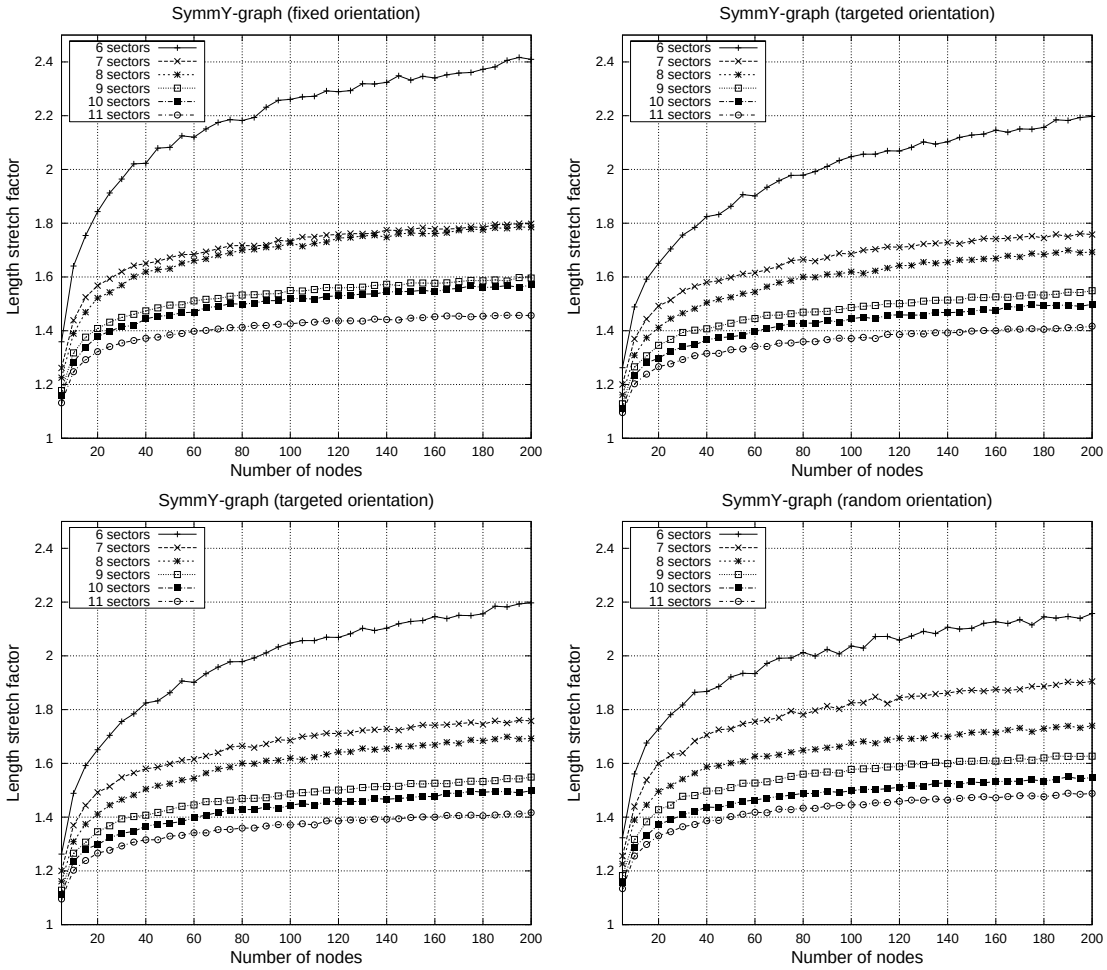

Figure 6.26: Maximum length stretch factors of SymmY-graph varying the number of sectors

that the values of the stretch factors of the Yao-graph converge to 1 if the number of sectors goes to infinity. The figures point out this behavior for all stretch factors. The curve progression of the maximum length stretch factor of the SymmY-graph using 6 senders per node differs from the characteristic of the other curves. It is interesting that the curves of a fixed sector orientation form a double pack: the curves representing the results using 7 and 8 senders as well as using 9 and 10 senders are nearly identical but there is a small gap between these two progressions. A targeted orientation balances the curves and a random orientation gives homogeneous curves without remarkable effects.

Number of Edges Figure 6.28 shows the number of edges of the Yao-graph and its variants unsing fixed and targeted sector orientation. On the one hand, the maximum number of edges of the Yao-graph is upper bounded by kn. Hence, using 8 senders per node we can have at most $8n$ edges. On the other hand, all three graphs are connected such that we have at least $n - 1$ edges. As you can see in the diagrams there is nearly no difference between the number of edges using different sector orientations. We could observe this behavior during all other simulations and

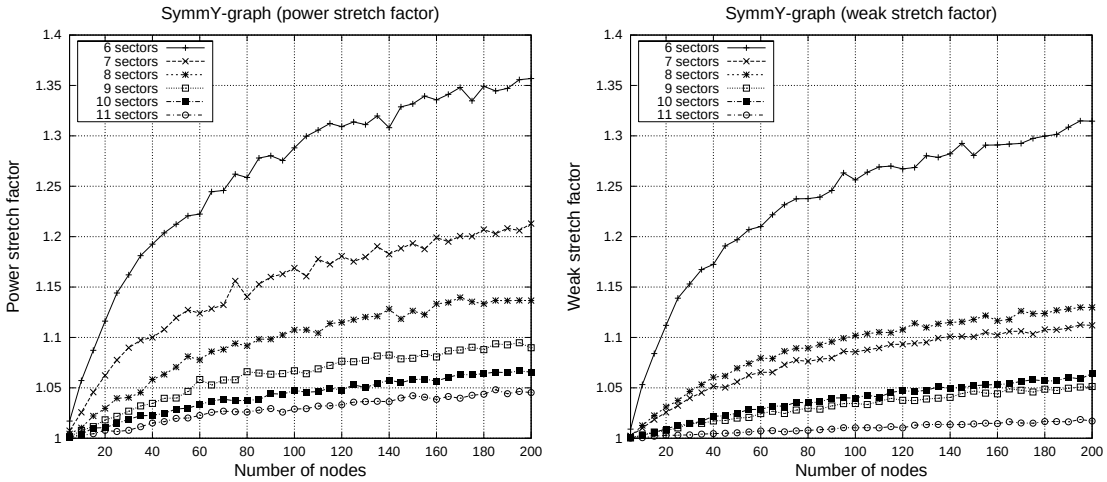

Figure 6.27: Maximum stretch factors of SymmY using targeted orientation

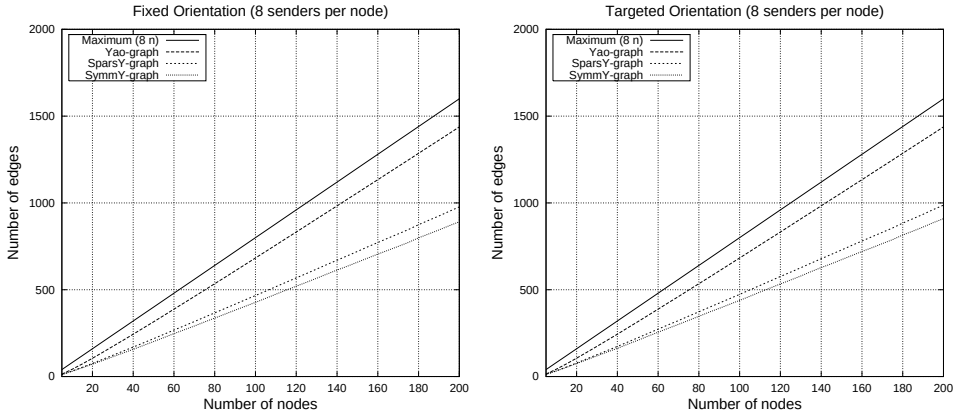

Figure 6.28: Number of edges in the Yao-graph and its variants

we were not wondered about that. Both diagrams show expected values: the Yao-graph has the highest number of edges, followed by the SparsY-graph and the SymmY-graph at position three.

Node Degrees In this paragraph we present the results concerning the maximum in-degree of a node. The in-degree is very important since there is only one transmission frequency given. A high in-degree can result in a high amount of interference. In this work the focus was not on improving the in-degree but for completeness we want to present the maximum in-degree of the graphs (Figure 6.29 left) and the average in-degree of a node (Figure 6.29 right). Simulations showed that the type of orientation does not influence the in-degrees appreciably.

The maximum in-degree of the Yao-graph can only be upper bounded by the trivial bound of $n-1$. The maximum in-degree of the other both variants converges relatively fast to the number of senders per node. On random vertex sets we can assume that the average in-degree of the Yao-graph is also given by a constant. The Yao-graph consists of at most kn edges and hence, the average in-degree of a node should converge to $kn/n = k$. This observation can be seen in the diagrams.

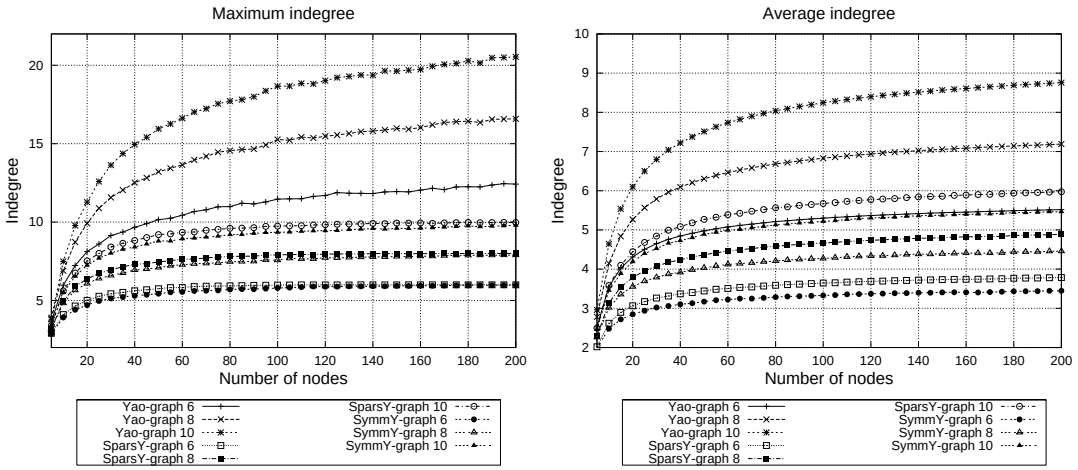

Figure 6.29: Maximum and average in-degree of the nodes using fixed sector orientation

Edge Lengths In order to spare energy in a wireless network we consider the edge lengths that appear in the sectorized graphs using different sector orientations. Figure 6.30 gives an overview of the maximum edge lengths.

Note that it is clear that a farthest orientation brings longest edges. Furthermore, the longest edge of the Yao-graph should be longer than the longest edge of the SparsY-graph which should be longer than the longest edge of the SymmY-graph. The figures point out this behavior. An interesting observation is that a random orientation yields to best values concerning longest edges in the Yao-graph. You have to notice that we performed 500 passes per measurement and this diagram points out that the extended communication model brings an improvement to energy consumption. In the sparser variants a fixed and a targeted orientation gives best results. Our simulations showed, looking at the average edge lengths, that there are only very small differences between the curves.

Network Energy Consumption Finally, we compare the topologies with regard to the energy-cost of the whole network structure. We sum up over the energy-cost of all existing communication links and present the results.

As expected the SymmY-graph has lowest energy consumption maintaining all edges, followed by the SparsY-graph and then by the Yao-graph (see Figure 6.31). We observe the same behavior as for the edge lengths: a random orientation is wise in case of the Yao-graph. Otherwise a fixed or a targeted orientation is adequate.

6.3 Conclusions

In this chapter we have presented the results of our extensive experimental evaluations. We have developed and implemented two different tools, SAHNE and ITGraP, to study topologies for the omndidirectional and the unidirectional communication model.

We have used our simulation environment SAHNE to analyze communication strategies using realistic communication models. SAHNE can be easily extended, e.g., for simulating (wire-

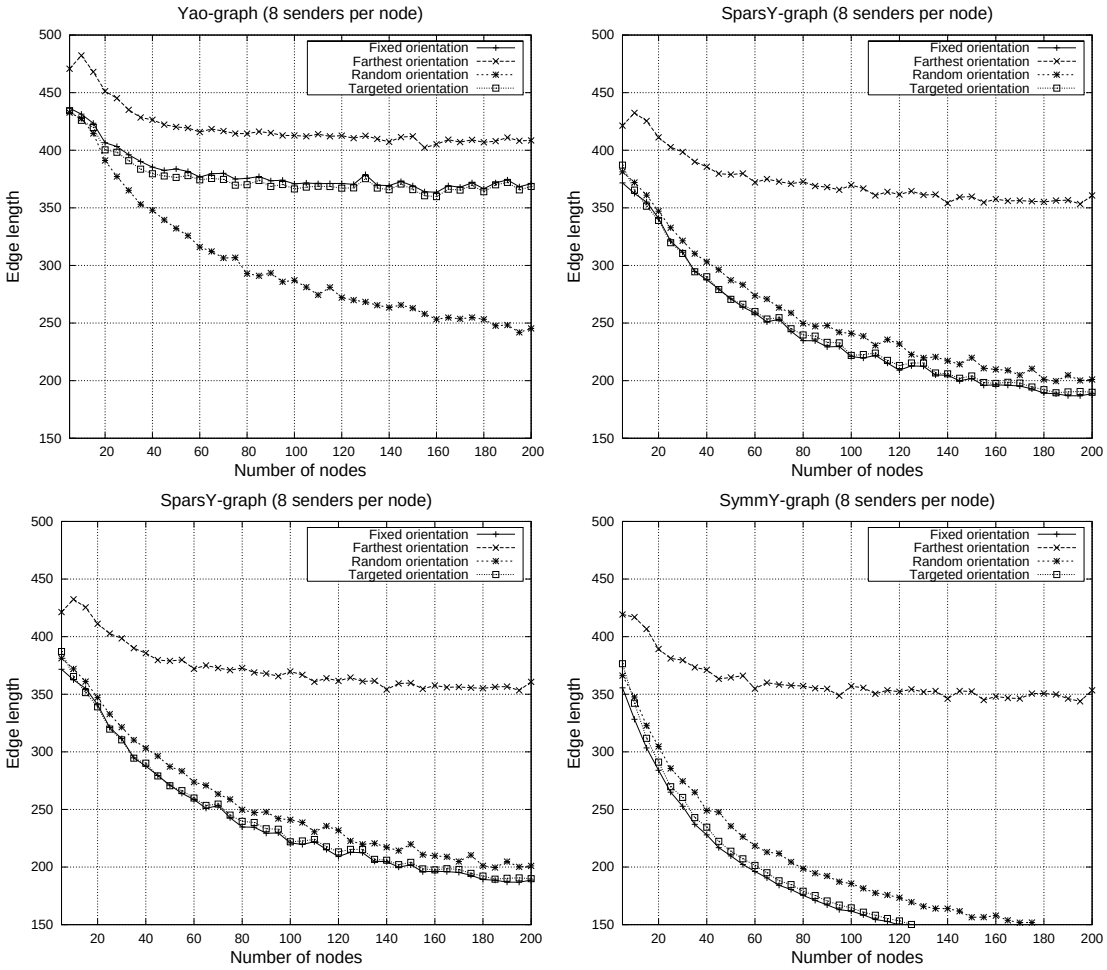

Figure 6.30: Maximum edge lengths

less) sensor networks or by implementing additional propagation models. For the omnidirectional communication model we have implemented and experimentally investigated the Hierarchical Layer Graph and for the unidirectional communication the Yao-graph and its variants. By simulations we have shown how these graphs can be used as congestion-efficient and/or energy-efficient topologies for wireless networks. Besides the use of omnidirectional antennae we have studied communication devices that can send and receive data in a fixed number of sectors in parallel with variable transmission power and proposed local, distributed algorithms to maintain the incoming and outgoing communication links of these topologies. To close the gap between abstract communication models used in the theoretical studies and realistic signal propagation and reception, we have extended our simulator SAHNE with well-known models for signal propagation and reception. The results of our simulation studies show that the Yao-graph can be constructed faster and yields smaller congestion values than the SparsY-graph and the SymmY-graph. However, the SparsY-graph is more energy-efficient than the Yao-graph since it uses shorter edges.

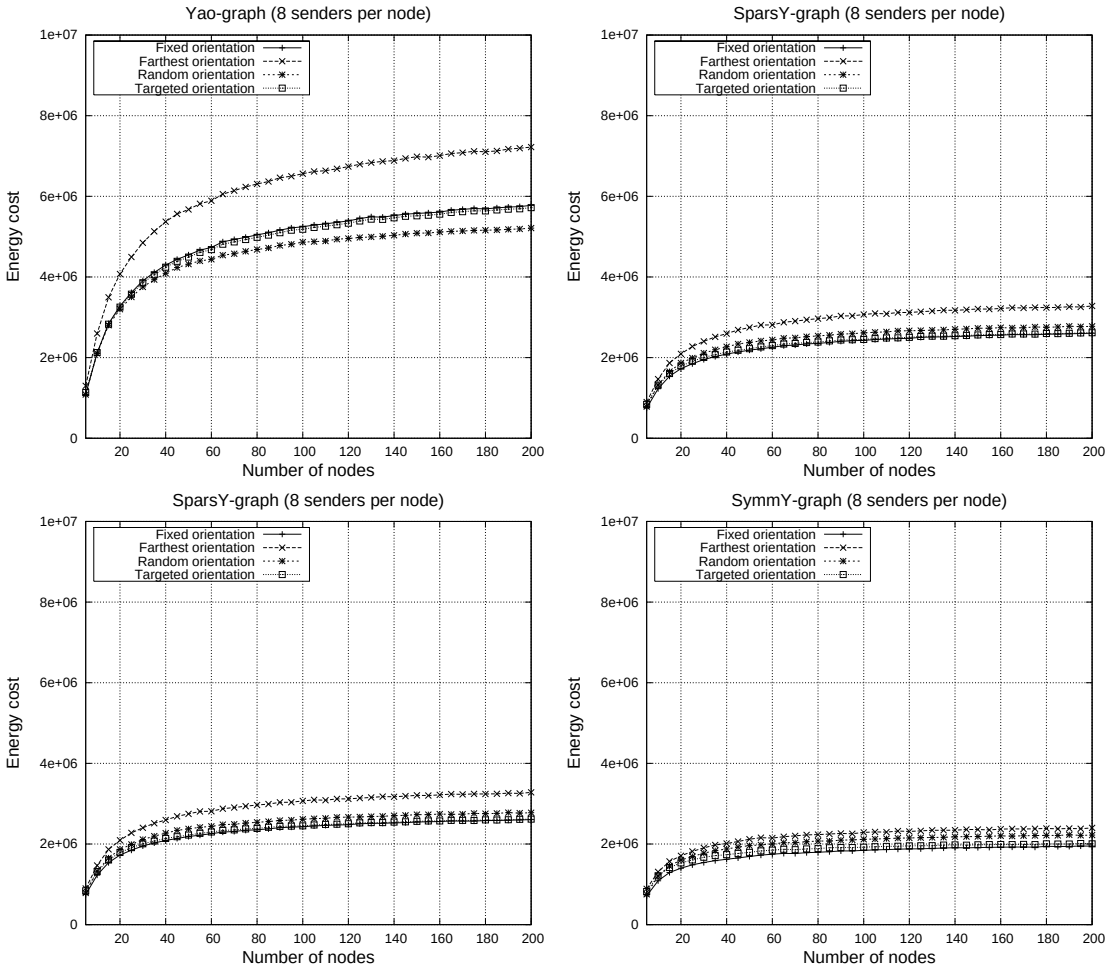

Figure 6.31: Network energy consumption: summation over all communication links

Furthermore, we have investigated an extended communication model where we allow each node to adjust the orientation of its senders. This is an important and interesting addition to variable and directional transmissions. We showed using simulations that the extended model allows us the improvement of the stretch factors of the Yao-graph and its variants.

For our experimental evaluation we implemented and used an interactive tool for checking graph properties. We presented new algorithms for computing stretch factors efficiently. We can exactly determine the length, the power, and the weak stretch factor of a graph consisting of n nodes and m edges in time $\mathcal{O}(n^2 \log n + nm)$. Since the Yao-graph and its variants are sparse graphs of at most $\mathcal{O}(n)$ edges, we need only time $\mathcal{O}(n^2 \log n)$ to calculate the stretch factors for these graphs. We used these results to give lower bounds to the stretch factors and applied this in our simulations.

For the extended communication model, we introduced new algorithms motivated theoretically and showed experimentally that a targeted orientation improves the results of the Yao-graph, the SparsY-graph, and the SymmY-graph with regard to energy consumption.

Finally, we want to point out some unsolved questions. It is (still) open whether the SparsY-graph is a spanner or not, in general. We extend this problem and ask whether it is possible to adjust the sectors of a node set or only of some nodes such that the SparsY-graph is a spanner depending on a specific orientation. Is it even possible to adjust some sectors of nodes of the SymmY-graph such that it results in a spanner, a weak spanner or power spanner? Our simulations showed that this holds on random vertex sets. On the other hand, further research can be done extending our communication model. For example, we could consider the case in which the size of the angle of each transmitter can also be controlled or the case where the number of sectors per device is variable. The first model presents new problems since the area around a node is not necessarily divided into non-overlapping regions. By the way, in real-world applications we have nearly always overlapping regions if we use unidirectional communication.

Summary and Outlook

Recently, wireless networks, especially mobile ad hoc networks and sensor networks, have become more important and many researchers as well as developers and engineers are trying to contribute to this field. Current topics are, e.g., heterogeneous mobile ad hoc networks or large-scale sensor networks.

In this thesis the focus was on topology control in power-variable, single frequency ad hoc networks using geometric spanners. We have used geometric graphs to model static, dynamic, and mobile ad hoc networks. Mainly, we have developed and analyzed algorithms for point-to-point communication using two different communication models. For the omnidirectional communication model we have suggested the Hierarchical Layer Graph and the Hierarchical Grid Graph. For the unidirectional communication model we have investigated the Yao-graph and two variants, namely the SparsY-graph and the SymmY-graph. Our goal was to construct ad hoc networks which are optimized for routing time and energy-consumption. We could relate methods in computational geometry and topology control in wireless networks. Furthermore, we have solved open problems stated by other researchers working on the same topic and could prove interesting relations, e.g., that every weak spanner is a power spanner, which can also be applied in other fields of research.

Besides our mathematical analyses we have also perfomed extensive simulations. For this purpose we have implemented two different platforms that enabled us to see whether our topologies are qualified for real-world applications. We used realistic settings and well-known models for signal propagation of (radio) waves.

Nevertheless, there are some open questions. First of all, one of the most interesting question is: is the SparsY-graph a spanner? This was also one of the most frequently asked question during this work and we have thought about it in almost the same manner. In the context of spanners, one can ask how optimal are our results on the relations, i.e. is there some $C = o(c^{4\mathcal{D}})$ such that any weak c-spanner is a (C, δ)-power spanner? Since we distinguished between two different communication models, one can ask for studies in which the combination of these models is investigated. Other heterogeneous properties may also be investigated. We presented lower and upper bounds for the routing time in ad hoc networks. Is it possible to improve these bounds/to close the gap? We introduced a new dimension to wireless networks using the unidirectional communication model, since we allow each node to adjust the orientation of its sectors/senders. Theoretical results are open. For physical purposes, it would be interesting to consider further models for signal propagation besides free space propagation or to account for physical effects in even more detail.

Mobility has been a major challenge in wireless networks. For example, what is realistic mobility? We tried to contribute to modelling of worst case movements, but there are some open questions. The modeling of interference of moving edges presented in this thesis is only a rough estimation. It is not clear how a mobile network design may look for a more accurate model. Furthermore, the distributed measurement and computation of the relative locations and relative speed vectors need to be further investigated.

Appendix

Notation

The following list summarizes some basic denotations used in this thesis:

- $\mathbb{N} = \{1, 2, 3, \ldots\}, \mathbb{N}_0 = \mathbb{N} \cup \{0\}$, $\mathbb{Z} = \{\ldots, -3, -2, -1, 0, 1, 2, 3, \ldots\}$
- $\mathbb{R}$ represents the set of all real numbers
- For $n \in \mathbb{N}$ we define $[n] := \{1, \ldots, n\}$
- Let $f(n)$ and $g(n)$ be two functions. Following [CLSR01] we denote by $\mathcal{O}(f(n))$, $\Omega(f(n))$, $\Theta(f(n))$, and $o(f(n))$ the sets of functions
  - $\mathcal{O}(f(n)) = \{\ g(n) \mid \exists c \in \mathbb{R}^+ \text{ and } n_o \in \mathbb{N} : \forall n \geq n_o\ f(n) \leq c \cdot g(n)\}$
  - $\Omega(f(n)) = \{\ g(n) \mid \exists c \in \mathbb{R}^+ \text{ and } n_o \in \mathbb{N} : \forall n \geq n_o\ f(n) \geq c \cdot g(n)\}$
  - $\Theta(f(n)) = \{\ g(n) \mid g(n) = \mathcal{O}(f(n)) \text{ and } g(n) = \Omega(f(n)\}$
  - $o(f(n)) = \{\ g(n) \mid \forall c \in \mathbb{R}^+\ \exists\ n_o \in \mathbb{N} : \forall n \geq n_o\ f(n) < c \cdot g(n)\}$
- For two functions $f(n)$ and $g(n)$ we mean by $f(n) = \mathcal{O}(g(n))$ that $f(n) \in \mathcal{O}(g(n))$; in an analogous manner, the same holds for $\Omega(f(n))$, $\Theta(f(n))$, and $o(f(n))$
- By $\log$ we mean the logarithm to the base 2, i.e. $\log_2$
- $|u - v|_2 = |u - v|$ is the Euclidean distance between u and v
- $|e|$ is the Euclidean length of the edge e
- $|x|_2 = |x|$ is the L_2-norm for an n-dimensional vector x
- $|M|$ is the cardinality of the set M
- For $x \in \mathbb{R}$ we define by $\lceil x \rceil$ the smallest $n \in \mathbb{N}$ with $n \geq x$
- For $x \in \mathbb{R}$ we define by $\lfloor x \rfloor$ the largest $n \in \mathbb{N}$ with $n \leq x$
- By *w.l.o.g.* we mean without loss of generality

- $\delta \in \mathbb{R}$: propagation exponent
- $\mathcal{D} \in \mathbb{N}$: dimension
- $\mathcal{D}_f \in \mathbb{R}$: fractal dimension or Hausdorff dimension
- $k_\mathcal{D} \in \mathbb{R}$: constant factor for the volume of a sphere $k_\mathcal{D} := \frac{\pi^{\mathcal{D}/2}}{(\mathcal{D}/2)!}$
- $\mathrm{BInt}(e), \mathrm{UInt}(e)$: set of edges bidirectionally/unidirectionally interfering with the edge e
- $\mathrm{BInt}(G), \mathrm{UInt}(G)$: bidirectional/unidirectional interference number of a graph G
- $\mathrm{BInt}_\alpha(G), \mathrm{BInt}_\alpha(e)$: the same as above but for worst case mobility for $\alpha \in \{\mathsf{v}, \mathsf{a}\}$
- $C_\mathcal{P}(e)$: congestion of an edge e in the network defined by the path system $\mathcal{P}$
- $C_{\alpha,\mathcal{P}}(e)$: $C_\mathcal{P}(e)$ using pedestrian or vehicular mobility, i.e. for $\alpha \in \{\mathsf{a}, \mathsf{v}\}$
- $g(V)$: diversity of a vertex set $V \subseteq \mathbb{R}^\mathcal{D}$

Bibliography

[ABBS01] B. Awerbuch, P. Berenbrink, A. Brinkmann, and C. Scheideler. Simple Routing Strategies for Adversarial Systems. In *IEEE Symposium on Foundations of Computer Science (FOCS'01)*, pages 158–167, 2001.

[AGK+98] S. Arora, M. Grigni, D. R. Karger, P. N. Klein, and A. Woloszyn. A polynomial-time approximation scheme for weighted planar graph TSP. In *Symposium on Discrete Algorithms (SODA'98)*, pages 33–41, 1998.

[ALW+03] K. Alzoubi, X.-Y. Li, Y. Wang, P.J. Wan, and O. Frieder. Geometric spanners for wireless ad hoc networks. *IEEE Transactions on Parallel and Distributed Systems*, 14(4):408–421, 2003.

[AS98] M. Adler and C. Scheideler. Efficient Communication Strategies for Ad-Hoc Wireless Networks (Extended Abstract). In *ACM Symposium on Parallel Algorithms and Architectures (SPAA'98)*, pages 259–268, 1998.

[AZ03] D. P. Agrawal and Q-A. Zeng. *Introduction to Wireless and Mobile Systems*. Brooks/Cole Publishing, 2003.

[BB99] S. Benedetto and E. Biglieri. *Principles of Digital Transmission*. Kluwer Academic / Plenum Publishers, 1999.

[Bet01a] C. Bettstetter. Mobility modeling in wireless networks: categorization, smooth movement, and border effects. *SIGMOBILE Mob. Comput. Commun. Rev.*, 5(3):55–66, 2001.

[Bet01b] C. Bettstetter. Smooth is Better than Sharp: A Random Mobility Model for Simulation of Wireless Networks. In *ACM Int. Workshop on Modeling, Analysis, and Simulation of Wireless and Mobile Systems (MSWiM'01)*, pages 19–27, 2001.

[Bet04] C. Bettstetter. *Mobility Modeling, Connectivity, and Adaptive Clustering in Ad Hoc Networks*. Utz Verlag, 2004.

[BGH99] J. Basch, L. J. Guibas, and J. Hershberger. Data Structures for Mobile Data. *Journal of Algorithms*, 31(1):1–28, 1999.

[BGLA02] L. Bao and J.J. Garcia-Luna-Aceves. Transmission scheduling in ad hoc networks with directional antennas. In *MobiCom'02*, pages 48–58. ACM Press, 2002.

[BH04] F. Bai and A. Helmy. A Survey of Mobility Modeling and Analysis in Wireless Adhoc Networks, Book Chapter of Wireless Ad Hoc and Sensor Networks, Kluwer. 2004.

[Bha98] V. Bharghavan. Performance Evaluation of Algorithms for Wireless Medium Access. In *International Computer Performance and Dependability Symposium*, pages 142–149, 1998.

[BV05] J.-Y. Le Boudec and M. Vojnovic. Perfect Simulation and Stationarity of a Class of Mobility Models. In *IEEE Infocom 2005*, accepted for publication, 2005.

[BvRWZ04] M. Burkhart, P. von Rickenbach, R. Wattenhofer, and A. Zollinger. Does topology control reduce interference? In *MobiHoc '04: Proceedings of the 5th ACM international symposium on Mobile ad hoc networking and computing*, pages 9–19, New York, NY, USA, 2004. ACM Press.

[CBD02] T. Camp, J. Boleng, and V. Davies. A Survey of Mobility Models for Ad Hoc Network Research. *Wireless Communications & Mobile Computing (WCMC): Special issue on Mobile Ad Hoc Networking: Research, Trends and Applications*, 2(5):483–502, 2002.

[Che86] L. P. Chew. There is a planar graph almost as good as the complete graph. In *2nd ACM Symposium on Computational Geometry (SoCG '86)*, pages 169–177, 1986.

[CJBM01] B. Chen, K. Jamieson, H. Balakrishnan, and R. Morris. Span: An Energy-Efficient Coordination Algorithm for Topology Maintenance in Ad Hoc Wireless Networks. In *Proceedings of the Seventh Annual ACM/IEEE International Conference on Mobile Computing and Networking (Mobicom)*, pages 85–96, Rome, Italy, July 2001.

[Cla87] K. Clarkson. Approximation algorithms for shortest path motion planning. In *Proceedings of the nineteenth annual ACM conference on Theory of computing*, pages 56–65. ACM Press, 1987.

[CLSR01] T. H. Cormen, C. E. Leiserson, C. Stein, and R. L. Rivest. *Introduction to Algorithms*. McGraw-Hill Higher Education, 2001.

[CNS01] I. Chatzigiannakis, S. Nikoletseas, and P. Spirakis. An efficient communication strategy for ad-hoc mobile networks. In *Proc. of the twentieth annual ACM symposium on Principles of distributed computing (PODC '01)*, pages 320–322, 2001.

[CPS04] A. E. F. Clementi, P. Penna, and R. Silvestri. On the power assignment problem in radio networks. *Mobile Networks and Applications*, 9(2):125–140, 2004.

[CS01] A. Czumaj and C. Sohler. Soft Kinetic Data Structures. In *Symposium on Discrete Algorithms (SODA'01)*, pages 865–872, 2001.

[CT00] J. Chang and L. Tassiulas. Energy conserving routing in wireless ad hoc networks. In *IEEE INFOCOM*, pages 22–31, March 2000.

[CYVR02] R. R. Choudhury, X. Yang, N. H. Vaidya, and R. Ramanathan. Using directional antennas for medium access control in ad hoc networks. In *MobiCom'02*, pages 59–70. ACM Press, 2002.

[DJ96] G. Dommety and R. Jain. Potential networking applications of global positioning systems (gps). Technical Report TR-24, CS Dept., The Ohio State University, 1996.

[DRWT97] R. Dube, C. D. Rais, K.-Y. Wang, and S. K. Tripathi. Signal Stability-Based Adaptive Routing (SSA) for Ad Hoc Mobile Networks. *IEEE Personal Communications*, 4(1):36–45, 1997.

[EGMT84] S. Even, O. Goldreich, S. Moran, and P. Tong. On the NP-Completeness of Certain Network-Testing Problems. 14(1):1–24, 1984.

[Eik03] M. Eikermann. Dynamic Source Routing: Implementierung, Erweiterung und Simulation. Bachelor thesis, University of Paderborn, 2003.

[Epp96] D. Eppstein. Beta-skeletons have unbounded dilation. Technical Report ICS-TR-96-15, 1996.

[Epp00] D. Eppstein. Spanning trees and spanners. In *Handbook of Computational Geometry*, chapter 9, pages 425–461. Elsevier, 2000.

[Epp05] D. Eppstein. The Geometry Junkyard: Fractals, www.ics.uci.edu/∼eppstein/junkyard/fractal.html, 2005.

[ET90] A. Ephremides and T.V. Truong. Scheduling broadcasts in multihop radio networks. 38(4):456–460, 1990.

[FLZ98] M. Fischer, T. Lukovszki, and M. Ziegler. Geometric searching in walkthrough animations with weak spanners in real time. In *6th Annual European Symposium on Algorithms (ESA '98)*, pages 163–174, 1998.

[FMS97] M. Fischer, F. Meyer auf der Heide, and W.-B. Strothmann. Dynamic data structures for realtime management of large geometric scenes. In *5th Annual European Symposium on Algorithms (ESA '97)*, pages 157–170, 1997.

[FV98] K. Fall and K. Varadhan. ns notes and documentation, web site at http://www.isi.edu/nsnam/ns. 1998.

[GGH+01a] J. Gao, L. J. Guibas, J. Hershberger, L. Zhang, and A. Zhu. Discrete Mobile Centers. In *Proc. of the 17th Symposium on Computational Geometry (SOCG'01)*, pages 188–196, 2001.

[GGH+01b] J. Gao, L. J. Guibas, J. Hershberger, L. Zhang, and A. Zhu. Geometric Spanner for Routing in Mobile Networks. In *ACM Symposium on Mobile Ad Hoc Networking and Computing (MOBICOM'01)*, pages 45–55, 2001.

[GK00] P. Gupta and P. Kumar. The Capacity of Wireless Networks. In *IEEE Transactions on Information Theory, Volume 46(2)*, pages 388–404, 2000.

[GLSV02] M. Grünewald, T. Lukovszki, C. Schindelhauer, and K. Volbert. Distributed Maintenance of Resource Efficient Wireless Network Topologies (Ext. Abstract). In *8th European Conference on Parallel Computing (EURO-PAR'02)*, **distinguished paper**, pages 935–946, 2002.

[GRSV03] M. Grünewald, U. Rückert, C. Schindelhauer, and K. Volbert. Directed power-variable infrared communications for the mini robot Khepera. In *Proceedings of the 2nd International Symposium on Autonomous Minirobots for Research and Edutainment (AMiRe '03)*, pages 113–122, 2003.

[GS69] K. R. Gabriel and R. R. Sokal. A new statistical approach to geographic variation analysis. In *Systematic Zoology (18)*, pages 259–278, 1969.

[GY04] S. Guo and O. W. Yang. Antenna orientation optimization for minimum-energy multicast tree construction in wireless ad hoc networks with directional antennas. In *MobiHoc'04*, pages 234–243, 2004.

[HBHMR+98] III H. B. Hunt, M. V. Marathe, V. Radhakrishnan, S. S. Ravi, D. J. Rosenkrantz, and R. E. Stearns. Nc-approximation schemes for np- and pspace-hard problems for geometric graphs. *J. Algorithms*, 26(2):238–274, 1998.

[HGPC99] X. Hong, M. Gerla, G. Pei, and C.-C. Chiang. A Group Mobility Model for Ad Hoc Wireless Networks. In *Proc. of the 2nd ACM int. workshop on Modeling, analysis and simulation of wireless and mobile systems*, pages 53–60, 1999.

[HP96] M. Horneffer and D. Plassmann. Directed antennas in mobile broadband systems. In *IEEE INFOCOM*, pages 704–712, 1996.

[HP00] Y. Hassin and D. Peleg. Sparse communication networks and efficient routing in the plane (ext. abstract). In *ACM Symposium on Principles of Distributed Computing (PODC '00)*, pages 41–50, 2000.

[HS02] Z. Huang and C.-C. Shen. A comparison study of omnidirectional and directional MAC protocols for ad hoc networks. In *IEEE Global Telecommunications Conference*, pages 57 – 61, 2002.

[HSS97] R. H. Hardin, N. J. A. Sloane, and W. Smith. Spherical Codes. Book in preparation, http://www.research.att.com/∼njas/coverings/index.html. 1997.

[IEE97] IEEE. IEEE Standard 802.11 - Wireless LAN Medium Access Control (MAC) and Physical Layer (PHY) Specification. 1997.

[JM96] D. B. Johnson and D. A. Maltz. Dynamic Source Routing in Ad Hoc Wireless Networks. In T. Imielinski and H. Korth, editors, *Mobile Computing*, volume 353, pages 152–181. Kluwer Academic Publishers, 1996.

[JRS03] L. Jia, R. Rajaraman, and C. Scheideler. On local algorithms for topology control and routing in ad hoc networks. In *Proc. of the 15th ACM symposium on parallel algorithms and architectures (SPAA '03)*, pages 220–229, 2003.

[JV02] E.-S. Jung and N. H. Vaidya. A power control mac protocol for ad hoc networks. In *Proceedings of the 8th annual international conference on Mobile computing and networking (Mobicom'02)*, pages 36–47. ACM Press, 2002.

[KB97] J. M. Kahn and J. R. Barry. Wireless Infrared Communications. *Proceedings of the IEEE*, 85:265–298, February 1997.

[KKKP00] L. M. Kirousis, E. Kranakis, D. Krizanc, and A. Pelc. Power consumption in packet radio networks. *Theoretical Computer Science*, 243(1-2):289–305, 2000.

[Kra88] J. D. Kraus. *Antennas*. McGraw-Hill, New York, 1988.

[KSV00] Y.-B. Ko, V. Shankarkumar, and N. H. Vaidya. Medium Access Control Protocols Using Directional Antennas in Ad Hoc Networks. In *IEEE INFOCOM*, pages 13–21, 2000.

[KTe00] K-Team S.A. *Khepera miniature mobile robot*, 2000. http://www.k-team.com/robots/khepera.

[Lei92] F. T. Leighton. *Introduction to Parallel Algorithms and Architectures Arrays, Trees, Hypercubes*. Morgan Kaufmann Publishers, Inc., San Mateo, California, 1992.

[LH99] B. Liang and Z. J. Haas. Predictive Distance-Based Mobility Management for PCS Networks. In *Proceedings of IEEE INFOCOM'99*, pages 1377–1384, 1999.

[LHB+01] L. Li, J. Halpern, P. Bahl, Y.-M. Wang, and R. Wattenhofer. Analysis of a cone-based distributed topology control algorithm for wireless multi-hop networks. In *ACM Symposium on Principle of Distributed Computing (PODC'01)*, pages 264–273, 2001.

[Li03a] X.-Y. Li. Applications of Computational Geometry in Wireless Ad Hoc Networks, Book Chapter of Ad Hoc Wireless Networking, Kluwer, edited by X. Z. Cheng, X. Huang, and D.-Z. Du. 2003.

[Li03b] X.-Y. Li. Topology Control in Wireless Ad Hoc Networks, Book Chapter of Ad Hoc Networking, IEEE Press, edited by S. Basagni, M. Conti, S. Giordano, and I. Stojmenovic. 2003.

[Li03c] X.-Y. Li. Wireless Sensor Networks and Computational Geometry, Book Chapter of Handbook of Sensor Networks, edited by Mohammad Ilyas et al. CRC Press. 2003.

[LL00] UCLA Parallel Computing Laboratory and Wireless Adaptive Mobility Laboratory. Glomosim: A scalable simulation environment for wireless and wired network systems, http://pcl.cs.ucla.edu/projects/glomosim. 2000.

[LLGH04] Y. Lu, H. Lin, Y. Gu, and A. Helmy. Towards Mobility-Rich Performance Analysis of Routing Protocols in Ad Hoc Networks: Using Contraction, Expansion and Hybrid Models. In *IEEE International Conference on Communications (ICC'04)*, 2004.

[LNR04] G. Lin, G. Noubir, and R. Rajaraman. Mobility models for ad-hoc network simulation. In *Proceedings of INFOCOM'04*, pages 454–463, 2004.

[LP99] P. H. Lehne and M. Pettersen. An Overview of Smart Antenna Technology for Mobile Communications Systems. *IEEE Communications Surveys*, 2(4):2–13, 1999.

[LWW01] X.-Y. Li, P.-J. Wan, and Y. Wang. Power Efficient and Sparse Spanner for Wireless Ad Hoc Networks. In *IEEE Int. Conference on Computer Communications and Networks (ICCCN '01)*, pages 564–567, 2001.

[MBH01] J. Monks, V. Bharghavan, and W.-M Hwu. A Power Controlled Multiple Access Protocol for Wireless Packet Networks. In *IEEE Infocom*, pages 1–11, 2001.

[MFG99] F. Mondada, E. Franzi, and A. Guignard. The development of khepera. In *Proceedings of the 1st International Khepera Workshop*, pages 7–13, Paderborn, Germany, December 10.-11. 1999.

[MMF98] H. Meyr, M. Moeneclaey, and S. A. Fechtel. *Digital Communication Receivers – Synchronization, Channel Estimation And Signal Processing*. John Wiley & Sons, Inc., 1998.

[MN99] K. Mehlhorn and S. Näher. *LEDA: A Platform for Combinatorial and Geometric Computing*. Cambridge University Press, 1999.

[MSVG02] F. Meyer auf der Heide, C. Schindelhauer, K. Volbert, and M. Grünewald. Energy, Congestion and Dilation in Radio Networks. In *ACM Symposium on Parallel Algorithms and Architectures (SPAA'02)*, pages 230–237, 2002.

[MSVG04] F. Meyer auf der Heide, C. Schindelhauer, K. Volbert, and M. Grünewald. Congestion, Dilation, and Energy in Radio Networks. *Theory of Computing Systems (TOCS'04)*, 37(3):343–370, 2004.

[NS00] G. Narasimhan and M. Smid. Approximating the stretch factor of euclidean graphs. *SIAM J. Comput.*, 30(3):978–989, 2000.

[Oka98] G. T. Okamoto. *Smart Antenna Systems and Wireless LANs*. Kluwer Academic Publishers, 1998.

[Par92] J.D. Parsons. *The Mobile Radio Propagation Channel*. Plentech Press, London, 1992.

[Per01] C. E. Perkins, editor. *Ad Hoc Networking*. Addision-Wesley, 2001.

[Pos03] T. Postler. Simulation von wahrscheinlichkeitsgesteuerten Kanalzugriffsstrategien in mobilen Ad-hoc-Netzwerken. Bachelor thesis, University of Paderborn, 2003.

[PS89] D. Peleg and A. A. Schaffer. Graph Spanners. *Journal of Graph Theory*, 13:99–116, 1989.

[Raj02] R. Rajaraman. Topology Control and Routing in Ad hoc Networks: A Survey. In *SIGACT News, June 2002*, pages 60–73, 2002.

[Ram01] R. Ramanathan. On the performance of ad hoc networks with beamforming antennas. In *MobiCom'01*, pages 95–105. ACM Press, 2001.

[Rap96] T. S. Rappaport. *Wireless Communications: Principles and Practices*. Prentice Hall, 1996.

[RH00] R. Ramanathan and R. Hain. Topology Control of Multihop Wireless Networks Using Transmit Power Adjustment. In *INFOCOM (2)*, pages 404–413, 2000.

[RM98] V. Rodoplu and T. Meng. Minimum energy mobile wireless networks. In *IEEE Int. Conference on Communications (ICC'98)*, pages 3:1633–1639, 1998.

[RP89] R. Ramaswami and K.K. Parhi. Distributed scheduling of broadcasts in a radio network. In *IEEE INFOCOM'89*, pages 497–504, 1989.

[RS91] J. Ruppert and R. Seidel. Approximating the d-dimensional complete Euclidean graph. In *3rd Canadian Conference on Computational Geometry (CCCG '91)*, pages 207–210, 1991.

[RS98] S. B. Rao and W. D. Smith. Approximating geometrical graphs via spanners and banyans. In *Proc. of the 30th annual ACM symposium on theory of computing (STOC'98)*, pages 540–550, 1998.

[RSVG03] S. Rührup, C. Schindelhauer, K. Volbert, and M. Grünewald. Performance of Distributed Algorithms for Topology Control in Wireless Networks. In *17th Int. Parallel and Distributed Processing Symposium (IPDPS'03)*, page 28(2), 2003.

[RT99] E. Royer and C. Toh. A review of current routing protocols for ad-hoc mobile wireless networks. *IEEE Personal Communications*, 4(2):46–55, 1999.

[Rüh02] S. Rührup. Topologieaufbau und -erhaltung in mobilen Ad-hoc-Netzwerken. Diploma thesis, University of Paderborn, 2002.

[San98] M. Sanchez. RE: Mobility pattern in a MANET, IETF MANET Mailing List, Sender: <misan@disca.upv.es>, http://www.disca.upv.es/misan/mobmodel.htm, June 25. 1998.

[SLRV03] C. Schindelhauer, T. Lukovszki, S. Rührup, and K. Volbert. Worst Case Mobility in Ad Hoc Networks. In *ACM Symposium on Parallel Algorithms and Architectures (SPAA'03)*, pages 230–239, 2003.

[Spo93] D. L. Spohn. *Data Network Design*. McGraw-Hill, Inc., 1993.

[SR98] S. Singh and C. Raghavendra. PAMAS - power aware multi-access protocol with signalling for ad hoc networks. *ACM Computer Comm. Review*, 28:5–26, 1998.

[SVZ04] C. Schindelhauer, K. Volbert, and M. Ziegler. Spanners, Weak Spanners, and Power Spanners for Wireless Networks. In *Proc. of the 15th International Symposium on Algorithms and Computation (ISAAC'04)*, pages 805–821, 2004.

[SW98] S. Singh and M. Woo. Power-Aware Routing in Mobile Ad Hoc Networks. In *Proc. of Mobile Computing and Networking*, pages 181–190, 1998.

[SW01] C. Schindelhauer and B. Weber. Tree-Approximations for the Weighted Cost-Distance Problem (Extended Abstract). In *Int. Symposium on Algorithms and Computation (ISAAC'01)*, pages 185–195, 2001.

[SWL04] W.-Z. Song, Y. Wang, and X.-Y. Li. Localized algorithms for energy efficient topology in wireless ad hoc networks. In *ACM symposium on mobile ad hoc networking and computing (MobiHoc'04)*, pages 98–108. ACM Press, 2004.

[Tan96] A. S. Tanenbaum. *Computer networks (4th ed.)*. Prentice-Hall, Inc., 1996.

[TMBR02] M. Takai, J. Martin, R. Bagrodia, and A. Ren. Directional virtual carrier sensing for directional antennas in mobile ad hoc networks. In *ACM symposium on mobile ad hoc networking and computing (MobiHoc'02)*, pages 183–193, 2002.

[Tri95] C. Tricot. *Curves and Fractal Dimension*. Springer, 1995.

[Val82] L. G. Valiant. A scheme for fast parallel communication. *SIAM Journal on Computing*, 11(2):350–361, 1982.

[Var01] A. Varga. The OMNeT++ Discrete Event Simulation System. In *Proceedings of the European Simulation Multiconference (ESM'2001)*, 2001.

[Vol01] K. Volbert. Simulative Analyse von Kommunikationsstrategien in mobilen Ad Hoc Netzwerken. Diploma thesis, University of Paderborn, 2001.

[Vol02] K. Volbert. A Simulation Environment for Ad Hoc Networks Using Sector Subdivision. In *10th Euromicro Workshop on Parallel, Distributed and Network-based Processing (PDP'02)*, pages 419–426, 2002.

[Vol04a] K. Volbert. Experimental Analysis of adjustable sectorized Topologies for Static Ad Hoc Networks. In *Proc. of the 2004 joint workshop on Foundations of Mobile Computing (DIAL M-POMC'04)*, pages 102–111, 2004.

[Vol04b] K. Volbert. Investigating sectorized topologies, http://wwwcs.upb.de/cs/ag-madh/www/english/kvolbert/yao.html. 2004.

[WK86] T. Williams and C. Kelley. Gnuplot, http://www.gnuplot.info/. 1986.

[WL02] Y. Wang and X.-Y. Li. Distributed spanner with bounded degree for wireless ad hoc networks. In *Proc. of the 16th International Parallel and Distributed Processing Symposium (IPDPS '02)*, page 120. IEEE Computer Society, 2002.

[WL03] Y. Wang and X.-Y. Li. Localized construction of bounded degree and planar spanner for wireless ad hoc networks. In *Proceedings of the 2003 joint workshop on Foundations of mobile computing*, pages 59–68. ACM Press, 2003.

[WLBW01] R. Wattenhofer, L. Li, P. Bahl, and Y.-M. Wang. Distributed Topology Control for Wireless Multihop Ad-hoc Networks. In *INFOCOM*, pages 1388–1397, 2001.

[WLWF02] Y. Wang, X.-Y. Li, P.-J. Wan, and O. Frieder. Sparse power efficient topology for wireless networks. In *Proc. ACM Hawaii International Conference on System Sciences (HICSS'02)*, page 296, 2002.

[XHE01] Y. Xu, J. Heidemann, and D. Estrin. Geography-informed Energy Conservation for Ad Hoc Routing. In *Proc. of 7th Annual Int. Conf. on Mobile Computing and Networking (Mobicom'01)*, pages 70–84, Rome, Italy, July 2001.

[Yao82] A. C.-C. Yao. On Constructing Minimum Spanning Trees in k-dimensional space and related problems. *SIAM J. Comput.*, 11:721–736, 1982.

[ZBG98] X. Zeng, R. Bagrodia, and M. Gerla. Glomosim: A library for parallel simulation of large-scale wireless networks. In *Workshop on Parallel and Distributed Simulation*, pages 154–161, 1998.